TESIS DE LA UNIVERSIDAD DE ZARAGOZA
2025
159

Adelaida Hernáiz Martorell

Biomarcadores epigenéticos y desarrollo de modelos celulares en scrapie ovino

Director/es
Martín Burriel, Inmaculada
Bolea Bailo, Rosa María

ISSN 2254-7606

Prensas de la Universidad
Universidad Zaragoza

Universidad de Zaragoza
Servicio de Publicaciones

ISSN 2254-7606

Universidad Zaragoza
1542

Tesis Doctoral

BIOMARCADORES EPIGENÉTICOS Y DESARROLLO DE MODELOS CELULARES EN SCRAPIE OVINO

Autor

Adelaida Hernáiz Martorell

Director/es

Martín Burriel, Inmaculada
Bolea Bailo, Rosa María

UNIVERSIDAD DE ZARAGOZA
Escuela de Doctorado

Programa de Doctorado en Ciencias Biomédicas y Biotecnológicas

2023

LABORATORIO DE GENÉTICA BIOQUÍMICA (LAGENBIO)

Departamento de Anatomía, Embriología y Genética Animal

Facultad de Veterinaria

UNIVERSIDAD DE ZARAGOZA

BIOMARCADORES EPIGENÉTICOS Y DESARROLLO DE MODELOS CELULARES EN SCRAPIE OVINO

Memoria presentada por:

Adelaida Hernaiz Martorell

Para optar al grado de Doctora por la Universidad de Zaragoza

Directoras:

Inmaculada Martín Burriel

Rosa María Bolea Bailo

ZARAGOZA, 2023

Departamento de Anatomía, Embriología y Genética Animal
Universidad Zaragoza

Departamento de Patología Animal
Universidad Zaragoza

Dra. Inmaculada Martín Burriel, Catedrática del Departamento de Anatomía, Embriología y Genética Animal, y Dra. Rosa María Bolea Bailo, Vicerrectora de Política Científica y Catedrática del Departamento de Patología Animal de la Facultad de Veterinaria (Universidad de Zaragoza),

CERTIFICAN:

Que Doña Adelaida Hernaiz Martorell ha realizado bajo nuestra dirección los trabajos correspondientes a su Tesis Doctoral titulada "Biomarcadores epigenéticos y desarrollo de modelos celulares en scrapie ovino" que se corresponde con el proyecto de tesis aprobado por la Comisión de Doctorado el 13 de septiembre de 2018. La Memoria presentada cumple los requisitos exigidos para optar al Grado de Doctor por la Universidad de Zaragoza, por lo que las directoras del trabajo autorizan su presentación como compendio de publicaciones para que pueda ser juzgada por el Tribunal correspondiente.

Lo que suscribimos como directoras del trabajo en Zaragoza, a 17 de enero de 2023.

Fdo.: Inmaculada Martín Burriel

Fdo.: Rosa M.ª Bolea Bailo

La realización de este trabajo de tesis doctoral ha sido posible gracias a la concesión de un contrato predoctoral del Gobierno de Aragón (Orden IIU/2023/2017), cofinanciado por el Fondo Social Europeo, y gracias a la financiación de los siguientes organismos y proyectos:

- Grupo de Investigación del Gobierno de Aragón A19-20R-LAGENBIO.
- Proyecto AGL2015-67945-P: Biomarcadores epigenéticos en enfermedades priónicas. Financiado por el Ministerio de Economía y Competitividad y por el Fondo Europeo de Desarrollo Regional (FEDER).
- Proyecto RTI2018-098711-B-I00: Transmisión, multiplicación, toxicidad y dianas terapéuticas de enfermedades priónicas en modelos celulares y bioensayos. Financiado por la Agencia Estatal de Investigación y por el Fondo Europeo de Desarrollo Regional (FEDER).

A mi familia.

"*Todos nuestros sueños pueden hacerse realidad, si tenemos el coraje de perseguirlos*"

Walt Disney

Agradecimientos

En estas líneas, me gustaría agradecer a todas aquellas personas que me han acompañado durante estos años de tesis con las que he compartido muchos momentos que siempre recordaré con mucho cariño.

A mis directoras de tesis, Inma y Rosa, por confiar en mí y darme la oportunidad de conocer el apasionante mundo de la investigación. Gracias a vosotras he conocido una salida profesional que al acabar la carrera no me había planteado, pero que ahora me encanta y quiero seguir formándome y aprendiendo cada día más. Inma, muchas gracias por todo, gracias por enseñarme y tener paciencia cuando a veces metía la pata en algún experimento, por escucharme y animarme en los momentos difíciles, incluidos los momentos de fenómenos paranormales con nuestras amigas las células, y también gracias por todas las risas y momentos divertidos que hemos vivido.

A mis compañeros de laboratorio de los que he aprendido muchas cosas y me han ayudado a lo largo de este recorrido. Gracias a todos mis compañeros del grupo LAGENBIO, Charo, Clemen, Laura Barrachina, Alina, Laura Moreno, Janne, Miriam, Leticia, Tresa, Ana Cris, Carmen, Raquel, Ana Solana, Arianne, Elvira, Paula, Pilar, por ayudarme cuando lo he necesitado, por animarme en los momentos duros y por todos los momentos bonitos que hemos compartido. También quiero dar las gracias a Marina, Mirta, Diego, Sonia, Alicia, Dani, Sandra y Belén por su ayuda a lo largo de la tesis.

A mis amigas, por estar siempre ahí durante todos estos años y espero que muchísimos más, gracias por apoyarme y darme ánimos.

A mi familia, en especial a mis padres, a mi hermano y a mi abuela, por vuestro apoyo incondicional, por creer siempre en mí y por darme ánimos y fuerza para seguir adelante, ahora y siempre.

A Carlos, gracias por escucharme y animarme, por sacarme siempre una sonrisa y estar ahí siempre que lo necesito.

Muchísimas gracias a todos.

La presente tesis doctoral está constituida por un compendio de trabajos previamente publicados e indexados en revistas científicas cuyo índice de impacto está incluido en el *Journal Citation Reports* (JCR). A continuación, se indican las referencias completas de los cuatro artículos publicados que forman parte de esta tesis por compendio de publicaciones, de acuerdo con la normativa de esta modalidad:

Hernaiz, Adelaida; Toivonen, Janne Markus; Bolea, Rosa; Martín-Burriel, Inmaculada. **Epigenetic Changes in Prion and Prion-like Neurodegenerative Diseases: Recent Advances, Potential as Biomarkers, and Future Perspectives.** *International Journal of Molecular Sciences. Vol. 23, pág. 12609, 2022.* doi:10.3390/IJMS232012609.

Hernaiz, Adelaida; Sanz, Arianne; Sentre, Sara; Ranera, Beatriz; Lopez-Pérez, Óscar; Zaragoza, Pilar; Badiola, Juan José; Filali, Hicham; Bolea, Rosa; Toivonen, Janne Markus; Martín-Burriel, Inmaculada. **Genome-Wide Methylation Profiling in the Thalamus of Scrapie Sheep.** *Frontiers in Veterinary Science. Vol. 0, pág. 29, 2022.* doi:10.3389/FVETS.2022.824677.

Hernaiz, Adelaida; Sentre, Sara; Betancor, Marina; López-Pérez, Óscar; Salinas-Pena, Mónica; Zaragoza, Pilar; Badiola, Juan José; Toivonen, Janne Markus; Bolea, Rosa; Martín-Burriel, Inmaculada. **5-Methylcytosine and 5-Hydroxymethylcytosine in Scrapie-Infected Sheep and Mouse Brain Tissues.** *International Journal of Molecular Sciences. Vol. 24, pág. 1621, 2023.* doi:10.3390/IJMS24021621.

García-mendívil, Laura; Mediano, Diego Rubén; Hernaiz, Adelaida; Sanz-rubio, David; Vázquez, Francisco José; Marín, Belén; López-pérez, Óscar; Otero, Alicia; Badiola, Juan José; Zaragoza, Pilar; Ordovás, Laura; Bolea, Rosa; Martín-Burriel, Inmaculada. **Effect of Scrapie Prion Infection in Ovine Bone Marrow-Derived Mesenchymal Stem Cells and Ovine Mesenchymal Stem Cell-Derived Neurons.** *Animals. Vol. 11, pág. 1137, 2021.* doi:10.3390/ANI11041137.

Además de los cuatro artículos ya publicados requeridos para presentar la tesis en la modalidad de compendio de publicaciones, se han incluido otros dos manuscritos todavía sin publicar que también forman parte de los obejtivos de esta tesis:

Hernaiz, Adelaida; Cobeta, Paula; Marín, Belén; Vázquez, Francisco José; Badiola, Juan José; Zaragoza, Pilar; Bolea, Rosa; Martín-Burriel, Inmaculada. **Susceptibility of ovine bone marrow-derived mesenchymal stem cell spheroids to scrapie prion infection.** Este manuscrito ha sido

enviado a la revista *Animals* para su publicación.

Hernaiz, Adelaida; Marín, Belén; Vázquez, Francisco José; Badiola, Juan José; Zaragoza, Pilar; Bolea, Rosa; Martín-Burriel, Inmaculada. **RNA-sequencing transcriptomic analysis of scrapie-infected ovine mesenchymal stem cells.** Este manuscrito será enviado próximamente para su posible publicación en la revista *Frontiers in Veterinary Science.*

Índice

ÍNDICE

Resumen/Abstract

Resumen

El scrapie es una enfermedad neurodegenerativa que pertenece al grupo de las encefalopatías espongiformes transmisibles (EETs) o enfermedades priónicas, las cuales están causadas por una isoforma patológica mal plegada de la proteína prion celular (PrP^{C}) conocida como PrP^{Sc}. Se trata de enfermedades fatales, actualmente sin cura y cuyos mecanismos patogénicos todavía no se conocen en su totalidad.

En esta tesis, se abordan dos campos de investigación diferentes en la enfermedad de scrapie. Por un lado, el estudio de cambios de metilación del DNA, mecanismo epigenético asociado recientemente con las enfermedades priónicas y con otras enfermedades neurodegenerativas, y por otro, el desarrollo de un modelo celular *in vitro* basado en el cultivo de células madre mesenquimales (MSCs) ovinas, dada la necesidad creciente de modelos celulares de especies naturalmente susceptibles a la enfermedad que permitan el estudio de las enfermedades priónicas de la manera más fidedigna posible.

En cuanto a los resultados obtenidos en los trabajos de metilación del DNA, en el tálamo de ovejas con scrapie, se han identificado genes con metilación diferencial asociados con distintas funciones reguladas por la PrP^{C}, así como con posibles funciones neuroprotectoras o agravantes del proceso neurodegenerativo. Algunos de estos genes con metilación diferencial también mostraron cambios de expresión en los animales con scrapie, indicando un posible efecto regulador de la metilación del DNA en la expresión génica. Además de estos cambios de metilación a nivel génico, en distintas regiones del sistema nervioso central de ovejas infectadas con scrapie y de un modelo murino transgénico de scrapie, se detectaron cambios en los niveles de las dos formas más abundantes de metilación del DNA, 5-metilcitosina (5mC) y 5-hidroximetilcitosina (5hmC), acompañados de cambios de expresión en algunos genes codificantes de enzimas reguladoras epigenéticas encargadas de regular los niveles de 5mC y 5hmC. Estos resultados indican que el mecanismo epigenético de metilación del DNA está involucrado en la patología de scrapie, existiendo tanto cambios globales en los perfiles de metilación como cambios específicos en genes concretos.

Por otro lado, los trabajos llevados a cabo en MSCs ovinas infectadas con scrapie han permitido evaluar la capacidad de estas células de infectarse y replicar PrP^{Sc}, así como el efecto de dicha infección sobre la viabilidad celular, tanto cultivadas en monocapa como en forma de esferoides tridimensionales. Al cultivar las MSCs en monocapa, observamos que en condiciones de crecimiento estas células no eran capaces de mantener el prion a lo largo del tiempo, a diferencia de las MSCs sometidas a diferenciación neurogénica que sí que fueron capaces de

captar y mantener el agente priónico. En ambas condiciones, la infección con scrapie produjo una toxicidad temprana disminuyendo la viabilidad de los cultivos. El cultivo en tres dimensiones en forma de esferoides, el cual se asemeja más a las condiciones de las células *in vivo*, parece afectar a la capacidad de infección de las MSCs en condiciones de crecimiento ya que, a diferencia de las MSCs cultivadas en monocapa, los esferoides de MSCs en crecimiento fueron capaces de mantener de manera estable los niveles de PrP^{Sc} a lo largo del tiempo de cultivo, indicando que el microambiente generado en los esferoides favorece la permisividad a la infección de las MSCs. Los esferoides en condiciones de diferenciación neurogénica también mantuvieron una señal estable de PrP^{Sc}. En este sistema en tres dimensiones, se observó igualmente cierta toxicidad acompañada de una disminución de la viabilidad celular. Este efecto tóxico provocado por la infección con scrapie se corroboró mediante un estudio transcriptómico de MSCs ovinas infectadas con scrapie en condiciones de crecimiento, en el cual se identificaron genes con expresión diferencial involucrados en distintas rutas biológicas relacionadas con la toxicidad y propagación priónicas. Estos resultados indican que las MSCs ovinas, además de ser permisivas a la infección con scrapie, son capaces de reproducir la toxicidad ejercida por el agente priónico, lo que las convierte en un modelo *in vitro* óptimo para el estudio de las enfermedades priónicas.

Abstract

Scrapie is a neurodegenerative disease that belongs to the group of transmissible spongiform encephalopathies (TSEs) or prion diseases, which are caused by a pathological misfolded isoform of the cellular prion protein (PrP^{C}) known as PrP^{Sc}. These diseases are fatal, currently without cure, and their pathogenic mechanisms are still not fully understood.

In this thesis, two different fields of research in scrapie disease are addressed. On the one hand, the study of DNA methylation changes, an epigenetic mechanism recently associated with prion diseases and other neurodegenerative diseases, and on the other hand, the development of an *in vitro* cell model based on the culture of ovine mesenchymal stem cells (MSCs), given the growing need for cell models of species naturally susceptible to the disease that allow the study of prion diseases in the most possible reliable way.

Regarding the results obtained in the work on DNA methylation, in the thalamus of scrapie sheep, differentially methylated genes associated with different functions regulated by PrP^{C}, as well as with possible neuroprotective or aggravating functions of the neurodegenerative process, have been identified. Some of these differentially methylated genes also showed expression changes in scrapie animals, indicating a possible regulatory effect of DNA methylation on gene expression. In addition to these methylation changes at gene level, changes in the levels of the two most abundant forms of DNA methylation, 5-methylcytosine (5mC) and 5-hydroxymethylcytosine (5hmC), accompanied by expression changes in some genes encoding epigenetic regulatory enzymes responsible for regulating the levels of 5mC and 5hmC, were detected in different regions of the central nervous system of scrapie-infected sheep and a transgenic murine model of scrapie. These results indicate that the epigenetic mechanism of DNA methylation is involved in the pathology of scrapie, with both global changes in methylation profiles and gene-specific changes.

On the other hand, the work carried out in scrapie-infected ovine MSCs has allowed the evaluation of the capacity of these cells to become infected and replicate PrP^{Sc}, as well as the analysis of the effect of this infection on cell viability, in monolayer-cultured cells and in three-dimensional spheroids. When MSCs were cultured in monolayer, we observed that under growth conditions these cells were not able to maintain the prion over time, in contrast to MSCs subjected to neurogenic differentiation that were able to capture and maintain the prion agent. In both conditions, the infection with scrapie resulted in early toxicity decreasing the viability of

the cultures. Three-dimensional culture in the form of spheroids, which more closely resembles *in vivo* cell conditions, appears to affect the infectivity of MSCs under growth conditions since, unlike MSCs cultured in monolayer, spheroids of growing MSCs were able to stably maintain PrP^{Sc} levels throughout the culture time, indicating that the microenvironment generated in the spheroids favors the permissiveness of MSCs to infection. Spheroids under neurogenic differentiation conditions also maintained a stable PrP^{Sc} signal. In this three-dimensional system, some toxicity accompanied by a decrease in cell viability was also observed. This toxic effect caused by scrapie infection was corroborated by a transcriptomic study of scrapie-infected ovine MSCs under growth conditions, in which differentially expressed genes involved in different biological pathways related to prion toxicity and propagation were identified. These results indicate that ovine MSCs, in addition to being permissive to scrapie infection, are capable of reproducing the toxicity exerted by the prion agent, which makes them an optimal *in vitro* model for the study of prion diseases.

Introducción general

1. Enfermedades priónicas

Las enfermedades priónicas, también conocidas como encefalopatías espongiformes transmisibles (EETs), son un conjunto de enfermedades neurodegenerativas que afectan tanto a seres humanos como a animales y que están causadas por un agente etiológico común: una proteína infecciosa conocida como prion. Se trata de trastornos fatales crónicos con largos periodos de incubación y con una patología similar que afecta al sistema nervioso central (SNC) [1].

En humanos, las enfermedades priónicas pueden ser de causa genética, adquiridas o desarrollarse esporádicamente (forma idiopática) [2]. La enfermedad de Creutzfeldt Jakob esporádica (sCJD) es la forma más común, representando un 85 % del total de casos [3]. Las enfermedades de causa genética están producidas por mutaciones en el gen que codifica la proteína prion conocido como gen *PRNP* [2]. Dentro de este grupo encontramos la enfermedad de CJD genética, el insomnio familiar fatal y la enfermedad de Gerstmann-Sträussler-Scheinker [4,5]. Por otro lado, las formas adquiridas son aquellas causadas por un contacto exógeno con el prion. En este grupo se encuentran el kuru [6], la variante de CJD y el CJD iatrogénico [7].

En el caso de los animales, la enfermedad es generalmente de causa adquirida y puede afectar a ovejas, cabras, vacas, cérvidos, felinos, visones y primates [8]. La enfermedad de scrapie, que afecta a ovejas y cabras, fue la primera EET descrita [9]. Se pueden distinguir dos formas de scrapie: el clásico y el atípico. Ambas formas presentan unas características específicas variando entre ellas los signos clínicos y las lesiones cerebrales de los animales afectados [10,11], así como los genotipos del gen *PRNP* asociados a la susceptibilidad de padecer la enfermedad [12,13]. Además, el scrapie clásico es de causa adquirida mientras que el atípico se considera una forma esporádica [14]. Los objetivos de esta tesis doctoral se desarrollan en torno a la forma clásica del scrapie ovino.

Otras dos EETs animales ampliamente estudiadas son la encefalopatía espongiforme bovina (BSE, de su denominación en inglés "*Bovine spongiform encephalopathy"*) y la enfermedad caquectizante crónica (CWD, de su denominación en inglés "*Chronic wasting disease"*). La BSE afecta al ganado vacuno, es zoonótica y es una de las enfermedades priónicas animales más conocidas debido a la epidemia originada en Reino Unido durante los años 80 [15]. El uso de harinas de carne y hueso contaminadas con priones para la alimentación del ganado vacuno se consideró la causa más probable de los casos de BSE en estos animales, que conllevó una posterior transmisión a humanos por consumo de productos contaminados con BSE. La prohibición del uso de estas harinas permitió el declive progresivo de la epidemia

[16]. Por otro lado, la CWD es una EET de elevada prevalencia en Norte América que afecta a varias especies de la familia de los cérvidos [17]. Es altamente contagiosa y persistente en el ambiente, lo que facilita su transmisión tanto en animales de granja como silvestres dificultando su control en las poblaciones de cérvidos [18,19].

1.1. Agente etiológico

1.1.1. Proteína prion celular

La proteína prion celular (PrP^C) se trata de una glicoproteína monomérica, soluble en detergentes, que consta de 250 aminoácidos [20]. Está codificada por el gen *PRNP*, altamente conservado en mamíferos [21]. Este gen presenta distintos sitios de unión para factores de transcripción, lo que permite un control dinámico de la expresión de PrP^C [22]. Los niveles más altos de expresión de PrP^C se encuentran en el SNC [23]. Se ha detectado tanto en neuronas como en astrocitos, oligodendrocitos y microglía [24–26]. Además de expresarse en el SNC, también se encuentra en el sistema nervioso periférico y en otros tejidos y células como, por ejemplo, el corazón, el páncreas, el intestino, el bazo, el hígado, los riñones y las células del sistema inmunitario [27–29].

Esta proteína está implicada en distintos procesos y rutas biológicas, siendo necesaria para un correcto funcionamiento del organismo. Entre las distintas funciones en las que participa, se pueden destacar las siguientes: homeostasis mitocondrial, control de los ritmos circadianos, unión a iones de cobre y regulación de los niveles de hierro, supervivencia y proliferación celular, mantenimiento de la mielina, modulación de la absorción de glucosa, modificación de la morfología celular, regulación de la adhesión celular, regulación de la autofagia y protección frente al estrés oxidativo [23].

Dado el carácter multifuncional de esta proteína, la pérdida de PrP^C durante el transcurso de las enfermedades priónicas se ha propuesto como un causante de exacerbar la patología neurodegenerativa y los efectos tóxicos de la proteína prion patológica en las EETs [20].

1.1.2. Proteína prion patológica

La proteína prion patológica conocida como PrP^{Sc}, siendo "Sc" la abreviatura de scrapie, es el agente causal de las enfermedades priónicas. Se trata de una isoforma infecciosa malplegada derivada de la conversión de PrP^C [30]. A diferencia de la PrP^C, PrP^{Sc} es parcialmente insoluble en detergentes, resistente a proteasas y es capaz de formar agregados que se depositan en los tejidos afectados por la enfermedad [30]. Comparado con la PrP^C, su secuencia de aminoácidos es idéntica pero posee mayor proporción de láminas beta en su estructura secundaria [31].

La conversión de PrP^{C} a PrP^{Sc} se produce por un mal plegamiento de la proteína prion celular al entrar en contacto con la PrP^{Sc}, la cual actúa como modelo o plantilla sobre la cual se pliega de forma anómala la PrP^{C}, propagándose de esta manera la isoforma mal plegada a lo largo del tejido nervioso [30].

La naturaleza infecciosa de las EETs radica en las propiedades de esta proteína que, además de propagarse en el tejido nervioso, puede detectarse en sangre [32], saliva [33] y orina [34] de animales infectados y puede ser transportada a través de la barrera intestinal tras su ingestión para iniciar posteriormente el proceso neuroinvasivo [35,36].

1.2. Scrapie clásico

1.2.1. Signos clínicos y lesiones histopatológicas

Esta enfermedad se suele presentar en ovejas de entre 2 y 5 años. Entre los signos clínicos más comunes se encuentran los cambios en el comportamiento, bruxismo, prurito, ataxia, movimientos hipermétricos, temblores de cabeza y pérdida de condición corporal [37]. Otros signos clínicos menos frecuentes son el ptialismo, nistagmo, reflejo pupilar alterado, hipoestesia, alteraciones cardíacas y respiratorias, compactación del rumen y reducción de la producción de leche [38–40].

Además de los signos clínicos, a nivel microscópico, se pueden detectar una serie de lesiones características en el SNC: degeneración espongiforme o vacuolización, gliosis y pérdida neuronal.

La degeneración espongiforme se produce en el pericarion neuronal y en el neuropilo de la sustancia gris, y suele ser bilateral y simétrica. Las principales áreas anatómicas del SNC donde se localiza la vacuolización son la médula espinal, la médula oblongada, el mesencéfalo, el hipotálamo, el tálamo y el área septal [41,42].

La gliosis se trata de una respuesta inespecífica de las células gliales frente a distintos estímulos. En el caso del scrapie, se puede observar astrogliosis y activación de la microglía, junto con los depósitos de PrP^{Sc}, la vacuolización y la degeneración neuronal. Los astrocitos y la microglía son capaces de acumular PrP^{Sc} tanto en casos naturales como experimentales de infección con scrapie clásico [43–45].

La degeneración y pérdida neuronal implica la presencia de neuronas necróticas diseminadas, acompañadas a veces de neuronofagia, neuritas distróficas y neuronas basofílicas [42].

1.2.2. Genotipo del gen PRNP ovino y su implicación en la susceptibilidad a la enfermedad

Existe una clara influencia del genotipo del gen *PRNP* ovino en la susceptibilidad a padecer el scrapie clásico. Los polimorfismos identificados en este gen en los codones 136 A (Alanina)/V (Valina), 154 R (Arginina)/H (Histidina) y 171 Q (Glutamina)/R/H están asociados con resistencia/susceptibilidad a la enfermedad [12,14]. El haplotipo VRQ es el que está asociado a mayor susceptibilidad, siendo los animales homocigotos para este haplotipo los que presentan mayor riesgo de padecer scrapie clásico. El haplotipo ancestral ARQ también se asocia con susceptibilidad a padecer scrapie, pero con menos riesgo que el haplotipo VRQ. Los haplotipos ARR y AHQ están asociados con resistencia a la enfermedad, pero solo si se presentan en homocigosis. Los animales heterocigotos que presentan haplotipos resistentes tienen menor riesgo de padecer la enfermedad [12,14].

Hay algunas razas de ovejas en las que algunos de estos genotipos no existen o se encuentran en una frecuencia muy baja como por ejemplo el VRQ en la raza Suffolk [46] o el ARR en la oveja islandesa [47]. En estos casos, la susceptibilidad a la enfermedad se asocia con el haplotipo ARQ y la resistencia con el haplotipo AHQ [48].

Atendiendo a estos criterios, se desarrolló una clasificación basada en el riesgo a contraer la enfermedad, siendo riesgo 1 la categoría de riesgo más bajo y riesgo 5 la categoría con el riesgo más elevado. En la Tabla 1 se muestran las distintas categorías de riesgos y sus genotipos asociados.

Tabla 1. Grupos de riesgo y genotipos asociados al scrapie clásico [14,48].

Grupo de riesgo	**Genotipos**
Riesgo 1	ARR/ARR
Riesgo 2	ARR/AHQ
	AHQ/AHQ
Riesgo 3	ARR/ARQ
	ARR/ARH
	ARQ/AHQ
	AHQ/ARH
Riesgo 4	ARH/ARH
	ARQ/ARH
	ARQ/ARQ
	ARR/VRQ

Riesgo 5	AHQ/VRQ
	ARQ/VRQ
	ARH/VRQ
	VRQ/VRQ

1.2.3. Patogenia

La transmisión natural del scrapie clásico ocurre principalmente de manera horizontal, por contacto directo entre los animales o de manera indirecta por contaminación presente en el ambiente. A mayor contacto o tiempo de exposición entre animales o con el entorno implica una mayor propagación de la enfermedad [14,49].

Los mecanismos patogénicos desarrollados durante el transcurso de la enfermedad dependen de la cepa, la dosis y la ruta de entrada del agente infeccioso, así como del genotipo del animal afectado [50,51]. En condiciones naturales, el prion penetra en el organismo por vía oral a través del tracto gastrointestinal. De manera experimental, también se han descrito otras rutas de entrada efectivas como la intracerebral, intraperitoneal, intravascular, intraocular, intranasal y conjuntival [14,52,53].

Tras su entrada al organismo por vía oral, los priones penetran en el tejido linfoide asociado al intestino, principalmente en las placas de Peyer. De esta forma, se introducen en el sistema linforeticular, acumulándose y replicándose en macrófagos y células dendríticas foliculares. Las tonsilas palatinas también se consideran una ruta de entrada al sistema linfoide [14,54,55].

Tras multiplicarse en el sistema linforeticular, los priones se dirigen al SNC mediante dos rutas principales: directamente a través del sistema nervioso periférico e indirectamente a través de los linfonodos, el bazo, las tonsilas y finalmente el sistema nervioso periférico [56]. La médula espinal torácica y el núcleo dorsal del nervio vago son las primeras regiones neuroanatómicas en las que se detectan depósitos de PrP^{Sc} [14,57].

1.2.4. Diagnóstico y tratamiento

El diagnóstico oficial de scrapie se realiza post-mortem en muestras de tejido de SNC mediante la identificación de la PrP^{Sc} utilizando anticuerpos específicos anti-PrP. Estos anticuerpos se usan en distintos inmunoensayos como western blot, ELISA, inmunohistoquímica, inmunocitoquímica e inmunoprecipitación [58].

El test post-mortem de elección en scrapie es el análisis inmunohistoquímico, el cual permite detectar la PrP^{Sc}, ver su distribución en el tejido y su localización celular, y observar las características morfológicas de su acumulación [59].

Como la PrP^{Sc} también puede diseminarse y acumularse en los tejidos linfoides durante el transcurso de la enfermedad, existe la posibilidad de un diagnóstico ante-mortem mediante el análisis inmunohistoquímico de los tejidos linfoides de las tonsilas [60], la conjuntiva del tercer párpado [61] y la mucosa rectal [62]. Sin embargo, un resultado negativo en estas pruebas ante-mortem debe interpretarse con cautela y reevaluarse posteriormente dado que existen una serie de factores como, por ejemplo, el tiempo de incubación y la extensión de la infección, que pueden afectar al resultado del test [58].

Por otro lado, recientemente se han desarrollado otras técnicas de detección que presentan una mayor sensibilidad para detectar PrP^{Sc}. Dos de ellas son el ensayo de conversión de proteína priónica inducida por agitación en tiempo real (RT-QuIC) y la amplificación cíclica de proteínas mal plegadas (PMCA) que permiten detectar de manera altamente sensible pequeñas cantidades de PrP^{Sc} [63–68]. Sin embargo, estas técnicas innovadoras todavía están en desarrollo y por ahora se utilizan con fines de investigación o como técnicas complementarias para la confirmación de un diagnóstico previo.

Teniendo en cuenta las distintas técnicas de diagnóstico mencionadas y el hecho de que a día de hoy el diagnóstico oficial sigue siendo en muestras post-mortem, existe una necesidad creciente del desarrollo de biomarcadores para un diagnóstico temprano de la enfermedad.

En cuanto al tratamiento, actualmente no existen terapias para tratar las enfermedades priónicas. En el caso de los animales, los brotes de enfermedad se controlan mediante una combinación de diferentes medidas: restricción de movimiento en las explotaciones afectadas, sacrificio de los animales afectados y, en el caso del scrapie clásico, selección genética de los genotipos resistentes [69].

2. Epigenética: mecanismos epigenéticos

La epigenética consiste en el estudio de cambios en la actividad o función de los genes que no se asocian con ningún cambio en la secuencia del DNA [70]. Dentro de este campo de estudio, se pueden definir tres mecanismos epigenéticos principales: la metilación del DNA, las modificaciones de histonas y los RNA no codificantes. Los dos primeros mecanismos actúan esencialmente alterando la estructura de la cromatina cercana de un gen o una región en particular, mientras que los RNA no codificantes, sobre todo los microRNA (miRNA), son capaces de regular la expresión sin necesidad de estar físicamente cerca de sus genes diana.

2.1. Metilación del DNA

2.1.1. Formas de metilación del DNA

La metilación del DNA es uno de los mecanismos epigenéticos más estudiados. Consiste en la unión covalente de un grupo metilo al carbono 5 del nucleótido citosina para formar una 5-metilcitosina (5mC) [71]. En los mamíferos, este proceso ocurre predominantemente en los residuos de citosinas presentes en los dinucleótidos CpG [72]. Se han identificado varias formas de metilación del DNA: la 5mC, su derivado hidroxilado conocido como 5-hidroximetilcitosina (5hmC) y sus productos oxidados resultantes conocidos como 5-formilcitosina (5fC) y 5-carboxilcitosina (5caC) [73]. De todas estas formas, 5mC y 5hmC son las más estables y abundantes en los genomas de mamíferos [74], mientras que 5fC y 5caC son menos frecuentes y se pueden eliminar de manera transitoria [75].

Este mecanismo epigenético está implicado en la regulación de la expresión génica. La forma 5mC está asociada predominantemente a silenciamiento génico [76], mientras que la forma 5hmC se encuentra presente en genes altamente expresados [77,78].

2.1.2. Enzimas reguladoras del proceso de metilación

Existen diferentes enzimas que actúan como mediadoras del proceso de metilación. Las DNA metiltransferasas (DNMTs) son las encargadas de producir la forma 5mC añadiendo de manera covalente un grupo metilo al carbono 5 de una citosina [70]. Las enzimas TET o "*ten-eleven translocation*", en cambio, son dioxigenasas encargadas de generar la forma 5hmC mediante la adición de un grupo hidroxilo a la forma 5mC [79].

Dentro de la familia de DNMTs, se pueden distinguir tres enzimas: DNMT1 (DNA metiltransferasa 1), DNMT3A (DNA metiltransferasa 3 alfa) y DNMT3B (DNA metiltransferasa 3 beta) [70]. Las enzimas DNMT3A y DNMT3B son de novo metiltransferasas, las cuales metilan citosinas previamente sin metilar en los dinucleótidos CpG, teniendo una preferencia similar por el DNA hemimetilado y sin metilar. Son esenciales para el proceso de metilación de novo del genoma durante el desarrollo [80]. La enzima DNMT1 es la encargada de preservar a lo largo de las divisiones celulares los patrones de metilación previamente establecidos. Se trata de una enzima de mantenimiento con preferencia por el DNA hemimetilado que preserva los sitios de metilación ya existentes [81].

En cuanto a las enzimas TET, podemos distinguir tres dioxigenasas de citosinas: TET1 (Tet metilcitosina dioxigenasa 1), TET2 (Tet metilcitosina dioxigenasa 2) y TET3 (Tet meticitosina dioxigenasa 3) [73].

2.2. Modificaciones de histonas

Las histonas son proteínas estructurales que junto con el DNA forman los nucleosomas, unidades fundamentales de la cromatina [82]. Estas proteínas pueden modificarse postraduccionalmente, existiendo un número diverso de modificaciones postraduccionales de histonas [83,84]. Estas modificaciones tienen lugar en las colas amino-terminales de las histonas produciendo cambios en la interacción de los nucleosomas y, por tanto, afectando a la estructura general de la cromatina. Los cambios inducidos por estas modificaciones afectan a distintos procesos del DNA como son la transcripción, la reparación del DNA, la replicación y la recombinación [84]. Las modificaciones postraduccionales más estudiadas son la acetilación, la fosforilación y la metilación.

2.2.1. Acetilación de histonas

La acetilación de histonas es un proceso sumamente dinámico que está regulado por dos familias de enzimas: las histonas acetiltransferasas (HATs) y las histonas deacetilasas (HDACs) [83].

Las HATs catalizan, mediante el uso de acetil coenzima A como cofactor, la transferencia de un grupo acetilo a los residuos de lisina de las histonas. La adición del grupo acetilo neutraliza la carga positiva de las lisinas de manera que se debilita la interacción entre las histonas y el DNA, resultando en una cromatina menos compacta y más activa para la transcripción [85]. Estas enzimas, por tanto, se consideran activadores transcripcionales y se pueden clasificar en dos grupos: tipo A y tipo B [85,86].

Por otra parte, las HDACs desempeñan una función opuesta a las HATs. Están encargadas de revertir la acetilación de los residuos de lisina, es decir, de eliminar los grupos acetilo, restaurando la carga positiva de las lisinas y estabilizando la interacción entre las histonas y el DNA, de manera que la cromatina se encuentra más compacta y menos activa. Debido a su modo de actuación, estas enzimas se consideran represores transcripcionales. Existen cuatro clases de HDACs: I, II, III y IV [84,86].

2.2.2. Fosforilación de histonas

Al igual que la acetilación, la fosforilación de histonas es un proceso dinámico. Este proceso se produce en los residuos de serina, treonina y tirosina de las histonas. La adición y retirada de grupos fosfato también está controlada por dos clases de enzimas conocidas como quinasas y fosfatasas [87].

Las enzimas quinasas son las encargadas de transferir un grupo fosfato al aminoácido diana correspondiente. Esta modificación añade carga negativa a las histonas, afectando

a la estructura de la cromatina y facilitando la transcripción del DNA [87]. La retirada de los grupos fosfato es llevada a cabo por las enzimas fosfatasas [88].

2.2.3. Metilación de histonas

La metilación de histonas tiene lugar en los residuos de lisina y arginina. A diferencia de la acetilación y la fosforilación, esta modificación no altera la carga de las histonas. Además, otra diferencia a tener en cuenta es que las lisinas pueden estar mono-, di- o tri-metiladas y las argininas mono- o di-metiladas [89].

Las enzimas metiltransferasas de histonas son las encargadas de la adición de grupos metilo. Las lisina metiltransferasas catalizan la adición de grupos metilo a los residuos de lisina, mientras que las arginina metiltransferasas añaden grupos metilo a los residuos de arginina [90,91]. Por otro lado, las demetilasas de histonas son las encargadas de eliminar los grupos metilo [92].

Al contrario que la acetilación y la fosforilación, en las cuales la presencia de un grupo acetilo o fosfato se asocia con activación de la transcripción y la ausencia con la represión de la transcripción, en el caso de la metilación de histonas, la posición de la metilación y el estado de metilación (mono-, di- o tri-metilación) determinan que dicha modificación tenga un efecto activador o represor de la transcripción [93,94].

2.3. MicroRNAs

Los microRNAs son pequeños RNA no codificantes, de unos 21-23 nucleótidos de longitud, capaces de regular la expresión génica a nivel transcripcional, postranscripcional o traduccional [95]. Aunque algunos miRNA pueden inducir la expresión génica en algunos casos por su interacción con los promotores de genes [96], su regulación de la expresión génica está basada en gran medida en la degradación o represión de la traducción de su RNA mensajero diana [97].

Muchos miRNA muestran un perfil de expresión específico de células o tejidos. Se pueden encontrar en la sangre y otros fluidos corporales como complejos libres (principalmente asociados a proteínas) o pueden estar contenidos en vesículas extracelulares. Estos miRNA circulantes pueden detectarse y medirse mediante métodos sensibles y específicos, como por ejemplo la PCR cuantitativa o las tecnologías de secuenciación de última generación, lo que los convierte en potenciales moléculas biomarcadoras [98].

2.4. Funciones de los mecanismos epigenéticos en el cerebro

2.4.1. Aprendizaje y memoria

La metilación del DNA y sus enzimas reguladoras están implicadas en la formación de la memoria [99,100]. Existe un equilibrio dinámico entre la metilación y desmetilación del DNA en genes reguladores de la plasticidad sináptica y de la formación de la memoria [100]. Las enzimas DNMTs parecen estar implicadas en la respuesta al miedo condicionado y en la formación de la memoria [100], mientras que las enzimas TET, mediante la desmetilación del DNA, juegan un papel fundamental en la activación de genes cruciales para la formación y consolidación de la memoria [101].

En cuanto a las modificaciones de histonas, la acetilación ha sido la modificación más estudiada a nivel cerebral, y está implicada en procesos de aprendizaje y en la adquisición de memorias a largo plazo [102,103].

Los miRNAs son capaces de controlar redes enteras de genes en las neuronas en respuesta a distintos procesos neuronales y pueden actuar en las dendritas regulando la síntesis local de determinadas proteínas cruciales para la plasticidad sináptica y la supervivencia celular [104,105].

2.4.2. Regulación de la neurogénesis

Un correcto estado de metilación del DNA es esencial para el mantenimiento y la diferenciación de los progenitores neuronales tanto en el cerebro adulto como durante el desarrollo embrionario [106]. Las enzimas DNMTs tienen un papel importante durante el desarrollo embrionario. Por ejemplo, DNMT1 está implicada en la regulación de la neurogénesis y la gliogénesis [107].

La acetilación y la metilación de histonas, así como sus enzimas asociadas también están implicadas en la neurogénesis del cerebro adulto, regulando la proliferación y la diferenciación de los progenitores neuronales [108–110].

Durante el desarrollo cerebral, los miRNAs intervienen en la formación y maduración de las sinapsis y en la dendritogénesis [104,105]. También se han descrito varios miRNAs implicados en el proceso de neurogénesis en el cerebro adulto [106].

2.4.3. Implicación en enfermedades neurodegenerativas priónicas y similares a priones

Así como el correcto funcionamiento de estos mecanismos epigenéticos se ha asociado con un adecuado funcionamiento del cerebro, la alteración o un mal funcionamiento de estos mecanismos se ha relacionado con distintas enfermedades neurodegenerativas incluidas las enfermedades priónicas y "*prion-like*" o similares a priones.

Las enfermedades *prion-like* son proteinopatías que presentan mecanismos patogénicos similares a los de las enfermedades priónicas, incluyendo la acumulación de proteínas mal plegadas en el SNC [111,112]. A este grupo de enfermedades pertenecen, entre otras, el Alzheimer, el Parkinson, el Huntington y la esclerosis lateral amiotrófica.

Los distintos hallazgos sobre la implicación de los mecanismos epigenéticos en las enfermedades priónicas y *prion-like* se detallan en profundidad en el manuscrito 1 de esta tesis.

3. Modelos celulares en las enfermedades priónicas

Los modelos celulares son herramientas que permiten estudiar los mecanismos moleculares implicados en las enfermedades priónicas, así como testar y descubrir nuevas moléculas terapéuticas.

Existen distintas líneas de cultivo celular capaces de infectarse de manera persistente con priones. En el estudio de las enfermedades priónicas, estos sistemas *in vitro* ofrecen una serie de ventajas: son más sencillos de manipular y económicamente más rentables que los modelos *in vivo*, ofrecen un alto rendimiento en las pruebas de cribado de potenciales moléculas terapéuticas, permiten estudiar mecanismos moleculares clave de las enfermedades priónicas dentro de un sistema celular intacto e incrementan la reproducibilidad y validez de los hallazgos científicos, todo ello evitando los problemas éticos que implica el uso de modelos animales o incluso de ciertas muestras humanas [113–115].

Para generar modelos celulares de enfermedades priónicas, generalmente se parte de una población de células que expresen la PrP^{C}. Estas células se inoculan con homogeneizados de cerebro infectados con priones. Tras su incubación, se retira dicho homogeneizado para asegurar que cualquier señal de PrP^{Sc} detectada sea resultado de la infección celular y no de la presencia del homogeneizado infectado [113]. En ocasiones, solo una fracción de células es capaz de infectarse con priones, siendo necesaria una posterior subclonación para crear líneas celulares que expresen altos niveles de PrP^{Sc} [116]. Para evaluar el éxito de la infección, normalmente se detecta la presencia de PrP^{Sc} en lisados celulares, aunque también se puede realizar en células intactas adheridas a una membrana [116]. Además, existen técnicas muy sensibles como el RT-QuIC y la PMCA capaces de detectar niveles muy bajos de infección priónica en las células [117–120].

3.1. Líneas celulares murinas inmortalizadas

Existen varias líneas celulares murinas inmortalizadas capaces de infectarse y propagar priones, pero, debido a que en el ratón no se desarrolla de manera natural la

enfermedad priónica, es necesario adaptar previamente las cepas priónicas mediante pases sucesivos en ratones para superar este fenómeno de barrera de especie [121].

Dos líneas celulares ampliamente utilizadas para el estudio de la propagación de priones son las células de neuroblastoma murino N2a [122] y las células hipotalámicas GT1 [123]. Otras líneas celulares neuronales capaces de infectarse con priones son las células de Schwann MSC-80 [124] y las células de la glía MG20 [125]. Por otro lado, hay otras líneas de origen no neuronal como los fibroblastos murinos NIH-3T3 y L929 [126] y los mioblastos C2C12 [127] que también son capaces de propagar priones.

Un aspecto importante a tener en cuenta en estas líneas celulares inmortalizadas es que, a pesar de ser capaces de propagar priones, generalmente la infección no induce ningún efecto citotóxico en las mismas. Por tanto, estas líneas son modelos muy útiles para el estudio de la propagación de priones pero no para estudiar la toxicidad inducida por la PrP^{Sc} [113].

3.2. Modelos celulares de especies naturalmente susceptibles

Aunque existen distintos modelos celulares murinos capaces de propagar priones, puede que estos modelos no reflejen exactamente las características patológicas de las enfermedades priónicas debido a que la especie murina no es un hospedador natural de la enfermedad y es necesaria una previa adaptación de las cepas de prion para que estos modelos celulares sean permisivos a la infección. Por este motivo, existe una necesidad creciente de desarrollar modelos celulares de especies naturalmente susceptibles para poder estudiar de manera más precisa los mecanismos patogénicos de estas enfermedades y testar potenciales terapias en modelos naturales de enfermedad.

Comparado con las diversas líneas murinas disponibles, el número de modelos celulares en especies naturalmente susceptibles es mucho más limitado. Sin embargo, se han conseguido desarrollar algunos modelos celulares capaces de propagar priones. Por ejemplo, el modelo hTERT de células de microglía ovinas es permisivo a la infección con scrapie clásico [128] y las células renales bovinas MDBK pueden replicar priones de BSE [129]. Los fibroblastos cerebrales de ciervo MDB también son capaces de replicar priones de CWD [130]. En humanos, también se ha conseguido desarrollar un modelo capaz de infectarse con priones de CJD a partir de astrocitos derivados de células madre pluripotentes inducidas (iPSCs) humanas [131].

3.3. Las células madre mesenquimales como modelo de enfermedad priónica

Las células madre mesenquimales (MSCs) son células multipotentes, con morfología similar a los fibroblastos, caracterizadas por su capacidad de autorrenovación y diferenciación hacia células de linaje mesodérmico (osteoblastos, adipocitos y condrocitos) [132]. Además, estas células también son capaces de diferenciarse *in vitro* hacia células neuronales [133,134].

Las MSCs de distintas especies, incluida la ovina, expresan la PrP^{C} [119,135,136], la cual parece tener un papel importante en el proceso de diferenciación neuronal de estas células [137–139]. Por otro lado, las MSCs derivadas de pacientes con sCJD expresan la PrP^{Sc} [136]. La expresión de PrP^{Sc} no se ha detectado en MSCs de ovejas infectadas con scrapie, pero sí que se ha observado una capacidad de proliferación menor en estas células comparado con las MSCs de ovejas sanas [119].

En la especie murina, estas células son capaces de migrar, por mediación de distintos factores quimiotácticos, hacia lesiones cerebrales producidas por priones [140–142], y la inyección *in vivo* de MSCs es capaz de prolongar la supervivencia de ratones infectados con la cepa priónica Chandler [140]. Además, las MSCs murinas pueden infectarse y propagar de manera persistente la cepa Fukuoka-1 y la variante de CJD [143–145].

La expresión de PrP^{C} y la capacidad de infección de estas células, las convierte en unas buenas candidatas para el desarrollo de modelos celulares en el campo de las enfermedades priónicas.

3.4. Sistemas de cultivo celular 3D en enfermedades priónicas

Los distintos modelos celulares mencionados hasta ahora son sistemas de cultivo en dos dimensiones (2D), es decir, células cultivadas en monocapa. A pesar de las múltiples ventajas que presentan estos sistemas, tienen la limitación de no ser capaces de reproducir el ambiente en el que se encuentran las células *in vivo* ni las interacciones celulares generadas en dicho ambiente [146,147].

Recientemente, con el objetivo de superar esta limitación, se han desarrollado plataformas de cultivo en tres dimensiones (3D). Estos sistemas parecen ser capaces de reproducir de manera bastante fidedigna el comportamiento de las células en condiciones *in vivo*, de manera que los estudios realizados en este tipo de modelos podrían aproximarse más a la realidad de las condiciones *in vivo* [148]. Existen distintos tipos de cultivo celular en 3D como, por ejemplo, los esferoides, los organoides, sistemas de hidrogel y biorreactores, entre otros [146,149].

Este tipo de modelos se ha utilizado para el estudio de distintas enfermedades incluidas enfermedades neurodegenerativas como el Alzheimer [150–153] y el Parkinson [154–157]. En el campo de las enfermedades priónicas, solo se han descrito dos estudios sobre organoides cerebrales derivados de iPSCs humanas capaces de infectarse y propagar priones de sCJD [158,159].

4. Objetivos de la tesis

Este trabajo de tesis desarrollado en el campo de estudio de las enfermedades priónicas, concretamente en la forma clásica del scrapie ovino, presenta dos objetivos generales. El primero de ellos, estudiar en la enfermedad de scrapie posibles cambios de metilación del DNA, así como la implicación de este mecanismo epigenético en los mecanismos patogénicos de la enfermedad. Por otro lado, el segundo objetivo está centrado en desarrollar un modelo celular *in vitro* de enfermedad priónica basado en el cultivo de células madre mesenquimales ovinas.

Para la consecución de estos objetivos generales, se han planteado los siguientes objetivos específicos:

1. Estudiar los cambios de metilación del DNA mediante secuenciación genómica de DNA transformado con bisulfito en muestras de tálamo de ovejas naturalmente infectadas con scrapie en fase clínica y evaluar el efecto de estos cambios de metilación en la expresión de determinados genes.
2. Estudiar la distribución inmunohistoquímica de los cambios de metilación e hidroximetilación en distintas regiones del SNC de ovejas infectadas de manera natural con scrapie y de un modelo murino transgénico de scrapie en fase clínica y preclínica.
3. Analizar la expresión de genes codificantes de enzimas reguladoras del proceso de metilación en muestras de tálamo de ovejas naturalmente infectadas con scrapie y de un modelo murino transgénico de scrapie en fase clínica y preclínica.
4. Infectar con scrapie células madre mesenquimales ovinas cultivadas en monocapa en condiciones de crecimiento y diferenciación neurogénica y analizar posteriormente su viabilidad celular y permisividad a la infección.
5. Infectar con scrapie células madre mesenquimales ovinas cultivadas como esferoides en tres dimensiones en condiciones de crecimiento y diferenciación neurogénica y analizar posteriormente su viabilidad celular y permisividad a la infección.

6. Realizar un estudio transcriptómico de células madre mesenquimales ovinas infectadas con scrapie e identificar las rutas moleculares y genes asociados con la capacidad de infección y la toxicidad priónica.

5. Justificación de los trabajos realizados

En este apartado, se enumera y presenta el compendio de publicaciones recogidas en esta tesis doctoral y se justifica la unidad temática de cada una de ellas. Los trabajos presentados desarrollan los objetivos generales y específicos de esta tesis:

- En el manuscrito 1 titulado "*Epigenetic Changes in Prion and Prion-like Neurodegenerative Diseases: Recent Advances, Potential as Biomarkers, and Future Perspectives*" se ha llevado a cabo una exhaustiva revisión bibliográfica sobre los distintos mecanismos epigenéticos implicados en las enfermedades neurodegenerativas priónicas y *prion-like*. Este artículo de revisión ha servido para perfilar y sentar las bases del primer objetivo general de esta tesis.
- En el manuscrito 2 titulado "*Genome-Wide Methylation Profiling in the Thalamus of Scrapie Sheep*" se ha completado el primer objetivo realizando un estudio genómico de los cambios de metilación del DNA en muestras de tálamo de ovejas naturalmente infectadas con scrapie en fase clínica, así como una evaluación del efecto de estos cambios de metilación en la expresión diferencial de determinados genes.
- En el manuscrito 3 titulado "*5-methylcytosine and 5-hydroxymethylcytosine in scrapie-infected sheep and mouse brain tissues*" se ha llevado a cabo un estudio inmuhistoquímico, en distintas regiones del SNC, de los niveles de 5mC y 5hmC, así como un análisis de expresión en la región del tálamo de genes codificantes de enzimas reguladoras epigenéticas en ovejas infectadas de manera natural con scrapie y en un modelo murino transgénico de scrapie en fase clínica y preclínica. Estos resultados se corresponden con los objetivos segundo y tercero de esta tesis.
- En el manuscrito 4 titulado "*Effect of Scrapie Prion Infection in Ovine Bone Marrow-Derived Mesenchymal Stem Cells and Ovine Mesenchymal Stem Cell-Derived Neurons*" se ha evaluado la capacidad de replicación del prion de las células madre mesenquimales ovinas infectadas con scrapie en condiciones de crecimiento y de diferenciación neurogénica en monocapa, así como el efecto de dicha infección en la viabilidad celular. Este estudio abarca el cuarto objetivo de la tesis.
- En el manuscrito 5 titulado "*Susceptibility of ovine bone marrow-derived mesenchymal stem cell spheroids to scrapie prion infection*" se ha evaluado el efecto

que tiene el cultivo en tres dimensiones en forma de esferoides sobre la permisividad a la infección y la viabilidad celular de las células madre mesenquimales ovinas infectadas con scrapie, tanto en condiciones de crecimiento como en condiciones de diferenciación neurogénica, completando así el quinto objetivo de esta tesis.

- En el manuscrito 6 titulado "*RNA-sequencing transcriptomic analysis of scrapie-infected ovine mesenchymal stem cells*" se ha llevado a cabo el último de los objetivos realizando un estudio transcriptómico en células madre mesenquimales ovinas infectadas con scrapie para la identificación de posibles procesos biológicos, rutas moleculares y genes que estén implicados en el proceso de infección y en la toxicidad priónica.

Compendio de trabajos

MANUSCRITO I

Epigenetic Changes in Prion and Prion-like Neurodegenerative Diseases: Recent Advances, Potential as Biomarkers, and Future Perspectives.

Hernaiz, Adelaida; Toivonen, Janne Markus; Bolea, Rosa; Martín-Burriel, Inmaculada.

International Journal of Molecular Sciences. Vol. 23, pág. 12609, 2022. doi:10.3390/IJMS232012609.

International Journal of
Molecular Sciences

MDPI

Review

Epigenetic Changes in Prion and Prion-like Neurodegenerative Diseases: Recent Advances, Potential as Biomarkers, and Future Perspectives

Adelaida Hernaiz [1], Janne Markus Toivonen [1,2], Rosa Bolea [3] and Inmaculada Martín-Burriel [1,2,3,*]

[1] Laboratorio de Genética Bioquímica (LAGENBIO), Facultad de Veterinaria, Universidad de Zaragoza, IA2, IIS Aragón, 50013 Zaragoza, Spain
[2] Centro de Investigación Biomédica en Red de Enfermedades Neurodegenerativas (CIBERNED), Instituto Carlos III, 28029 Madrid, Spain
[3] Centro de Encefalopatías y Enfermedades Transmisibles Emergentes (CEETE), Facultad de Veterinaria, Universidad de Zaragoza, IA2, IIS Aragón, 50013 Zaragoza, Spain
* Correspondence: minma@unizar.es; Tel.: +34-976761662

Citation: Hernaiz, A.; Toivonen, J.M.; Bolea, R.; Martín-Burriel, I. Epigenetic Changes in Prion and Prion-like Neurodegenerative Diseases: Recent Advances, Potential as Biomarkers, and Future Perspectives. *Int. J. Mol. Sci.* **2022**, *23*, 12609. https://doi.org/10.3390/ijms232012609

Academic Editors: Roberta Mancuso and Simone Agostini

Received: 6 September 2022 Accepted: 18 October 2022
Published: 20 October 2022

Abstract: Prion diseases are transmissible spongiform encephalopathies (TSEs) caused by a conformational conversion of the native cellular prion protein (PrP^{C}) to an abnormal, infectious isoform called PrP^{Sc}. Amyotrophic lateral sclerosis, Alzheimer's, Parkinson's, and Huntington's diseases are also known as prion-like diseases because they share common features with prion diseases, including protein misfolding and aggregation, as well as the spread of these misfolded proteins into different brain regions. Increasing evidence proposes the involvement of epigenetic mechanisms, namely DNA methylation, post-translational modifications of histones, and microRNA-mediated post-transcriptional gene regulation in the pathogenesis of prion-like diseases. Little is known about the role of epigenetic modifications in prion diseases, but recent findings also point to a potential regulatory role of epigenetic mechanisms in the pathology of these diseases. This review highlights recent findings on epigenetic modifications in TSEs and prion-like diseases and discusses the potential role of such mechanisms in disease pathology and their use as potential biomarkers.

Keywords: epigenetics; DNA methylation; histone modifications; microRNA; prion diseases; prionlike diseases

1. Introduction

Epigenetics is the study of heritable changes in gene activity or function that is not associated with any change in the DNA sequence itself [1]. Three major epigenetic mechanisms have been described: DNA methylation and histone modifications essentially alter the structure of the nearby chromatin of a particular gene or region, whereas non-coding RNAs, especially microRNAs (miRNAs), may regulate expression without the necessity for the physical vicinity for their target genes.

DNA methylation involves the covalent transfer of a methyl group to the C-5 position of the nucleobase cytosine to form 5-methylcytosine. In mammals, DNA methylation may occur at cytosines in any context of the genome [1] and can participate in the regulation of gene expression. Histones are structural proteins that form DNA nucleosomes and are frequently subjected to covalent post-translational modifications. They are involved in the expression and repression of target genes generally via chromatin modification [2]. The most studied histone modifications are acetylation, methylation, and phosphorylation, but also other modifications exist, including citrullination, ubiquitination, ADP-ribosylation, deamination, and proline isomerization [2,3].

MicroRNAs are small non-coding RNAs (21–23 nucleotides in length) that may regulate gene expression at transcriptional, posttranscriptional, or translational levels [4]. Although miRNAs may induce gene expression in some cases by their interaction with gene promoters [5], miRNA-based regulation is thought to rely largely on the repression of target mRNA translation or its sequence-dependent degradation. Several miRNAs display a cell- or tissue-specific expression profile, while others are widely expressed. They can be found in blood and other biofluids as free (mainly protein-associated) complexes or can be contained by extracellular vesicles. Moreover, circulating miRNAs can be detected and measured by highly sensitive and specific methods (e.g., quantitative PCR and nextgeneration sequencing). All these characteristics have facilitated studies of miRNAs as potential biomarker molecules [6].

The mentioned epigenetic mechanisms are involved in several aspects of brain development as well as in normal aging [7,8]. DNA methylation and histone acetylation are essential in memory acquirement, learning, and acquisition of long-term memories [8–10], and miRNAs are crucial for the formation and maturation of synapses and for dendritogenesis in early brain development [11–13]. Considering the central role of epigenetics in neural plasticity, it is not surprising that dysregulation of these processes has been associated with different neurodegenerative diseases, either by mediating interactions between genetic and environmental risk factors or by directly interacting with disease-specific pathological factors [7,8]. The neurodegenerative disorders where epigenetics seem to have a key role include Alzheimer's (AD), Parkinson's (PD), and Huntington's (HD) diseases, amyotrophic lateral sclerosis (ALS), prion diseases, stroke, and global ischemia [7,8]. The first four are also known as prion-like diseases because they are proteinopathies that share common pathogenic mechanisms with prion diseases, including the accumulation of misfolded proteins in the central nervous system (CNS) [14,15].

Prion diseases, also referred to as transmissible spongiform encephalopathies (TSEs), are a group of neurodegenerative disorders affecting humans and other animals [16] and are caused by a conformational conversion of the cellular prion protein (PrP^{C}) to an infectious isoform, partially resistant to proteases and prone to form aggregates called PrP^{Sc} [17].

Research in yeast has revealed that certain proteins that adopt prion conformation, such as URE3 or PSI^{+}, can be considered as an epigenetic mechanism that can be inherited through mitosis and meiosis. These self-templating conformations of prion proteins interact with nucleic acids (DNA and RNA) and can regulate gene expression through the modification of chromatin remodeling, nucleic acid translation, and replication, providing beneficial phenotypes in stressful conditions [18]. If prions in yeast possess these characteristics, it could be expected that alteration of the prion protein and other proteins with similar characteristics in mammals will also affect epigenetic mechanisms. Increasing evidence suggests involvement of epigenetic mechanisms in the pathogenesis of prion-like diseases and other neurodegenerative disorders. However, current knowledge about the association of epigenetics with prion diseases is scarce.

Given that some of the affected mechanisms may be shared with TSEs and prionlike diseases, this review summarizes the latest findings on epigenetic modifications in prion-like diseases and reports the recently discovered roles of epigenetic mechanisms in TSEs.

2. Epigenetic Changes in Prion-Like Diseases

2.1. DNA Methylation

2.1.1. DNA Methylation Profiles

Altered DNA methylation patterns have been associated with the neuropathology of prion-like diseases. Several studies have identified sets of genes containing differentially methylated regions (DMRs) and differentially methylated positions (DMPs) between patients and healthy controls, primarily in peripheral blood [19–26] and brain tissue [27–35] and to a lesser extent in saliva [23] and using in vitro models [36,37]. Table 1 summarizes global and gene-specific DNA methylation changes reported in these diseases.

When comparing the DMRs and DMPs identified in each prion-like disease (Supplementary Table S1) using the InteractiVenn software [38], no common DMRs and DMPs were found between all four diseases, but some regions and positions matched between two or three of these diseases

(Figure 1). Regarding the DMRs, the disease pairs that shared the highest number of common regions were first PD and HD, second PD and ALS, and third PD and AD (Figure 1a). On the other hand, PD and AD are the only diseases that share a relatively high number of DMPs (Figure 1b). Although these comparisons between the DMRs and DMPs identified in prion-like diseases allow an overview of common differentially methylated genes shared between some of these diseases, there are limitations that could affect the number of regions and positions identified in each disease and must be taken into account: (1) the compared studies were performed in different tissues and body fluids which could lead to different methylation profiles inherent to each tissue; (2) the number of studies developed in each disease is different, being AD and PD the most studied ones; and (3) the methodology used in the different works varies. Most studies were performed using the 450 K methylation array, and whole genome bisulfite sequencing was used only in one study of PD [37]. This methodology detects DMPs in non-annotated sequences such as lincRNAs, pseudogenes, and antisense or unknown miRNAs, which explains in part why the number of DMPs and DMRs in PD is substantially higher than in other diseases.

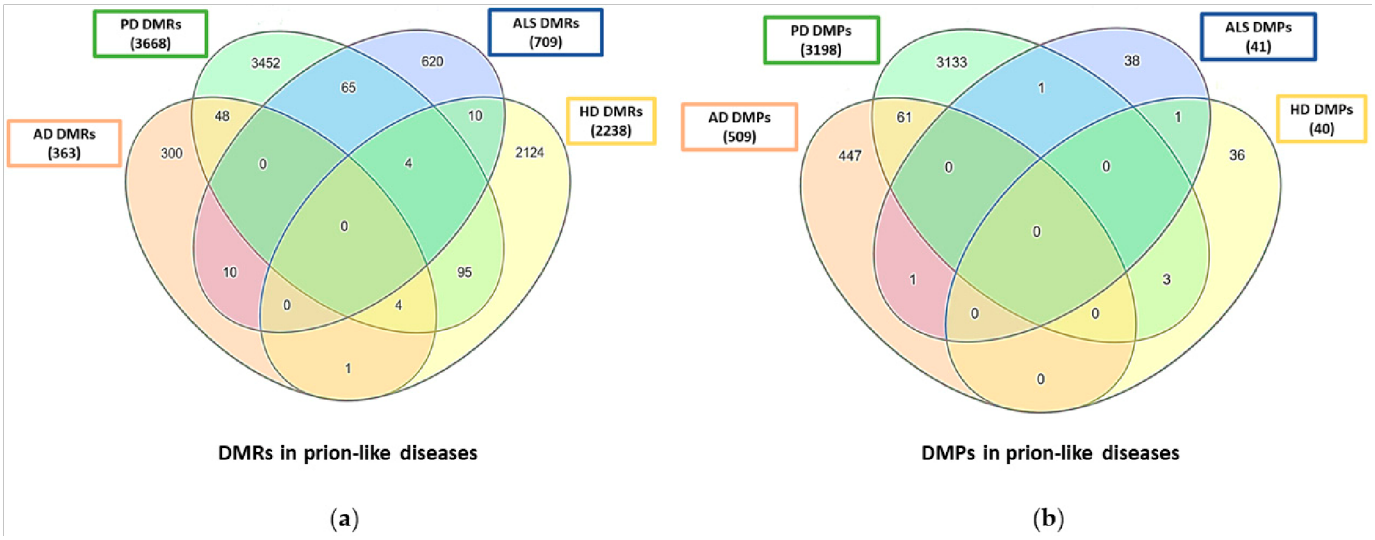

Figure 1. Comparison of differentially methylated regions (DMRs) and positions (DMPs) in prion-like diseases. Venn diagrams indicate the number of common and unique DMRs (**a**) and DMPs (**b**) in AD, PD, ALS, and HD.

Studies on the DNA methylation process have concentrated on different areas of the CNS depending on their relevance with the pathogenesis of each disease. Epigenome-wide studies on AD patients have identified DMRs in the superior temporal gyrus, a region that displays a marked gene dysregulation in AD [27,28]. Most of these DMRs were found to be in gene promoters and associated with AD pathology. Significant DNA methylation changes are also found in PD-affected brain areas, namely the dorsal motor nucleus of the vagus, substantia nigra, and cingulate gyrus [32]. In HD, DNA methylation studies performed so far have shown disparate results. A genome-wide DNA methylation profile of cortex tissues from HD patients suggests that DNA methylation may have a minimal association with HD status but could be correlated with the age of disease onset and contribute to the tissuespecific expression patterns of huntingtin (*HTT*) [39]. In contrast, using the same methodology but analyzing multiple CNS regions, another study identified 11 co-methylation modules associated with HD status in cortical regions and observed an accelerated epigenetic age in specific brain regions (frontal lobe, parietal lobe, and cingulate gyrus) of HD patients [35], measured by combining DNA methylation levels of known CpGs [40].

Genome-wide studies have detected DNA modifications in specific genes that have been analyzed in detail to elucidate their role in neurodegeneration. Epigenetic control of enhancers seems to be involved in AD as loss of CpH (most frequently at CpA sites) methylation of enhancers, which is normal in aging neurons but is accelerated and occurs early in AD neurons. This modification seems to prompt the reactivation of cell cycle and neurogenesis pathways and, in

the case of the enhancer of *DSCAML1* that codes for Down Syndrome cell adhesion molecule-like protein 1, precedes the onset of neurofibrillary tangle pathology [41]. Hypomethylation of *DSCAML1* gene enhancer is associated with an upregulation of *BACE1* (beta-secretase 1) transcripts and an increase in amyloid plaques, neurofibrillary tangles, and cognitive decline [41]. These results support an early involvement of epigenetic changes in AD.

In the same disease, a protective role has been suggested for *PM20D1* (peptidase M20 domain containing 1). DNA methylation and RNA expression of this gene are associated with AD, and its overexpression in cells is neuroprotective against AD stressors [42].

Methylation changes in other genes have been related to prion-like disease pathogenesis, although its role is still unknown. In PD, patients show hypomethylation of the promoter region of *SNCA*, the gene encoding α-synuclein protein [43]. Moreover, several ALS-related genes (*DENND11*, *COL15A1*, *TARDBP*, *RANGAP1*, and *IGHMBP2*) and DNA repair genes (*OGG1*, *APEX1*, *PNKP*, and *APTX*) are differentially methylated in ALS patients [44–46]. Differential DNA methylation has also been observed in specific genes in HD, namely *HES4*, a transcription factor involved in neural stem cell regeneration, and *BDNF*, encoding brain-derived neurotrophic factor [47,48]. *HES4* promoter hypermethylation is associated with reduced expression of the gene and with striatal degeneration and age of onset of HD patients. Consistently, inhibition of *HES4* by shRNA increases mutant HTT aggregates in a cell model of the disease. *BDNF* promoter hypermethylation in the blood of HD patients did not correlate with motor or cognitive status but may represent a biomarker for HD-associated psychiatric symptoms.

Most of the reported studies reveal that changes in DNA methylation can be associated with pathogenic processes of these neurodegenerative diseases, but there does not appear to be a universal mechanism relating DNA methylation and protein aggregates. Studies performed in human patients are normally carried out at the late stages of the disease when it is difficult to differentiate if changes in DNA methylation are a cause or a consequence of neurodegeneration. Analysis of this epigenetic process in animal or cellular models could possibly allow us to elucidate this question.

A limitation of most of these studies is the technology used for the determination of DNA methylation. Methylation arrays or NGS-sequencing-based methods did not differentiate between methyl Cytosines (mC) and their oxidized product hydroxymethyl Cytosines (hmC), which has regulatory functions and could be an epigenetic mark in its own right [49]. Antibody-based techniques have already been used in these diseases to specifically detect 5mC and 5hmC methylation forms [50,51]. However, these techniques cannot identify specific genes of interest. Third-generation sequencers [52] could help elucidate which epigenetic mark is involved in a gene-specific regulation.

2.1.2. Biomarkers Based on DNA Methylation

DNA methylation as a potential biomarker has been investigated in easily accessible tissues at both genomic and gene-specific levels. Both sporadic (SALS) and familial ALS (FALS) patients show increased global 5-methylcytosine levels in blood DNA [53]. At the gene level, hypermethylation of the promoter for *C9orf72*, a gene responsible for the majority of the FALS cases (as well as for those of frontotemporal dementia), correlates with its reduced mRNA expression levels in a clinical cohort of *C9orf72* pathological expansion carriers [54]. A significant association between DNA methylation age-acceleration, disease duration, and age of onset has also been observed in *C9orf72* carriers [55]. The second most common cause of FALS is mutations in superoxide dismutase 1 (*SOD1*), with nearly 200 mutations described, some of which show incomplete penetrance and great phenotypic variability. ALS patients carrying not fully penetrant *SOD1* mutations display an increase in global DNA methylation, and DNA methylation levels correlate positively with disease duration [56]. However, since the promoters of four major ALS genes (*C9orf72*, *SOD1*, *TARDBP*, and *FUS)* were not methylated in the study subjects, it was concluded that the increased methylation is likely to occur in other gene regions. In this study, no

repeat expansion was observed in *C9orf72*, which supports the previous finding [51] that genespecific methylation in the *C9orf72* locus is dependent on this pathological feature.

In contrast, DNA hypomethylation seems to be a key mark in PD patients, finding several hypomethylated and upregulated genes in blood and saliva samples associated with systemic immune response pathways and mitochondrial dysfunction [21,23]. In addition, in leukocytes from PD patients, hypomethylation of *NPAS2* (neuronal PAS domain protein 2) [57] and *DRD2* (dopamine receptor D2) [57] has been proposed as a novel biomarker for PD.

In blood from AD patients, *B3GALT4* (beta-1,3-galactosyltransferase 4), a gene associated with AD onset and progression, and *PTGR3* (prostaglandin reductase 3), associated with AD risk, are hypomethylated and correlate with memory performance and cerebrospinal fluid (CSF) levels of Aβ and tau [58]. Moreover, hypomethylation of *BIN1* (bridging integrator 1), a gene associated with AD pathogenesis, and hypermethylation of estrogen receptor α (*ESR1*) gene promoter, which is related to impaired cognitive function and quality of life of AD patients, have been also reported [59,60]. Another potential biomarker of this disease could be the hypomethylation in *TOMM40* (translocase of outer mitochondrial membrane 40) and *APOE* (apolipoprotein E) gene promoters observed in the hippocampus, cerebellum, and peripheral blood of AD patients, which correlated with increasing *APOE* and decreasing *TOMM40* expression [61]. Besides these promising results, very few have been subjected to clinical trials. Only methylation levels on *COASY* (Coenzyme A synthase) and *SPINT1* (Serine peptidase inhibitor Kunitz type 1) promoter regions have been considered convenient and useful biomarkers for AD [62].

In HD, DNA methylation status in peripheral blood does not seem to be affected as, after a microarray study of blood samples, no distinctive patterns were observed in the covered CpG sites and their associated genes [25].

2.1.3. In Vitro Studies

Cellular models are particularly useful for analyzing the effect of DNA methylation and investigating the role of methylation in candidate genes and potential treatments. DNA methylation changes in prion-like diseases have been investigated in vitro using cell models. A whole-genome bisulfite sequencing study using induced pluripotent stem cell (iPSC) -derived dopaminergic neurons from sporadic PD and monogenic *LRRK2* (Leucine-rich repeat kinase 2)-associated PD patients revealed global DNA hypermethylation associated with disease [37], conversely to the hypomethylation observed in blood and saliva. In ALS, a study that evaluated the methylation status of human embryonic stem cells (hESCs) and iPSCs both carrying the *C9orf72* mutation showed that hESCs were completely unmethylated at the *C9orf72* repeats, whereas iPSCs were hypermethylated. This methylation status remained unchanged after the differentiation of hESCs and iPSCs into neural precursors. The hypermethylation observed in the *C9orf72* repeats of iPSCs was proposed as a possible neuroprotective mechanism attenuating the accumulation of potentially toxic repeat-containing mRNAs in neurons, given that hESCs presented a more severe phenotype than iPSCs [63].

Hypomethylation of the *SNCA* gene has been described in early onset PD patients [43], and lowered methylation status is likely to increase *SNCA* expression, contributing to the accumulation of α-synuclein in this disease. With the purpose of maintaining normal physiological levels of α-synuclein, Kantor et al. [64] experimentally methylated the *SNCA* gene using a system based on CRISPR-deactivated Cas9 fused with the catalytic domain of *DNMT3A* (DNA methyltransferase 3 alpha). This technique was applied to iPSC-derived dopaminergic neurons from a PD patient resulting in hypermethylation of the *SNCA* gene, downregulation of the SNCA expression, and a reversion of disease-related phenotypic perturbations [65]. The same hypermethylation-based approach has been recently used to manipulate the levels of amyloid-beta (Aβ) precursor (APP) in cultured neurons from AD mice, resulting in decreased Aβ peptide levels, decreased Aβ42/40 ratio, and increased cell survival [66]. Importantly, further studies in vivo indicated that lentiviral injection of dCas9-Dnmt3a in mouse brain induces efficient DNA methylation editing, decreases the levels of APP, and improves the cognitive defects associated with this AD model.

2.1.4. Mitochondrial DNA Methylation

Finally, in addition to nuclear DNA, mitochondrial DNA (mtDNA) methylation has also been observed in humans and animal models. In ALS, *SOD1* mutation carriers display increased levels of mtDNA and demethylation of the mitochondrial D-loop, a noncoding region critical for both mtDNA replication and transcription. This could represent an attempt to compensate for the disease-associated loss of mitochondrial function by mtDNA upregulation in carriers of ALS-linked *SOD1* mutations [67]. While D-loop is also hypomethylated in the hippocampus of a mouse model of AD (APP/PS1), this is associated with decreased mtDNA copy number [68]. Thus, while altered methylation of mtDNA suggests a possible role for this epigenetic mechanism in ALS and AD, the fact that the outcome in the level of mtDNA is opposite in the two cases warrants further studies on the topic.

Table 1. Global and gene-specific DNA methylation in prion-like diseases.

Disease	Species/Model	Tissue Type	Methylation Finding	References
Alzheimer's disease	Human	Brain, peripheral blood	Methylation profiles of AD patients. Identification of differentially methylated positions (DMPs)	[19,20,30,31]
	Human	Brain	Methylation profile of AD patients. Identification of differentially methylated regions (DMRs)	[27]
	Human	Superior temporal gyrus	Hypermethylated DMRs	[28,29]
	APP/PS1 mice	Hippocampus	Changes in mitochondrial DNA methylation	[68]
	Human	Neurons	Hypomethylated enhancers in *DSCAML1* gene	[41]
	Human	Hippocampus, cerebellum, peripheral blood	Hypomethylation in *TOMM40* and *APOE* gene promoters	[61]
	Human	Frontal cortex	Methylation of *PM20D1* gene	[42]
	Human	Peripheral blood	Hypomethylation of *B3GALT4* and *ZADH2* genes	[57]
	Human	Peripheral blood	Hypomethylation of *BIN1* gene	[58]
	Human	Peripheral blood	Hypermethylation of *ERα* gene promoter	[59]
Parkinson's disease	Human	Peripheral blood	Identification of DMRs between PD patients and healthy controls	[22]
	Human	Brain	Identification of DMRs in PD-affected brain areas	[32]
	Human	iPSC-derived dopaminergic neurons	Global DNA hypermethylation changes	[36,37]
	Human	Peripheral blood, saliva	Global DNA hypomethylation changes	[21,23]
	Human	Peripheral blood, iPSC-derived dopaminergic neurons	Hypomethylation of *SNCA* gene promoter. Reversion of disease symptoms via CRISPR/Cas9-mediated *SNCA* hypermethylation	[43,65]
	Human	Leukocytes	Hypomethylation of *NPAS2* and *DRD2* genes	[60,63]
Amyotrophic lateral sclerosis	Human	Peripheral blood	Methylation profile of ALS patients. Identification of DMPs	[24]
	Human	Brain	Methylation profile of ALS patients. Identification of DMRs	[33]
	Human	Peripheral blood	Increased global 5-methylcytosines levels in sALS and FALS	[53]
	Human	Peripheral blood	Hypermethylation of the *C9orf72* promoter and association of DNA methylation age-acceleration with disease duration and age of onset in *C9orf72* expansion carriers	[54,55]

	Human	Peripheral blood	Increase in global DNA methylation and demethylation of the mitochondrial D-loop region in *SOD1* mutation carriers	[56,67]
	Human	hESCs, iPSCs	hESCs unmethylated and iPSCs hypermethylated at the *C9orf72* repeats	[64]
	Human	Brain, motor neurons	Differential methylation of *KIAA1147*, *IGHMBP2*, *COL15A1*, *TARDBP*, *RANGAP1*, *IGHMBP2*, *OGG1*, *APEX1*, *PNKP*, and *APTX*	[44–46]

Table 1. *Cont.*

Disease	Species/Model	Tissue Type	Methylation Finding	References
Huntington's disease	YAC128 mice	Brain	Methylation profile. Identification of DMRs	[34]
	Human	Peripheral blood	Methylation profile of HD patients. Identification of DMPs	[26]
	Human	Brain	Minimal association of DNA methylation with HD status	[39]
	Human	Peripheral blood	No significant changes between patients and controls	[25]
	Human	Brain	11 co-methylation modules associated with HD status	[35]
	Human	Brain	*HES4* promoter hypermethylation	[47]
	Human	Plasma, saliva	*BDNF* promoter hypermethylation	[48]

2.2. Histone Modifications

The most studied histone modification in prion-like diseases is acetylation. Global levels of acetylated histones and differential expression of the enzymes in charge of their acetylation or deacetylation have been related to the pathology of these diseases. Moreover, pharmacological modulation of these enzymes could ultimately result in a potential treatment strategy. Table 2 summarizes the main results in this subject.

Widespread acetylome variation has been observed in different brain areas of AD patients, and this epigenetic modification can be induced by pathological tau [69,70]. Acetylation of a lysine residue in histone 3 (H3K27) varies in the vicinity of several known AD risk genes (*APP*, *CR1*, *MAPT*, *PSEN1*, *PSEN2*, and *TOMM40*) and is robustly associated with the disease [69]. Similarly, altered histone acetylation has been linked to PD-associated neurodegeneration. PD neurotoxins specifically increase histone acetylation through an autophagy-mediated reduction of histone deacetylases (HDACs) in PD patients' dopaminergic neurons [71].

The modulation of epigenetic enzymes involved in acetylation, mainly HDACs, also has a role in the development and progression of prion-like diseases. HDACs can be divided into four subtypes, classes I, II, and IV being classical HDACs and class III consisting of NAD^+-dependent silent information regulator 2 family members (sirtuins). HDAC activities are unbalanced in fibroblasts from PD patients, which is associated with impaired mitophagy and increased cell death [72].

In addition, changes in expression levels of particular HDACs have been described, but their modifications are not always in accordance with studies. Modifications can be different depending on the disease and CNS cell populations. HDAC1 and HDAC2 levels are strongly decreased in the frontal cortex of AD patients, and HDAC1 is also reduced in the hippocampus [73]. HDAC2 downregulation seems to contribute to cholinergic nucleus basalis of Meynert neuronal dysfunction, neurofibrillary tangles pathology, and cognitive decline during the clinical progression of AD [74]. On the contrary, HDAC2 is upregulated in the microglia from the substantia nigra of PD patients [75]. Additionally, nuclear accumulation of HDAC4, which is normally localized at the cytoplasm, seems to promote neuronal apoptosis in PD-affected dopaminergic neurons [76].

The levels of class II HDACs (4, 5, and 6) are increased in the skeletal muscle of *SOD1*-ALS mice with severe neuromuscular impairment [77]. Although this increase was not observed in motor neurons, Class II HDACs could also contribute to motor neuron degeneration as their pharmacological inhibition is able to restore the expression and function of glutamate transporter EAAT2 in the spinal cord of ALS [78]. However, HDAC4 expression is decreased in the skeletal muscle of ALS patients [79], and the skeletal musclespecific ablation of HDAC4 is sufficient to induce an earlier onset of the disease, a decrease in neuromuscular junctions' size, and muscle denervation and atrophy in *SOD1*-ALS mice [80]. Finally, an in vivo brain assessment of HDAC alterations by positron emission tomography showed no significant differences in HDAC expression levels between ALS patients and healthy controls [81], suggesting that HDAC alterations may have a more profound effect on the disease in peripheral tissues. Given that the skeletal muscle function is compromised in ALS, the implication that HDAC4 could be protective in ALS skeletal muscle has questioned the use of broad-range HDAC inhibitors as a strategy for ALS treatment [82]. However, research on the role of HDACs in different tissues warrants further investigation because the discovery of highly selective inhibitors for HDACs could eliminate the potential negative effects of more broad-range targeting in the future.

In AD patient-derived neurons and triple transgenic (3xTg-AD, carrying mutated forms of *APP*, *PSEN1*, and *MAPT*/tau) mouse model, inhibition of HDAC3 (Class I) decreases pathological tau phosphorylation and acetylation, reduces Aβ protein expression, increases Aβ degradation, improves learning and memory and normalizes several AD-related genes [83]. Importantly, HDAC6 seems to influence tau phosphorylation, autophagic flux, and tubulin acetylation [84], and its inhibition stimulates pathological tau degradation in ADLP APT mice (carrying six mutations in *APP*, *PSEN1*, and *MAPT*/tau) and AD patient-derived brain organoids [85]. The inhibition of HDAC6 has

also been proposed as a therapeutic strategy for PD, as this enzyme contributes to oxidative injury and dopaminergic neurotoxicity through mediating deacetylation of peroxiredoxins 1 and 2 in oxidopamine-induced PD mice [86]. In the PD mouse model expressing mutated *LRRK2* (R1441G), HDAC inhibition by valproic acid has a neuroprotective effect through modulation of neuroinflammation and improvement of PD-like symptoms [87]. Inhibition of histone sirtuin-2 deacetylase (SIRT2) also has therapeutic effects protecting degenerating dopaminergic neurons, reducing microglia activation, and facilitating the trafficking and clearance of misfolded proteins [88,89].

This therapeutic approach of HDAC inhibition has also been investigated in ALS models. HDAC inhibition in spinal cord-dorsal root ganglion cultures enables the heat shock response, which manages a load of aberrant proteins in a stress-dependent manner in cultured spinal motor neurons and also rescues the DNA repair response in iPSC-derived motor neurons carrying the *FUS* mutation [90]. Similarly, global histone hypoacetylation was observed in a *FUS* murine model. The restoration of histone acetylation levels in these mice by HDAC inhibition ameliorated the disease phenotype and significantly extended their lifespan [91]. In addition, HDAC6 inhibition restored axonal transport defects and mitochondrial and endoplasmic reticulum vesicle transport defects in ALS patient-derived motor neurons by increasing the α-tubulin acetylation level [92,93].

In HD rats and mouse models, HDAC inhibition produces a variety of neuroprotective beneficial effects, including partial reversal of behavioral symptoms, reversion of aberrant neuronal differentiation [94], prevention of striatal neuronal atrophy, improvement of motor performance [95], amelioration of disease phenotypes in a transgenerational manner [96] and reestablishment of pyruvate dehydrogenase activity improving mitochondrial function and bioenergetics [97]. Moreover, a multiomic study has proposed that the positive effect of HDAC4 knockdown in rescuing synaptic function in HD mice could be a consequence of synaptic vesicle trafficking regulation, and HDAC4 could interact with htt via association with htt-interacting proteins [98]. Other HDACs have also been proposed as therapeutic targets in HD. Striatal HDAC2 levels are reduced in the YAC128 HD mouse model subjected to dietary restriction, which could contribute to improving the disease phenotype [99]. In addition, inhibition of HDAC3 improves motor deficits, suppresses striatal CAG repeat expansions, and reduces the accumulation of oligomeric forms of mutant htt in HD transgenic mice [100,101]. In contrast, genetic deletion of HDAC6 exacerbates social impairments and hypolocomotion in HD R6/1 mice [102].

Although there are fewer works analyzing this epigenetic mechanism compared to DNA methylation or microRNAs, the results obtained seem to be promising, not as a source of biomarkers but as a possible target for therapies.

Other histone modifications have been studied, but the number of these studies is even lower. A genome-wide study in human brains has identified differential enrichment of trimethylated lysine 4 of histone 3 (H3K4me3) mark between HD and control samples [103]. Interestingly, in a Drosophila melanogaster HD model, the activity reduction of the H3K27specific demethylase, Utx, ameliorated neurodegeneration and diminished htt aggregation [104]. Conversely, in this same model, histone methyltransferase dSETDB1/ESET was identified as a mediator of mutant htt-induced degeneration [105].

Table 2. Histone post-translational modifications in prion-like diseases.

Disease	Species/Model	Tissue Type	Main Finding	References
Alzheimer's disease	Human	Brain	Widespread acetylomic variation associated with AD, possibly induced by pathological tau	[69,70]
	Human	Frontal cortex, hippocampus	Decreased levels of HDAC1	[73]
	Human	Frontal cortex	Decreased levels of HDAC2 contributing to neuronal dysfunction, neurofibrillary tangles pathology, and cognitive decline	[73,74]

	3xTg-AD mice, Human	Human iPSC-derived neurons	HDAC3 inhibition decreases pathological tau phosphorylation and acetylation	[75]
	ADLP^{APT} mice, Human	Human-derived brain organoids	HDAC6 inhibition stimulates pathological tau degradation	[77]
Parkinson's disease	Human	Dopaminergic neurons	PD neurotoxins increase histone acetylation through an autophagy-mediated HDACs reduction mechanism	[71]
	Human	Fibroblasts	Imbalance between total HATs and HDACs activities	[72]
	LRRK2 R1441G mice	Brain	HDAC inhibition has a neuroprotective effect through modulation of neuroinflammation and improvement of PD-like behaviors	[79]
	Sirt2 −/− C57-BL6 mice, Human	Brain	Sirtuin-2 deacetylase inhibition protects degenerating dopaminergic neurons, reduces microglial activation, and facilitates the trafficking and clearance of misfolded proteins	[80,81]
	Human	Microglia from the substantia nigra	Upregulation of HDAC2	[83]
	E13-14 mice	Dopaminergic neurons	HDAC4 accumulation promotes neuronal apoptosis	[84]
	C57-BL6 mice	Brain	HDAC6 could contribute to oxidative injury	[86]
Amyotrophic lateral sclerosis	*SOD1*-ALS mice	Skeletal muscle	Increase in class II HDACs (4, 5, and 6) involved in modulating the expression and function of glutamate transporter	[85,86]
	Human	iPSC-derived motor neurons	HDAC inhibition rescues the DNA repair response	[90]
	Tg *FUS* +/+ mice	Spinal cord	Global histone hypoacetylation. Restoration of histone acetylation ameliorates the disease phenotype	[91]
	Human	iPSC-derived motor neurons	HDAC6 inhibition restores axonal transport defects and mitochondrial and endoplasmic reticulum vesicle transport defects	[92,93]
	Human	Brain	No significant differences in HDAC expression levels between patients and controls	[97]
	SOD1-ALS mice, Human	Skeletal muscle	Decreased expression of HDAC4 associated with an earlier onset of the disease	[87,88]
Huntington's disease	tgHD rats, BACHD, R6/2, YAC128 mice	Brain	HDAC inhibition produces neuroprotective beneficial effects	[94–97]
	HttQ20, HttQ140 mice	Brain	HDAC4 regulates synaptic vesicle trafficking and interacts with htt	[98]
	YAC128 mice	Brain	Reduction of HDAC2 could contribute to improving the disease phenotype	[99]
	N171-82Q, HdhQ^{111} knock-in mice	Brain	HDAC3 inhibition improves motor deficits, suppresses striatal CAG repeat expansions, and reduces accumulation of mutant huntingtin oligomeric forms	[100,101]
	R6/1 mice	In vivo assessment	HDAC6 deletion exacerbates social impairments and hypolocomotion	[102]
	Human	Brain	Differentially enrichment of H3K4me3 mark	[103]
	Drosophila melanogaster	Brain, eye	Activity reduction of Utx ameliorates neurodegeneration and diminishes htt aggregation. dSETDB1/ESET might be a mediator of mutant htt-induced degeneration	[104,105]

2.3. MicroRNAs

A large number of human proteins containing prion-like domains are RNA or DNA-binding proteins [106]. The first protein with these motifs associated with neurodegeneration was TDP-43 (trans-activation response element DNA-binding protein 43) [107,108], which is the major pathological protein in sporadic ALS. This protein plays a role in many RNA-related functions, including microRNA biogenesis. Afterward, many other proteins related to neurodegenerative diseases have been discovered that play a role in RNA metabolism, and amyloids coaggregate with endogenous nucleic acids [109,110]. Although different RNA species may be altered in prion-like

diseases, we focus on the role of microRNA in these pathologies. These biomolecules have been widely studied in neurodegenerative diseases. Changes in miRNA expression profiles may serve as biomarkers, and these molecules seem to play important roles in the neuropathology of these diseases.

2.3.1. MicroRNA Profiles

Several studies have measured miRNA expression profiles in tissues and body fluids from patients and in different in vitro and animal models of prion-like diseases. Sets of microRNAs altered in each prion-like disease seem to be largely different, as summarized in Table 3.

In AD patients, miRNA profiles have been analyzed in brain [111–114], blood [115,116], serum [117,118], CSF [119] and extracellular vesicles (EVs) [120–122]. Brain and EVs miRNA profiles have as well been characterized in AD mouse models [123–125]. Comparing the different profiles, only one miRNA, miR-324-3p, is commonly downregulated in the brain, body fluids, and EVs of AD patients, but its expression is not altered in AD mouse models. MiRNA profiles have been also characterized in brain [126–129], gut [130], blood [128], plasma [131,132], serum [133], CSF [134,135], saliva [136], and EVs [131,137] of PD patients; in brain of a PD mouse model [135]; in blood of a PD rat model [138]; and in a PD in vitro model [139]. Although no common miRNAs are found when comparing all the abovementioned PD profiles, there are common miRNAs between some tissues and body fluids. MicroRNA miR-451a is upregulated in the brain, gut, and CSF of PD patients and also in the brains of PD mice, and miR-19b-3p is downregulated in the brain, blood, plasma, and saliva of PD patients.

In ALS patients, microRNAs have been studied in brain [140,141], skeletal muscle [142,143], blood [143–146], plasma [147], serum [148–150], CSF [151] and EVs [152–155]. Distinctive ALS miRNA profiles are also present in mouse skeletal muscle [156] and serum [157] and in in vitro models [154,158]. Three miRNAs, miR-125a-3p, miR-193a-5p, and miR-455-3p, are commonly downregulated in the brain, skeletal muscle, blood, and serum from ALS patients, and the expression of miR-125a-5p, which is downregulated in the brain and skeletal muscle of ALS patients, is also reduced in ALS mouse models and in vitro models. A smaller number of studies have explored the miRNA profiles in HD. These profiles are found in the brain [159–161], plasma [162], and CSF [163] of HD patients and in the brain of HD mouse models [164–167]. No common miRNAs are found between the profiles performed in HD patients, but there are two miRNAs, miR-10b-5p and miR-10a-5p, that are upregulated in the brain of both HD patients and mouse models.

When comparing the human miRNA profiles of the four prion-like diseases, there are two miRNAs, miR-144-3p and miR-22-5p, that appear upregulated in all four pathologies (Figure 2a). The β-amyloid precursor protein (APP) has been identified as a target gene of miR-144-3p, which seems to have a role in mitochondrial function maintenance [168], and a potential neuroprotective role has been predicted for miR-22 related to the regulation of targets implicated in HD such as HDAC4 [169]. Further analyses are necessary to verify if these two microRNAs display important roles in misfolded protein-related diseases.

Conversely, although there are miRNAs similarly downregulated between two or three prion-like diseases, no common downregulated miRNAs are found between the four diseases (Figure 2b). The existence of differently regulated microRNA in different diseases can be used as a source of biomarkers for differential diagnosis. Supplementary Table S2 lists common upregulated and downregulated miRNAs for combinations of different prion-like diseases and the datasets used to generate the Venn diagrams.

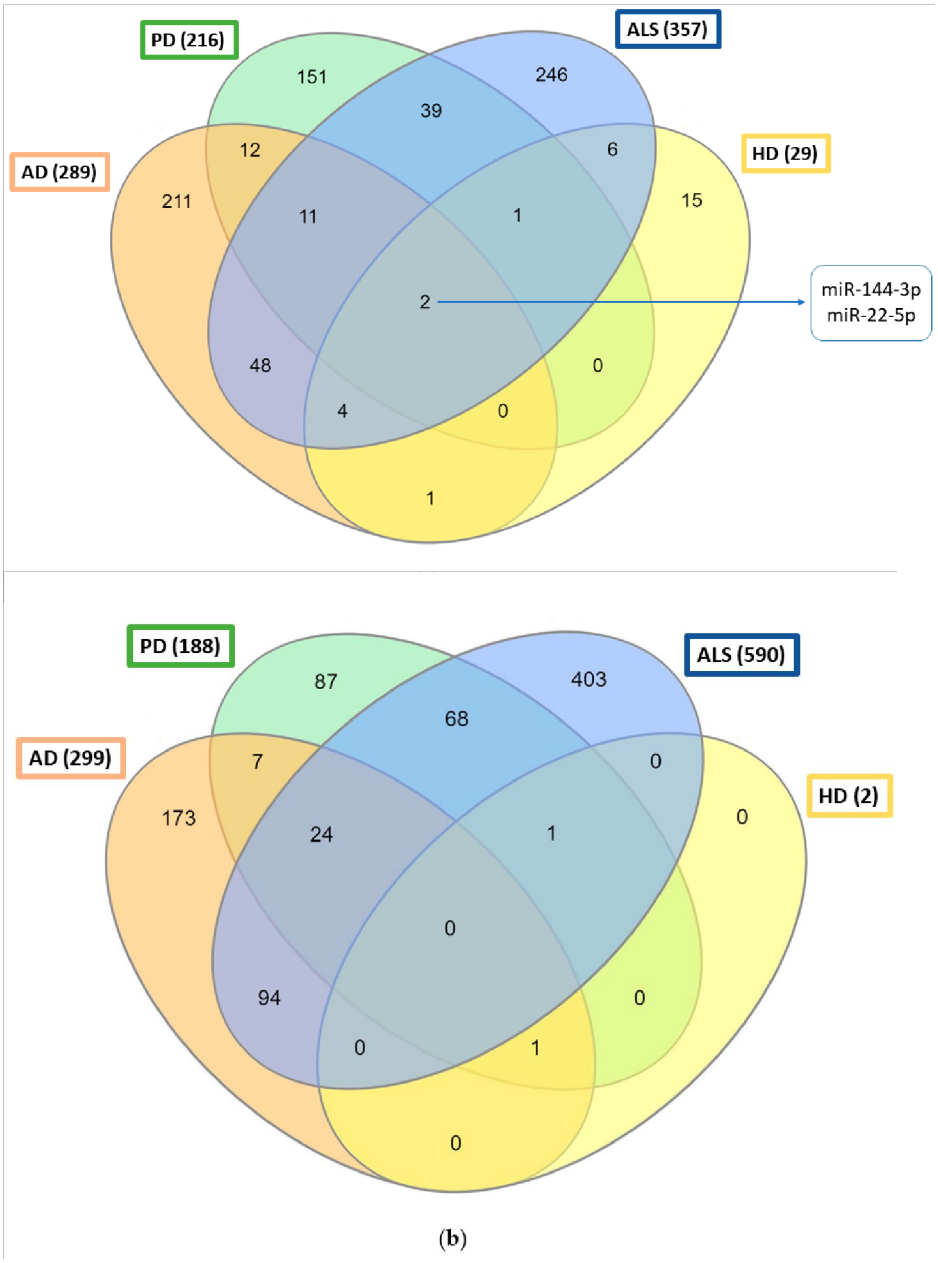

Figure 2. Venn diagrams of miRNA profiles in prion-like diseases: (**a**) upregulated miRNAs in prion-like disease patients; (**b**) downregulated miRNAs in patients suffering from prion-like diseases.

2.3.2. The Role of microRNAs in Prion-Like Diseases

In addition to miRNA profiles that could reveal potential disease biomarkers, some studies have shed light on the functions or possible roles of different miRNAs in prion-like diseases.

In AD pathology, several miRNAs seem to have neuroprotective roles attenuating Aβ accumulation and its associated neurotoxicity. In particular, the following miRNAs have been associated with this neuroprotective function: miR-193a-3p [170] and miR -133b [171] in human serum, miR-335-5p [172] and miR-361-3p [173] in the human brain, miR-200a-3p [174] in plasma from AD patients, miR-107 [175] in human neuroblast cell lines, and miR-340 [176] in the hippocampus from senescence-accelerated (SAMP8) mice that show increased oxidative damage associated with APP overproduction. Moreover, in rat hippocampus, miR-134-5p [177] is involved in rescuing AD synaptic plasticity deficit, and miR-124 [178] and miR-200a-3p [174] are involved in alleviating tau pathology in murine and in vitro models, respectively. On the other hand, miR-34c [179] and miR-124 [180] mediate synaptic and memory deficits in AD. Other miRNAs recently described to likely participate in AD risk and progression are miR-146a, miR-181a, detected in blood from AD patients, and miR-142-3p [181,182] in the human brain. All aforementioned miRNAs have been proposed as potential diagnostic biomarkers and/or therapeutic targets for AD pathology.

Dysregulation of miRNAs is also implicated in PD pathogenesis. The upregulation of several miRNAs, including miR-150 [183] in human serum, miR-let-7a [184], and miR -190 [185] in C57BL/6 mouse model and miR-135b [186] in in vitro models, ameliorates PD-associated neuroinflammation. By inhibiting SP1, a transcription factor expressed in the brain, miR-375 decreases dopaminergic neurons' damage, reduces oxidative stress, and diminishes inflammation in PD, and miR-29c also attenuates dopaminergic neuron loss, neuroinflammatory response, and α-synuclein accumulation [187,188]. Furthermore, in a PD rat model, miR-3557 and miR-324 seem to be involved in delaying PD neurodegeneration [189], and overexpression of miR-410 in a PD cellular model appears to exert neuroprotective effects against apoptosis and reactive oxygen species production [190]. In contrast, overexpression of miR-326 has been described to promote autophagy of dopaminergic neurons, and miR-195 downregulation might induce microglia-mediated neuroinflammation activation [191,192]. On the other hand, miR-7 seems to be involved in regulating *BDNF* expression in the early stages of PD, and miR-376a could also be implicated in PD pathogenesis, possibly by regulating the expression of mitochondrial-related genes [193,194].

Several studies also report miRNA changes in ALS, suggesting that these molecules could play a role in the development and progression of the disease. In serum from ALS patients, downregulation of miR-335-5p may enhance mitophagy, autophagy, and apoptosis pathways [195]. Interestingly, in the spinal cord of an ALS mouse model, downregulated miR-375-3p appears to control various target structures that intervene at different sites of the apoptosis pathway [196]. In contrast, in the cerebellum of an ALS mouse model, increased miR-29b-3p seems to downregulate proapoptotic factors, leading to neuroprotection [197]. Regarding to axon degeneration, several miRNAs, namely miR-126-5p [198], miR-494-3p [199] and miR-1825 [200], might facilitate this pathological feature in ALS. On the other hand, upregulated miR-338-3p is responsible for decreased glycogenolysis and subsequent glycogen accumulation within the spinal cord of *SOD1*-ALS mice [201], and miR-105 and miR-9 seem to potentially contribute to the pathogenesis of intermediate filament inclusions in ALS [202]. Furthermore, it has been described that extracellular miR-218 released from dying motor neurons in ALS can be taken up by neighboring astrocytes and negatively affect astrocyte function [203]. In the skeletal muscle of FALS patients, it has been reported an upregulation of miR-206, involved in the neuromuscular junction, regeneration, and muscle atrophy, and also an increase in inflammatory miRNAs (miR-27a, miR-221, miR-155) [79]. miR-206, a microRNA that was consistently altered during the course of the disease in the skeletal muscle of the *SOD1*-G93A ALS mouse model, is also increased in serum from ALS patients [155]. Mechanistically, it has been suggested that increased miR-206 is an attempt to promote maintenance and/or repair of neuromuscular junctions by targeting and

inhibiting HDAC4, which leads to a fibroblast growth factor (FGF)-stimulated reinnervation [204]. Finally, reduced expression of the miR-17~92 cluster has been associated with the vulnerability of limb-innervating lateral motor column motor neurons to ALS-related degeneration [205].

In HD, a consistent association between expression profiles of CSF-miRNAs and the earliest prodromal stages of the disease has been reported [162]. In contrast, a study in a knock-in mouse model of HD (Hdh mice) suggests that miRNA regulation may have a limited global role in responding to HD in the striatum and cortex of these mice [206]. A decrease in miR-132 has been observed in the brain of another model of HD (HD R6/2 mice), and restoration of miR-132 deficiency seems to confer amelioration in motor function and lifespan of these mice [207]. In neural progenitors and differentiated neural cells of a transgenic HD nonhuman primate model and in HD murine primary neurons, miR-196a has shown neuroprotective effects, including improvement of cell survival and mitochondrial functions, reduction of cytotoxicity and apoptosis and enhancement of neuronal morphology and differentiation [208,209]. Regarding htt, miR-27a has been reported to reduce mutant htt aggregation in R6/2-derived neuronal stem cells [210]. Interestingly, artificial miRNAs have also been used to successfully reduce mutant htt levels in a transgenic HD sheep model and in a humanized Hu128/21 HD mouse model [211,212].

As reported, the role of microRNAs in these neurodegenerative diseases is better known than the ones of the other epigenetic mechanisms. We have the tools to analyze the effect of overexpressing or repressing the expression of these molecules using expression vectors or antisense oligonucleotides in cellular models. This could facilitate the research in therapies modifying dysregulated microRNAs.

Table 3. MicroRNAs in prion-like diseases.

Disease	Species/Model	Tissue Type	miRNA	Main Finding	References
Alzheimer's disease	Human	Brain, peripheral blood, serum, CSF, serum and CSF exosomes, and plasma extracellular vesicles	miRNA profiles	Differential miRNA expression profiles in AD patients	[111–122]
	APP/PS1 and 5XFAD mice	Brain and urinary exosomes	miRNA profiles	Differential miRNA expression profiles in AD mouse models	[123–125]
	Human	Serum	miR-193a-3p, miR-133b	Neuroprotective roles attenuating Aβ accumulation and its associated neurotoxicity	[170,171]
	Human	Brain	miR-335-5p, miR-361-3p		[172,173]
			miR-340		
	Human	SH-SY5Y, SK-N-SH cells	miR-107		[176]
	SAMP8 mice	Hippocampus			[175]
	Human	Blood plasma	miR-200a-3p		[174]
	Rat	Hippocampus	miR-134-5p	Involved in rescuing AD synaptic plasticity	[177]
	C57BL/6J, Tg2576 mice	Hippocampus	miR-124	Alleviates tau pathology and mediates synaptic and memory deficits	[178,180]
	SAMP8 mice, Human	Hippocampus, serum	miR-34c	Mediates synaptic and memory deficits	[179]
	Human	Blood, Brain	miR-146a, miR-181a, miR-142-3p	Associated with AD risk and progression	[181,182]
	Human	Brain, gut, plasma, serum, CSF, saliva, plasma exosomes, serum extracellular vesicles, and iPSC-derived dopaminergic neurons	miRNA profiles	Differential miRNA expression profiles in PD patients	[126–137]
					[139]

Parkinson's disease	Rat	Peripheral blood	miRNA profile	Differential miRNA expression profile in a PD rat model	[138]
	Human	Serum	miR-150		[183]
	C57BL/6 mice	Brain	miR-let-7a, miR-190	Amelioration of PD-associated neuroinflammation	[184,185]
	Human, rat	SH-SY5Y, PC-12 cells	miR-135b		[186]
	Wistar rats, C57BL/6 mice, Human	Brain, SH-SY5Y cells	miR-375, miR-29c	Decrease in dopaminergic neurons' damage and neuroinflammatory response	[187,188]
	Sprague–Dawley rats	Brain	miR-3557, miR-324	Involved in delaying PD neurodegeneration	[189]
	Human, rat	SH-SY5Y, PC-12 cells	miR-410	Overexpression exerts neuroprotective effects against apoptosis and reactive oxygen species production	[190]
	C57BL/6 mice	Brain	miR-326	Overexpression promotes autophagy of dopaminergic neurons	[191]
	Mouse	BV2 cells	miR-195	Downregulation might induce microglia-mediated neuroinflammation activation	[192]
	Sprague–Dawley rats	Peripheral blood, brain	miR-7	Involved in regulating brain-derived neurotrophic factor expression in early stages of PD	[193]
	Human	PBMCs, SH-SY5Y cells	miR-376a	Implicated in PD pathogenesis regulating the expression of mitochondrial-related genes	[194]

Table 3. *Cont.*

Disease	Species/Model	Tissue Type	miRNA	Main Finding	References
Amyotrophic lateral sclerosis	Human	Brain, spinal cord, skeletal muscle, neuromuscular junctions, plasma, serum, leukocytes, CSF, plasma, serum, brain and spinal cord extracellular vesicles, motor neuron-derived exosomes, iPSC-derived motor neurons, and motor neuron progenitors	miRNA profiles	Differential miRNA expression profiles in ALS patients	[140–155] [158]
	$SOD1^{G86R}$ and $SOD1^{G91A}$ mice	Serum, skeletal muscle	miRNA profiles	Differential miRNA expression profiles in ALS mouse models	[156,157]
	Human	Serum	miR-335-5p	Downregulation may enhance mitophagy, autophagy, and apoptosis pathways	[195]
	Wobbler mice	Spinal cord	miR-375-3p	Regulates target structures that intervene at the apoptosis pathway	[196]
	Wobbler mice	Cerebellum	miR-29b-3p	Downregulates proapoptotic factors, leading to neuroprotection	[197]
	$SOD1^{G93A}$ mice	Muscle	miR-126-5p	Involved in axon degeneration	[198]
	Human	Astrocytes	miR-494-3p		[199]
	Human	CNS	miR-1825		[200]
	SOD1 mice	Spinal cord	miR-338-3p	Upregulation decreases glycogenolysis causing glycogen accumulation within the spinal cord	[201]
	Human	Spinal cord	miR-105, miR-9	Contribute to intermediate filament aggregation in ALS	[202]
	Mouse	Astrocytes	miR-218	Affects astrocyte function negatively	[203]
	Human, $SOD1^{G93A}$ mice	Skeletal muscle, serum, plasma	miR-206	Upregulated. Involved in neuromuscular junction, regeneration, and muscle atrophy	[79,156]

	Human	Skeletal muscle	miR-27a, miR-221, miR-155	Increased in FALS patients	[79]
	Human, $SOD1^{G93A}$ mice	Motor neurons	miR-17~92 cluster	Associated with vulnerability of motor neurons to ALS-related degeneration	[205]
Huntington's disease	C57BL/6, R6/1 and BACHD mice	Brain	miRNA profiles	Differential miRNA expression profiles in HD mouse models	[164–167]
	Human	Brain, plasma, CSF	miRNA profiles	Differential miRNA expression profiles in HD patients. Association between CSF-miRNAs expression profiles and the earliest prodromal stages of HD	[172–176]
	Hdh mice	Striatum, cortex	miRNA profiles	miRNA regulation may have a limited global role in responding to HD	[206]
	R6/2 mice	Brain	miR-132	Decreased levels, whose restoration confers amelioration in motor function and lifespan	[207]
	FVB mouse embryos, HD1/HD7/WT monkey	Neural progenitors, neural cells	miR-196a	Neuroprotective effects	[208,209]
	R6/2 mice	Neuronal stem cells	miR-27a	Reduces mutant htt aggregation	[210]
	Hu128/21 mice, sheep	Striatum	Artificial miRNAs	Reduce mutant htt levels	[211,212]

3. Epigenetic Changes in Prion Diseases

Compared to prion-like diseases, there are very few studies on the involvement of epigenetic changes in transmissible spongiform encephalopathies.

It is known that the prion protein (PrP) is able to bind to RNA and DNA molecules [213]. As these nucleic acids can induce PrP aggregation, they have been proposed as catalysts in the conversion of the PrPC to the pathologic form PrPSc [214]. Different DNA molecules are capable of binding to recombinant PrP (rPrP), resulting in complex aggregates [215]. Interestingly, the GC content of these DNA molecules seems to be important in the binding, affinity, stability, and aggregation abilities and in the toxic species generation [215]. A recent study has evaluated the neurotoxic effect of the inoculation of a PrP-DNA complex in the lateral ventricle of Swiss mice, which, after inoculation, showed cognitive impairment, hippocampal synapse loss, and intense glial activation [216]. In contrast, in human neuroblastoma cell cultures, PrP cytotoxicity is attenuated when combined with DNA molecules, which stabilize PrP structure and reduce its pathogenic properties [217].

Different RNA molecules can also bind to PrP and trigger its aggregation and conversion to PrPSc, the efficiency of the conversion depending on the RNA source [216,218,219]. Some of these RNA molecules, specifically RNA aptamers, are able to bind and stabilize PrPC and reduce PrPSc levels in infected mouse neuronal cells [220]. Further studies are needed in order to evaluate the involvement of these nucleic acids in prion pathology and to develop potential therapeutic strategies.

3.1. DNA Methylation Profiles

DNA methylation might also be involved in the pathogenesis of prion diseases. A study of the mouse prion protein gene (*PRNP*) encoding the PrP^C protein has reported an association between DNA methylation and *PRNP* gene expression. The *PRNP* gene promoter region seems to be unmethylated, and the methylation status of one of the *PRNP* enhancer regions was negatively correlated with *PRNP* expression [221]. In addition, during neuronal differentiation of mouse embryonic carcinoma P19C6 cells, the expression of *PRNP* was markedly increased, while CpG

methylation was significantly reduced, suggesting that DNA methylation could be implicated in mediating *PRNP* expression regulation [222].

Only three studies have analyzed the methylome of prion diseases. A genome-wide methylation study has shown differentially methylated positions in blood from sporadic Creutzfeldt–Jakob disease (sCJD) patients compared with healthy controls, some of these positions correlated with disease progression [223]. Furthermore, another genome-wide methylation study of the CNS of sheep naturally infected with scrapie has identified differentially methylated regions between control and scrapie animals, belonging some of them to genes with possible neuroprotective roles and to genes that may contribute to scrapie disease progression [224]. Interestingly, a recent study was able to identify different DNA methylation patterns in tonsil and appendix lymphoreticular tissues between sCJD patients and healthy individuals [225], pointing to a potential source of diagnostic biomarkers in prion diseases.

Although these three works have been performed in different tissues (blood, CNS, and lymphoid tissues) and species (CJD human patients and scrapie-infected sheep) and have used different methodologies (450k methylation array for humans and whole genome bisulfite sequencing), we have compared the genes detected in each work containing either DMR or DMP. Twelve genes were differentially methylated in both ovine CNS and CJD blood. Further studies are necessary to confirm the role of these common genes in prion diseases. Supplementary Table S4 shows the common DMR and DMP in prion and prion-like diseases.

We have compared the methylation DMR and DMP profiles between these studies and those performed in prion-like diseases. As different methodology has been used, only DMPs obtained in CJD samples were compared with the other diseases. Only 2 DMPs identified in CJD blood were found in common with AD, 3 with PD, and 1 with ALS. However, of a total of 8907 DMRs observed in CNS of scrapie-infected sheep, 634 are also altered in PD, 60 in Alzheimer's, 51 in ALS, and 61 in HD. This large difference is due to the fact that PD and scrapie were analyzed using the same methodology, bisulfite-treated DNA sequencing. More such studies are needed in the other prion-like diseases to determine whether or not there are common genes differentially methylated in all prion-misfolded pathologies.

3.2. Histone Modifications

Yeast ESI+, for expressed sub-telomeric information, is the prion form of the Set3C histone deacetylase scaffold Snt1 (NCOR1 in humans). This prion, in response to cell cycle arrest, is able to activate gene expression through H4 acetylation and RNA polymerase II recruitment [226]. Other histone deacetylases, namely HDAC6 and sirtuin-1 (SIRT1), have shown protective effects during prion infection. Although many studies in prion-like diseases are addressed to inhibit HDAC6 as a potential therapeutic approach, in cerebral cortical neurons, overexpression of HDAC6 alleviates prion peptide-mediated neuronal cell death and toxicity [227]. On the other hand, overexpression of SIRT1, which is decreased in the brains of scrapie-infected rodents and in prion-infected SMB-S15 cells, reduces PrP^{Sc} levels and protects against prion protein-induced neuronal cell death and mitochondrial dysfunction [228–230]. Therefore, although HDAC inhibition is proposed as a potential therapeutic strategy in prion-like diseases, this approach does not seem the best choice for treating prion diseases. Further analysis will be necessary to find out the role of other HDACs in prion diseases and to design novel therapies that maybe could be focused on the overexpression of HDACs.

3.3. MicroRNA Profiles

A number of studies have reported changes in miRNA expression profiles during prion infection in the CNS, plasma, and synaptoneurosomes of preclinical and clinical scrapie-infected mice [231–233], in the serum of elk infected with the chronic wasting disease (CWD) [234] and in plasma of naturally infected classical scrapie sheep [235]. When comparing these profiles with the ones reported in prion-like diseases, there are some miRNAs commonly altered in the two groups of diseases. Table 4 shows the common upregulated, and downregulated miRNAs, and

Supplementary Table S3 lists the datasets generated from the different miRNA profile studies in prion diseases. The prion-like disease with more miRNAs in common with prion diseases is ALS, whereas the one with fewer miRNAs in common is HD. More studies are required in order to find specific miRNAs that are only altered in prion diseases, even only in each type of prion disease, specifically for their use as diagnostic biomarkers.

Table 4. MicroRNAs commonly upregulated and downregulated in prion and prion-like diseases. (+) = Upregulated and (−) = Downregulated.

miRNA	Prion Diseases	AD	PD	ALS	HD	Upregulated (+)/Downregulated (−)
miR-5100	+		+	+		Upregulated
miR-342-3p	+/−	−	+/−	+/−		Upregulated/Downregulated
let-7f-5p	+		+	+		Upregulated
miR-146b-5p	+	+	+	+		Upregulated
let-7a-5p	+	+		+		Upregulated
miR-378c	+	+		+		Upregulated
miR-27a-3p	+	+		+		Upregulated
miR-339-3p	+	+		+		Upregulated
miR-142-5p	+	+	+	+		Upregulated
miR-146a-5p	+	+				Upregulated
miR-320a-3p	+/−	+	+	−		Upregulated/Downregulated
miR-10a-5p	+				+	Upregulated
miR-326	+			+		Upregulated
miR-21-5p	+			+		Upregulated
miR-324-5p	+			+		Upregulated
miR-103a-3p	+			+		Upregulated
miR-331-3p	+/−		−	+/−		Upregulated/Downregulated
miR-107	+			+		Upregulated
miR-142-3p	+			+		Upregulated
miR-129-5p	−		−	−		Downregulated
miR-423-5p	−		−	−		Downregulated
miR-125a-5p	−		−	−		Downregulated
miR-148a-3p	−		−	−		Downregulated

Table 4. *Cont.*

miRNA	Prion Diseases	AD	PD	ALS	HD	Upregulated (+)/Downregulated (−)
miR-186-5p	−		−	−		Downregulated
miR-141-3p	−		−	−		Downregulated
miR-149-5p	−			−		Downregulated
miR-200a-3p	−			−		Downregulated
miR-200b	−			−		Downregulated
miR-323-3p	−			−		Downregulated
miR-338-3p	−	−		−		Downregulated
miR-342-5p	−			−		Downregulated
miR-382	−			−		Downregulated
miR-383	−			−		Downregulated
miR-433	−			−		Downregulated
miR-455-5p	−			−		Downregulated
let-7b	−			−		Downregulated
let-7c	−			−		Downregulated

miR-486-3p	–			–	Downregulated
miR-183-5p	–			–	Downregulated
miR-100-5p	–			–	Downregulated
miR-125b-5p	–			–	Downregulated
miR-99a-5p	–			–	Downregulated
miR-145-3p	–			–	Downregulated
miR-410-3p	–			–	Downregulated
miR-181d-5p	–			–	Downregulated
miR-375	–			–	Downregulated
miR-99b-5p	–			–	Downregulated
miR-30e-3p	–	–	–	–	Downregulated
miR-129-2-3p	–	–	–	–	Downregulated
miR-223-3p	–	–	–	–	Downregulated
miR-493-3p	–	–			Downregulated
miR-182-3p	–	–			Downregulated
miR-877-5p	–	–		–	Downregulated
miR-182-5p	–	–		–	Downregulated
miR-144-5p	–	–		–	Downregulated
miR-181c-5p	–	–		–	Downregulated

Although the potential role of most of these alterations in TSE pathology is unknown, multiple miRNAs regulate PrP^{C} levels both directly and indirectly in human neuroectodermal cell lines [236]. On the other hand, miR-16, which is increased in hippocampal neurons during presymptomatic prion disease, could decrease neurite length and branching, probably via the downregulation of components of the MAPK/ERK pathway [237]. Additionally, a single nucleotide polymorphism in miR-146a has been associated with susceptibility to FFI (fatal familial insomnia) and with the appearance of some clinical features in sCJD patients [238]. Interestingly, artificial miRNAs have also been used to reduce PrP^{C} and subsequently suppress PrP^{Sc} propagation in primary mixed neuronal and glial cells culture [239].

4. Concluding Remarks

It is evident that epigenetic mechanisms, namely DNA methylation, histone posttranslational modifications, and microRNAs, are involved in the pathophysiology of neurodegenerative diseases. Increasing evidence in prion-like diseases and, more recently, in prion diseases has shown that epigenetic modifications can modulate different pathogenic mechanisms occurring in these neurodegenerative disorders. Nevertheless, these epigenetic mechanisms seem to act differently in each of these diseases. Global DNA methylation changes have been detected in prion diseases and prion-like diseases in a variety of tissues and in several specific genes, showing different trends in the global methylation profile of each disease and several genes harboring differentially methylated regions and positions that match between some of these diseases. Modulation of HDAC enzymes seems to also be a common epigenetic mechanism in these diseases. Interestingly, among all the HDACs, the enzyme HDAC6 is involved in both prion diseases and prion-like diseases, although the mechanism of action is different between the two groups of diseases. On the other hand, other HDCAs, namely HDAC2, HDAC3, and HDAC4, are associated with different aspects of prion-like diseases. Additionally, miRNA profiles seem to be the most specific of each disease. However, there are two miRNAs, miR-144-3p and miR-22-5p, that seem to be commonly upregulated in the four prion-like diseases but not in prion diseases, and other miRNAs, such as miR-335-5p, miR-375, and miR-27a, have functions in AD, PD, HD, and ALS, but they seem to regulate different pathways in each disease. Prion and prion-like diseases also share several miRNAs in common, ALS being the prion-like disease with the highest number of common miRNAs. In addition, artificial miRNAs have successfully been used in both HD and prion diseases to reduce misfolded protein levels. Further research is still needed, especially in prion diseases where knowledge is still scarce, in order to elucidate the exact molecular

pathways by which these epigenetic mechanisms perform their regulatory roles and to identify potential epigenetic diagnostic and therapeutic biomarkers.

Supplementary Materials: The following supporting information can be downloaded at: https://www.mdpi.com/article/10.3390/ijms232012609/s1. References[19–37,111–122,126–137,140–155,159–163,231–235] are cited in the Supplementary Materials.

Author Contributions: Conceptualization, A.H. and I.M.-B.; writing—original draft preparation, A.H.; writing—review and editing, I.M.-B. and J.M.T.; visualization, A.H.; supervision, I.M.-B., J.M.T., and R.B.; funding acquisition, I.M.-B. and R.B. All authors have read and agreed to the published version of the manuscript.

Funding: This work was supported by Gobierno de Aragón and the European Social Fund cofinanced predoctoral grant Order IIU/2023/2017, AGL2015-67945-P funded by MINECO, reference group A19-20R funded by Gobierno de Aragón co-financed with FEDER 2014-2020 *Construyendo Europa desde Aragón* and the European Regional Development Fund (ERDF).

Institutional Review Board Statement: Not applicable.

Informed Consent Statement: Not applicable.

Data Availability Statement: Data sharing is not applicable to this article.

Conflicts of Interest: The authors declare no conflict of interest.

References

1. Moore, L.D.; Le, T.; Fan, G. DNA Methylation and Its Basic Function. *Neuropsychopharmacology* **2013**, *38*, 23–38. [CrossRef] [PubMed]
2. Audia, J.E.; Campbell, R.M. Histone Modifications and Cancer. *Cold Spring Harb. Perspect. Biol.* **2016**, *8*, a019521. [CrossRef] [PubMed]
3. Zhang, J.; Jing, L.; Li, M.; He, L.; Guo, Z. Regulation of histone arginine methylation/demethylation by methylase and demethylase (Review). *Mol. Med. Rep.* **2019**, *19*, 3963–3971. [CrossRef] [PubMed]
4. Huang, W. MicroRNAs: Biomarkers, diagnostics, and therapeutics. *Methods Mol. Biol.* **2017**, *1617*, 57–67.
5. Place, R.F.; Li, L.C.; Pookot, D.; Noonan, E.J.; Dahiya, R. MicroRNA-373 induces expression of genes with complementary promoter sequences. *Proc. Natl. Acad. Sci. USA* **2008**, *105*, 1608–1613. [CrossRef]
6. Bottani, M.; Banfi, G.; Lombardi, G. Perspectives on miRNAs as Epigenetic Markers in Osteoporosis and Bone Fracture Risk: A Step Forward in Personalized Diagnosis. *Front. Genet.* **2019**, *10*, 1044. [CrossRef]
7. Lardenoije, R.; Iatrou, A.; Kenis, G.; Kompotis, K.; Steinbusch, H.W.; Mastroeni, D.; Coleman, P.; Lemere, C.A.; Hof, P.R.; van den Hove, D.L.A.; et al. The epigenetics of aging and neurodegeneration. *Prog. Neurobiol.* **2015**, *131*, 21–64. [CrossRef]
8. Hwang, J.Y.; Aromolaran, K.A.; Zukin, R.S. The emerging field of epigenetics in neurodegeneration and neuroprotection. *Nat. Rev. Neurosci.* **2017**, *18*, 347–361. [CrossRef]
9. Heyward, F.D.; Sweatt, J.D. DNA Methylation in Memory Formation: Emerging Insights. *Neuroscientist* **2015**, *21*, 475–489. [CrossRef] 10. Miller, C.A.; Sweatt, J.D. Covalent Modification of DNA Regulates Memory Formation. *Neuron* **2007**, *53*, 857–869. [CrossRef]
11. Hu, Z.; Li, Z. miRNAs in synapse development and synaptic plasticity. *Curr. Opin. Neurobiol.* **2017**, *45*, 24–31. [CrossRef] [PubMed]
12. Woldemichael, B.T.; Mansuy, I.M. Micro-RNAs in cognition and cognitive disorders: Potential for novel biomarkers and therapeutics. *Biochem. Pharmacol.* **2016**, *104*, 1–7. [CrossRef] [PubMed]
13. Aksoy-Aksel, A.; Zampa, F.; Schratt, G. MicroRNAs and synaptic plasticity-a mutual relationship. *Philos. Trans. R. Soc. B Biol. Sci.* **2014**, *369*, 20130515. [CrossRef]
14. Jaunmuktane, Z.; Brandner, S. Invited Review: The role of prion-like mechanisms in neurodegenerative diseases. *Neuropathol. Appl. Neurobiol.* **2019**, *46*, 522–545. [CrossRef]
15. Masnata, M.; Sciacca, G.; Maxan, A.; Bousset, L.; Denis, H.L.; Lauruol, F.; David, L.; Saint-Pierre, M.; Kordower, J.H.; Melki, R.; et al. Demonstration of prion-like properties of mutant huntingtin fibrils in both in vitro and in vivo paradigms. *Acta Neuropathol.* **2019**, *137*, 981–1001. [CrossRef] [PubMed]
16. Ma, J.; Wang, F. Prion disease and the 'protein-only hypothesis'. *Essays Biochem.* **2014**, *56*, 181–191. [CrossRef]
17. Prusiner, S. Novel proteinaceous infectious particles cause scrapie. *Science* **1982**, *216*, 136–144. [CrossRef]
18. Chakravarty, A.K.; Jarosz, D.F. More than Just a Phase: Prions at the Crossroads of Epigenetic Inheritance and Evolutionary Change. *J. Mol. Biol.* **2018**, *430*, 4607–4618. [CrossRef]
19. Li, H.; Guo, Z.; Guo, Y.; Li, M.; Yan, H.; Cheng, J.; Wang, C.; Hong, G. Common DNA methylation alterations of Alzheimer's disease and aging in peripheral whole blood. *Oncotarget* **2016**, *7*, 19089–19098. [CrossRef]
20. Li, Q.S.; Vasanthakumar, A.; Davis, J.W.; Idler, K.B.; Nho, K.; Waring, J.F.; Saykin, A.J.; for the Alzheimer's Disease Neuroimaging Initiative (ADNI). Association of peripheral blood DNA methylation level with Alzheimer's disease progression. *Clin. Epigenetics* **2021**, *13*, 191. [CrossRef]

21. Wang, C.; Chen, L.; Yang, Y.; Zhang, M.; Wong, G. Identification of potential blood biomarkers for Parkinson's disease by gene expression and DNA methylation data integration analysis. *Clin. Epigenet.* **2019**, *11*, 24. [CrossRef] [PubMed]
22. Henderson, A.R.; Wang, Q.; Meechoovet, B.; Siniard, A.L.; Naymik, M.; de Both, M.; Huentelman, M.J.; Caselli, R.J.; DriverDunckley, E.; Dunckley, T. DNA Methylation and Expression Profiles of Whole Blood in Parkinson's Disease. *Front. Genet.* **2021**, *12*, 640266. [CrossRef] [PubMed]
23. Chuang, Y.-H.; Paul, K.C.; Bronstein, J.M.; Bordelon, Y.; Horvath, S.; Ritz, B. Parkinson's disease is associated with DNA methylation levels in human blood and saliva. *Genome Med.* **2017**, *9*, 76. [CrossRef] [PubMed]
24. Hop, P.J.; Zwamborn, R.A.; Hannon, E.; Shireby, G.L.; Nabais, M.F.; Walker, E.M.; van Rheenen, W.; van Vugt, J.J.; Dekker, A.M.; Westeneng, H.-J.; et al. Genome-wide study of DNA methylation shows alterations in metabolic, inflammatory, and cholesterol pathways in ALS. *Sci. Transl. Med.* **2022**, *14*, eabj0264. [CrossRef]
25. Zadel, M.; Maver, A.; Kovanda, A.; Peterlin, B. DNA methylation profiles in whole blood of Huntington's disease patients. *Front. Neurol.* **2018**, *9*, 655. [CrossRef]
26. Lu, A.T.; Narayan, P.; Grant, M.J.; Langfelder, P.; Wang, N.; Kwak, S.; Wilkinson, H.; Chen, R.Z.; Chen, J.; Bawden, C.S.; et al. DNA methylation study of Huntington's disease and motor progression in patients and in animal models. *Nat. Commun.* **2020**, *11*, 4529. [CrossRef]
27. Zhao, J.; Zhu, Y.; Yang, J.; Li, L.; Wu, H.; de Jager, P.L.; Jin, P.; Bennett, D.A. A genome-wide profiling of brain DNA hydroxymethylation in Alzheimer's disease. *Alzheimer's Dement.* **2017**, *13*, 674–688. [CrossRef]
28. Watson, C.T.; Roussos, P.; Garg, P.; Ho, D.J.; Azam, N.; Katsel, P.L.; Haroutunian, V.; Sharp, A.J. Genome-wide12 DNA methylation profiling in the superior temporal gyrus reveals epigenetic signatures associated with Alzheimer's disease. *Genome Med.* **2016**, *8*, 5. [CrossRef]
29. Gao, Z.; Fu, H.; Zhao, L.; Sun, Z.; Yang, Y.; Zhu, H. Aberrant DNA methylation associated with Alzheimer's disease in the superior temporal gyrus. *Exp. Ther. Med.* **2017**, *15*, 103–108. [CrossRef]
30. Altuna, M.; Casado, A.U.; de Gordoa, J.S.-R.; Zelaya, M.V.; Labarga, A.; Lepesant, J.M.J.; Roldán, M.; Blanco-Luquin, I.; Perdones, Á.; Larumbe, R.; et al. DNA methylation signature of human hippocampus in Alzheimer's disease is linked to neurogenesis. *Clin. Epigenetics* **2019**, *11*, 91. [CrossRef]
31. Smith, A.; Smith, R.G.; Pishva, E.; Hannon, E.; Roubroeks, J.A.Y.; Burrage, J.; Troakes, C.; Al-Sarraj, S.; Sloan, C.; Mill, J.; et al. Parallel profiling of DNA methylation and hydroxymethylation highlights neuropathology-associated epigenetic variation in Alzheimer's disease. *Clin. Epigenetics* **2019**, *11*, 52. [CrossRef] [PubMed]
32. Young, J.I.; Sivasankaran, S.K.; Wang, L.; Ali, A.; Mehta, A.; Davis, D.A.; Dykxhoorn, D.M.; Petito, C.K.; Beecham, G.W.; Martin, E.R.; et al. Genome-wide brain DNA methylation analysis suggests epigenetic reprogramming in Parkinson disease. *Neurol. Genet.* **2019**, *5*, e342. [CrossRef] [PubMed]
33. Appleby-Mallinder, C.; Schaber, E.; Kirby, J.; Shaw, P.; Cooper-Knock, J.; Heath, P.R.; Highley, J.R. TDP43 proteinopathy is associated with aberrant DNA methylation in human amyotrophic lateral sclerosis. *Neuropathol. Appl. Neurobiol.* **2020**, *47*, 61–72. [CrossRef] [PubMed]
34. Wang, F.; Yang, Y.; Lin, X.; Wang, J.-Q.; Wu, Y.-S.; Xie, W.; Wang, D.; Zhu, S.; Liao, Y.-Q.; Sun, Q.; et al. Genome-wide loss of 5-hmC is a novel epigenetic feature of Huntington's disease. *Hum. Mol. Genet.* **2013**, *22*, 3641–3653. [CrossRef]
35. Horvath, S.; Langfelder, P.; Kwak, S.; Aaronson, J.; Rosinski, J.; Vogt, T.F.; Eszes, M.; Faull, R.L.M.; Curtis, M.A.; Waldvogel, H.J.; et al. Huntington's disease accelerates epigenetic aging of human brain and disrupts DNA methylation levels. *Aging* **2016**, *8*, 1485–1512. [CrossRef]
36. Fernández-Santiago, R.; Carballo-Carbajal, I.; Castellano, G.; Torrent, R.; Richaud, Y.; Sánchez-Danés, A.; Vilarrasa-Blasi, R.; Sánchez-Pla, A.; Mosquera, J.L.; Soriano, J.; et al. Aberrant epigenome in iPSC-derived dopaminergic neurons from Parkinson's disease patients. *EMBO Mol. Med.* **2015**, *7*, 1529–1546. [CrossRef]
37. Fernández-Santiago, R.; Merkel, A.; Castellano, G.; Heath, S.; Raya, A.; Tolosa, E.; Martí, M.J.; Consiglio, A.; Ezquerra, M. Whole-genome DNA hyper-methylation in iPSC-derived dopaminergic neurons from Parkinson's disease patients. *Clin. Epigenet.* **2019**, *11*, 108. [CrossRef]
38. Heberle, H.; Meirelles, G.V.; Da Silva, F.R.; Telles, G.P.; Minghim, R. InteractiVenn: A Web-Based Tool for the Analysis of Sets through Venn Diagrams. *BMC Bioinform.* **2015**, *16*, 169. [CrossRef]
39. De Souza, R.A.; Islam, S.A.; McEwen, L.M.; Mathelier, A.; Hill, A.; Mah, S.M.; Wasserman, W.W.; Kobor, M.S.; Leavitt, B.R. DNA methylation profiling in human Huntington's disease brain. *Hum. Mol. Genet.* **2016**, *25*, 2013–2030. [CrossRef]
40. Horvath, S. DNA methylation age of human tissues and cell types. *Genome Biol.* **2013**, *14*, R115.
41. Li, P.; Marshall, L.; Oh, G.; Jakubowski, J.L.; Groot, D.; He, Y.; Wang, T.; Petronis, A.; Labrie, V. Epigenetic dysregulation of enhancers in neurons is associated with Alzheimer's disease pathology and cognitive symptoms. *Nat. Commun.* **2019**, *10*, 2246. [CrossRef] [PubMed]
42. Sanchez-Mut, J.V.; Glauser, L.; Monk, D.; Gräff, J. Comprehensive analysis of PM20D1 QTL in Alzheimer's disease. *Clin. Epigenet.* **2020**, *12*, 20. [CrossRef] [PubMed]
43. Eryilmaz, I.E.; Cecener, G.; Erer, S.; Egeli, U.; Tunca, B.; Zarifoglu, M.; Elibol, B.; Tokcaer, A.B.; Saka, E.; Demirkiran, M.; et al. Epigenetic approach to early-onset Parkinson's disease: Low methylation status of *SNCA* and *PARK2* promoter regions. *Neurol. Res.* **2017**, *39*, 965–972. [CrossRef]

44. Taskesen, E.; Mishra, A.; van der Sluis, S.; Ferrari, R.; International FTD-Genomics Consortium; Veldink, J.H.; van Es, M.A.; Smit, A.B.; Posthuma, D.; Pijnenburg, Y. Susceptible genes and disease mechanisms identified in frontotemporal dementia and frontotemporal dementia with Amyotrophic Lateral Sclerosis by DNA-methylation and GWAS. *Sci. Rep.* **2017**, *7*, 8899. [CrossRef] [PubMed]
45. Ebbert, M.; Ross, C.A.; Pregent, L.J.; Lank, R.J.; Zhang, C.; Katzman, R.B.; Jansen-West, K.; Song, Y.; da Rocha, E.L.; Palmucci, C.; et al. Conserved DNA methylation combined with differential frontal cortex and cerebellar expression distinguishes C9orf72associated and sporadic ALS, and implicates SERPINA1 in disease. *Acta Neuropathol.* **2017**, *134*, 715–728. [CrossRef]
46. Kim, B.W.; Jeong, Y.E.; Wong, M.; Martin, L.J. DNA damage accumulates and responses are engaged in human ALS brain and spinal motor neurons and DNA repair is activatable in iPSC-derived motor neurons with SOD1 mutations. *Acta Neuropathol. Commun.* **2020**, *8*, 7. [CrossRef]
47. Bai, G.; Cheung, I.; Shulha, H.P.; Coelho, J.E.; Li, P.; Dong, X.; Jakovcevski, M.; Wang, Y.; Grigorenko, A.; Jiang, Y.; et al. Epigenetic dysregulation of hairy and enhancer of split 4 (HES4) is associated with striatal degeneration in postmortem Huntington brains. *Hum. Mol. Genet.* **2014**, *24*, 1441–1456. [CrossRef]
48. Gutierrez, A.; Corey-Bloom, J.; Thomas, E.A.; Desplats, P. Evaluation of Biochemical and Epigenetic Measures of Peripheral Brain-Derived Neurotrophic Factor (BDNF) as a Biomarker in Huntington's Disease Patients. *Front. Mol. Neurosci.* **2020**, *12*, 335. [CrossRef]
49. Bachman, M.; Uribe-Lewis, S.; Yang, X.; Williams, M.; Murrell, A.; Balasubramanian, S. 5-Hydroxymethylcytosine is a predominantly stable DNA modification. *Nat. Chem.* **2014**, *6*, 1049–1055. [CrossRef]
50. Ellison, E.M.; Abner, E.L.; Lovell, M.A. Multiregional analysis of global 5-methylcytosine and 5-hydroxymethylcytosine throughout the progression of Alzheimer's disease. *J. Neurochem.* **2016**, *140*, 383–394. [CrossRef]
51. Kaut, O.; Kuchelmeister, K.; Moehl, C.; Wüllner, U. 5-methylcytosine and 5-hydroxymethylcytosine in brains of patients with multiple system atrophy and patients with Parkinson's disease. *J. Chem. Neuroanat.* **2019**, *96*, 41–48. [CrossRef] [PubMed]
52. Laszlo, A.H.; Derrington, I.M.; Brinkerhoff, H.; Langford, K.W.; Nova, I.C.; Samson, J.M.; Bartlett, J.J.; Pavlenok, M.; Gundlach, J.H. Detection and mapping of 5-methylcytosine and 5-hydroxymethylcytosine with nanopore MspA. *Proc. Natl. Acad. Sci. USA* **2013**, *110*, 18904–18909. [CrossRef] [PubMed]
53. Hamzeiy, H.; Savas¸, D.; Tunca, C.; S¸en, N.E.; Gündogdu Eken, A.; S¸ahbaz, I.; Calini, D.; Tiloca, C.; Ticozzi, N.; Ratti, A.; et al.˘ Elevated Global DNA Methylation Is Not Exclusive to Amyotrophic Lateral Sclerosis and Is Also Ob-served in Spinocerebellar Ataxia Types 1 and 2. *Neurodegener. Dis.* **2018**, *18*, 38–48. [CrossRef] [PubMed]
54. Jackson, J.L.; Finch, N.A.; Baker, M.C.; Kachergus, J.M.; DeJesus-Hernandez, M.; Pereira, K.; Christopher, E.; Prudencio, M.; Heckman, M.G.; Thompson, E.A.; et al. Elevated methylation levels, reduced expression levels, and frequent contractions in a clinical cohort of C9orf72 expansion carriers. *Mol. Neurodegener.* **2020**, *15*, 7. [CrossRef] [PubMed]
55. Zhang, M.; Tartaglia, M.C.; Moreno, D.; Sato, C.; McKeever, P.; Weichert, A.; Keith, J.; Robertson, J.; Zinman, L.; Rogaeva, E. DNA methylation age-acceleration is associated with disease duration and age at onset in *C9orf72* patients. *Acta. Neuropathol.* **2017**, *134*, 271–279. [CrossRef]
56. Coppedè, F.; Stoccoro, A.; Mosca, L.; Gallo, R.; Tarlarini, C.; Lunetta, C.; Marocchi, A.; Migliore, L.; Penco, S. Increase in DNA methylation in patients with amyotrophic lateral sclerosis carriers of not fully penetrant SOD1 mutations. *Amyotroph. Lateral Scler. Front. Degener.* **2018**, *19*, 93–101. [CrossRef]
57. Madrid, A.; Hogan, K.J.; Papale, L.A.; Clark, L.R.; Asthana, S.; Johnson, S.C.; Alisch, R.S. DNA Hypomethylation in Blood Links B3GALT4 and ZADH2 to Alzheimer's Disease. *J. Alzheimer's Dis.* **2018**, *66*, 927–934. [CrossRef]
58. Salcedo-Tacuma, D.; Melgarejo, J.D.; Mahecha, M.F.; Ortega-Rojas, J.; Arboleda-Bustos, C.E.; Pardo-Turriago, R.; Arboleda, H. Differential Methylation Levels in CpGs of the BIN1 Gene in Individuals with Alzheimer Disease. *Alzheimer Dis. Assoc. Disord.* **2019**, *33*, 321–326. [CrossRef]
59. Li, K.-X.; Sun, Q.; Wei, L.-L.; Du, G.-H.; Huang, X.; Wang, J.-K. ERα Gene Promoter Methylation in Cognitive Function and Quality of Life of Patients with Alzheimer Disease. *J. Geriatr. Psychiatry Neurol.* **2019**, *32*, 221–228. [CrossRef]
60. Mao, W.; Zhao, C.; Ding, H.; Liang, K.; Xue, J.; Chan, P.; Cai, Y. Pyrosequencing analysis of methylation levels of clock genes in leukocytes from Parkinson's disease patients. *Neurosci. Lett.* **2018**, *668*, 115–119. [CrossRef]
61. Shao, Y.; Shaw, M.; Todd, K.; Khrestian, M.; D'Aleo, G.; Barnard, P.J.; Zahratka, J.; Pillai, J.; Yu, C.-E.; Keene, C.D.; et al. DNA methylation of TOMM40-APOE-APOC2 in Alzheimer's disease. *J. Hum. Genet.* **2018**, *63*, 459–471. [CrossRef] [PubMed]
62. Kobayashi, N.; Shinagawa, S.; Nagata, T.; Shimada, K.; Shibata, N.; Ohnuma, T.; Kasanuki, K.; Arai, H.; Yamada, H.; Nakayama, K.; et al. Usefulness of DNA Methylation Levels in COASY and SPINT1 Gene Promoter Regions as Biomarkers in Diagnosis of Alzheimer's Disease and Amnestic Mild Cognitive Impairment. *PLoS ONE* **2016**, *11*, e0168816. [CrossRef] [PubMed]
63. Ozaki, Y.; Yoshino, Y.; Yamazaki, K.; Ochi, S.; Iga, J.; Nagai, M.; Nomoto, M.; Ueno, S. DRD2 methylation to differentiate dementia with Lewy bodies from Parkinson's disease. *Acta Neurol. Scand.* **2019**, *141*, 177–182. [CrossRef] [PubMed]
64. Cohen-Hadad, Y.; Altarescu, G.; Eldar-Geva, T.; Levi-Lahad, E.; Zhang, M.; Rogaeva, E.; Gotkine, M.; Bartok, O.; Ashwal-Fluss, R.; Kadener, S.; et al. Marked Differences in C9orf72 Methylation Status and Isoform Expression between C9/ALS Human Embryonic and Induced Pluripotent Stem Cells. *Stem Cell Rep.* **2016**, *7*, 927–940. [CrossRef]

65. Kantor, B.; Tagliafierro, L.; Gu, J.; Zamora, M.E.; Ilich, E.; Grenier, C.; Huang, Z.Y.; Murphy, S.; Chiba-Falek, O. Downregulation of SNCA Expression by Targeted Editing of DNA Methylation: A Potential Strategy for Precision Therapy in PD. *Mol. Ther.* **2018**, *26*, 2638–2649. [CrossRef]
66. Park, H.; Shin, J.; Kim, Y.; Saito, T.; Saido, T.C.; Kim, J. CRISPR/dCas9-Dnmt3a-mediated targeted DNA methylation of APP rescues brain pathology in a mouse model of Alzheimer's disease. *Transl. Neurodegener.* **2022**, *11*, 41. [CrossRef]
67. Stoccoro, A.; Mosca, L.; Carnicelli, V.; Cavallari, U.; Lunetta, C.; Marocchi, A.; Migliore, L.; Coppedè, F. Mitochondrial DNA copy number and D-loop region methylation in carriers of amyotrophic lateral sclerosis gene mutations. *Epigenomics* **2018**, *10*, 1431–1443. [CrossRef]
68. Xu, Y.; Xu, L.; Han, M.; Liu, X.; Li, F.; Zhou, X.; Wang, Y.; Bi, J. Altered mitochondrial DNA methylation and mitochondrial DNA copy number in an APP/PS1 transgenic mouse model of Alzheimer disease. *Biochem. Biophys. Res. Commun.* **2019**, *520*, 41–46. [CrossRef]
69. Marzi, S.; Leung, S.K.; Ribarska, T.; Hannon, E.; Smith, A.R.; Pishva, E.; Poschmann, J.; Moore, K.; Troakes, C.; Al-Sarraj, S.; et al. A histone acetylome-wide association study of Alzheimer's disease identifies disease-associated H3K27ac differences in the entorhinal cortex. *Nat. Neurosci.* **2018**, *21*, 1618–1627. [CrossRef]
70. Klein, H.-U.; McCabe, C.; Gjoneska, E.; Sullivan, S.E.; Kaskow, B.J.; Tang, A.; Smith, R.V.; Xu, J.; Pfenning, A.R.; Bernstein, B.E.; et al. Epigenome-wide study uncovers large-scale changes in histone acetylation driven by tau pathology in aging and Alzheimer's human brains. *Nat. Neurosci.* **2018**, *22*, 37–46. [CrossRef]
71. Park, G.; Tan, J.; Garcia, G.; Kang, Y.; Salvesen, G.; Zhang, Z. Regulation of Histone Acetylation by Autophagy in Parkinson Disease. *J. Biol. Chem.* **2016**, *291*, 3531–3540. [CrossRef] [PubMed]
72. Yakhine-Diop, S.M.S.; Niso-Santano, M.; Rodríguez-Arribas, M.; Gómez-Sánchez, R.; Martínez-Chacón, G.; Uribe-Carretero, E.; Navarro-García, J.A.; Ruiz-Hurtado, G.; Aiastui, A.; Cooper, J.M.; et al. Impaired Mitophagy and Protein Acetylation Levels in Fibroblasts from Parkinson's Disease Patients. *Mol. Neurobiol.* **2019**, *56*, 2466–2481. [CrossRef] [PubMed]
73. Schueller, E.; Paiva, I.; Blanc, F.; Wang, X.L.; Cassel, J.C.; Boutillier, A.L.; Bousiges, O. Dysregulation of histone acetylation pathways in hippocampus and frontal cortex of Alzheimer's disease patients. *Eur. Neuropsychopharmacol.* **2020**, *33*, 101–116. [CrossRef] [PubMed]
74. Mahady, L.; Nadeem, M.; Malek-Ahmadi, M.; Chen, K.; Perez, S.E.; Mufson, E.J. HDAC 2 dysregulation in the nucleus basalis of Meynert during the progression of Alzheimer's disease. *Neuropathol. Appl. Neurobiol.* **2019**, *45*, 380–397. [CrossRef] [PubMed]
75. Tan, Y.; Delvaux, E.; Nolz, J.; Coleman, P.D.; Chen, S.; Mastroeni, D. Upregulation of histone deacetylase 2 in laser capture nigral microglia in Parkinson's disease. *Neurobiol. Aging* **2018**, *68*, 134–141. [CrossRef]
76. Wu, Q.; Yang, X.; Zhang, L.; Zhang, Y.; Feng, L. Nuclear Accumulation of Histone Deacetylase 4 (HDAC4) Exerts Neurotoxicity in Models of Parkinson's Disease. *Mol. Neurobiol.* **2017**, *54*, 6970–6983. [CrossRef]
77. Buonvicino, D.; Felici, R.; Ranieri, G.; Caramelli, R.; Lapucci, A.; Cavone, L.; Muzzi, M.; Di Pietro, L.; Bernardini, C.; Zwergel, C.; et al. Effects of Class II-Selective Histone Deacetylase Inhibitor on Neuromuscular Function and Disease Progression in SOD1-ALS Mice. *Neuroscience* **2018**, *379*, 228–238. [CrossRef]
78. Lapucci, A.; Cavone, L.; Buonvicino, D.; Felici, R.; Gerace, E.; Zwergel, C.; Valente, S.; Mai, A.; Chiarugi, A. Effect of Class II HDAC inhibition on glutamate transporter expression and survival in SOD1-ALS mice. *Neurosci. Lett.* **2017**, *656*, 120–125. [CrossRef]
79. Pegoraro, V.; Marozzo, R.; Angelini, C. MicroRNAs and HDAC4 protein expression in the skeletal muscle of ALS patients. *Clin. Neuropathol.* **2020**, *39*, 105–114. [CrossRef]
80. Pigna, E.; Simonazzi, E.; Sanna, K.; Bernadzki, K.M.; Proszynski, T.; Heil, C.; Palacios, D.; Adamo, S.; Moresi, V. Histone deacetylase 4 protects from denervation and skeletal muscle atrophy in a murine model of amyo-trophic lateral sclerosis. *eBioMedicine* **2019**, *40*, 717–732. [CrossRef]
81. Dios, A.M.; Babu, S.; Granucci, E.J.; Mueller, K.; Mills, A.; Alshikho, M.J.; Zürcher, N.R.; Cernasov, P.; Gilbert, T.; Glass, J.D.; et al. Class I and II histone deacetylase expression is not altered in human amyotrophic lateral sclerosis: Neuropathological and positron emission tomography molecular neuroimaging evidence. *Muscle Nerve* **2019**, *60*, 443–452. [CrossRef] [PubMed]
82. Boutillier, A.-L.; Tzeplaeff, L.; Dupuis, L. The dark side of HDAC inhibition in ALS. *eBioMedicine* **2019**, *41*, 38–39. [CrossRef]
83. Janczura, K.J.; Volmar, C.H.; Sartor, G.C.; Rao, S.J.; Ricciardi, N.R.; Lambert, G.; Brothers, S.P.; Wahlestedt, C. Inhibition of HDAC3 reverses Alzheimer's disease-related pathologies in vitro and in the 3xTg-AD mouse model. *Proc. Natl. Acad. Sci. USA* **2018**, *115*, E11148–E11157. [CrossRef] [PubMed]
84. Esteves, A.; Palma, A.; Gomes, R.; Santos, D.; Silva, D.; Cardoso, S. Acetylation as a major determinant to microtubule-dependent autophagy: Relevance to Alzheimer's and Parkinson disease pathology. *Biochim. Biophys. Acta (BBA) Mol. Basis Dis.* **2018**, *1865*, 2008–2023. [CrossRef] [PubMed]
85. Choi, H.; Kim, H.J.; Yang, J.; Chae, S.; Lee, W.; Chung, S.; Kim, J.; Choi, H.; Song, H.; Lee, C.K.; et al. Acetylation changes tau interactome to degrade tau in Alzheimer's disease animal and organoid models. *Aging Cell.* **2020**, *19*, e13081. [CrossRef]
86. Jian, W.; Wei, X.; Chen, L.; Wang, Z.; Sun, Y.; Zhu, S.; Lou, H.; Yan, S.; Li, X.; Zhou, J.; et al. Inhibition of HDAC6 increases acetylation of peroxiredoxin1/2 and ameliorates 6-OHDA induced dopaminergic injury. *Neurosci. Lett.* **2017**, *658*, 114–120. [CrossRef]
87. Kim, T.; Song, S.; Park, Y.; Kang, S.; Seo, H. HDAC inhibition by valproic acid induces neuroprotection and improvement of PD-like behaviors in LRRK2 R1441G transgenic mice. *Exp. Neurobiol.* **2019**, *28*, 504–515. [CrossRef]

88. Harrison, I.F.; Smith, A.D.; Dexter, D.T. Pathological histone acetylation in Parkinson's disease: Neuroprotection and inhibition of microglial activation through SIRT 2 inhibition. *Neurosci. Lett.* **2017**, *666*, 48–57. [CrossRef]
89. Esteves, A.R.; Arduíno, D.M.; Silva, D.F.; Viana, S.D.; Pereira, F.C.; Cardoso, S.M. Mitochondrial Metabolism Regulates Microtubule Acetylome and Autophagy Trough Sirtuin-2: Impact for Parkinson's Disease. *Mol. Neurobiol.* **2018**, *55*, 1440–1462. [CrossRef]
90. Kuta, R.; Larochelle, N.; Fernandez, M.; Pal, A.; Minotti, S.; Tibshirani, M.; St.Louis, K.; Gentil, B.J.; Nalbantoglu, J.N.; Hermann, A.; et al. Depending on the stress, histone deacetylase inhibitors act as heat shock protein co-inducers in motor neurons and potentiate arimoclomol, exerting neuroprotection through multiple mechanisms in ALS models. *Cell Stress Chaperones* **2020**, *25*, 173–191. [CrossRef]
91. Rossaert, E.; Pollari, E.; Jaspers, T.; van Helleputte, L.; Jarpe, M.; van Damme, P.; de Bock, K.; Moisse, M.; van den Bosch, L. Restoration of histone acetylation ameliorates disease and metabolic abnormalities in a FUS mouse model. *Acta Neuropathol. Commun.* **2019**, *7*, 107. [CrossRef]
92. Guo, W.; Naujock, M.; Fumagalli, L.; Vandoorne, T.; Baatsen, P.; Boon, R.; Ordovás, L.; Patel, A.; Welters, M.; Vanwelden, T.; et al. HDAC6 inhibition reverses axonal transport defects in motor neurons derived from FUS-ALS patients. *Nat. Commun.* **2017**, *8*, 861. [CrossRef] [PubMed]
93. Guo, W.; Bosch, L.V.D. Therapeutic potential of HDAC6 in amyotrophic lateral sclerosis. *Cell Stress* **2018**, *2*, 14–16. [CrossRef] [PubMed]
94. Siebzehnrübl, F.A.; Raber, K.A.; Urbach, Y.K.; Schulze-Krebs, A.; Canneva, F.; Moceri, S.; Habermeyer, J.; Achoui, D.; Gupta, B.; Steindler, D.A.; et al. Early postnatal behavioral, cellular, and molecular changes in models of Huntington disease are reversible by HDAC inhibition. *Proc. Natl. Acad. Sci. USA* **2018**, *115*, E8765–E8774. [CrossRef] [PubMed]
95. Chopra, V.; Quinti, L.; Khanna, P.; Paganetti, P.; Kuhn, R.; Young, A.B.; Kazantsev, A.G.; Hersch, S. LBH589, A Hydroxamic Acid-Derived HDAC Inhibitor, is Neuroprotective in Mouse Models of Huntington's Disease. *J. Huntingtons. Dis.* **2016**, *5*, 347–355. [CrossRef]
96. Jia, H.; Morris, C.D.; Williams, R.M.; Loring, J.F.; Thomas, E.A. HDAC inhibition imparts beneficial transgenerational effects in Huntington's disease mice via altered DNA and histone methylation. *Proc. Natl. Acad. Sci. USA* **2014**, *112*, E56–E64. [CrossRef]
97. Naia, L.; Cunha-Oliveira, T.; Rodrigues, J.; Rosenstock, T.R.; Oliveira, A.; Ribeiro, M.; Carmo, C.; Oliveira-Sousa, S.I.; Duarte, A.I.; Hayden, M.R.; et al. Histone Deacetylase Inhibitors Protect Against Pyruvate Dehydrogenase Dysfunction in Huntington's Disease. *J. Neurosci.* **2017**, *37*, 2776–2794. [CrossRef]
98. Federspiel, J.D.; Greco, T.M.; Lum, K.K.; Cristea, I.M. Hdac4 Interactions in Huntington's Disease Viewed Through the Prism of Multiomics. *Mol. Cell. Proteom.* **2019**, *18*, S92–S113. [CrossRef]
99. Moreno, C.L.; Ehrlich, M.E.; Mobbs, C.V. Protection by dietary restriction in the YAC128 mouse model of Huntington's disease: Relation to genes regulating histone acetylation and HTT. *Neurobiol. Dis.* **2016**, *85*, 25–34. [CrossRef]
100. Jia, H.; Wang, Y.; Morris, C.D.; Jacques, V.; Gottesfeld, J.; Rusche, J.R.; Thomas, E.A. The Effects of Pharmacological Inhibition of Histone Deacetylase 3 (HDAC3) in Huntington's Disease Mice. *PLoS ONE* **2016**, *11*, e0152498. [CrossRef]
101. Suelves, N.; Kirkham-McCarthy, L.; Lahue, R.S.; Ginés, S. A selective inhibitor of histone deacetylase 3 prevents cognitive deficits and suppresses striatal CAG repeat expansions in Huntington's disease mice. *Sci. Rep.* **2017**, *7*, 6082. [CrossRef]
102. Ragot, A.; Pietropaolo, S.; Vincent, J.; Delage, P.; Zhang, H.; Allinquant, B.; Leinekugel, X.; Fischer, A.; Cho, Y.H. Genetic deletion of the Histone Deacetylase 6 exacerbates selected behavioral deficits in the R6/1 mouse model for Huntington's disease. *Brain Behav.* **2015**, *5*, e00361. [CrossRef] [PubMed]
103. Dong, X.; Tsuji, J.; Labadorf, A.; Roussos, P.; Chen, J.-F.; Myers, R.H.; Akbarian, S.; Weng, Z. The Role of H3K4me3 in Transcriptional Regulation Is Altered in Huntington's Disease. *PLoS ONE* **2015**, *10*, e0144398. [CrossRef]
104. Song, W.; Zsindely, N.; Faragó, A.; Marsh, J.L.; Bodai, L. Systematic genetic interaction studies identify histone demethylase Utx as potential target for ameliorating Huntington's disease. *Hum. Mol. Genet.* **2017**, *27*, 649–666. [CrossRef] [PubMed]
105. Lee, J.; Hwang, Y.J.; Kim, Y.; Lee, M.Y.; Hyeon, S.J.; Lee, S.; Kim, D.H.; Jang, S.; Im, H.; Min, S.-J.; et al. Remodeling of heterochromatin structure slows neuropathological progression and prolongs survival in an animal model of Huntington's disease. *Acta Neuropathol.* **2017**, *134*, 729–748. [CrossRef] [PubMed]
106. March, Z.M.; King, O.D.; Shorter, J. Prion-like domains as epigenetic regulators, scaffolds for subcellular organization, and drivers of neurodegenerative disease. *Brain Res.* **2016**, *1647*, 9–18. [CrossRef] [PubMed]
107. Chen-Plotkin, A.S.; Lee, V.M.-Y.; Trojanowski, J.Q. TAR DNA-binding protein 43 in neurodegenerative disease. *Nat. Rev. Neurol.* **2010**, *6*, 211–220. [CrossRef]
108. Guo, L.; Shorter, J. Biology and Pathobiology of TDP-43 and Emergent Therapeutic Strategies. *Cold Spring Harb. Perspect. Med.* **2016**, *7*, a024554. [CrossRef]
109. Harrison, A.F.; Shorter, J. RNA-binding proteins with prion-like domains in health and disease. *Biochem. J.* **2017**, *474*, 1417–1438. [CrossRef]
110. Murakami, K.; Ono, K. Interactions of amyloid coaggregates with biomolecules and its relevance to neurodegeneration. *FASEB J.* **2022**, *36*, e22493. [CrossRef]
111. Henriques, A.D.; Machado-Silva, W.; Leite, R.E.P.; Suemoto, C.K.; Leite, K.R.M.; Srougi, M.; Pereira, A.C.; Jacob-Filho, W.; Nóbrega, O.T. Genome-wide profiling and predicted significance of post-mortem brain microRNA in Alzheimer's disease. *Mech. Ageing Dev.* **2020**, *191*, 111352. [CrossRef] [PubMed]

112. Moradifard, S.; Hoseinbeyki, M.; Ganji, S.M.; Minuchehr, Z. Analysis of microRNA and Gene Expression Profiles in Alzheimer's Disease: A Meta-Analysis Approach. *Sci. Rep.* **2018**, *8*, 4767. [CrossRef] [PubMed]
113. Nunez-Iglesias, J.; Liu, C.-C.; Morgan, T.E.; Finch, C.E.; Zhou, X.J. Joint Genome-Wide Profiling of miRNA and mRNA Expression in Alzheimer's Disease Cortex Reveals Altered miRNA Regulation. *PLoS ONE* **2010**, *5*, e8898. [CrossRef] [PubMed]
114. Watson, C.N.; Begum, G.; Ashman, E.; Thorn, D.; Yakoub, K.M.; Al Hariri, M.; Nehme, A.; Mondello, S.; Kobeissy, F.; Belli, A.; et al. Co-Expression Analysis of microRNAs and Proteins in Brain of Alzheimer's Disease Patients. *Cells* **2022**, *11*, 163. [CrossRef] [PubMed]
115. Ren, R.J.; Zhang, Y.F.; Dammer, E.B.; Zhou, Y.; Wang, L.L.; Liu, X.H.; Feng, B.L.; Jiang, G.X.; Chen, S.D.; Wang, G.; et al. Peripheral Blood MicroRNA Expression Profiles in Alzheimer's Disease: Screening, Validation, Association with Clinical Phenotype and Implications for Molecular Mechanism. *Mol. Neurobiol.* **2016**, *53*, 5772–5781. [CrossRef]
116. Wang, Z.; Shen, L.; Wang, Y.; Huang, S. Integrated analysis of miRNA and mRNA expression in the blood of patients with Alzheimer's disease. *Mol. Med. Rep.* **2020**, *22*, 1053–1062. [CrossRef]
117. Dong, H.; Li, J.; Huang, L.; Chen, X.; Li, D.; Wang, T.; Hu, C.; Xu, J.; Zhang, C.; Zen, K.; et al. Serum MicroRNA Profiles Serve as Novel Biomarkers for the Diagnosis of Alzheimer's Disease. *Dis. Markers* **2015**, *2015*, 625659. [CrossRef]
118. Lu, L.; Dai, W.-Z.; Zhu, X.-C.; Ma, T. Analysis of Serum miRNAs in Alzheimer's Disease. *Am. J. Alzheimer's Dis. Other Dementias* **2021**, *36*. [CrossRef]
119. Dangla-Valls, A.; Molinuevo, J.L.; Altirriba, J.; Sánchez-Valle, R.; Alcolea, D.; Fortea, J.; Rami, L.; Balasa, M.; Muñoz-García, C.; Ezquerra, M.; et al. CSF microRNA Profiling in Alzheimer's Disease: A Screening and Validation Study. *Mol. Neurobiol.* **2016**, *54*, 6647–6654. [CrossRef]
120. Dong, Z.; Gu, H.; Guo, Q.; Liang, S.; Xue, J.; Yao, F.; Liu, X.; Li, F.; Liu, H.; Sun, L.; et al. Profiling of Serum Exosome MiRNA Reveals the Potential of a MiRNA Panel as Diagnostic Biomarker for Alzheimer's Disease. *Mol. Neurobiol.* **2021**, *58*, 3084–3094. [CrossRef]
121. McKeever, P.M.; Schneider, R.; Taghdiri, F.; Weichert, A.; Multani, N.; Brown, R.A.; Boxer, A.L.; Karydas, A.; Miller, B.; Robertson, J.; et al. MicroRNA Expression Levels Are Altered in the Cerebrospinal Fluid of Patients with Young-Onset Alzheimer's Disease. *Mol. Neurobiol.* **2018**, *55*, 8826–8841. [CrossRef] [PubMed]
122. Serpente, M.; Fenoglio, C.; D'Anca, M.; Arcaro, M.; Sorrentino, F.; Visconte, C.; Arighi, A.; Fumagalli, G.G.; Porretti, L.; Cattaneo, A.; et al. MiRNA Profiling in Plasma Neural-Derived Small Extracellular Vesicles from Patients with Alzheimer's Disease. *Cells* **2020**, *9*, 1443. [CrossRef] [PubMed]
123. Ma, N.; Tie, C.; Yu, B.; Zhang, W.; Wan, J. Identifying lncRNA-miRNA-mRNA networks to investigate Alzheimer's disease pathogenesis and therapy strategy. *Aging* **2020**, *12*, 2897–2920. [CrossRef] [PubMed]
124. Song, Z.; Qu, Y.; Xu, Y.; Zhang, L.; Zhou, L.; Han, Y.; Zhao, W.; Yu, P.; Zhang, Y.; Li, X.; et al. Microarray microRNA profiling of urinary exosomes in a 5XFAD mouse model of Alzheimer's disease. *Anim. Model. Exp. Med.* **2021**, *4*, 233–242. [CrossRef]
125. Li, Z.-R.; Liu, R.; Zeng, L.; Jiang, H.-L.; Ashraf, G.M. MicroRNA and mRNA profiling of cerebral cortex in a transgenic mouse model of Alzheimer's disease by RNA sequencing. *Neural Regen. Res.* **2021**, *16*, 2099–2108. [CrossRef]
126. Cardo, L.F.; Coto, E.; Ribacoba, R.; Menéndez, M.; Moris, G.; Suárez, E.; Alvarez, V. MiRNA Profile in the Substantia Nigra of Parkinson's Disease and Healthy Subjects. *J. Mol. Neurosci.* **2014**, *54*, 830–836. [CrossRef]
127. Hoss, A.G.; Labadorf, A.; Beach, T.G.; Latourelle, J.C.; Myers, R.H. microRNA Profiles in Parkinson's Disease Pre-frontal Cortex. *Front. Aging Neurosci.* **2016**, *8*, 36. [CrossRef]
128. Schulz, J.; Takousis, P.; Wohlers, I.; Itua, I.O.; Dobricic, V.; Rücker, G.; Binder, H.; Middleton, L.; Ioannidis, J.P.; Perneczky, R.; et al. Meta-analyses identify differentially expressed microRNAs in Parkinson's disease. *Ann. Neurol.* **2019**, *85*, 835–851. [CrossRef]
129. Tatura, R.; Kraus, T.; Giese, A.; Arzberger, T.; Buchholz, M.; Höglinger, G.; Müller, U. Parkinson's disease: SNCA-, PARK2-, and LRRK2-targeting microRNAs elevated in cingulate gyrus. *Park. Relat. Disord.* **2016**, *33*, 115–121. [CrossRef]
130. Kurz, A.; Kumar, R.; Northoff, B.H.; Wenk, C.; Schirra, J.; Donakonda, S.; Höglinger, G.U.; Schwarz, J.; Rozanski, V.; Hübner, R.; et al. Differential expression of gut miRNAs in idiopathic Parkinson's disease. *Park. Relat. Disord.* **2021**, *88*, 46–50. [CrossRef]
131. Cai, M.; Chai, S.; Xiong, T.; Wei, J.; Mao, W.; Zhu, Y.; Li, X.; Wei, W.; Dai, X.; Yang, B.; et al. Aberrant Expression of Circulating MicroRNA Leads to the Dysregulation of Alpha-Synuclein and Other Pathogenic Genes in Parkinson's Disease. *Front. Cell Dev. Biol.* **2021**, *9*, 695007. [CrossRef]
132. Cardo, L.F.; Coto, E.; de Mena, L.; Ribacoba, R.; Moris, G.; Menéndez, M.; Álvarez, L.D.M. Profile of microRNAs in the plasma of Parkinson's disease patients and healthy controls. *J. Neurol.* **2013**, *260*, 1420–1422. [CrossRef] [PubMed]
133. Ruf, W.; Freischmidt, A.; Grozdanov, V.; Roth, V.; Brockmann, S.; Mollenhauer, B.; Martin, D.; Haslinger, B.; Fundel-Clemens, K.; Otto, M.; et al. Protein Binding Partners of Dysregulated miRNAs in Parkinson's Disease Serum. *Cells* **2021**, *10*, 791. [CrossRef] [PubMed]
134. dos Santos, M.C.T.; Barreto-Sanz, M.A.; Correia, B.R.S.; Bell, R.; Widnall, C.; Perez, L.T.; Berteau, C.; Schulte, C.; Scheller, D.; Berg, D.; et al. miRNA-based signatures in cerebrospinal fluid as potential diagnostic tools for early stage Parkinson's disease. *Oncotarget* **2018**, *9*, 17455–17465. [CrossRef] [PubMed]
135. Mo, M.; Xiao, Y.; Huang, S.; Cen, L.; Chen, X.; Zhang, L.; Luo, Q.; Li, S.; Yang, X.; Lin, X.; et al. MicroRNA expressing profiles in A53T mutant alpha-synuclein transgenic mice and Parkinsonian. *Oncotarget* **2016**, *8*, 15–28. [CrossRef]

136. Jiang, Y.; Chen, J.; Sun, Y.; Li, F.; Wei, L.; Sun, W.; Deng, J.; Yuan, Y.; Wang, Z. Profiling of Differentially Expressed MicroRNAs in Saliva of Parkinson's Disease Patients. *Front. Neurol.* **2021**, *12*, 738530. [CrossRef]
137. He, S.; Huang, L.; Shao, C.; Nie, T.; Xia, L.; Cui, B.; Lu, F.; Zhu, L.; Chen, B.; Yang, Q. Several miRNAs derived from serum extracellular vesicles are potential biomarkers for early diagnosis and progression of Parkinson's disease. *Transl. Neurodegener.* **2021**, *10*, 25. [CrossRef]
138. Yadav, S.K.; Pandey, A.; Sarkar, S.; Yadav, S.S.; Parmar, D.; Yadav, S. Identification of Altered Blood MicroRNAs and Plasma Proteins in a Rat Model of Parkinson's Disease. *Mol. Neurobiol.* **2022**, *59*, 1781–1798. [CrossRef]
139. Tolosa, E.; Botta-Orfila, T.; Morató, X.; Calatayud, C.; Ferrer-Lorente, R.; Martí, M.J.; Fernández, M.; Gaig, C.; Raya, A.; Consiglio, A.; et al. MicroRNA alterations in iPSC-derived dopaminergic neurons from Parkinson disease patients. *Neurobiol. Aging* **2018**, *69*, 283–291. [CrossRef]
140. Campos-Melo, D.; Droppelmann, C.A.; He, Z.; Volkening, K.; Strong, M.J. Altered microRNA expression profile in amyotrophic lateral sclerosis: A role in the regulation of NFL mRNA levels. *Mol. Brain* **2013**, *6*, 26. [CrossRef]
141. Wakabayashi, K.; Mori, F.; Kakita, A.; Takahashi, H.; Utsumi, J.; Sasaki, H. Analysis of microRNA from archived formalin-fixed paraffin-embedded specimens of amyotrophic lateral sclerosis. *Acta Neuropathol. Commun.* **2014**, *2*, 173. [CrossRef] [PubMed]
142. Aksu-Menges, E.; Balci-Hayta, B.; Bekircan-Kurt, C.E.; Aydinoglu, A.T.; Erdem-Ozdamar, S.; Tan, E. Two distinct skeletal muscle microRNA signatures revealing the complex mechanism of sporadic ALS. *Acta Neurol. Belg.* **2021**, 1–11. [CrossRef] [PubMed] 143. De Felice, B.; Manfellotto, F.; Fiorentino, G.; Annunziata, A.; Biffali, E.; Pannone, R.; Federico, A. Wide-Ranging Analysis of MicroRNA Profiles in Sporadic Amyotrophic Lateral Sclerosis Using Next-Generation Sequencing. *Front. Genet.* **2018**, *9*, 310. [CrossRef] [PubMed]
144. Chen, Y.; Wei, Q.; Chen, X.; Li, C.; Cao, B.; Ou, R.; Hadano, S.; Shang, H.-F. Aberration of miRNAs Expression in Leukocytes from Sporadic Amyotrophic Lateral Sclerosis. *Front. Mol. Neurosci.* **2016**, *9*, 69. [CrossRef] [PubMed]
145. De Felice, B.; Guida, M.; Guida, M.; Coppola, C.; de Mieri, G.; Cotrufo, R. A miRNA signature in leukocytes from sporadic amyotrophic lateral sclerosis. *Gene* **2012**, *508*, 35–40. [CrossRef]
146. Liguori, M.; Nuzziello, N.; Introna, A.; Consiglio, A.; Licciulli, F.; D'Errico, E.; Scarafino, A.; Distaso, E.; Simone, I.L. Dysregulation of MicroRNAs and Target Genes Networks in Peripheral Blood of Patients With Sporadic Amyotrophic Lateral Sclerosis. *Front. Mol. Neurosci.* **2018**, *11*, 288. [CrossRef]
147. Takahashi, I.; Hama, Y.; Matsushima, M.; Hirotani, M.; Kano, T.; Hohzen, H.; Yabe, I.; Utsumi, J.; Sasaki, H. Identification of plasma microRNAs as a biomarker of sporadic Amyotrophic Lateral Sclerosis. *Mol. Brain* **2015**, *8*, 67. [CrossRef]
148. Freischmidt, A.; Müller, K.; Zondler, L.; Weydt, P.; Volk, A.E.; Božic˘, A.L.; Walter, M.; Bonin, M.; Mayer, B.; von Arnim, C.A.F.; et al. Serum microRNAs in patients with genetic amyotrophic lateral sclerosis and pre-manifest mutation carriers. *Brain* **2014**, *137*, 2938–2950. [CrossRef]
149. Joilin, G.; Gray, E.; Thompson, A.G.; Bobeva, Y.; Talbot, K.; Weishaupt, J.; Ludolph, A.; Malaspina, A.; Leigh, P.N.; Newbury, S.F.; et al. Identification of a potential non-coding RNA biomarker signature for amyotrophic lateral sclerosis. *Brain Commun.* **2020**, *2*, fcaa053. [CrossRef]
150. Taguchi, Y.-H.; Wang, H. Exploring microRNA Biomarker for Amyotrophic Lateral Sclerosis. *Int. J. Mol. Sci.* **2018**, *19*, 1318. [CrossRef]
151. Benigni, M.; Ricci, C.; Jones, A.R.; Giannini, F.; Al-Chalabi, A.; Battistini, S. Identification of miRNAs as Potential Biomarkers in Cerebrospinal Fluid from Amyotrophic Lateral Sclerosis Patients. *NeuroMolecular Med.* **2016**, *18*, 551–560. [CrossRef] [PubMed]
152. Katsu, M.; Hama, Y.; Utsumi, J.; Takashina, K.; Yasumatsu, H.; Mori, F.; Wakabayashi, K.; Shoji, M.; Sasaki, H. MicroRNA expression profiles of neuron-derived extracellular vesicles in plasma from patients with am-yotrophic lateral sclerosis. *Neurosci. Lett.* **2019**, *708*, 134176. [CrossRef] [PubMed]
153. Lo, T.-W.; Figueroa-Romero, C.; Hur, J.; Pacut, C.; Stoll, E.; Spring, C.; Lewis, R.; Nair, A.; Goutman, S.A.; Sakowski, S.A.; et al. Extracellular Vesicles in Serum and Central Nervous System Tissues Contain microRNA Signatures in Sporadic Amyotrophic Lateral Sclerosis. *Front. Mol. Neurosci.* **2021**, *14*, 739016. [CrossRef] [PubMed]
154. Rizzuti, M.; Melzi, V.; Gagliardi, D.; Resnati, D.; Meneri, M.; Dioni, L.; Masrori, P.; Hersmus, N.; Poesen, K.; Locatelli, M.; et al. Insights into the identification of a molecular signature for amyotrophic lateral sclerosis exploiting integrated microRNA profiling of iPSC-derived motor neurons and exosomes. *Cell. Mol. Life Sci.* **2022**, *79*, 189. [CrossRef]
155. Saucier, D.; Wajnberg, G.; Roy, J.; Beauregard, A.P.; Chacko, S.; Crapoulet, N.; Fournier, S.; Ghosh, A.; Lewis, S.M.; Marrero, A.; et al. Identification of a circulating miRNA signature in extracellular vesicles collected from amyotrophic lateral sclerosis patients. *Brain Res.* **2019**, *1708*, 100–108. [CrossRef]
156. Toivonen, J.M.; Manzano, R.; Oliván, S.; Zaragoza, P.; García-Redondo, A.; Osta, R. MicroRNA-206: A Potential Circulating Biomarker Candidate for Amyotrophic Lateral Sclerosis. *PLoS ONE* **2014**, *9*, e89065. [CrossRef]
157. Matamala, J.M.; Arias-Carrasco, R.; Sanchez, C.; Uhrig, M.; Bargsted, L.; Matus, S.; Maracaja-Coutinho, V.; Abarzua, S.; van Zundert, B.; Verdugo, R.; et al. Genome-wide circulating microRNA expression profiling reveals potential biomarkers for amyotrophic lateral sclerosis. *Neurobiol. Aging* **2018**, *64*, 123–138. [CrossRef]
158. Rizzuti, M.; Filosa, G.; Melzi, V.; Calandriello, L.; Dioni, L.; Bollati, V.; Bresolin, N.; Comi, G.P.; Barabino, S.; Nizzardo, M.; et al. MicroRNA expression analysis identifies a subset of downregulated miRNAs in ALS motor neuron progenitors. *Sci. Rep.* **2018**, *8*, 10105. [CrossRef]
159. Dong, X.; Cong, S. Bioinformatic analysis of microRNA expression in Huntington's disease. *Mol. Med. Rep.* **2018**, *18*, 2857–2865. [CrossRef]

160. Hoss, A.G.; Kartha, V.K.; Dong, X.; Latourelle, J.C.; Dumitriu, A.; Hadzi, T.C.; Macdonald, M.E.; Gusella, J.F.; Akbarian, S.; Chen, J.-F.; et al. MicroRNAs Located in the Hox Gene Clusters Are Implicated in Huntington's Disease Pathogenesis. *PLoS Genet.* **2014**, *10*, e1004188. [CrossRef]
161. Wang, Z.M.; Dong, X.Y.; Cong, S.Y. Bioinformatic analysis of a microRNA regulatory network in Huntington's disease. *J. Integr. Neurosci.* **2020**, *19*, 641–650. [CrossRef] [PubMed]
162. Díez-Planelles, C.; Sánchez-Lozano, P.; Crespo, M.; Gil-Zamorano, J.; Ribacoba, R.; González, N.; Suárez, E.; Martínez-Descals, A.; Martínez-Camblor, P.; Álvarez, V.; et al. Circulating microRNAs in Huntington's disease: Emerging mediators in metabolic impairment. *Pharmacol. Res.* **2016**, *108*, 102–110. [CrossRef] [PubMed]
163. Reed, E.R.; Latourelle, J.C.; Bockholt, J.H.; Bregu, J.; Smock, J.; Paulsen, J.S.; Myers, R.H. PREDICT-HD CSF ancillary study investigators MicroRNAs in CSF as prodromal biomarkers for Huntington disease in the PREDICT-HD study. *Neurology* **2017**, *90*, e264–e272. [CrossRef] [PubMed]
164. Dubois, C.; Kong, G.; Tran, H.; Li, S.; Pang, T.Y.; Hannan, A.J.; Renoir, T. Small Non-coding RNAs Are Dysregulated in Huntington's Disease Transgenic Mice Independently of the Therapeutic Effects of an Environmental Intervention. *Mol. Neurobiol.* **2021**, *58*, 3308–3318. [CrossRef]
165. Langfelder, P.; Gao, F.; Wang, N.; Howland, D.; Kwak, S.; Vogt, T.F.; Aaronson, J.S.; Rosinski, J.; Coppola, G.; Horvath, S.; et al. MicroRNA signatures of endogenous Huntingtin CAG repeat expansion in mice. *PLoS ONE* **2018**, *13*, e0190550. [CrossRef] 166. Olmo, I.G.; Olmo, R.P.; Gonçalves, A.N.A.; Pires, R.G.W.; Marques, J.T.; Ribeiro, F.M. High-Throughput Sequencing of BACHD Mice Reveals Upregulation of Neuroprotective miRNAs at the Pre-Symptomatic Stage of Huntington's Disease. *ASN Neuro* **2021**, *13*. [CrossRef]
167. Pircs, K.; Petri, R.; Madsen, S.; Brattås, P.L.; Vuono, R.; Ottosson, D.R.; St-Amour, I.; Hersbach, B.; Matusiak-Brückner, M.; Lundh, S.H.; et al. Huntingtin Aggregation Impairs Autophagy, Leading to Argonaute-2 Accumulation and Global MicroRNA Dysregulation. *Cell Rep.* **2018**, *24*, 1397–1406. [CrossRef]
168. Li, K.; Zhang, J.; Ji, C.; Wang, L. MiR-144-3p and Its Target Gene β-Amyloid Precursor Protein Regulate 1-Methyl-4-Phenyl-1,23,6-Tetrahydropyridine-Induced Mitochondrial Dysfunction. *Mol. Cells* **2016**, *39*, 543–549. [CrossRef]
169. Jovicic, A.; Zaldivar Jolissaint, J.F.; Moser, R.; de Fatima Silva Santos, M.; Luthi-Carter, R. MicroRNA-22 (miR-22) Overexpression Is Neuroprotective via General Anti-Apoptotic Effects and May also Target Specific Huntington's Disease-Related Mechanisms. *PLoS ONE* **2013**, *8*, e54222.
170. Cao, F.; Liu, Z.; Sun, G. Diagnostic value of miR-193a-3p in Alzheimer's disease and miR-193a-3p attenuates amyloid-β induced neurotoxicity by targeting PTEN. *Exp. Gerontol.* **2019**, *130*, 110814. [CrossRef]
171. Yang, Q.; Zhao, Q.; Yin, Y. miR-133b is a potential diagnostic biomarker for Alzheimer's disease and has a neuroprotective role. *Exp. Ther. Med.* **2019**, *18*, 2711–2718. [CrossRef] [PubMed]
172. Wang, D.; Fei, Z.; Luo, S.; Wang, H. MiR-335-5p Inhibits β-Amyloid (Aβ) Accumulation to Attenuate Cognitive Deficits Through Targeting c-jun-N-terminal Kinase 3 in Alzheimer's Disease. *Curr. Neurovasc. Res.* **2020**, *17*, 93–101. [CrossRef] [PubMed]
173. Ji, Y.; Wang, D.; Zhang, B.; Lu, H. MiR-361-3p inhibits β-amyloid accumulation and attenuates cognitive deficits through targeting BACE1 in Alzheimer's disease. *J. Integr. Neurosci.* **2019**, *18*, 285–291. [CrossRef] [PubMed]
174. Wang, L.; Liu, J.; Wang, Q.; Jiang, H.; Zeng, L.; Li, Z.; Liu, R. MicroRNA-200a-3p Mediates Neuroprotection in Alzheimer-Related Deficits and Attenuates Amyloid-Beta Overproduction and Tau Hyperphosphorylation via Coregulating BACE1 and PRKACB. *Front. Pharmacol.* **2019**, *10*, 806. [CrossRef] [PubMed]
175. Xu, W.; Li, K.; Fan, Q.; Zong, B.; Han, L. Knockdown of long non-coding RNA SOX21-AS1 attenuates amyloid-β-induced neuronal damage by sponging miR-107. *Biosci. Rep.* **2020**, *40*, BSR20194295. [CrossRef]
176. Tan, X.; Luo, Y.; Pi, D.; Xia, L.; Li, Z.; Tu, Q. miR-340 reduces accumulation of amyloid-β through targeting BACE1 (β-site amyloid precursor protein cleaving enzyme 1) in Alzheimer' s disease. *Curr. Neurovasc. Res.* **2020**, *17*, 86–92. [CrossRef]
177. Baby, N.; Alagappan, N.; Dheen, S.T.; Sajikumar, S. MicroRNA-134-5p inhibition rescues long-term plasticity and synaptic tagging/capture in an Aβ(1–42)-induced model of Alzheimer's disease. *Aging Cell* **2020**, *19*, e13046. [CrossRef]
178. Hou, T.Y.; Zhou, Y.; Zhu, L.S.; Wang, X.; Pang, P.; Wang, D.Q.; Liuyang, Z.Y.; Man, H.; Lu, Y.; Zhu, L.Q.; et al. Correcting abnormalities in miR-124/PTPN1 signaling rescues tau pathology in Alzheimer's disease. *J. Neurochem.* **2020**, *154*, 441–457. [CrossRef]
179. Shi, Z.; Zhang, K.; Zhou, H.; Jiang, L.; Xie, B.; Wang, R.; Xia, W.; Yin, Y.; Gao, Z.; Cui, D.; et al. Increased miR-34c mediates synaptic deficits by targeting synaptotagmin 1 through ROS-JNK-p53 pathway in Alzheimer's Disease. *Aging Cell* **2020**, *19*, e13125. [CrossRef]
180. Wang, X.; Liu, D.; Huang, H.Z.; Wang, Z.H.; Hou, T.Y.; Yang, X.; Pang, P.; Wei, N.; Zhou, Y.F.; Dupras, M.J.; et al. A Novel MicroRNA124/PTPN1 Signal Pathway Mediates Synaptic and Memory Deficits in Alzheimer's Disease. *Biol. Psychiatry* **2018**, *83*, 395–405. [CrossRef]
181. Ansari, A.; Maffioletti, E.; Milanesi, E.; Marizzoni, M.; Frisoni, G.B.; Blin, O.; Richardson, J.C.; Bordet, R.; Forloni, G.; Gennarelli, M.; et al. miR-146a and miR-181a are involved in the progression of mild cognitive impairment to Alzheimer's disease. *Neurobiol. Aging* **2019**, *82*, 102–109. [CrossRef] [PubMed]
182. Ghanbari, M.; Munshi, S.T.; Ma, B.; Lendemeijer, B.; Bansal, S.; Adams, H.H.; Wang, W.; Goth, K.; Slump, D.E.; van den Hout, M.C.G.N.; et al. A functional variant in the miR-142 promoter modulating its expression and conferring risk of Alzheimer disease. *Hum. Mutat.* **2019**, *40*, 2131–2145. [CrossRef] [PubMed]

183. Li, H.; Yu, L.; Li, M.; Chen, X.; Tian, Q.; Jiang, Y.; Li, N. MicroRNA-150 serves as a diagnostic biomarker and is involved in the inflammatory pathogenesis of Parkinson's disease. *Mol. Genet. Genom. Med.* **2020**, *8*, e1189. [CrossRef]
184. Zhang, J.; Zhou, D.; Zhang, Z.; Qu, X.; Bao, K.; Lu, G.; Duan, J. miR-let-7a suppresses α-Synuclein-induced microglia inflammation through targeting STAT3 in Parkinson's disease. *Biochem. Biophys. Res. Commun.* **2019**, *519*, 740–746. [CrossRef] [PubMed]
185. Sun, Q.; Wang, S.; Chen, J.; Cai, H.; Huang, W.; Zhang, Y.; Wang, L.; Xing, Y. MicroRNA-190 alleviates neuronal damage and inhibits neuroinflammation via Nlrp3 in MPTP-induced Parkinson's disease mouse model. *J. Cell. Physiol.* **2019**, *234*, 23379–23387. [CrossRef] [PubMed]
186. Zeng, R.; Luo, D.-X.; Li, H.-P.; Zhang, Q.-S.; Lei, S.-S.; Chen, J.-H. MicroRNA-135b alleviates MPP^+-mediated Parkinson's disease in in vitro model through suppressing FoxO1-induced NLRP3 inflammasome and pyroptosis. *J. Clin. Neurosci.* **2019**, *65*, 125–133. [CrossRef] [PubMed]
187. Cai, L.J.; Tu, L.; Li, T.; Yang, X.L.; Ren, Y.P.; Gu, R.; Zhang, Q.; Yao, H.; Qu, X.; Wang, Q.; et al. Up-regulation of microRNA-375 ameliorates the damage of dopaminergic neurons, reduces oxidative stress and inflammation in Parkinson's disease by inhibiting SP1. *Aging* **2020**, *12*, 672–689. [CrossRef]
188. Wang, R.; Yang, Y.; Wang, H.; He, Y.; Li, C. MiR-29c protects against inflammation and apoptosis in Parkinson's disease model in vivo and in vitro by targeting SP1. *Clin. Exp. Pharmacol. Physiol.* **2019**, *47*, 372–382. [CrossRef]
189. Liu, W.; Li, L.; Liu, S.; Wang, Z.; Kuang, H.; Xia, Y.; Tang, C.; Yin, D. MicroRNA Expression Profiling Screen miR-3557/324-Targeted CaMK/mTOR in the Rat Striatum of Parkinson's Disease in Regular Aerobic Exercise. *Biomed Res. Int.* **2019**, *2019*, 7654798. [CrossRef]
190. Ge, H.; Yan, Z.; Zhu, H.; Zhao, H. MiR-410 exerts neuroprotective effects in a cellular model of Parkinson's disease induced by 6-hydroxydopamine via inhibiting the PTEN/AKT/mTOR signaling pathway. *Exp. Mol. Pathol.* **2019**, *109*, 16–24. [CrossRef]
191. Zhao, X.H.; Wang, Y.B.; Yang, J.; Liu, H.Q.; Wang, L.L. MicroRNA-326 suppresses iNOS expression and promotes autophagy of dopaminergic neurons through the JNK signaling by targeting XBP1 in a mouse model of Parkinson's disease. *J. Cell. Biochem.* **2019**, *120*, 14995–15006. [CrossRef] [PubMed]
192. Ren, Y.; Li, H.; Xie, W.; Wei, N.; Liu, M. MicroRNA-195 triggers neuroinflammation in Parkinson's disease in a Rho-associated kinase 1-dependent manner. *Mol. Med. Rep.* **2019**, *19*, 5153–5161. [CrossRef] [PubMed]
193. Li, B.; Jiang, Y.; Xu, Y.; Li, Y.; Li, B. Identification of miRNA-7 as a regulator of brain-derived neurotrophic fac-tor/A-synuclein axis in atrazine-induced Parkinson's disease by peripheral blood and brain microRNA profiling. *Chemosphere* **2019**, *233*, 542–548. [CrossRef] [PubMed]
194. Baghi, M.; Delavar, M.R.; Yadegari, E.; Peymani, M.; Pozo, D.; Nasr-Esfahani, M.H.; Ghaedi, K. Modified level of miR-376a is associated with Parkinson's disease. *J. Cell. Mol. Med.* **2020**, *24*, 2622–2634. [CrossRef] [PubMed]
195. De Luna, N.; Turon-Sans, J.; Cortes-Vicente, E.; Carrasco-Rozas, A.; Illán-Gala, I.; Dols-Icardo, O.; Clarimón, J.; Lleó, A.; Gallardo, E.; Illa, I.; et al. Downregulation of miR-335-5P in Amyotrophic Lateral Sclerosis Can Contribute to Neuronal Mitochondrial Dysfunction and Apoptosis. *Sci. Rep.* **2020**, *10*, 4308. [CrossRef]
196. Rohm, M.; May, C.; Marcus, K.; Steinbach, S.; Theis, V.; Theiss, C.; Matschke, V. The microRNA miR-375-3p and the tumor suppressor NDRG2 are involved in sporadic amyotrophic lateral sclerosis. *Cell. Physiol. Biochem.* **2019**, *52*, 1412–1426.
197. Klatt, C.L.; Theis, V.; Hahn, S.; Theiss, C.; Matschke, V. Deregulated miR-29b-3p Correlates with Tissue-Specific Activation of Intrinsic Apoptosis in An Animal Model of Amyotrophic Lateral Sclerosis. *Cells* **2019**, *8*, 1077. [CrossRef]
198. Maimon, R.; Ionescu, A.; Bonnie, A.; Sweetat, S.; Wald-Altman, S.; Inbar, S.; Gradus, T.; Trotti, D.; Weil, M.; Behar, O.; et al. miR126-5p Downregulation Facilitates Axon Degeneration and NMJ Disruption via a Non-Cell-Autonomous Mechanism in ALS. *J. Neurosci.* **2018**, *38*, 5478–5494. [CrossRef]
199. Varcianna, A.; Myszczynska, M.A.; Castelli, L.M.; O'Neill, B.; Kim, Y.; Talbot, J.; Nyberg, S.; Nyamali, I.; Heath, P.R.; Stopford, M.J.; et al. Micro-RNAs secreted through astrocyte-derived extracellular vesicles cause neuronal network degeneration in C9orf72 ALS. *eBioMedicine* **2019**, *40*, 626–635. [CrossRef]
200. Helferich, A.M.; Brockmann, S.J.; Reinders, J.; Deshpande, D.; Holzmann, K.; Brenner, D.; Andersen, P.M.; Petri, S.; Thal, D.R.; Michaelis, J.; et al. Dysregulation of a novel miR-1825/TBCB/TUBA4A pathway in sporadic and familial ALS. *Cell. Mol. Life Sci.* **2018**, *75*, 4301–4319. [CrossRef]
201. Li, C.; Wei, Q.; Gu, X.; Chen, Y.; Chen, X.; Cao, B.; Ou, R.; Shang, H. Decreased Glycogenolysis by miR-338-3p Promotes Regional Glycogen Accumulation Within the Spinal Cord of Amyotrophic Lateral Sclerosis Mice. *Front. Mol. Neurosci.* **2019**, *12*, 114. [CrossRef] [PubMed]
202. Hawley, Z.C.E.; Campos-Melo, D.; Strong, M.J. MiR-105 and miR-9 regulate the mRNA stability of neuronal intermediate filaments. Implications for the pathogenesis of amyotrophic lateral sclerosis (ALS). *Brain Res.* **2019**, *1706*, 93–100. [CrossRef] [PubMed]
203. Hoye, M.L.; Regan, M.R.; A Jensen, L.; Lake, A.M.; Reddy, L.V.; Vidensky, S.; Richard, J.-P.; Maragakis, N.J.; Rothstein, J.D.; Dougherty, J.D.; et al. Motor neuron-derived microRNAs cause astrocyte dysfunction in amyotrophic lateral sclerosis. *Brain* **2018**, *141*, 2561–2575. [CrossRef] [PubMed]
204. Williams, A.H.; Valdez, G.; Moresi, V.; Qi, X.; McAnally, J.; Elliott, J.L.; Bassel-Duby, R.; Sanes, J.R.; Olson, E.N. MicroRNA-206 Delays ALS Progression and Promotes Regeneration of Neuromuscular Synapses in Mice. *Science* **2009**, *326*, 1549–1554. [CrossRef]

205. Tung, Y.-T.; Peng, K.-C.; Chen, Y.-C.; Yen, Y.-P.; Chang, M.; Thams, S.; Chen, J.-A. Mir-17~92 Confers Motor Neuron Subtype Differential Resistance to ALS-Associated Degeneration. *Cell Stem Cell* **2019**, *25*, 193–209.e7. [CrossRef]
206. Mégret, L.; Nair, S.S.; Dancourt, J.; Aaronson, J.; Rosinski, J.; Neri, C. Combining feature selection and shape analysis uncovers precise rules for miRNA regulation in Huntington's disease mice. *BMC Bioinform.* **2020**, *21*, 75. [CrossRef]
207. Fukuoka, M.; Takahashi, M.; Fujita, H.; Chiyo, T.; Popiel, H.A.; Watanabe, S.; Furuya, H.; Murata, M.; Wada, K.; Okada, T.; et al. Supplemental Treatment for Huntington's Disease with miR-132 that Is Deficient in Huntington's Disease Brain. *Mol. Ther. Nucleic Acids* **2018**, *11*, 79–90. [CrossRef]
208. Kunkanjanawan, T.; Carter, R.L.; Prucha, M.S.; Yang, J.; Parnpai, R.; Chan, A.W.S. miR-196a Ameliorates Cytotoxicity and Cellular Phenotype in Transgenic Huntington's Disease Monkey Neural Cells. *PLoS ONE* **2016**, *11*, e0162788. [CrossRef]
209. Her, L.-S.; Mao, S.-H.; Chang, C.-Y.; Cheng, P.-H.; Chang, Y.-F.; Yang, H.-I.; Chen, C.-M.; Yang, S.-H. miR-196a Enhances Neuronal Morphology through Suppressing RANBP10 to Provide Neuroprotection in Huntington's Disease. *Theranostics* **2017**, *7*, 2452–2462. [CrossRef]
210. Ban, J.-J.; Chung, J.-Y.; Lee, M.; Im, W.; Kim, M. MicroRNA-27a reduces mutant hutingtin aggregation in an in vitro model of Huntington's disease. *Biochem. Biophys. Res. Commun.* **2017**, *488*, 316–321. [CrossRef]
211. Pfister, E.L.; DiNardo, N.; Mondo, E.; Borel, F.; Conroy, F.; Fraser, C.; Gernoux, G.; Han, X.; Hu, D.; Johnson, E.; et al. Artificial miRNAs Reduce Human Mutant Huntingtin Throughout the Striatum in a Transgenic Sheep Model of Huntington's Disease. *Hum. Gene Ther.* **2018**, *29*, 663–673. [CrossRef] [PubMed]
212. Caron, N.S.; Southwell, A.L.; Brouwers, C.C.; Cengio, L.D.; Xie, Y.; Black, H.F.; Anderson, L.M.; Ko, S.; Zhu, X.; van Deventer, S.J.; et al. Potent and sustained huntingtin lowering via AAV5 encoding miRNA preserves striatal volume and cognitive function in a humanized mouse model of Huntington disease. *Nucleic Acids Res.* **2019**, *48*, 36–54. [CrossRef] [PubMed]
213. Cordeiro, Y.; Macedo, B.; Silva, J.L.; Gomes, M.P.B. Pathological implications of nucleic acid interactions with proteins associated with neurodegenerative diseases. *Biophys. Rev.* **2014**, *6*, 97–110. [CrossRef] [PubMed]
214. Cordeiro, Y.; Silva, J.L. The Hypothesis of the Catalytic Action of Nucleic Acid on the Conversion of Prion Protein. *Protein Pept. Lett.* **2005**, *12*, 251–255. [CrossRef]
215. Macedo, B.; Millen, T.A.; Braga, C.A.C.A.; Gomes, M.P.B.; Ferreira, P.S.; Kraineva, J.; Winter, R.; Silva, J.; Cordeiro, Y. Nonspecific Prion Protein–Nucleic Acid Interactions Lead to Different Aggregates and Cytotoxic Species. *Biochemistry* **2012**, *51*, 5402–5413. [CrossRef]
216. Gomes, M.P.B.; Millen, T.A.; Ferreira, P.S.; e Silva, N.L.C.; Vieira, T.C.R.G.; Almeida, M.; Silva, J.L.; Cordeiro, Y. Prion Protein Complexed to N2a Cellular RNAs through Its N-terminal Domain Forms Aggregates and Is Toxic to Murine Neuroblastoma Cells. *J. Biol. Chem.* **2008**, *283*, 19616–19625. [CrossRef]
217. Tandon, A.; Subramani, V.K.; Kim, K.K.; Park, S.H. Interaction of Prion Peptides with DNA Structures. *ACS Omega* **2021**, *7*, 176–186. [CrossRef]
218. Adler, V.; Zeiler, B.; Kryukov, V.; Kascsak, R.; Rubenstein, R.; Grossman, A. Small, highly structured RNAs participate in the conversion of human recombinant PrPSen to PrPRes in vitro. *J. Mol. Biol.* **2003**, *332*, 47–57. [CrossRef]
219. Deleault, N.R.; Lucassen, R.W.; Supattapone, S. RNA molecules stimulate prion protein conversion. *Nature* **2003**, *425*, 717–720. [CrossRef]
220. Mashima, T.; Nishikawa, F.; Kamatari, Y.O.; Fujiwara, H.; Saimura, M.; Nagata, T.; Kodaki, T.; Nishikawa, S.; Kuwata, K.; Katahira, M. Anti-prion activity of an RNA aptamer and its structural basis. *Nucleic Acids Res.* **2012**, *41*, 1355–1362. [CrossRef]
221. Dalai, W.; Matsuo, E.; Takeyama, N.; Kawano, J.; Saeki, K. CpG site DNA methylation patterns reveal a novel regulatory element in the mouse prion protein gene. *J. Vet. Med. Sci.* **2017**, *79*, 100–107. [CrossRef] [PubMed]
222. Dalai, W.; Matsuo, E.; Takeyama, N.; Kawano, J.; Saeki, K. Increased expression of prion protein gene is accompanied by demethylation of CpG sites in a mouse embryonal carcinoma cell line, P19C6. *J. Vet. Med. Sci.* **2017**, *79*, 644–648. [CrossRef] [PubMed]
223. Dabin, L.C.; Guntoro, F.; Campbell, T.; Bélicard, T.; Smith, A.R.; Smith, R.G.; Raybould, R.; Schott, J.M.; Lunnon, K.; Sarkies, P.; et al. Altered DNA methylation profiles in blood from patients with sporadic Creutzfeldt–Jakob disease. *Acta Neuropathol.* **2020**, *140*, 863–879. [CrossRef] [PubMed]
224. Hernaiz, A.; Sanz, A.; Sentre, S.; Ranera, B.; Lopez-Pérez, O.; Zaragoza, P.; Badiola, J.J.; Filali, H.; Bolea, R.; Toivonen, J.M.; et al. Genome-Wide Methylation Profiling in the Thalamus of Scrapie Sheep. *Front. Vet. Sci.* **2022**, *9*, 824677. [CrossRef]
225. Guntoro, F.; Viré, E.; Giordani, C.; Darwent, L.; Hummerich, H.; Linehan, J.; Sinka, K.; Jaunmuktane, Z.; Brandner, S.; Collinge, J.; et al. DNA methylation analysis of archival lymphoreticular tissues in Creutzfeldt–Jakob disease. *Acta Neuropathol.* **2022**, *144*, 785–787. [CrossRef]
226. Harvey, Z.H.; Chakravarty, A.K.; Futia, R.A.; Jarosz, D.F. A Prion Epigenetic Switch Establishes an Active Chromatin State. *Cell* **2020**, *180*, 928–940.e14. [CrossRef]
227. Zhu, T.; Zhao, D.; Song, Z.; Yuan, Z.; Li, C.; Wang, Y.; Zhou, X.; Yin, X.; Hassan, M.F.; Yang, L. HDAC6 alleviates prion peptide-mediated neuronal death via modulating PI3K-Akt-mTOR pathway. *Neurobiol. Aging* **2016**, *37*, 91–102. [CrossRef]
228. Seo, J.-S.; Moon, M.-H.; Jeong, J.-K.; Seol, J.-W.; Lee, Y.-J.; Park, B.-H.; Park, S.-Y. SIRT1, a histone deacetylase, regulates prion protein-induced neuronal cell death. *Neurobiol. Aging* **2012**, *33*, 1110–1120. [CrossRef]
229. Jeong, J.-K.; Moon, M.-H.; Lee, Y.-J.; Seol, J.-W.; Park, S.-Y. Autophagy induced by the class III histone deacetylase Sirt1 prevents prion peptide neurotoxicity. *Neurobiol. Aging* **2012**, *34*, 146–156. [CrossRef]
230. Wang, J.; Zhang, J.; Shi, Q.; Zhang, B.-Y.; Chen, C.; Chen, L.-N.; Sun, J.; Wang, H.; Xiao, K.; Dong, X.-P. Scrapie Infection in

Experimental Rodents and SMB-S15 Cells Decreased the Brain Endogenous Levels and Activities of Sirt1. *J. Mol. Neurosci.* **2014**, *55*, 1022–1030. [CrossRef]

231. Boese, A.S.; Saba, R.; Campbell, K.; Majer, A.; Medina, S.; Burton, L.; Booth, T.F.; Chong, P.; Westmacott, G.; Dutta, S.M.; et al. MicroRNA abundance is altered in synaptoneurosomes during prion disease. *Mol. Cell. Neurosci.* **2016**, *71*, 13–24. [CrossRef] [PubMed]
232. Gao, C.; Wei, J.; Zhang, B.-Y.; Shi, Q.; Chen, C.; Wang, J.; Shi, Q.; Dong, X.-P. MiRNA expression profiles in the brains of mice infected with scrapie agents 139A, ME7 and S15. *Emerg. Microbes Infect.* **2016**, *5*, 1–10. [CrossRef] [PubMed]
233. Toivonen, J.M.; Sanz-Rubio, D.; López-Pérez, Ó.; Marín-Moreno, A.; Bolea, R.; Osta, R.; Badiola, J.J.; Zaragoza, P.; Espinosa, J.-C.; Torres, J.-M.; et al. MicroRNA Alterations in a Tg501 Mouse Model of Prion Disease. *Biomolecules* **2020**, *10*, 908. [CrossRef] [PubMed]
234. Slota, J.; Medina, S.J.; Klassen, M.; Gorski, D.; Mesa, C.M.; Robertson, C.; Mitchell, G.; Coulthart, M.B.; Pritzkow, S.; Soto, C.; et al. Identification of circulating microRNA signatures as potential biomarkers in the serum of elk infected with chronic wasting disease. *Sci. Rep.* **2019**, *9*, 19705. [CrossRef]
235. Rubio, D.S.; López-Pérez, Ó.; de Andrés Pablo, A.; Bolea, R.; Osta, R.; Badiola, J.J.; Zaragoza, P.; Martín-Burriel, I.; Toivonen, J.M. Increased circulating microRNAs miR-342-3p and miR-21-5p in natural sheep prion disease. *J. Gen. Virol.* **2017**, *98*, 305–310. [CrossRef]
236. Pease, D.; Scheckel, C.; Schaper, E.; Eckhardt, V.; Emmenegger, M.; Xenarios, I.; Aguzzi, A. Genome-wide identification of microRNAs regulating the human prion protein. *Brain Pathol.* **2018**, *29*, 232–244. [CrossRef]
237. Burak, K.; Lamoureux, L.; Boese, A.; Majer, A.; Saba, R.; Niu, Y.; Frost, K.; Booth, S.A. MicroRNA-16 targets mRNA involved in neurite extension and branching in hippocampal neurons during presymptomatic prion disease. *Neurobiol. Dis.* **2018**, *112*, 1–13. [CrossRef]
238. Gao, C.; Shi, Q.; Wei, J.; Zhou, W.; Xiao, K.; Wang, J.; Shi, Q.; Dong, X.-P. The associations of two SNPs in miRNA-146a and one SNP in ZBTB38-RASA2 with the disease susceptibility and the clinical features of the Chinese patients of sCJD and FFI. *Prion* **2018**, *12*, 34–41. [CrossRef]
239. Kang, S.-G.; Kim, C.; Aiken, J.; Yoo, H.S.; McKenzie, D. Dual MicroRNA to Cellular Prion Protein Inhibits Propagation of Pathogenic Prion Protein in Cultured Cells. *Mol. Neurobiol.* **2017**, *55*, 2384–2396. [CrossRef]

MANUSCRITO II

Genome-Wide Methylation Profiling in the Thalamus of Scrapie Sheep.

Hernaiz, Adelaida; Sanz, Arianne; Sentre, Sara; Ranera, Beatriz; Lopez-Pérez, Óscar; Zaragoza, Pilar; Badiola, Juan José; Filali, Hicham; Bolea, Rosa; Toivonen, Janne Markus; Martín-Burriel, Inmaculada.

Frontiers in Veterinary Science. Vol. 0, pág. 29, 2022. doi:10.3389/FVETS.2022.824677.

frontiers in Veterinary Science

ORIGINAL RESEARCH
published: 16 February 2022
doi: 10.3389/fvets.2022.824677

Genome-Wide Methylation Profiling in the Thalamus of Scrapie Sheep

Adelaida Hernaiz[1], Arianne Sanz[1], Sara Sentre[1], Beatriz Ranera[2], Oscar Lopez-Pérez[1,3], Pilar Zaragoza[1], Juan J. Badiola[3], Hicham Filali[3], Rosa Bolea[3], Janne M. Toivonen[1,4†] and Inmaculada Martín-Burriel[1,3,4†]*

[1] Laboratorio de Genética Bioquímica (LAGENBIO), Facultad de Veterinaria, Universidad de Zaragoza-IA2, IIS, Zaragoza, Spain, [2] Facultad de Ciencias de la Salud, Universidad San Jorge, Zaragoza, Spain, [3] Centro de Encefalopatías y Enfermedades Transmisibles Emergentes (CEETE), Facultad de Veterinaria, Universidad de Zaragoza-IA2, IIS, Zaragoza, Spain, [4] Centro de Investigación Biomédica en Red de Enfermedades Neurodegenerativas (CIBERNED), Instituto de Salud Carlos III, Madrid, Spain

Scrapie is a neurodegenerative disorder belonging to the group of transmissible spongiform encephalopathy (TSE). Scrapie occurs in sheep and goats, which are considered good natural animal models of these TSE. Changes in DNA methylation occur in the central nervous system (CNS) of patients suffering from prion-like neurodegenerative diseases, such as Alzheimer's disease. Nevertheless, potential DNA methylation alterations have not yet been investigated in the CNS of any prion disease model or naturally infected cases, neither in humans nor in animals. Genome-wide DNA methylation patterns were studied in the thalamus obtained from sheep naturally infected with scrapie at a clinical stage ($n = 4$) and from controls ($n = 4$) by performing a whole-genome bisulfite sequencing (WGBS) analysis. Ewes carried the scrapie-susceptible ARQ/ARQ *PRNP* genotype and were sacrificed at a similar age (4–6 years). Although the average genomic methylation levels were similar between the control and the scrapie animals, we identified 8,907 significant differentially methylated regions (DMRs) and 39 promoters (DMPs). Gene Ontology analysis revealed that hypomethylated DMRs were enriched in genes involved in transmembrane transport and cell adhesion, whereas hypermethylated DMRs were related to intracellular signal transduction genes. Moreover, genes highly expressed in specific types of CNS cells and those previously described to be differentially expressed in scrapie brains contained DMRs. Finally, a quantitative PCR (qPCR) validation indicated differences in the expression of five genes (*PCDH19*, *SNCG*, *WDR45B*, *PEX1*, and *CABIN1*) that matched the methylation changes observed in the genomic study. Altogether, these results suggest a potential regulatory role of DNA methylation in prion neuropathology.

Keywords: DNA methylation, thalamus, ovine scrapie, prion, whole genome bisulfite sequencing

OPEN ACCESS

Edited by:
Cristina Lecchi,
University of Milan, Italy

Reviewed by:
Cemal ÜN,
Ege University, Turkey
James Hope,
Animal and Plant Health Agency, United Kingdom

****Correspondence:***
Inmaculada Martín-Burriel
minma@unizar.es

† These authors have contributed equally to this work

Specialty section:
This article was submitted to Veterinary Experimental and Diagnostic Pathology, a section of the journal Frontiers in Veterinary Science

Received: *29 November 2021*
Accepted: *05 January 2022*
Published: *16 February 2022*

Citation:
Hernaiz A, Sanz A, Sentre S, Ranera B, Lopez-Pérez O, Zaragoza P, Badiola JJ, Filali H, Bolea R, Toivonen JM and Martín-Burriel I (2022) Genome-Wide Methylation Profiling in the Thalamus of Scrapie Sheep. Front. Vet. Sci. 9:824677. doi: 10.3389/fvets.2022.824677

INTRODUCTION

Prion diseases are fatal and transmissible neurodegenerative disorders that occur in humans and animals (1). These diseases are caused by the conformational conversion of the cellular prion protein (PrP^{C}) to an infectious isoform PrP^{Sc}, which is partially resistant to proteases and prone to form aggregates (2). The accumulation of PrP^{Sc} in the central nervous system (CNS)

causes spongiform neuronal degeneration, activation of glial cells, and neuronal loss (3). Ovine scrapie was the first reported transmissible spongiform encephalopathy (TSE) (4) and has been widely studied. Several transcriptomic studies performed in sheep have reported differentially expressed genes (DEGs) and proteins that seem to be involved in the pathogenesis of scrapie and other neurodegenerative diseases including human prion diseases (5–8). These common findings between scrapie and human prion diseases support the use of scrapie sheep as a good natural animal model to study the molecular mechanisms of prion neuropathology and to identify potential diagnostic and therapeutic biomarkers for prion diseases.

Functional genomics provides important tools to investigate molecular mechanisms of the disease and potential disease biomarkers. In previous studies, using custom arrays, we described significant changes in the CNS transcriptome of sheep naturally infected with scrapie at the early and late stages of the disease (5, 6). Dysregulated genes were associated with ion binding and transport, nucleotide binding, structural molecules, immune system, secreted extracellular proteins, lysosomal proteases, and phospho-proteins.

Gene expression can be modulated by epigenetic mechanisms. DNA methylation at the C5 position of Cytosine (mC) is one of the main epigenetic regulatory mechanisms, which is essential for the adequate development of the organism. Methylation usually occurs in CpG islands (CGIs) located in promoter regions or regulatory domains and also within intergenic regions (9). Environmental variables, such as nutrition and stress exposure, can induce alterations in DNA methylation (10). Many of these may constitute epigenetic drift; that is, they are not translated into phenotypic effect. However, some environmental changes may display a relevant effect in the modulation of gene expression in disease-associated status (11).

Epigenetics regulate neural activity in the brain (12), and DNA methylation seems to be important in memory formation and aging-related cognitive decline (13, 14). Regulation by DNA methylation of specific genes in Alzheimer's disease (AD) (15, 16) and in Parkinson's disease (PD) (17) has been demonstrated. Distinct methylation observed in PD patients involves genes previously associated with the disease, and concordant alterations between the brain and peripheral blood leukocytes have been found (18). Hypermethylation also occurs in the G4C2 repeat expansion in C9orf72, which is the most common known cause of amyotrophic lateral sclerosis (ALS) and frontotemporal lobar degeneration (FTLD). The hypermethylation seems to be associated with the presence of the expansion, which could be responsible for C9orf72 downregulation in the disease (19). Global methylation is also altered in the spinal cord of sporadic ALS patients where both hyper- and hypomethylation can directly modulate the expression of adjacent genes (20).

The abovementioned evidence from other neurodegenerative diseases suggests that DNA methylation status may also contribute to the development of prion diseases. The mouse gene coding PrP^{C} contains a CGI in its promotor that seems to modulate the expression of this protein in a tissue-specific manner (21). However, methylation has not been observed in the promoter of the rat *PRNP* gene, at least in PC12 cells (22). Regarding prion diseases, DNA methylation studies at a genomic level have only been performed in blood from patients with sporadic Creutzfeldt–Jakob disease (sCJD), the most common human prion disease (23). To the best of our knowledge, no genome-wide DNA methylation studies have yet been reported in the CNS of any prion disease models or naturally infected cases. We present here a whole-genome bisulfite sequencing (WGBS) analysis of the thalamus obtained from sheep naturally infected with scrapie. The study revealed a number of differentially methylated regions (DMRs) between the control and scrapie animals, as well as an enrichment of several cellular and molecular functions that could contribute to prion-related neuropathology. We compared these results with previously described transcriptomic changes and performed a gene expression analysis that revealed significant changes in the expression of several genes with differential methylation. Of these, several also correlated with prion-related lesions.

MATERIALS AND METHODS

Animals and Tissue Selection

Thalamus samples from eight Rasa Aragonesa sheep were used for WGBS analysis. Four of them were controls, and the other four were naturally infected with scrapie. All the ewes were aged from 4 to 6 years and carried the ARQ/ARQ genotype for the *PRNP* gene (**Supplementary Table S1**). These animals correspond to those used previously in an association study between gene expression profiles and scrapie-related lesions in the medulla oblongata of scrapie-infected sheep (5). All scrapie animals displayed clear symptomatology. The time the animals were maintained until sacrifice is shown in **Supplementary Table S1**. Histopathological lesions related to prion diseases (PrP^{Sc} deposition, neuronal vacuolation, spongiosis, and gliosis) were semiquantified in a previous study (24) and are shown in **Supplementary Table S1**.

The expression of selected differentially methylated genes (DMGs) was evaluated by quantitative PCR (qPCR) using a different set of thalamus samples, with five tissues obtained from control sheep and eight from naturally infected scrapie animals.

Whole-Genome Bisulfite Sequencing Library Preparation and Sequencing

Genomic DNA was isolated from the thalamus using the Quick-DNA Midiprep Plus kit (Zymo Research, Irvine, CA, USA). Before library construction, degradation of DNA was checked by agarose gel electrophoresis, DNA purity (260/280 ratio) was assessed using NanoDrop spectrophotometer (Thermo Fisher Scientific, Waltham, MA, USA), and the quality and quantity of DNA were determined using Qubit® 2.0 fluorometer (Life Technologies, Carlsbad, CA, USA).

Sequencing libraries were constructed for the different genomic DNA samples. Approximately 2.5 μg of genomic DNA spiked with 12.5 ng of lambda DNA was fragmented by sonication to 200–400 bp with Biorupter, followed by end repair and adenylation. EZ DNA Methylation-Gold Kit (Zymo Research) was used to treat DNA fragments with bisulfite. Afterwards, fragments were selected by size and PCR amplified

using KAPA HiFi HotStart Uracil + ReadyMix (2×). Library DNA concentration was firstly quantified with Qubit2.0 and then diluted to 1 ng/?l before checking insert size on Agilent 2100 (Agilent Technologies, Santa Clara, CA, USA) and quantified with more accuracy by qPCR (effective concentration of library >2 nM). Libraries were then sequenced on the Illumina HiSeq Xten platform, and 150-bp paired-end reads were generated according to Illumina's protocol. Raw and processed WGBS data are stored at the National Center for Biotechnology Information (NCBI) GEO Series record GSE184767. Library preparation and WGBS were performed by Novogene (UK) Company Limited (Cambridge, UK).

Data Analysis

Raw reads were saved as fastq format files, and Trimmomatic (v0.36) tool was used to filter out the contaminated adapter sequence and low-quality reads with default parameters. FastQC (v0.11.3) was also performed on the clean data obtained from trimming. Bisulfite-treated reads were aligned with the reference genome (Oar_v4.0) using the Bismark (v0.12.5) software (25) with default parameters. After alignment, Bismark was used to calculate read coverage and sequencing depth, distribution of genome coverage, distribution of chromosome depth and coverage, and coverage depth of each cytosine site context (CpG, CHH, and CHG, where H = A, C, or G) and to identify methylated sites by comparison of read base and the reference genome base at the same position. The bigWig format files containing mapping results, as well as corresponding reference genome and gene annotation files, were visualized using the IGV (Integrative Genomic Viewer) software. In order to find accurate methylated sites, sequencing depth $\geq$5 and q-values $\leq$0.05 were set as thresholds in the analysis (26, 27). For methylated sites, the methylation level was calculated using the formula ML = mCc/(mCc + umCc), where ML represents the methylation level, and mCc and umCc represent the methylated and unmethylated read counts, respectively. The average methylation level of the whole genome was calculated in each sample with 10 kb as a bin. The average methylation level of all the covered cytosine sites on each chromosome was also calculated. The average methylated level in different cytosine contexts was evaluated in different functional genomic regions such as promotor [2-kb region above a transcriptional start site (TSS)], 5′UTR, exon, intron, CGI, and CGI shore. Functional areas of each gene were divided into 20 bins. Finally, motif characteristics around the positions of methylated cytosines were determined in high-methylated (methylation level higher than 75% in CG context and higher than 25% in non-CG context) and low-methylated sites and in all mC sites.

Differentially Methylated Region Analysis

DMRs between scrapie and control groups were determined by employing the Bsseq (v0.6.2) software from the Bioconductor (v2.13) package (28) (http://www.bioconductor.org/packages/release/bioc/html/bsseq.html) with default parameters. Bsseq is based on the BSmooth algorithm and targeted for WGBS data. As more variations may occur between scrapie samples than between control samples, the variance was estimated using data from the control group. To identify differentially methylated sites, *t*-test and quantile-based screening (cutoff set as [2.5%, 97.5%], namely, false discovery rate (FDR) < 0.05) were performed. Differentially methylated sites were merged and filtered to obtain the final DMRs with a threshold of at least 0.1 difference in methylation level and at least 3 cytosine sites in every DMR, being two adjacent cytosine sites not beyond 300 bp. DMRs were annotated when overlapping with functional elements (exon, intron, or promoters) of associated genes.

Differentially Methylated Promoter Analysis

Differentially methylated promoters (DMPs) were identified by testing for each cytosine in each context (CG, CHG, and CHH) of the promoter region using Fisher's exact test. Then, the p-value was corrected applying an FDR < 0.05 and an absolute difference of the methylation levels between the scrapie and the control group >0.2. The promoter region was set as the upstream 2 kb of TSS. Hierarchical clustering methods were adopted to analyze the methylation level of DMPs in scrapie and control thalami.

Enrichment Analysis

Gene Ontology (GO; http://www.geneontology.org/) and Kyoto Encyclopedia of Genes and Genomes (KEGG) pathways analysis were performed to identify the significant function and pathways of genes associated with DMRs and DMPs (DMGs). GO and KEGG terms with corrected $p < 0.05$ were considered significantly enriched by DMGs.

To investigate if DMGs were expressed in a specific type of CNS cell, a comparison of DMGs with proteins defined as tenfold more abundant in oligodendrocytes, astrocytes, microglia, and cortical neurons in the mouse brain (29) was performed using the InteractiVenn software (30). Afterwards, an enrichment analysis in Reactome (31) was conducted in order to reveal possible pathways with DMGs.

New Microarray Proof Annotation and Comparison With Identified Differentially Methylated Regions

In a previous study using custom arrays, significant changes in the expression profile of several genes were found in the CNS of sheep naturally infected with scrapie compared to healthy animals (5). As the tissues of this former report belonged to the same animals used in our study, the datasets that contained differentially expressed probes between symptomatic and non-symptomatic animals were used to perform a new annotation. The BLAST-Like Alignment Tool (BLAT) (32) was used to identify the chromosome, the strand, and the location of the beginning and the end of the alignment from the probe in the reference Oar v3.1 genome. That information was included as new information in the original dataset.

Subsequently, the data were loaded into a data.frame object in R (version 3.6.1), and the biomaRt (33, 34) package was used to retrieve annotation information and identifier cross-references from Ensembl. Oar v3.1 reference genome from Ensembl was used as the dataset. Attributes to query the database were as follows: chromosome_name, start_position, end_position, strand,

external_gene_name, refseq_mrna_predicted, refseq_mrna, description, external_synonym, and wikigene_name in order to obtain the annotated gene for the probe. Subsequently, annotated genes were included in the new dataset and exported into a comma-separated file.

Those probe sequences without any hit by biomaRt were manually annotated, using the Genome Data Viewer from the NCBI and, again, the Oar v3.1 reference genome (https://www.ncbi.nlm.nih.gov/genome/gdv/browser/genome/?id=GCF_000298735.1).

These genes differentially expressed in scrapie animals were then compared with the identified DMRs using the InteractiVenn software (30).

RNA/cDNA Preparation and Quantitative Real-Time PCR Analysis

Real-time qPCR was used to validate the biological functionality of a set of DMRs and DMPs by analyzing the expression levels of their linked DMGs. DMRs were selected for validation according to their level of methylation variation, the functionality of their associated genes, and their position in regulatory regions. Similarly, we chose DMPs taking into account the role of DMGs, the number of differentially regulated cytosines, and the level of change.

Total RNA was isolated using the RNeasy Lipid Tissue Mini kit (Qiagen, Valencia, CA, USA). The quality and quantity of RNA were determined using a NanoDrop instrument (Thermo Fisher Scientific, Waltham, MA, USA). cDNA samples were synthesized from 200 ng of total RNA using the reverse transcription (RT) reagent qScript cDNA SuperMix (Quantabio, Beverly, MA, USA). All procedures were performed following the manufacturer's recommended instructions.

The primers used for qPCR are listed in **Supplementary Table S2**. The reactions were performed on a QuantStudio 3 Real-Time PCR System (Thermo Fisher Scientific). Each PCR was performed by triplicate in a total volume of 10 μl, using 2 μl of cDNA, 300 nM of each primer, and Fast SYBR™ Green Master Mix (Applied Biosystems, Thermo Fisher Scientific). The comparative quantification of the results was standardized by the $2^{-\Delta\Delta Ct}$ method (35), using the geometric mean of *GAPDH*, *G6PDH*, and *SDHA* as a normalizer (36). Student's *t*-test was applied to identify differences between groups, which were considered significant at $p < 0.05$.

Correlation Between Methylation Levels, Gene Expression, and Prion-Related Lesions

Tissues analyzed in this work were used in previous studies to validate expression changes of candidate genes in different CNS areas, including the thalamus (24, 37). In these previous works, PrP^{Sc} deposition profiles, neuronal vacuolization, neuropil spongiosis, and gliosis were evaluated and semiquantitatively scored. These published scores were used to analyze any possible relationship between the degree of lesions and whole methylation levels in the different mC context or expression levels of DMGs using Pearson's correlation.

RESULTS

DNA Methylation Patterns

Between 832,778,776 and 1,152,563,414 sequencing raw reads were obtained per sample corresponding to 125 and 173 Gb of raw data, respectively. **Supplementary Table S3** shows the data quality of the resulting sequences. More than 97.5% of bases displayed a quality higher than Q20, and the percentage of bases showing higher quality (Q30) was higher than 93.7%. The percentage of bisulfite conversion was higher than 99.88% in all samples analyzed.

After raw data cleaning and trimming, the reads were mapped to the reference genome (Oar_v4.0). Between 258,079,070 and 339,064,958 clean reads were mapped on the genome with a percentage of unique mapping reads higher than 53% and covering more than 25 times the genome (**Table 1**). The percentage of genome bases with a minimum 5× coverage was higher than 85% and higher than 73% for a 10× coverage.

No significant differences were observed between scrapie and control sheep in the overall methylation level (**Supplementary Table S4**) for each cytosine context (mC in CG, CHG, and CHH), nor in the total percentage of methylated cytosines or in the percentages of methylated cytosines in these contexts (**Supplementary Table S5**), being the higher percentage of mC found in CpG context. Compared with the controls, the scrapie samples displayed higher variability in the percentages of methylated cytosines (**Supplementary Table S5**) and in the whole-genome methylation level (**Figure 1**). Sequence preferences flanking the 9 bp sequences around methylated C sites were similar in all samples (**Supplementary Figure S1**). No specific sequences were found in CG contexts, and CAG and CAC were the most frequent motifs in high and low methylation regions in CHG and CHH contexts, respectively.

Correlation Between PrP^{Sc} Accumulation and Methylation Levels

In order to explain the variability observed within the scrapie group, we compared global methylated cytosines in the different sites with the degree of PrP^{Sc} deposition in the thalamus within the analyzed animals. We obtained a significant negative correlation between PrP^{Sc} deposits and the percentage of methylated CHG sites ($r = -0.972$, $p = 0.028$) and a negative trend correlation with the percentages of mC sites ($r = -0.942$, $p = 0.057$) and mCHH sites ($r = -0.936$, $p = 0.064$) (**Figure 2A**).

Similarly, significant negative correlations were found between % mC ($r = -0.965$, $p = 0.03$) and % mCHH ($r = -0.976$, $p = 0.02$) and spongiosis in scrapie thalamus and a trend to signification between this lesion and % mCHG ($r = -0.933$, $p = 0.06$) (**Figure 2B**). On the contrary, a positive correlation was found between % mCHG ($r = 0.753$, $p = 0.03$) and reactive gliosis in the whole set of animals, but not when the group of scrapie sheep were analyzed separately (**Figure 2C**).

Finally, the time the animal was showing clinical symptoms could also explain the observed variation because animals showing the highest PrP^{Sc} deposition scores are those maintained for longer periods (**Supplementary Table S1**).

TABLE 1 | Overview of mapping and genome coverage.

Sample	Mapped reads	Unique mapping rate (%)[a]	Duplication rate (%)[b]	Sites coverage mean[c]	5× coverage[d]	10× coverage[e]
C1	339,064,958	59.64	15.94	31.94	85.26	74.66
C2	280,226,053	53.03	13.26	27.23	85.04	73.82
C3	298,189,223	69.19	13.11	29.07	86.39	75.28
C4	287,338,062	55.24	12.21	28.30	85.30	74.55
Sc1	294,158,670	71.52	11.76	29.15	86.79	76.62
Sc2	289,367,126	64.95	11.7	28.67	85.02	74.01
Sc3	292,893,236	71.15	12.13	28.84	86.22	75.75
Sc4	258,079,070	61.95	13.51	24.99	86.10	74.13

[a]*Percentage of uniquely mapped reads in the filtered clean reads used for mapping.*
[b]*Percentage of duplication reads.*
[c]*Sites coverage mean: the average base coverage of the genome.*
[d]*Percentage of bases with a minimum 5× coverage of the genome.*
[e]*Percentage of bases with a minimum 10× coverage of the genome.*

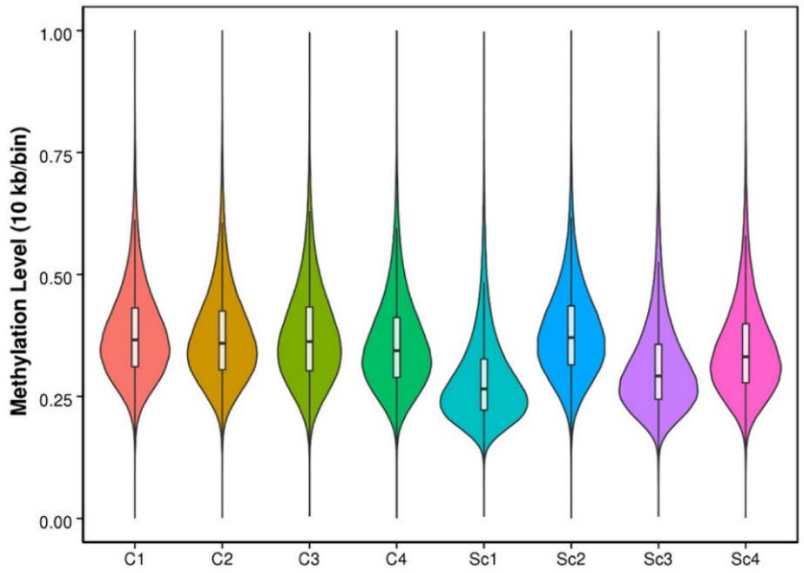

FIGURE 1 | Violin plot for the overall distribution of methylation levels using 10 kb/bin. The abscissa represents the different control (C) and scrapie (S) samples; the ordinate represents the level of methylation of the samples; and the width of each violin represents the density of the point at that methylation level.

Differentially Methylated Cytosines, Regions, and Promoters in Scrapie

DNA methylation level was investigated in different genome components including promoters, exons, and introns. Average methylation levels were similar in all samples, with exons having the features with a lower degree of methylation in all samples (**Supplementary Figure S2**).

Besides this lack of overall methylation changes, DMRs between the control and scrapie groups were identified using the Bsseq package. We identified 8,907 DMRs between scrapie and control tissues, from which 4,630 were hypermethylated and 4,277 hypomethylated (**Supplementary Table S6**). These DMRs were mainly distributed in introns (7,511), followed by exons (2,426) and 955 located in annotated promoters (**Figure 3**). A total of 3,568 annotated genes were associated with these DMRs.

As methylation plays an important role in the regulation of gene expression, we performed an analysis to determine DMPs. After filtering and identifying promoters with an absolute difference of the methylation levels >0.2 and with an FDR lower than 0.05, we identified 39 DMPs, 15 of which were hypermethylated and 24 hypomethylated (**Supplementary Table S7**).

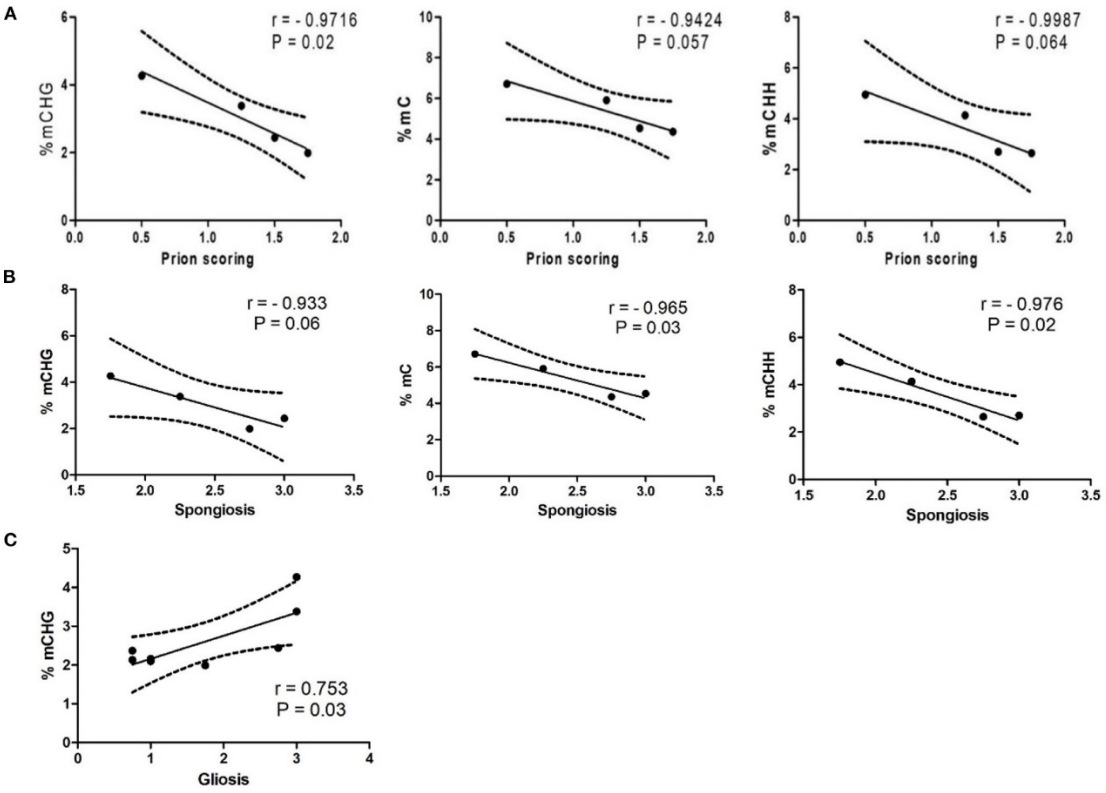

FIGURE 2 | (A) Correlation between PrP^{Sc} deposition scores and percentage of methylated cytosines in different motifs. **(B)** Correlation between spongiosis and percentage of methylated cytosines in different motifs. **(C)** Correlation between gliosis and percentage of methylated CHG sites.

Enrichment Analysis of Genes Related to Hyper- and Hypomethylated Differentially Methylated Regions

In order to determine if different molecular functions can be activated or repressed in scrapie brains, the identified DMRs were directionally separated, and GO enrichment was performed in hypermethylated (**Figure 4A**, **Supplementary Table S8**) and hypomethylated (**Figure 4B**, **Supplementary Table S9**) DMR-associated genes. Biological processes showing a significant increase of hypermethylated DMRs were related to the regulation of small GTPase mediated signal transduction, intracellular signal transduction and its regulation, homophilic cell adhesion via plasma membrane adhesion molecules, and cell–cell adhesion via plasma–membrane adhesion molecules, the last being also enriched in hypomethylated DMRs. In addition, the transmembrane transport biological process was also enriched in hypomethylated DMRs. Genes related to hyper- and hypomethylated DMRs were significantly enriched for myosin complex cellular components, and genes with hypermethylated DMRs were enriched in components of the actin cytoskeleton. Some molecular functions were found to be enriched in both hyper- and hypomethylated DMRs, such as those related to protein, ATP, ion or ribonucleotide binding, and motor activity. However, hypermethylated DMRs were enriched in calcium ion binding, cytoskeletal protein binding, or acting binding, whereas molecular functions related to purine binding, hydrolase, and kinase activity were enriched in hypomethylated DMRs (**Figure 4**).

KEGG pathway analysis revealed a significant enrichment of hypermethylated DMRs in the calcium signaling pathway and ABC transporters (**Figure 5A**, **Supplementary Table S10**), whereas hypomethylated DMRs appeared enriched in calcium signaling, circadian entrainment, and cAMP signaling pathways (**Figure 5B**, **Supplementary Table S11**).

Due to the relatively low number of DMPs found, GO enrichment analysis did not display any biological process, molecular component, or molecular function with a statistically significant corrected p-value. Although KEGG pathway analysis detected no significant pathways enriched, in hypomethylated DMPs, some pathways displayed a trend toward significance after multiple corrections including terms like apoptosis, lysosomes, protein processing in the endoplasmic reticulum, or AD (**Supplementary Table S12**).

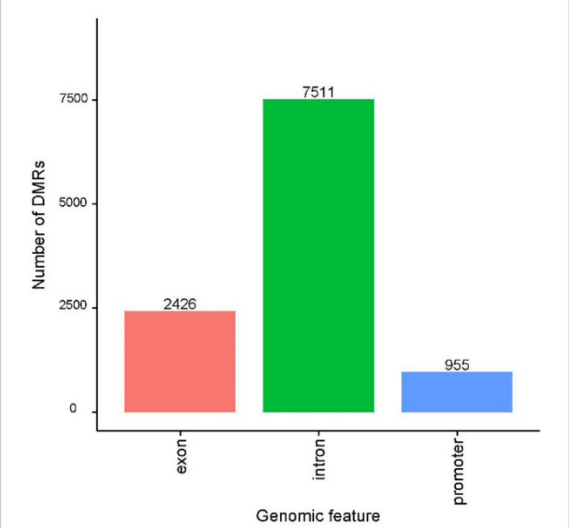

FIGURE 3 | Distribution of differentially methylated regions (DMRs) within functional regions.

To investigate if DMGs were expressed in a specific type of CNS cell, we compared DMGs with proteins defined as tenfold more abundant in oligodendrocytes, astrocytes, microglia, and cortical neurons in the mouse brain (29). A total of 206 DMGs corresponded to genes encoding for abundant proteins in neurons (46% of described abundant proteins). An enrichment analysis in Reactome (31) revealed enriched pathways corresponding to unblocking of NMDA receptors, glutamate binding, and activation (**Supplementary Table S13**). In the analysis of abundant proteins in microglia, we found a total of 83 DMGs (32% of abundant proteins in these cells). Three Reactome pathways were enriched in this set of DMGs: immune system, innate immune system, and neutrophil degranulation (**Supplementary Table S13**). More than half of the genes encoding proteins abundant in oligodendrocytes displayed DMRs, although we did not find any enriched pathways. Finally, close to 40% of genes encoding known abundant proteins in astrocytes had DMRs. Pathways enriched were related to laminin interactions, post-translational protein phosphorylation, IL6 signaling, and extracellular matrix organization and interactions (**Supplementary Table S13**).

Microarray-Identified Genes Differentially Expressed in Scrapie Contain Differentially Methylated Regions

To identify DEGs previously described in scrapie animals (5) containing DMRs, we enriched the annotation of the published set of DEGs with the identified DMRs. Of the total of annotated genes ($n = 125$) (**Supplementary Table S14**), 21 were found to harbor DMRs (**Figure 6**). These DMRs were hyper- or hypomethylated, and the majority of them were located in intron regions (**Figure 7**).

Expression Analysis of Genes With Significant Hypo- and Hypermethylated Differentially Methylated Regions and Differentially Methylated Promoters

In order to evaluate the effect of DNA methylation on gene expression in scrapie, we selected, among all the significant hypo- and hypermethylated DMRs and DMPs, a series of genes (DMGs) (**Tables 2**, **3**) with important functions in the nervous system and in other neurodegenerative diseases. The expression of these genes was analyzed by qPCR and correlated with their methylation state and the position (promoter, exon, or intron) of their significant DMRs.

As shown in **Tables 2**, **3** and **Figure 8**, significant changes were found between the control and scrapie animals in the expression of four genes (*PCDH19*, *SNCG*, *PEX1*, and *CABIN1*) and a trend toward significance in the expression of gene *WDR45B*.

Correlation Between Differentially Methylated Gene Expression, PrP^{Sc} Accumulation, and Prion-Related Lesions

In order to find a possible association between DMG expression, PrP^{Sc} deposits, and prion-related lesions (spongiosis, gliosis, and vacuolization) (24), a correlation analysis was performed. A significant negative correlation was found between PrP^{Sc} accumulation and the expression of *PEX1* ($r = -0.6471$, $p = 0.0431$) (**Figure 9B**) and *Metazoa_SRP* ($r = -0.6649$, $p = 0.0256$) (**Figure 9A**). Regarding spongiosis, a significant negative correlation with *PEX1* ($r = -0.6709$, $p = 0.0337$) (**Figure 9B**) and *Metazoa_SRP* ($r = -0.7383$, $p = 0.0095$) (**Figure 9A**) expressions and a positive correlation with *KCNK4* expression ($r = 0.7473$, $p = 0.0082$) (**Figure 9C**) were also observed. *Metazoa_SRP* expression was as well negatively correlated with gliosis ($r = -0.7328$, $p = 0.0103$) (**Figure 9A**), and this prion-related lesion also showed a significant positive correlation with *MTSS1L* expression ($r = 0.6725$, $p = 0.0234$) (**Figure 9D**). Finally, a positive correlation between vacuolization and the expression of *CABIN1* ($r = 0.6875$, $p = 0.0194$) (**Figure 9E**) and *SGSM2* ($r = 0.6608$, $p = 0.0269$) (**Figure 9F**) was obtained.

DISCUSSION

DNA methylation has been studied as a possible epigenetic regulatory mechanism in the pathogenesis of several neurodegenerative diseases. DNA methylation might have a role in the progression and pathways linked to AD (38) and PD (39). These diseases are also identified as prion-like diseases because they share common pathogenic mechanisms with prion diseases, such as the accumulation of misfolded proteins in the CNS (40). These facts suggest that DNA methylation may also have a role in prion diseases.

To the best of our knowledge, and in contrast to AD (38), PD (41), and ALS (42), only one study has analyzed the genome-wide methylation profile in prion diseases, and this was performed

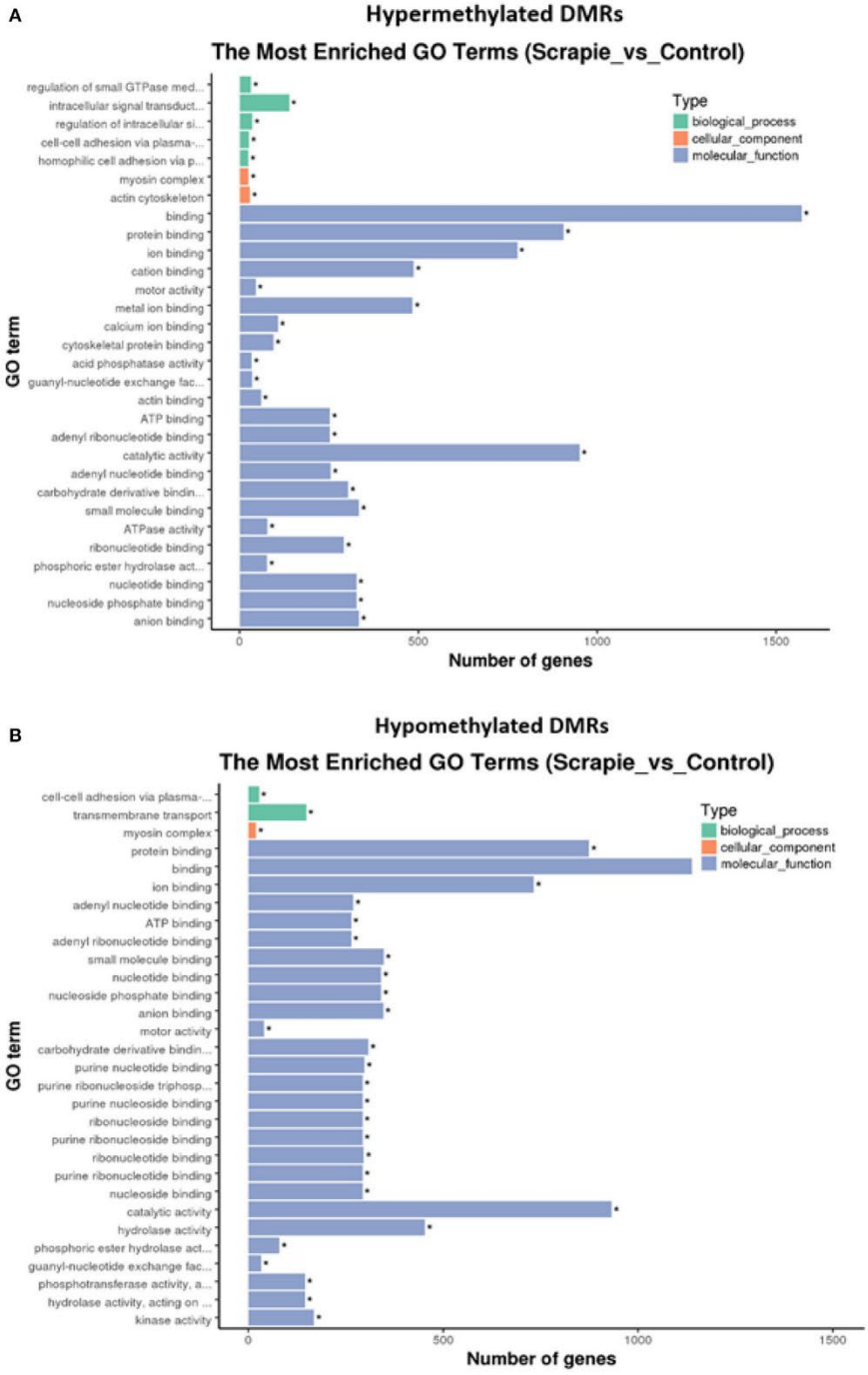

FIGURE 4 | Biological processes, cellular components, and molecular functions enriched in hypermethylated **(A)** and hypomethylated **(B)** differentially methylated regions (DMRs).

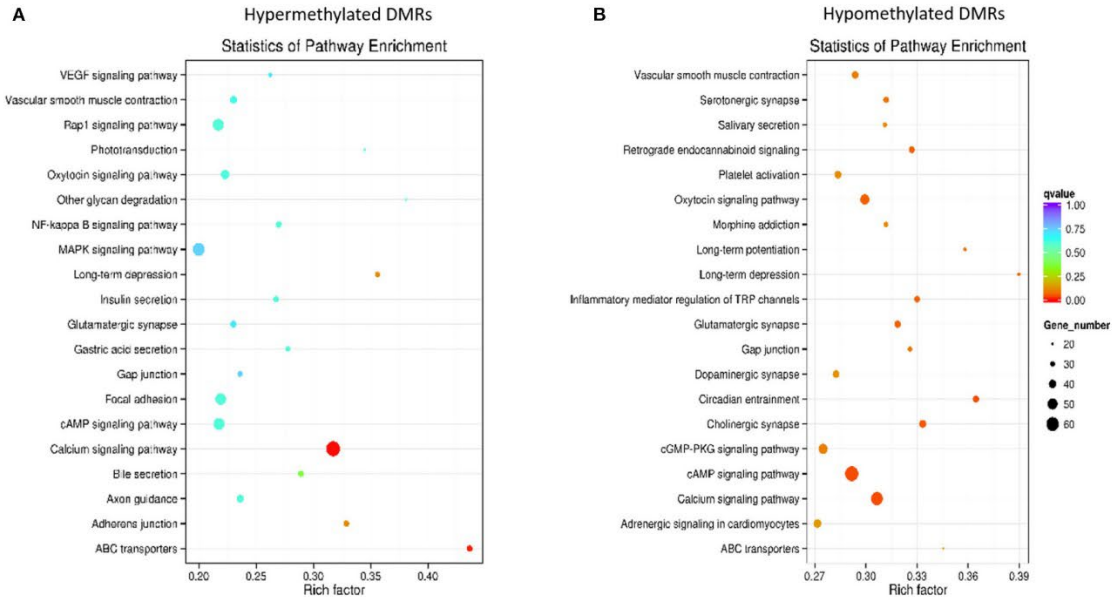

FIGURE 5 | Kyoto Encyclopedia of Genes and Genomes (KEGG) pathway enrichment in hypermethylated **(A)** and hypomethylated **(B)** differentially methylated regions (DMRs).

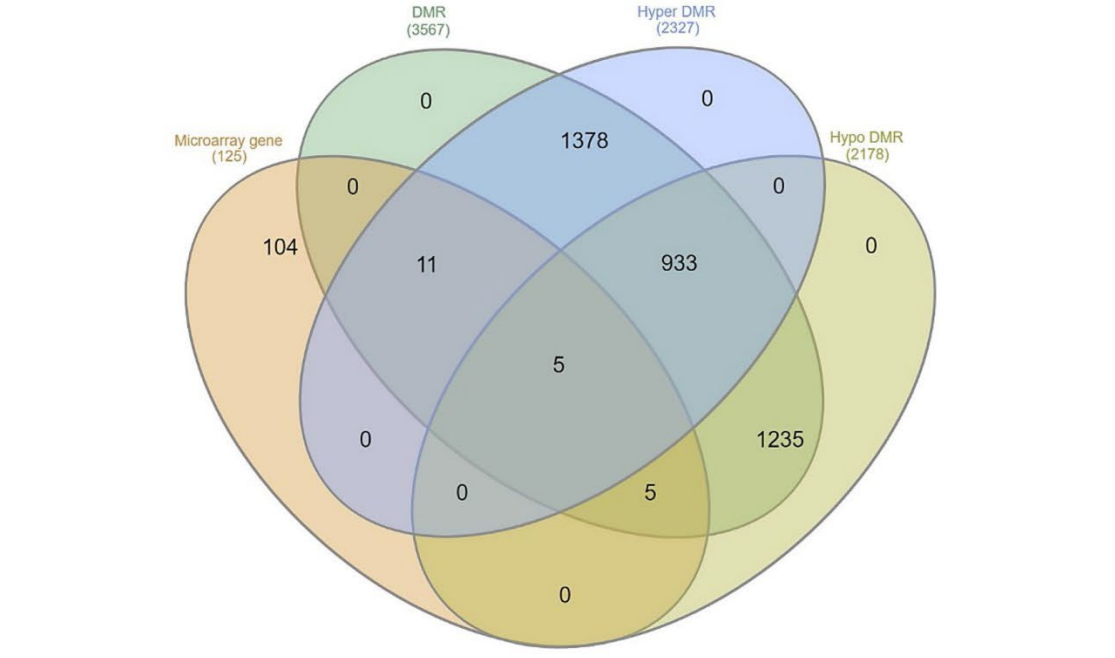

FIGURE 6 | Microarray-annotated genes containing differentially methylated regions (DMRs).

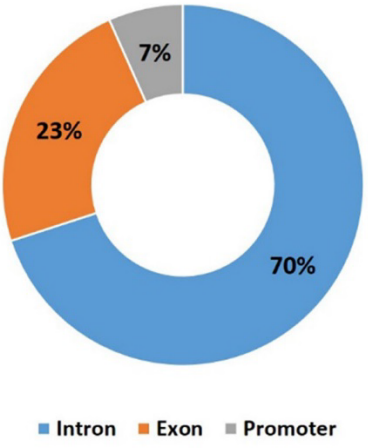

FIGURE 7 | Differentially methylated region (DMR) positions (intron, exon, and promoter) of the microarray-annotated genes.

in peripheral blood of sCJD patients (23). We report here the first WGBS study carried out in the CNS of any prion disease model. The study was performed in ovine classical scrapie, a natural animal model of prion disease. After neuroinvasion, PrP^{Sc} deposits in this form of scrapie are first observed in the spinal cord and obex, and from there they spread to the cerebellum, diencephalon, and prefrontal cortex (43). A previous work from our group revealed the similar intensity of PrP^{Sc} immunohistochemical signals in the obex (tissue selected for classical scrapie diagnosis), cervical spinal cord, and thalamus, although there was some variability between individuals showing a lesser degree of injury in some cases (44). In the present study, we have analyzed thalamus-derived DNA from a set of individuals whose obex was used in a previous transcriptomic analysis (5) and compared our methylation results with the reported expression changes. Although these techniques have been performed in different areas of the CNS, we believe that this approach would still be appropriate because previous validation of the expression changes observed in the array by qPCR showed similar results in the obex and diencephalon (thalamus and hypothalamus) (37). The sample size used in this study is limited (four scrapie vs. four control tissues) but adequate for the WGBS approach (45–49).

Although no significant differences were seen in global methylation levels between scrapie and control animals, significant correlations of methylation levels with PrP^{Sc} accumulation and prion-related lesions were evidenced in the scrapie group. However, significant correlations were seen in the total percentage of methylated cytosine and in motifs other than CpG, which was the most frequent methylated motif. Furthermore, this study allowed the identification of a great number of DMRs between the control and scrapie animals.

GO enrichment and KEGG pathway analyses of DMGs revealed an enrichment of several molecular and cellular functions in scrapie-affected animals. The most prominent enriched functions include intracellular signal transduction, transmembrane transport, protein and cellular binding, calcium signaling pathway, cAMP signaling pathway, cholinergic synapse, circadian entrainment, and apoptosis pathway. Interestingly, the PrP^{C} seems to have a role in all these processes. Several hypotheses suggest that PrP^{C} modulates components involved in proliferation, cell adhesion, transmembrane signaling, differentiation, and trafficking signaling pathways (50). In addition, PrP^{C} might also regulate synaptic transmission and plasticity, preserving normal synaptic structure and function (51). Regarding circadian entrainment, the role of PrP^{C} in sleep homeostasis and sleep continuity has been described (51). Stimulating the cAMP signaling pathway, PrP^{C} seems to promote cell survival, neurite outgrowth (52), and myelin maintenance (51). It has also been reported that PrP^{C} may regulate intracellular calcium homeostasis and exert control on mitochondria-associated apoptotic signaling (52). Therefore, the enrichment observed in all these functions when the PrP^{C} has lost its function due to its conversion to the pathological prion protein suggests a possible epigenetic regulation of all these processes.

Among the epigenetic mechanisms, DNA methylation has been described to participate in gene expression regulation. It is known that the position of the methylation in the transcriptional unit influences its relationship to the control of gene expression (53). Depending on whether the methylation is in a promoter, exon, or intron region, the effect on gene expression is different. Methylation in the promoter region is commonly associated with gene repression, whereas methylation in the gene body (exons) is associated with gene activation (53). Also, there is an inverse correlation between DNA methylation of the first intron and gene expression that could be due to the presence of intronic enhancers interacting with the promoters (54). With the purpose of studying the effect of DNA methylation on gene expression in Scrapie, we selected, among all the identified significant DMRs, a series of genes that have important functions in the nervous system and in some neurodegenerative diseases. Of all the selected genes, significant changes between the control and scrapie animals were found in the expression of five genes: *PCDH19*, *SNCG*, *WDR45B*, *PEX1*, and *CABIN1*.

The expression of the gene encoding Protocadherin 19 (*PCDH19*) was downregulated. This gene is located on chromosome X and belongs to the protocadherin family involved in signal transduction at synapses and in the establishment of neuronal connections. Protocadherins are mainly expressed in the CNS and participate in neuronal development, migration, segregation, and synaptic plasticity. Accordingly, the highest expression levels of *PCDH19* are found in the nervous system, although it is also expressed in several embryonic and adult tissues such as the kidney, lungs, and trachea (55). This gene has a role in the proliferation of neuronal progenitors, the formation of neuronal circuits, and the regulation of neuronal activity (56). Moreover, *PCDH19* seems to participate in GABAergic transmission, migration, and morphological maturation of neurons (57). Autism, intellectual disabilities, and epilepsy are related to defects in the expression or function of protocadherins, and mutations in *PCDH19* gene cause early infantile epileptic

TABLE 2 | Expression levels of genes with differentially methylated regions (DMRs).

Gene	DMR methylation state	DMR position	$2^{-\Delta\Delta Ct}$	Gene expression *p*-value
A1BG	1 H	Promoter	0.7331	NS
CABIN1	10 H/12 h	Intron/exon	0.7180	$p = 0.03$
CD81	1 H	Promoter	0.7706	NS
MAD1L1	5 H	Promoter/intron	0.8738	NS
Metazoa_SRP	1 h	Exon/promoter	1.1784	NS
PCDH19	1 H	Promoter	0.7022	$p = 0.03$
PEX1	1 H/2 h	Exon	1.3468	$p = 0.01$
PLA2G5	1 H/2 h	Exon	0.9899	NS
PSMG4	2 H	Intron	0.9229	NS
SNX33	2 H	Promoter/intron	0.8682	NS
WDR45B	1 H	Exon	1.1992	$p = 0.11$

Methylation state, number of DMRs and state (H, hypermethylated, h, hypomethylated); DMR position, positions of the DMR; $2^{-\Delta\Delta Ct}$; relative gene expression in terms of $2^{-\Delta\Delta Ct}$ and gene expression p-value of significant differentially expressed genes; NS, no significant changes.

TABLE 3 | Expression levels of genes with differentially methylated promoters (DMPs).

Gene	DMP methylation state	$2^{-\Delta\Delta Ct}$	Gene expression p-value
CAPN1	h	1.1886	NS
GSTA4	h	0.8821	NS
INTS1	H	0.9869	NS
KCNK4	h	0.7392	NS
MTSS1L	H	0.8599	NS
NARS	h	0.8130	NS
PLCL2	h	1.2551	NS
SNCG	H	0.3663	$p = 0.02$
WSCD2	H	0.7505	NS

Methylation state, DMP state (H, hypermethylated, h, hypomethylated); $2^{-\Delta\Delta Ct}$, relative gene expression in terms of $2^{-\Delta\Delta Ct}$ and gene expression p-value of significant differentially expressed genes; NS, no significant changes.

encephalopathy-9 (EIEE9) in humans (55). To the best of our knowledge, *PCDH19* methylation has only been studied in hepatocellular carcinoma in which hypermethylation of the promoter region correlated with a downregulation of the gene expression was observed (58). Here, a decrease in the expression of this gene was in accordance with promoter hypermethylation in naturally infected scrapie animals. Given the important role of *PCDH19* in the maintenance of neuronal homeostasis and neuronal connections, its downregulation observed in scrapie animals could be associated with earlier onset and/or the augmented progression of the prion disease.

Another DMG was γ-synuclein (*SNCG*), a member of the synuclein family that encompasses an important class of intrinsically disordered neural proteins. It is known that this protein has pathogenic implications in both neurodegeneration and cancer (59). γ-Synuclein is physiologically expressed by astrocytes in the human nervous system stimulating the cell cycle and participating in the expression and release of extracellular brain-derived neurotrophic factor (BNDF) (60). γ-Synuclein may also inhibit the aggregation propensity of α-synuclein, a protein present in Lewy bodies whose aggregation is a hallmark in PD (61). In contrast, overexpression of γ-synuclein in the neurons of transgenic mice induces a severe neurodegenerative pathology characterized by substantial depletion of neurofilaments in neuronal processes and, ultimately, death of motor neurons (62). In AD patients, γ-synuclein is also increased extracellularly in the brain and cerebrospinal fluid (60). In addition, upregulation of γ-synuclein is considered a prognostic marker in neurodegenerative conditions (62) and multiple invasive cancers (63, 64). Taking all these data into consideration, the downregulation and promoter hypermethylation observed in naturally infected scrapie animals suggest a possible neuroprotective role of this gene at astrocytes that are known to be involved in prion replication and spread.

WD repeat domain 45B (*WDR45B*/*WIPI3*) belongs to the WIPI protein family and was overexpressed in scrapie animals. All human WIPI proteins (WIPI1, WIPI2, WIPI3, and WIPI4) are known to have a role in the control of the autophagy process. In fact, *WDR45B* seems to participate in the formation of functional autophagosomes (65). Autophagy is a quality control mechanism for the degradation of misfolded proteins and damaged organelles and plays an important role in the maintenance of neural homeostasis (66). Dysregulation of the autophagy process has been described in different natural and experimental animal models of prion diseases (67–70) and other neurodegenerative diseases (71). In addition, *WDR45B* is associated in humans with a neurodevelopmental syndrome characterized by spastic quadriplegia, epilepsy, intellectual disability, and cerebral hypoplasia (72). *WDR45B* knockout mice display deficits and cognitive defects (66). The fact that neuronal homeostasis and autophagy are dysregulated in scrapie could possibly explain the *WDR45B* upregulation observed in naturally infected scrapie animals. The increased expression of this gene could be a host response that aims for the proper maintenance of the autophagic capacity and balanced neuronal homeostasis to slow down the prion disease progression.

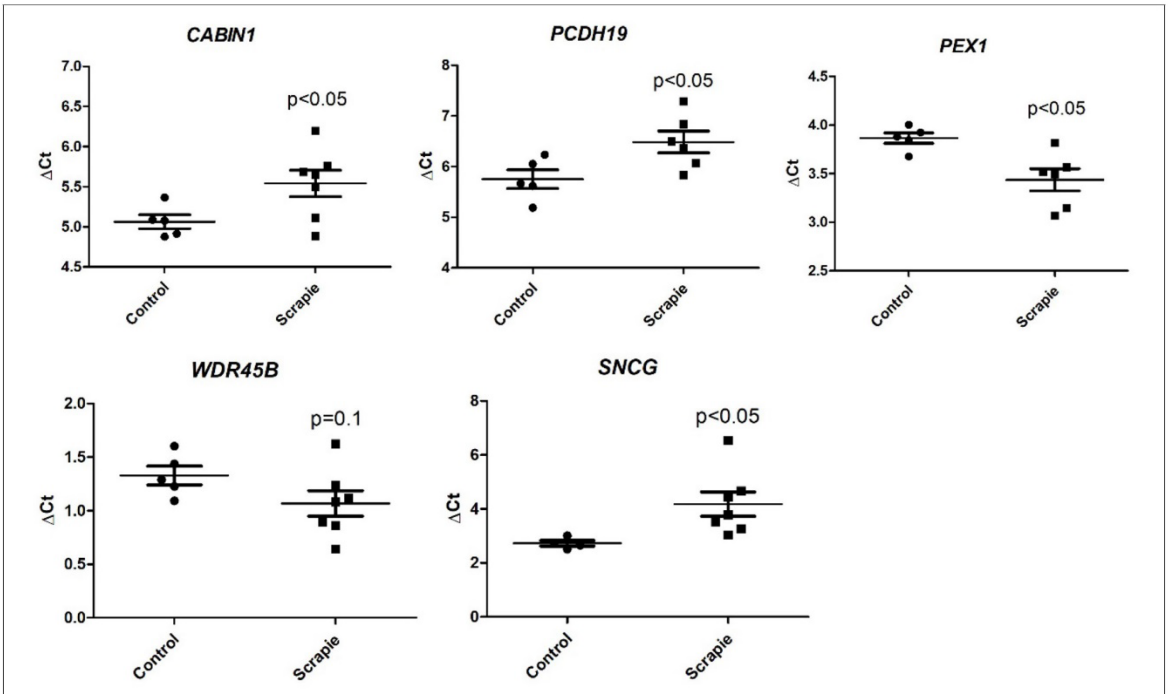

FIGURE 8 | Gene expression profile of significant differentially expressed genes (*CABIN1*, *PCDH19*, *PEX1*, *SNCG*, and *WDR45B*). Data are shown in terms of relative gene expression (ΔCt) between control and scrapie animals.

Peroxisomal biogenesis factor 1 (*PEX1*) is a gene encoding the peroxin 1 protein that is involved in the peroxisome biogenesis specifically in importing peroxisomal matrix proteins (73) and was upregulated in scrapie animals. Peroxisomes are important metabolic organelles that contribute to cellular lipid metabolism and redox balance (74). Even though peroxisomes are present in most mammalian cell types, their contribution to the CNS function is related to the biosynthesis of ether phospholipids. These are important components of myelin in the synthesis of docosahexaenoic acid (DHA), which plays an important role in nervous system signaling, and to the degradation of toxic compounds and D-amino acids, which would protect brain structures and modulate synaptic signaling, respectively (75). Neurological diseases such as AD, autism, ALS (75), and PD (74) present dysfunction of peroxisomes or dysregulation of peroxisomal metabolites. As an example, patients with pronounced AD pathology display an inefficient peroxisome transport between neurites and soma and dysregulation in peroxisomal lipid metabolism. These alterations contribute to AD pathology aggravating disease progression. However, whether they are a secondary phenomenon or play a causative role in AD pathogenesis remains to be determined (74). In our study, we detected an upregulation of *PEX1* gene in naturally infected scrapie animals that were significantly correlated with spongiosis and PrP^{Sc} accumulation, suggesting that peroxisome activity might as well be compromised in scrapie. Although further research is needed, this finding could also indicate a possible role of peroxisomes in the pathogenesis of prion diseases.

Calcineurin-binding protein 1 (*CABIN1*) is a gene that acts as a calcium-dependent repressor of calcineurin in the CNS (76). Calcineurin is a serine/threonine phosphatase widely expressed in different cell types and structures including neurons, where it is involved in synaptic transmission and neurotransmitter release (77). The chronic aberrant activation of this protein in neurons contributes to synaptic dysfunction in AD. In contrast, calcineurin inhibition can improve synaptic morphology in AD mouse models (78). Synaptic dysfunction and synaptic loss are as well prominent and early events in prion diseases (51). Moreover, calcineurin activation mediated by human prion protein triggers neuronal cell death (79). Altogether, these data suggest that the downregulation of *CABIN1* observed in scrapie animals, which showed a significant association with vacuolization, could trigger calcineurin activation contributing, along with other pathogenic mechanisms, to the synaptic impairment and neuronal cell death observed in scrapie disease.

Although we found no significant changes in the expression of *Metazoa_SRP* (Metazoan signal recognition particle RNA) between the control and scrapie animals, we observed a significant negative correlation between the expression of this gene and PrP^{Sc} accumulation, spongiosis, and gliosis. *Metazoa_SRP* is a noncoding RNA (ncRNA). This type of molecule is abundantly expressed in the brain, and some of

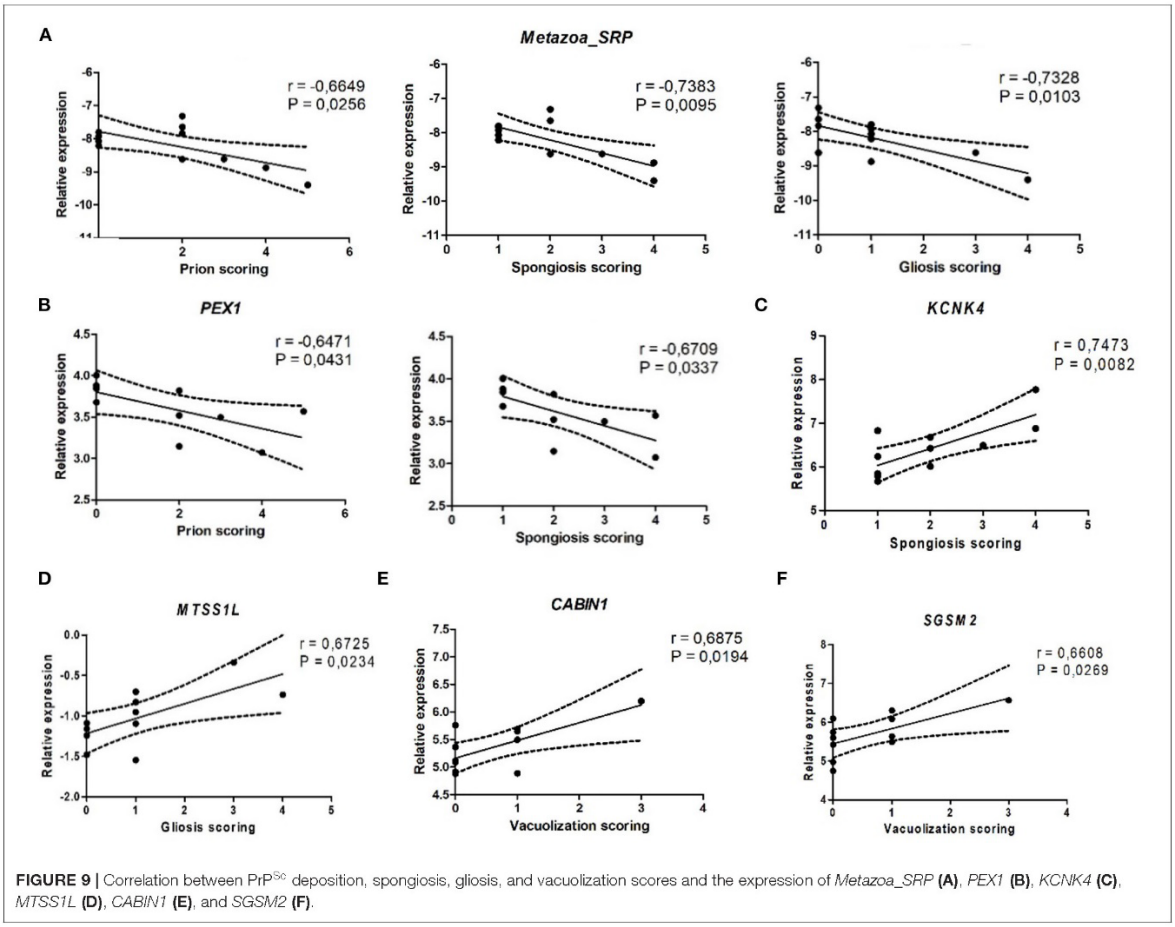

FIGURE 9 | Correlation between PrP^{Sc} deposition, spongiosis, gliosis, and vacuolization scores and the expression of *Metazoa_SRP* **(A)**, *PEX1* **(B)**, *KCNK4* **(C)**, *MTSS1L* **(D)**, *CABIN1* **(E)**, and *SGSM2* **(F)**.

them have been reported to be dysregulated in neurodegenerative diseases. In addition, ncRNAs have been proposed as potential biomarkers for neural disorders (80, 81). Deregulation of different types of ncRNAs, namely, microRNAs, long noncoding RNAs, and circular RNAs, has been described in AD (82, 83) and PD (84, 85) and also in prion diseases including scrapie (86, 87). Although further research is warranted, the association of *Metazoa_SRP* with prion-related lesions could indicate a possible implication of this ncRNA in scrapie pathology.

Finally, in addition to the expression study of genes with functions in the nervous system and in some neurodegenerative diseases, we compared genes previously described to be differentially expressed in scrapie (5) with our set of identified DMRs finding that some of these genes also harbored DMRs. This fact suggests that DNA methylation could also be implicated in the expression of these previously described genes.

In conclusion, our study shows a potential regulatory role of DNA methylation in prion pathology. We identified many DMRs between the control and scrapie animals, some of them belonging to genes with possible neuroprotective roles against neurodegeneration (*SNCG* and *WDR45B*) and to genes that may facilitate or contribute to scrapie disease progression (*PCDH19*, *PEX1*, and *CABIN1*). Additionally, an enrichment in a variety of molecular and cellular functions in which the PrP^{C} is involved was found in naturally infected scrapie animals, supporting the idea that epigenetic regulation could have an important role in prion diseases. Due to the limitations of sample size and regions studied, replication of the study using a larger number of animals and other CNS areas is warranted in the future.

DATA AVAILABILITY STATEMENT

The raw and processed sequencing data generated for this study have been deposited in NCBI's Gene Expression Omnibus (88) and are accessible through GEO Series accession number GSE184767 (https://www.ncbi.nlm.nih.gov/geo/query/acc.cgi?acc=GSE184767).

ETHICS STATEMENT

The animal study was reviewed and approved by Comisión Ética Asesora para la Experimentación Animal de la Universidad de Zaragoza.

AUTHOR CONTRIBUTIONS

AH: validation, formal analysis, investigation, and writing—original draft. AS and SS: validation, formal analysis, and investigation. BR: software, formal analysis, and investigation. OL-P: investigation. PZ and JB: funding acquisition. HF: formal analysis and investigation. RB: supervision, project administration, and funding acquisition. JT: conceptualization, methodology, investigation, project administration, and funding acquisition. IM-B: conceptualization, methodology, investigation, writing—review and editing, supervision, project administration, and funding acquisition. All authors reviewed the final version of the manuscript.

FUNDING

AH and OL-P were supported by research grants from Gobierno de Aragón (Order IIU/2023/2017 and C012/2014) co-financed by the European Social Fund. This research was partially funded by the following projects: AGL2015-67945-P funded by MINECO; RTI2018-098711-B-I00 funded by MCIN/AEI/10.13039/501100011033 FEDER Una manera de hacer Europa; reference group A19-20R funded by the Government of Aragón co-financed with FEDER 2014-2020 Construyendo Europa desde Aragón and the European Regional Development Fund (ERDF), and EFA 148/16 REDPRION funded by Spain-France-Andorra Cooperation Program (POCTEFA). POCTEFA aims to reinforce the economic and social integration of the French–Spanish–Andorran border. Its support is focused on developing economic, social, and environmental cross-border activities through joint strategies, favoring sustainable territorial development.

SUPPLEMENTARY MATERIAL

The Supplementary Material for this article can be found online at: https://www.frontiersin.org/articles/10.3389/fvets.2022.824677/full#supplementary-material

REFERENCES

1. Prusiner SB. The prion diseases. *Brain Pathol.* (1998) 8:499–513. doi: 10.1111/j.1750-3639.1998.tb00171.x
2. Prusiner SB. Novel proteinaceous infectious particles cause scrapie. *Science.* (1982) 216:136–44. doi: 10.1126/science.6801762
3. Bell JE, Ironside JW. Neuropathology of spongiform encephalopathies in humans. *Br Med Bull.* (1993) 49:738–77. doi: 10.1093/oxfordjournals.bmb.a072645
4. Pattison IH, Jones KM. The astrocytic reaction in experimental scrapie in the rat. *Res Vet Sci.* (1967) 8:160–5. doi: 10.1016/S0034-5288(18)34630-7
5. Filali H, Martin-Burriel I, Harders F, Varona L, Lyahyai J, Zaragoza P, et al. Gene expression profiling and association with prion-related lesions in the Medulla Oblongata of symptomatic natural scrapie animals. *PLoS ONE.* (2011) 6:e19909. doi: 10.1371/journal.pone.0019909
6. Filali H, Martin-Burriel I, Harders F, Varona L, Serrano C, Acín C, et al. Medulla oblongata transcriptome changes during presymptomatic natural scrapie and their association with prion-related lesions. *BMC Genomics.* (2012) 13:399. doi: 10.1186/1471-2164-13-399
7. Zetterberg H, Bozzetta E, Favole A, Corona C, Cavarretta MC, Ingravalle F, et al. Neurofilaments in blood is a new promising preclinical biomarker for the screening of natural scrapie in sheep. *PLoS ONE.* (2019) 14:e0226697. doi: 10.1371/journal.pone.0226697
8. López-Pérez Ó, Bernal-Martín M, Hernaiz A, Llorens F, Betancor M, Otero A, et al. BAMBI and CHGA in prion diseases: Neuropathological assessment and potential role as disease biomarkers. *Biomolecules.* (2020) 10:706. doi: 10.3390/biom10050706
9. Sandoval J, Esteller M. Cancer epigenomics: beyond genomics. *Curr Opin Genet Dev.* (2012) 22:50–5. doi: 10.1016/j.gde.2012.02.008
10. Heijmans BT, Tobi EW, Stein AD, Putter H, Blauw GJ, Susser ES, et al. Persistent epigenetic differences associated with prenatal exposure to famine in humans. *Proc Natl Acad Sci U S A.* (2008) 105:17046–9. doi: 10.1073/pnas.0806560105
11. Bjornsson HT, Fallin MD, Feinberg AP. An integrated epigenetic and genetic approach to common human disease. *Trends Genet.* (2004) 20:350–8. doi: 10.1016/j.tig.2004.06.009
12. Mehler MF. Epigenetics and the nervous system. *Ann Neurol.* (2008) 64:602–17. doi: 10.1002/ana.21595
13. Miller CA, Sweatt JD. Covalent modification of DNA regulates memory formation. *Neuron.* (2007) 53:857–69. doi: 10.1016/j.neuron.2007.02.022
14. Oliveira AMM, Hemstedt TJ, Bading H. Rescue of aging-associated decline in Dnmt3a2 expression restores cognitive abilities. *Nat Neurosci.* (2012) 15:1111–3. doi: 10.1038/nn.3151
15. De Jager PL, Srivastava G, Lunnon K, Burgess J, Schalkwyk LC Yu L, et al. Alzheimer's disease: early alterations in brain DNA methylation at ANK1, BIN1, RHBDF2 and other loci. *Nat Neurosci.* (2014) 17:1156–63. doi: 10.1038/nn.3786
16. Sanchez-Mut J V, Aso E, Panayotis N, Lott I, Dierssen M, Rabano A, et al. DNA methylation map of mouse and human brain identifies target genes in Alzheimer's disease. *Brain.* (2013) 136:3018–27. doi: 10.1093/brain/awt237
17. Kaut O, Schmitt I, Wüllner U. Genome-scale methylation analysis of Parkinson's disease patients' brains reveals DNA hypomethylation and increased mRNA expression of cytochrome P450 2E1. *Neurogenetics.* (2012) 13:87–91. doi: 10.1007/s10048-011-0308-3
18. Masliah E, Dumaop W, Galasko D, Desplats P. Distinctive patterns of DNA methylation associated with Parkinson disease: identification of concordant epigenetic changes in brain and peripheral blood leukocytes. *Epigenetics.* (2013) 8:1030–8. doi: 10.4161/epi.25865
19. Xi Z, Zinman L, Moreno D, Schymick J, Liang Y, Sato C, et al. Hypermethylation of the CpG island near the G4C2 repeat in ALS with a C9orf72 expansion. *Am J Hum Genet.* (2013) 92:981–9. doi: 10.1016/j.ajhg.2013.04.017
20. Figueroa-Romero C, Hur J, Bender DE, Delaney CE, Cataldo MD, Smith AL, et al. Identification of epigenetically altered genes in sporadic amyotrophic lateral sclerosis. Le W, editor. *PLoS ONE.* (2012) 7:e52672. doi: 10.1371/journal.pone.0052672
21. Dalai W, Matsuo E, Takeyama N, Kawano J, Saeki K. CpG site DNA methylation patterns reveal a novel regulatory element in the mouse prion protein gene. *J Vet Med Sci.* (2017) 79:100–7. doi: 10.1292/jvms.16-0390
22. Zawlik I, Witusik M, Hulas-Bigoszewska K, Piaskowski S, Szybka M, Golanska E, et al. Regulation of PrPC expression: Nerve growth factor (NGF) activates the prion gene promoter through the MEK1 pathway in PC12 cells. *Neurosci Lett.* (2006) 400:58–62. doi: 10.1016/j.neulet.2006.02.021
23. Dabin LC, Guntoro F, Campbell T, Bélicard T, Smith AR, Smith RG, et al. Altered DNA methylation profiles in blood from patients with sporadic Creutzfeldt–Jakob disease. *Acta Neuropathol.* (2020) 140:863–79. doi: 10.1007/s00401-020-02224-9
24. Serrano C, Bolea R, Lyahyai J, Filali H, Varona L, Marcos-Carcavilla A, et al. Changes in HSP gene and protein expression in natural scrapie with brain damage. *Vet Res.* (2011) 42:13. doi: 10.1186/1297-9716-42-13
25. Krueger F, Andrews SR. Bismark: A flexible aligner and methylation caller for Bisulfite-Seq applications. *Bioinformatics.* (2011) 27:1571–2. doi: 10.1093/bioinformatics/btr167
26. Habibi E, Brinkman AB, Arand J, Kroeze LI, Kerstens HHD, Matarese F, et al. Whole-genome bisulfite sequencing of two distinct interconvertible DNA

methylomes of mouse embryonic stem cells. *Cell Stem Cell.* (2013) 13:360–9. doi: 10.1016/j.stem.2013.06.002
27. Gifford CA, Ziller MJ, Gu H, Trapnell C, Donaghey J, Tsankov A, et al. Transcriptional and epigenetic dynamics during specification of human embryonic stem cells. *Cell.* (2013) 153:1149–63. doi: 10.1016/j.cell.2013.04.037
28. Hansen KD, Langmead B, Irizarry RA. BSmooth: from whole genome bisulfite sequencing reads to differentially methylated regions. *Genome Biol.* (2012) 13:R83. doi: 10.1186/gb-2012-13-10-r83
29. Sharma K, Schmitt S, Bergner CG, Tyanova S, Kannaiyan N, Manrique-Hoyos N, et al. Cell type- and brain region-resolved mouse brain proteome. *Nat Neurosci.* (2015) 18:1819–31. doi: 10.1038/nn.4160
30. Heberle H, Meirelles VG, da Silva FR, Telles GP, Minghim R. InteractiVenn: A web-based tool for the analysis of sets through Venn diagrams. *BMC Bioinformatics.* (2015) 16:169. doi: 10.1186/s12859-015-0611-3
31. Jassal B, Matthews L, Viteri G, Gong C, Lorente P, Fabregat A, et al. The reactome pathway knowledgebase. *Nucleic Acids Res.* (2020) 48:D498–503. doi: 10.1093/nar/gkz1031
32. Kent WJ. BLAT—The BLAST-Like Alignment Tool. *Genome Res.* (2002) 12:656–64. doi: 10.1101/gr.229202
33. Durinck S, Spellman PT, Birney E, Huber W. Mapping identifiers for the integration of genomic datasets with the R/ Bioconductor package biomaRt. *Nat Protoc.* (2009) 4:1184–91. doi: 10.1038/nprot.2009.97
34. Durinck S, Moreau Y, Kasprzyk A, Davis S, De Moor B, Brazma A, et al. BioMart and Bioconductor: A powerful link between biological databases and microarray data analysis. *Bioinformatics.* (2005) 21:3439–40. doi: 10.1093/bioinformatics/bti525
35. Livak KJ, Schmittgen TD. Analysis of relative gene expression data using real-time quantitative PCR and the 2-ΔΔCT method. *Methods.* (2001) 25:402–8. doi: 10.1006/meth.2001.1262
36. Lyahyai J, Serrano C, Ranera B, Badiola JJ, Zaragoza P, Martin-Burriel I. Effect of scrapie on the stability of housekeeping genes. *Anim Biotechnol.* (2010) 21:1–13. doi: 10.1080/10495390903323851
37. Filali H, Vidal E, Bolea R, Márquez M, Marco P, Vargas A, et al. Gene and protein patterns of potential prion-related markers in the central nervous system of clinical and preclinical infected sheep. *Vet Res.* (2013) 44:14. doi: 10.1186/1297-9716-44-14
38. Sharma VK, Mehta V, Singh TG. Alzheimer's Disorder: Epigenetic connection and associated risk factors. *Curr Neuropharmacol.* (2020) 18:740–53. doi: 10.2174/1570159X18666200128125641
39. Young JI, Sivasankaran SK, Wang L, Ali A, Mehta A, Davis DA, et al. Genome-wide brain DNA methylation analysis suggests epigenetic reprogramming in Parkinson disease. *Neurol Genet.* (2019) 5:e342. doi: 10.1212/NXG.0000000000000342
40. Jaunmuktane Z, Brandner S. Invited Review: The role of prion-like mechanisms in neurodegenerative diseases. *Neuropathol Appl Neurobiol.* (2019) 46:522–45. doi: 10.1111/nan.12592
41. Henderson-Smith A, Fisch KM, Hua J, Liu G, Ricciardelli E, Jepsen K, et al. DNA methylation changes associated with Parkinson's disease progression: outcomes from the first longitudinal genome-wide methylation analysis in blood. *Epigenetics.* (2019) 14:365–82. doi: 10.1080/15592294.2019.1588682
42. Jackson JL, Finch NCA, Baker MC, Kachergus JM, Dejesus-Hernandez M, Pereira K, et al. Elevated methylation levels, reduced expression levels, and frequent contractions in a clinical cohort of C9orf72 expansion carriers. *Mol Neurodegener.* (2020) 15:7. doi: 10.1186/s13024-020-0359-8
43. Wemheuer WM, Benestad SL, Wrede A, Wemheuer WE, Brenig B, Bratberg B, et al. PrP Sc spreading patterns in the brain of sheep linked to different prion types. *Vet Res.* (2011) 42:1–14. doi: 10.1186/1297-9716-42-32
44. Bolea R, Monleón E, Schiller I, Raeber AJ, Acín C, Monzón M, et al. Comparison of immunohistochemistry and two rapid tests for detection of abnormal prion protein in different brain regions of sheep with typical scrapie. *J Vet Diagn Invest.* (2005) 17:467–9. doi: 10.1177/104063870501700511
45. Fan Y, Liang Y, Deng K, Zhang Z, Zhang G, Zhang Y, et al. Analysis of DNA methylation profiles during sheep skeletal muscle development using whole-genome bisulfite sequencing. *BMC Genomics.* (2020) 21:327. doi: 10.1186/s12864-020-6751-5
46. Zhang Y, Li F, Feng X, Yang H, Zhu A, Pang J, et al. Genome-wide analysis of DNA Methylation profiles on sheep ovaries associated with prolificacy using whole-genome Bisulfite sequencing. *BMC Genomics.* (2017) 18:759. doi: 10.1186/s12864-017-4068-9
47. Chen Y, Hu S, Liu M, Zhao B, Yang N, Li J, et al. Analysis of genome DNA methylation at inherited coat color dilutions of rex rabbits. *Front Genet.* (2021) 11:603528. doi: 10.3389/fgene.2020.603528
48. Laufer BI, Hwang H, Vogel Ciernia A, Mordaunt CE, LaSalle JM. Whole genome bisulfite sequencing of Down syndrome brain reveals regional DNA hypermethylation and novel disorder insights. *Epigenetics.* (2019) 14:672. doi: 10.1080/15592294.2019.1609867
49. Li C, Li Y, Zhou G, Gao Y, Ma S, Chen Y, et al. Whole-genome bisulfite sequencing of goat skins identifies signatures associated with hair cycling. *BMC Genomics.* (2018) 19:638. doi: 10.1186/s12864-018-5002-5
50. Atkinson CJ, Zhang K, Munn AL, Wiegmans A, Wei MQ. Prion protein scrapie and the normal cellular prion protein. *Prion.* (2016) 10:63–82. doi: 10.1080/19336896.2015.1110293
51. Wulf MA, Senatore A, Aguzzi A. The biological function of the cellular prion protein: An update. *BMC Biology.* (2017) 15:34. doi: 10.1186/s12915-017-0375-5
52. Gavín R, Lidón L, Ferrer I, Río JA del. The quest for cellular prion protein functions in the aged and neurodegenerating brain. *Cells.* (2020) 9:591. doi: 10.3390/cells9030591
53. Jones PA. Functions of DNA methylation: Islands, start sites, gene bodies and beyond. *Nat Rev Genet.* (2012) 13:484–92. doi: 10.1038/nrg3230
54. Anastasiadi D, Esteve-Codina A, Piferrer F. Consistent inverse correlation between DNA methylation of the first intron and gene expression across tissues and species. *Epigenetics and Chromatin.* (2018) 11:37. doi: 10.1186/s13072-018-0205-1
55. Gerosa L, Francolini M, Bassani S, Passafaro M. The role of protocadherin 19 (PCDH19) in neurodevelopment and in the pathophysiology of early infantile epileptic encephalopathy-9 (EIEE9). *Dev Neurobiol.* (2019) 79:75–84. doi: 10.1002/dneu.22654
56. Fujitani M, Zhang S, Fujiki R, Fujihara Y, Yamashita T. A chromosome 16p13.11 microduplication causes hyperactivity through dysregulation of miR-484/protocadherin-19 signaling. *Mol Psychiatry.* (2017) 22:364–74. doi: 10.1038/mp.2016.106
57. Bassani S, Cwetsch AW, Gerosa L, Serratto GM, Folci A, Hall IF, et al. The female epilepsy protein PCDH19 is a new GABAAR-binding partner that regulates GABAergic transmission as well as migration and morphological maturation of hippocampal neurons. *Hum Mol Genet.* (2018) 27:1027–38. doi: 10.1093/hmg/ddy019
58. Zhang T, Guan G, Chen T, Jin J, Zhang L, Yao M, et al. Methylation of PCDH19 predicts poor prognosis of hepatocellular carcinoma. *Asia Pac J Clin Oncol.* (2018) 14:e352–8. doi: 10.1111/ajco.12982
59. Roy S, Bhat R. Suppression, disaggregation, and modulation of γ-Synuclein fibrillation pathway by green tea polyphenol EGCG. *Protein Sci.* (2019) 28:382–402. doi: 10.1002/pro.3549
60. Winham CL, Le T, Jellison ER, Silver AC, Levesque AA, Koob AO. γ-Synuclein induces human cortical astrocyte proliferation and subsequent BDNF expression and release. *Neuroscience.* (2019) 410:41–54. doi: 10.1016/j.neuroscience.2019.04.057
61. Sanjeev A, Mattaparthi VSK. Computational study on the role of γ-synuclein in inhibiting the α-synuclein aggregation. *Cent Nerv Syst Agents Med Chem.* (2018) 19:24–30. doi: 10.2174/1871524918666181012160439
62. Ninkina N, Peters O, Millership S, Salem H, van der Putten H, Buchman VL. Gamma-synucleinopathy: neurodegeneration associated with overexpression of the mouse protein. *Hum Mol Genet.* (2009) 18:1779–94. doi: 10.1093/hmg/ddp090
63. Bakula D, Müller AJ, Zuleger T, Takacs Z, Franz-Wachtel M, Thost AK, et al. WIPI3 and WIPI4 β-propellers are scaffolds for LKB1-AMPK-TSC signalling circuits in the control of autophagy. *Nat Commun.* (2017) 8:15637. doi: 10.1038/ncomms15637
64. Ji C, Zhao H, Li D, Sun H, Hao J, Chen R, et al. Role of Wdr45b in maintaining neural autophagy and cognitive function. *Autophagy.* (2019) 16:615–25. doi: 10.1080/15548627.2019.1632621
65. Hibi T, Mori T, Fukuma M, Yamazaki K, Hashiguchi A, Yamada T, et al. Synuclein-gamma is closely involved in perineural invasion and distant metastasis in mouse models and is a novel prognostic

factor in pancreatic cancer. *Clin Cancer Res.* (2009) 15:2864–71. doi: 10.1158/1078-0432.CCR-08-2946
66. Martini-Stoica H, Xu Y, Ballabio A, Zheng H. The autophagy-lysosomal pathway in neurodegeneration: A TFEB perspective. *Trends Neurosci.* (2016) 39:221–34. doi: 10.1016/j.tins.2016.02.002
67. Suleiman J, Allingham-Hawkins D, Hashem M, Shamseldin HE, Alkuraya FS, El-Hattab AW. WDR45B-related intellectual disability, spastic quadriplegia, epilepsy, and cerebral hypoplasia: A consistent neurodevelopmental syndrome. *Clin Genet.* (2018) 93:360–4. doi: 10.1111/cge.13054
68. Waterham HR, Ferdinandusse S, Wanders RJA. Human disorders of peroxisome metabolism and biogenesis. *Biochim Biophys Acta - Mol Cell Res.* (2016) 1863:922–33. doi: 10.1016/j.bbamcr.2015.11.015
69. Islinger M, Voelkl A, Fahimi HD, Schrader M. The peroxisome: an update on mysteries 2.0. *Histochem Cell Biol.* (2018) 150:443–71. doi: 10.1007/s00418-018-1722-5
70. Berger J, Dorninger F, Forss-Petter S, Kunze M. Peroxisomes in brain development and function. *Biochim Biophys Acta - Mol Cell Res.* (2016) 1863:934–55. doi: 10.1016/j.bbamcr.2015.12.005
71. Hammond DR, Udvadia AJ. Cabin1 expression suggests roles in neuronal development. *Dev Dyn.* (2010) 239:2443–51. doi: 10.1002/dvdy.22367
72. Tarasova EO, Gaydukov AE, Balezina OP. Calcineurin and Its Role in Synaptic Transmission. *Biochemistry (Moscow).* (2018) 83:674–89. doi: 10.1134/S0006297918060056
73. Hopp SC, Bihlmeyer NA, Corradi JP, Vanderburg C, Cacace AM, Das S, et al. Neuronal calcineurin transcriptional targets parallel changes observed in Alzheimer disease brain. *J Neurochem.* (2018) 147:24–39. doi: 10.1111/jnc.14469
74. Hong JM, Moon JH, Park SY. Human prion protein-mediated calcineurin activation induces neuron cell death via AMPK and autophagy pathway. *Int J Biochem Cell Biol.* (2020) 119:105680. doi: 10.1016/j.biocel.2019.105680
75. Subhramanyam CS, Hu Q. Non-coding RNA in brain development and disorder. *Curr Med Chem.* (2017) 24:1983–97. doi: 10.2174/0929867324666170124151436
76. Salvatori B, Biscarini S, Morlando M. Non-coding RNAs in Nervous System Development and Disease. *Front Cell Dev Biol.* (2020) 8:273. doi: 10.3389/fcell.2020.00273
77. Liu W, Zhang Q, Zhang J, Pan W, Zhao J, Xu Y. Long non-coding RNA MALAT1 contributes to cell apoptosis by sponging miR-124 in Parkinson disease. *Cell Biosci.* (2017) 7:19. doi: 10.1186/s13578-017-0147-5
78. Boellaard JW, Schlote W, Tateishi J. Neuronal autophagy in experimental Creutzfeldt-Jakob's disease. *Acta Neuropathol.* (1989) 78:410–8. doi: 10.1007/BF00688178
79. Sanz-Rubio D, López-Pérez Ó, Pablo ÁDA, Bolea R, Osta R, Badiola JJ, et al. Increased circulating microRNAs miR-342-3p and miR-21-5p in natural sheep prion disease. *J Gen Virol.* (2017) 98:305–10. doi: 10.1099/jgv.0.000685
80. Edgar R, Domrachev M, Lash A. Gene Expression Omnibus: NCBI gene expression and hybridization array data repository. *Nucleic Acids Res.* (2002) 30:207–10. doi: 10.1093/nar/30.1.207
81. Burak K, Lamoureux L, Boese A, Majer A, Saba R, Niu Y, et al. MicroRNA-16 targets mRNA involved in neurite extension and branching in hippocampal neurons during presymptomatic prion disease. *Neurobiol Dis.* (2018) 112:1–13. doi: 10.1016/j.nbd.2017.12.011
82. López-Pérez Ó, Bolea R, Marín B, Badiola JJ, Martín-Burriel I. Autophagy impairment in highly prion-affected brain areas of sheep experimentally infected with atypical scrapie. *Vet Microbiol.* (2019) 233:78–84. doi: 10.1016/j.vetmic.2019.04.026
83. Li H, Yu L, Li M, Chen X, Tian Q, Jiang Y, et al. MicroRNA-150 serves as a diagnostic biomarker and is involved in the inflammatory pathogenesis of Parkinson's disease. *Mol Genet Genomic Med.* (2020) 8:e1189. doi: 10.1002/mgg3.1189
84. Jiang Y, Liu YE, Goldberg ID, Shi YE. Gamma synuclein, a novel heat-shock protein-associated chaperone, stimulates ligand-dependent estrogen receptor alpha signaling and mammary tumorigenesis. *Cancer Res.* (2004) 64:4539–46. doi: 10.1158/0008-5472.CAN-03-3650
85. Cervera-Carles L, Dols-Icardo O, Molina-Porcel L, Alcolea D, Cervantes-Gonzalez A, Muñoz-Llahuna L, et al. Assessing circular RNAs in Alzheimer's disease and frontotemporal lobar degeneration. *Neurobiol Aging.* (2020) 92:7–11. doi: 10.1016/j.neurobiolaging.2020.03.017
86. López-Pérez Ó, Otero A, Filali H, Sanz-Rubio D, Toivonen JM, Zaragoza P, et al. Dysregulation of autophagy in the central nervous system of sheep naturally infected with classical scrapie. *Sci Rep.* (2019) 9:1911. doi: 10.1038/s41598-019-38500-2
87. Yang Q, Zhao Q, Yin Y. miR-133b is a potential diagnostic biomarker for Alzheimer's disease and has a neuroprotective role. *Exp Ther Med.* (2019) 18:2711–8. doi: 10.3892/etm.2019.785
88. López-Pérez Ó, Toivonen JM, Otero A, Solanas L, Zaragoza P, Badiola JJ, et al. Impairment of autophagy in scrapie-infected transgenic mice at the clinical stage. *Lab Investig.* (2020) 100:52–63. doi: 10.1038/s41374-019-0312-z

Conflict of Interest: The authors declare that the research was conducted in the absence of any commercial or financial relationships that could be construed as a potential conflict of interest.

MANUSCRITO III

5-Methylcytosine and 5-Hydroxymethylcytosine in Scrapie-Infected Sheep and Mouse Brain Tissues.

Hernaiz, Adelaida; Sentre, Sara; Betancor, Marina; López-Pérez, Óscar; Salinas-Pena, Mónica; Zaragoza, Pilar; Badiola, Juan José; Toivonen, Janne Markus; Bolea, Rosa; Martín-Burriel, Inmaculada.

International Journal of Molecular Sciences. Vol. 24, pág. 1621, 2023. doi:10.3390/IJMS24021621.

International Journal of
Molecular Sciences

MDPI

Article

5-Methylcytosine and 5-Hydroxymethylcytosine in Scrapie-Infected Sheep and Mouse Brain Tissues

Adelaida Hernaiz [2], Sara Sentre [1], Marina Betancor [2], Óscar López-Pérez [1], Mónica Salinas-Pena [1], Pilar Zaragoza [1,3], Juan José Badiola [2], Janne Markus Toivonen [1,3], Rosa Bolea [2] and Inmaculada Martín-Burriel [1,2,3,*]

[1] Laboratorio de Genética Bioquímica (LAGENBIO), Facultad de Veterinaria, Universidad de Zaragoza, IA2, IIS Aragón, 50013 Zaragoza, Spain
[2] Centro de Encefalopatías y Enfermedades Transmisibles Emergentes (CEETE), Facultad de Veterinaria, Universidad de Zaragoza, IA2, IIS Aragón, 50013 Zaragoza, Spain
[3] Centro de Investigación Biomédica en Red de Enfermedades Neurodegenerativas (CIBERNED), Instituto Carlos III, 28029 Madrid, Spain
* Correspondence: minma@unizar.es; Tel.: +34-976-761662

check for updates

Citation: Hernaiz, A.; Sentre, S.; Betancor, M.; López-Pérez, Ó.; Salinas-Pena, M.; Zaragoza, P.; Badiola, J.J.; Toivonen, J.M.; Bolea, R.; Martín-Burriel, I. 5-Methylcytosine and 5-Hydroxymethylcytosine in Scrapie-Infected Sheep and Mouse Brain Tissues. *Int. J. Mol. Sci.* **2023**, *24*, 1621. https://doi.org/10.3390/ijms24021621

Academic Editor: Roberta Mancuso

Received: 28 November 2022
Revised: 10 January 2023
Accepted: 11 January 2023
Published: 13 January 2023

Abstract: Scrapie is a neurodegenerative disorder belonging to the group of transmissible spongiform encephalopathies or prion diseases, which are caused by an infectious isoform of the innocuous cellular prion protein (PrP^{C}) known as PrP^{Sc}. DNA methylation, one of the most studied epigenetic mechanisms, is essential for the proper functioning of the central nervous system. Recent findings point to possible involvement of DNA methylation in the pathogenesis of prion diseases, but there is still a lack of knowledge about the behavior of this epigenetic mechanism in such neurodegenerative disorders. Here, we evaluated by immunohistochemistry the 5-methylcytosine (5mC) and 5-hydroxymethylcytosine (5hmC) levels in sheep and mouse brain tissues infected with scrapie. Expression analysis of different gene coding for epigenetic regulatory enzymes (*DNMT1*, *DNMT3A*, *DNMT3B*, *HDAC1*, *HDAC2*, *TET1*, and *TET2*) was also carried out. A decrease in 5mC levels was observed in scrapie-affected sheep and mice compared to healthy animals, whereas 5hmC displayed opposite patterns between the two models, demonstrating a decrease in 5hmC in scrapie-infected sheep and an increase in preclinical mice. 5mC correlated with prion-related lesions in mice and sheep, but 5hmC was associated with prion lesions only in sheep. Differences in the expression changes of epigenetic regulatory genes were found between both disease models, being differentially expressed *Dnmt3b*, *Hdac1*, and *Tet1* in mice and *HDAC2* in sheep. Our results support the evidence that DNA methylation in both forms, 5mC and 5hmC, and its associated epigenetic enzymes, take part in the neurodegenerative course of prion diseases.

Keywords: 5-methylcytosine; 5-hydroxymethylcytosine; prion diseases; scrapie

1. Introduction

Epigenetics is a field of study focused on heritable changes in gene activity or function that are not associated with any change in the DNA sequence itself [1]. One of the most studied epigenetic modifications is DNA methylation, which consists of the covalent addition of a methyl group to the C-5 position of the nucleobase cytosine to form 5-methylcytosine (5mC) [2]. In mammals, this DNA methylation process occurs predominantly at cytosine residues within CpG dinucleotides [3]. Moreover, multiple forms of DNA methylation have been identified including 5mC, its hydroxylated derivative 5-hydroxymethylcytosine (5hmC), and its ensuing oxidation products 5-formylcytosine (5fC) and 5-carboxylcytosine (5caC) [4]. Among these forms, 5mC and 5hmC are relatively stable and abundant in mammalian genomes [5], whereas 5fC and 5caC are rarer and can be transiently removed [6].

Different enzymes act as mediators of the DNA methylation process. DNA methyltransferases (DNMTs) are responsible for producing 5mC by covalently adding a methyl

group at the C-5 position of cytosines. There are three members of the DNMT family that directly catalyze the addition of methyl groups onto DNA: DNMT1 (DNA methyltransferase 1), DNMT3A (DNA methyltransferase 3 alpha), and DNMT3B (DNA methyltransferase 3 beta) [1]. DNMT3A and DNMT3B are de novo methyltransferases that target cytosines of previously unmethylated CpG dinucleotides, having an equal preference for hemimethylated and unmethylated DNA, and are essential in the de novo methylation of the genome during development [7]. On the other hand, established DNA methylation patterns are stably preserved over cell divisions by DNMT1, a maintenance enzyme that preserves existing methylated sites with a preference for hemimethylated DNA [8].

DNA methylation is involved in the regulation of gene expression and the 5mC form is predominantly associated with gene silencing [9]. DNMT1, DNMT3A, and DNMT3B can repress transcription through an association with histone deacetylases HDAC1 (histone deacetylase 1) and HDAC2 (histone deacetylase 2), enzymes that remove acetyl groups from histones facilitating chromatin compaction and repressing transcription [10].

The 5hmC form results from the addition of a hydroxyl group to 5mC by the ten-eleven translocation enzymes (TETs) [11]. This TET enzyme family comprises three cytosine dioxygenases: TET1 (tet methylcytosine dioxygenase 1), TET2 (tet methylcytosine dioxygenase 2), and TET3 (tet methylcytosine dioxygenase 3) [4]. As previously mentioned, among the three oxidated forms of 5mC, 5hmC is the most stable varying its presence significantly between tissues [12]. Recent findings report that 5hmC is predominantly enriched in the vicinity of transcription factor binding sites, including distal regulatory elements and gene bodies of highly expressed genes, and is less abundant at gene promoter regions [13,14]. This distribution suggests that 5hmC may be associated with stable regulation of gene expression across the genome, potentially counteracting the gene repression produced by 5mC [4].

The regulation of the de novo methylation and demethylation is of great importance for the differentiation and maturation of the mammalian central nervous system (CNS) [1]. DNMTs act coordinated, regulating the 5mC methylation patterns of the neural populations and organizing neuronal development [15]. Moreover, DNMT1 and DNMT3A are involved in the synaptic plasticity of postmitotic neurons and play a role in learning and memory in the adult brain [16]. In addition to 5mC, 5hmC is highly enriched in the CNS in comparison to other tissues [17] and, although less is known about the functions of 5hmC in the brain, some studies suggest the involvement of 5hmC in neurodevelopment and neurological function [18,19].

Just like DNA methylation, in both 5mC and 5hmC forms, it is associated with normal development and function of the CNS; altered DNA methylation patterns have been related to a variety of neurological and neurodegenerative disorders, including Alzheimer's (AD) [20,21] and Parkinson's (PD) [22,23] diseases, as well as Transmissible Spongiform Encephalopathies (TSEs), or prion diseases [24,25].

Prion diseases are a group of neurodegenerative disorders affecting humans and other animals [26] that are caused by an infectious isoform of the innocuous cellular prion protein (PrP^{C}), partially resistant to proteases and prone to form aggregates, called PrP^{Sc} [27]. The accumulation of the PrP^{Sc} in the CNS causes spongiform degeneration, glial cell activation, and neuronal loss [28]. Among the various types of TSEs, ovine scrapie was the first discovered and is considered a good model for the study of different aspects of prion diseases [29,30].

Although recent studies have shed light on the possible roles of DNA methylation in the pathogenesis of prion diseases [24,25,31–33], knowledge in this field is still scarce. Little is known about how 5mC patterns and DNA methylation enzymes behave throughout the course of these diseases and, to the best of our knowledge, no study has yet explored the role of 5hmC in prion pathology. The present study aimed to evaluate the 5mC and 5hmC brain profiles in a transgenic scrapie mouse model and sheep naturally infected with scrapie. Moreover, expression analysis of the genes coding different enzymes involved in the DNA methylation process was performed along with a correlation analysis in order to find possible associations between the brain levels of 5mC and 5hmC with the expression levels of genes encoding DNA methylation enzymes and with prion-related lesions.

2. Results

2.1. Scrapie Characterization

Figure 1 shows the PrP^{Sc} deposition and vacuolation of the analyzed brain areas in Tg338 mice. The obex, mesencephalon, thalamus, and hypothalamus were the areas with higher PrP^{Sc} deposits. Regarding vac vacuolation, obex, mesencephalon, hypothalamus, and septal area/striatum were the areas that showed higher levels of spongiosis.

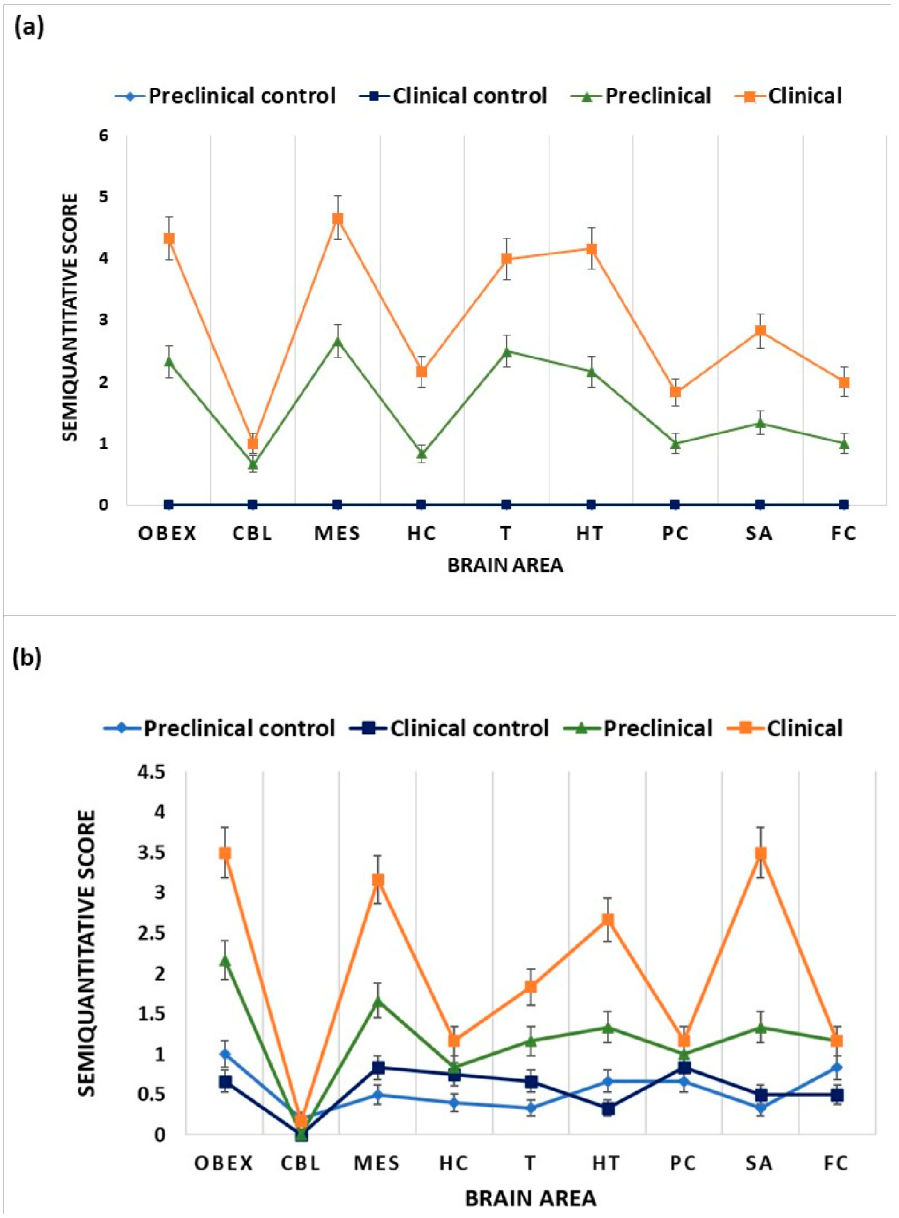

Figure 1. Semiquantitative evaluation in Tg338 mice of (**a**) PrP^{Sc} deposits and (**b**) vacuolation on a semiquantitative scale being 0 for lack of staining/vacuolation and 5 for the staining/vacuolation present at maximum intensity. In (**a**) preclinical control and clinical control display the same levels of PrP^{Sc} deposits. Data are shown as mean values ± SEM in the following brain areas: OBEX, cerebellum (CBL), mesencephalon (MES), hippocampus (HC), thalamus (T), hypothalamus (HT), parietal cortex (PC), septal area/striatum (SA), and frontal cortex (FC).

The scrapie characterization of the sheep used in this study was performed previously in an earlier publication from our group [34].

2.2. Expression Levels of Genes Involved in Epigenetic Regulation

2.2.1. Gene Expression Profile in Tg338 Mice

The expression profile of seven genes described to be involved in epigenetic regulation (*Dnmt1*, *Dnmt3a*, *Dnmt3b*, *Hdac1*, *Hdac2*, *Tet1*, and *Tet2*) was analyzed by quantitative real-time PCR (RT-qPCR) in the thalamus of Tg338 mice, a transgenic scrapie mouse model expressing a transgenic VRQ allele of the ovine *PRNP* gene under the ovine PrP promoter [35,36]. The mice were divided into four groups of

study: clinical and preclinical mice infected with scrapie and their corresponding controls, designated as clinical control and preclinical control, respectively.

In all the studied genes, preclinical mice showed lower expression levels compared to their controls. This decreased expression was statistically significant in *Dnmt3b* ($p < 0.05$) and *Tet1* ($p < 0.05$), and showed a trend to signification ($p = 0.1$) in *Dnmt1*, *Dnmt3a*, *Hdac2*, and *Tet2*. Moreover, the expression of these genes in preclinical mice was also significantly lower than the one observed in clinical mice, the difference being statistically significant for *Dnmt3b* ($p < 0.05$) and *Hdac1* ($p < 0.05$), and with a trend to signification for *Dnmt1* ($p = 0.1$). On the contrary, no significant differences were observed between clinical mice and their controls (Figure 2). Ct values of the RT-qPCR analysis are presented in Supplementary Table S1.

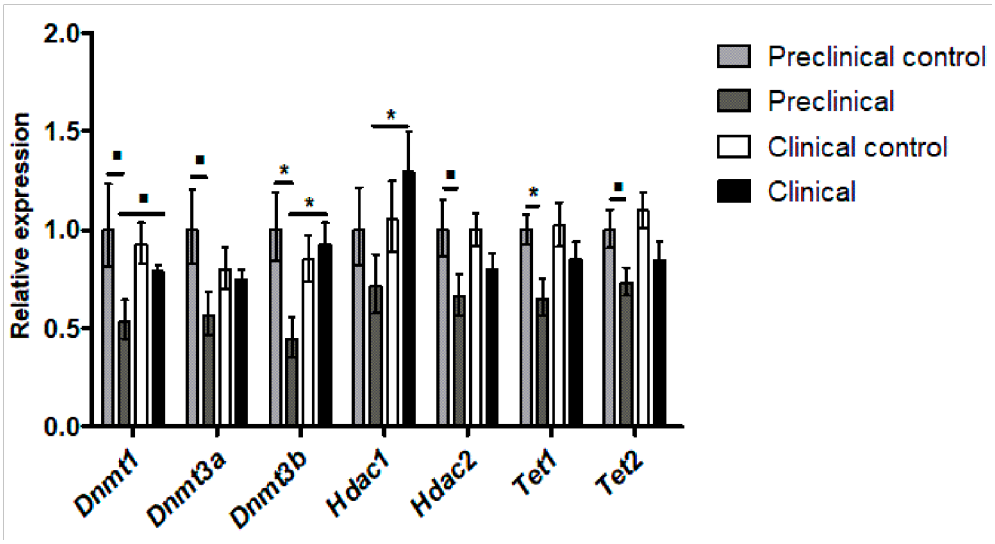

Figure 2. Relative expression levels in terms of $2^{-\Delta\Delta Ct}$ of epigenetic regulatory genes in the thalamus of Tg338 mice. $p = 0.1$; * $p < 0.05$.

In order to test if the lack of statistical significance was due to age differences within the group that could modify gene expression, we calculated the correlation between gene expression Ct values and age in controls. No significant Pearson correlation values were found ($p > 0.05$) for any of the analyzed genes.

2.2.2. Gene Expression Profile in Sheep

In sheep, the expression profile of six genes (*DNMT1*, *DNMT3A*, *DNMT3B*, *HDAC1*, *HDAC2*, and *TET1*) was also analyzed by RT-qPCR in the thalamus region. The sheep were divided into three groups of study: preclinical scrapie-infected sheep, clinical scrapieinfected sheep, and healthy control sheep.

No significant differences were observed in the expression levels of *DNMT1*, *DNMT3A*, and *DNMT3B* genes between the different groups of animals. However, a trend to signification ($p = 0.1$) between control and preclinical sheep, and between control and clinical sheep was observed in *TET1*, whose expression levels, just like in mice, were lower in clinical and preclinical sheep compared to the control ones. In addition, downregulation of *HDAC2* was observed in preclinical sheep compared to controls and clinical animals ($p < 0.05$). These expression trends in the *HDAC2* gene were like those observed in preclinical Tg338 mice. A downregulation of *HDAC1* expression was also observed in clinical scrapie sheep compared to controls ($p = 0.1$), in contrast with the increased expression displayed by the clinical Tg338 mice (Figure 3). Ct values of the RT-qPCR analysis are shown in Supplementary Table S2. Similar to mice, gene expression levels did not correlate with age in controls.

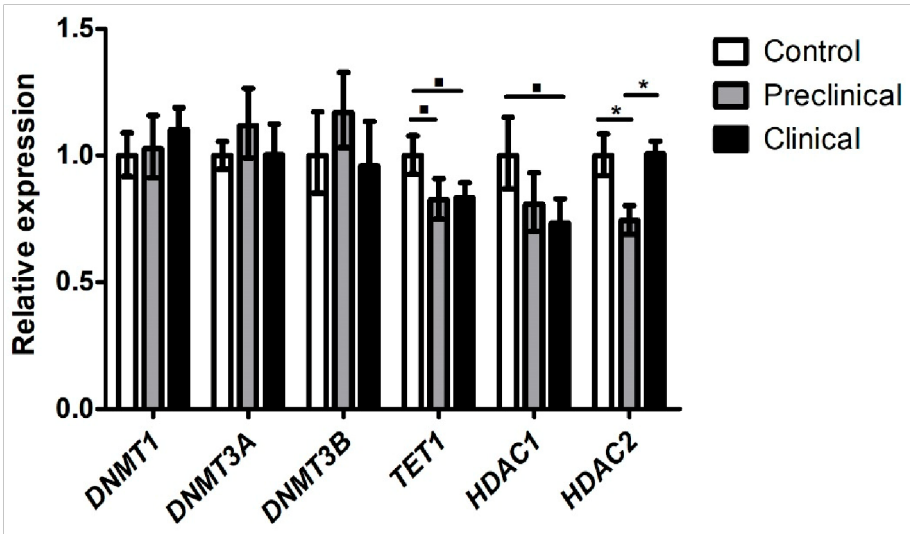

Figure 3. Relative expression levels in terms of $2^{-\Delta\Delta Ct}$ of genes involved in epigenetic regulation in the thalamus of sheep. $p = 0.1$; * $p < 0.05$.

2.3. 5-Methylcytosine and 5-Hydroxymethylcytosine Brain Profiles of Tg338 Mice and Sheep 2.3.1. 5mC and 5hmC Levels in Tg338 Mice Brains

Immunohistochemistry was performed in CNS tissue sections from Tg338 mice for the detection of 5mC and 5hmC. Nine brain areas were studied in the four groups of mice: the frontal cortex, parietal cortex, thalamus, hypothalamus, hippocampus, mesencephalon, cerebellum, obex, and septal area/striatum.

In all the studied brain areas, 5mC and 5hmC displayed intranuclear staining in neurons and glial cells.

Regarding 5mC levels, clinical and preclinical mice displayed similar levels across all the studied brain areas (Figure 4). The same trend was observed between preclinical mice and their respective controls (Figure 4). The obex was the only area that showed a significant difference, namely a decrease in 5mC levels in clinical compared to control mice ($p < 0.05$) (Figures 4 and 5). To determine whether the lack of significance between the different groups was a consequence of differences in age at the sacrifice, we calculated Pearson's correlation between age and immunohistochemical parameters in the animals of control groups, finding only a significant positive correlation ($p < 0.05$) in the cerebellum (r = 0.68) and hypothalamus (r = 0.70).

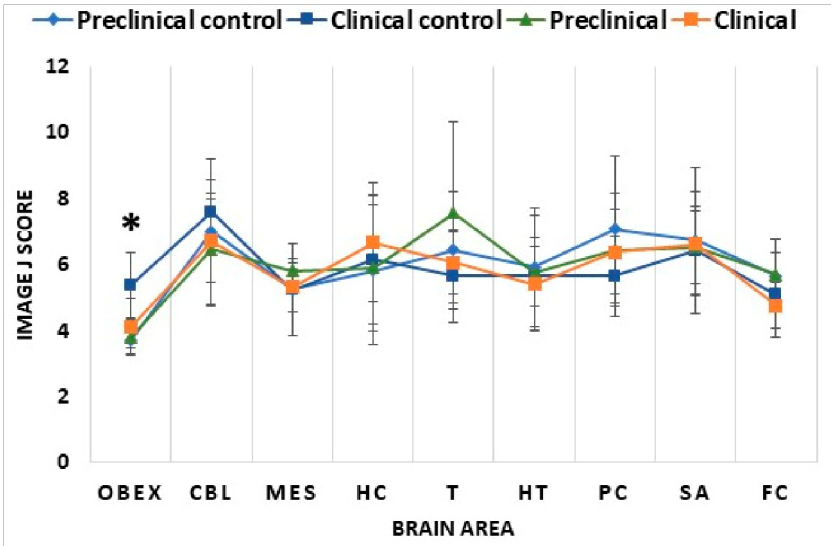

Figure 4. Comparison of 5mC Image J scores of the studied brain areas in the different mice groups: preclinical control, clinical control, preclinical, and clinical mice. The nine studied areas were the obex, cerebellum (CBL), mesencephalon

(MES), hippocampus (HC), thalamus (T), hypothalamus (HT), parietal cortex (PC), septal area/striatum (SA), and frontal cortex (FC). The data are presented as mean values ± SEM. * Significant difference between clinical control and clinical mice ($p < 0.05$).

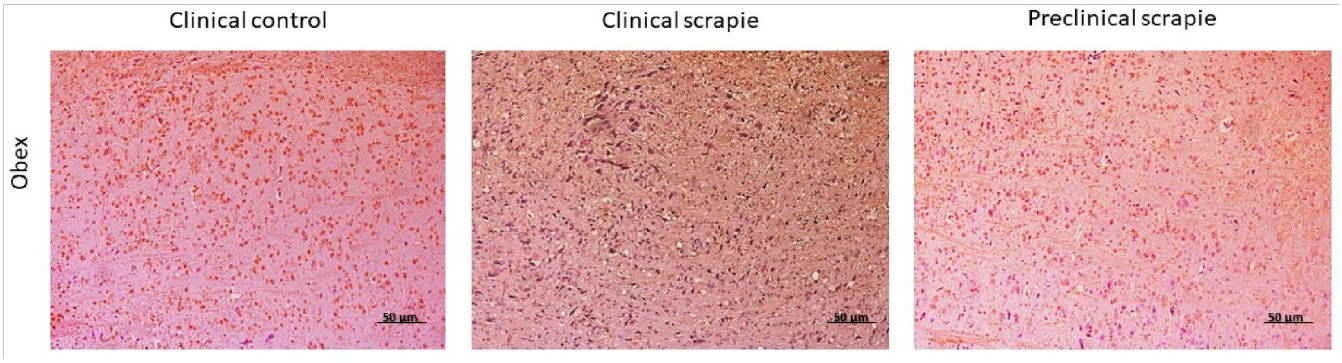

Figure 5. Representative images of 5mC immunostaining in the obex of clinical control mice and clinical and preclinical mice.

A different pattern was observed for 5hmC. Clinical mice showed similar levels to their controls in all studied brain areas (Figure 6). In contrast, 5hmC levels were increased in preclinical mice compared to their controls and the clinical mice (Figure 6). This increase was significant in some of the analyzed brain areas, including in the parietal cortex and cerebellum between preclinical and control mice ($p < 0.05$) and in the thalamus ($p < 0.05$), hypothalamus ($p < 0.01$), parietal cortex ($p < 0.01$), and cerebellum ($p < 0.05$) between preclinical and clinical mice (Figures 6 and 7). Hydroxymethylation did not display a significant correlation with age in any of the analyzed areas (Pearson's correlation $p > 0.05$).

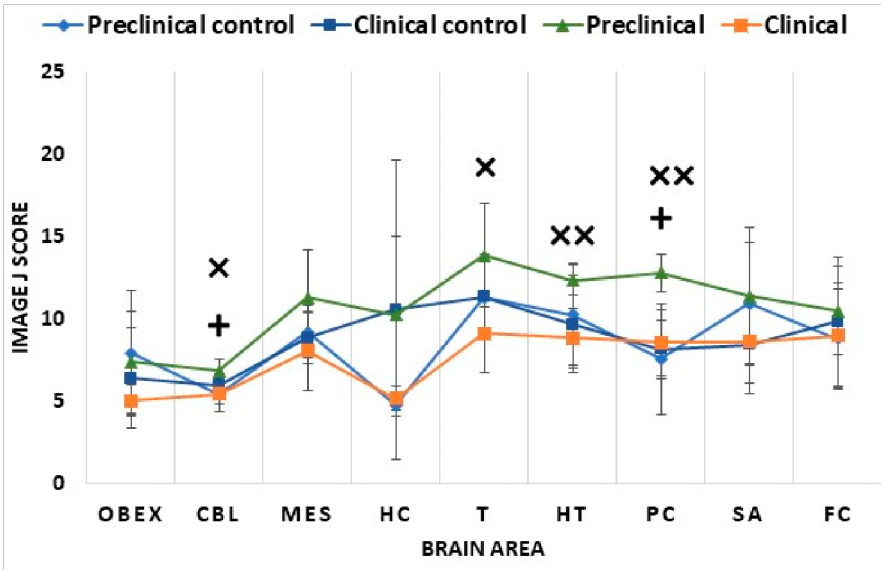

Figure 6. Comparison of 5hmC Image J scores of the studied brain areas in the different mice groups: preclinical control, clinical control, preclinical, and clinical mice. The nine studied areas were the obex, cerebellum (CBL), mesencephalon (MES), hippocampus (HC), thalamus (T), hypothalamus (HT), parietal cortex (PC), septal area/striatum (SA), and frontal cortex (FC). The data are presented as mean values ± SEM. + Significant difference between preclinical control and preclinical mice ($p < 0.05$); × significant difference between preclinical and clinical mice ($p < 0.05$); ×× significant difference between preclinical and clinical mice ($p < 0.01$).

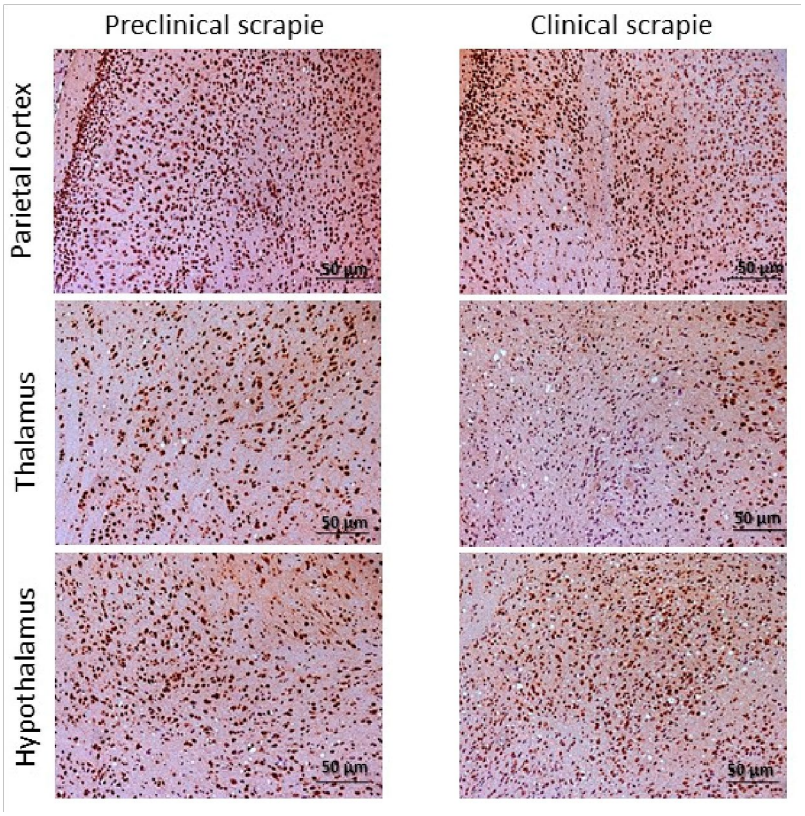

Figure 7. Immunostaining patterns of 5hmC in the parietal cortex, thalamus, and hypothalamus of preclinical and clinical Tg338 mice.

2.3.2. 5mC and 5hmC Levels in Scrapie Sheep Brains

In sheep CNS tissue sections, immunohistochemistry was performed to detect 5mC and 5hmC in eight areas: the frontal cortex, basal ganglia cortex, basal ganglia, parietal cortex, thalamus, hippocampus, mesencephalon, and obex.

Both 5mC and 5hmC showed nuclear and perinuclear staining in neurons and glial cells. The levels of 5mC negatively correlated with age in the thalamus of control sheep ($r = -0.95$, $p = 0.02$). No significant correlations were found in any other areas for 5mC or 5hmC.

Like what was observed in mice, clinical and preclinical sheep showed similar 5mC levels in all studied brain areas (Figure 8). However, infected animals displayed lower values of 5mC signal than controls (Figure 8). This reduction was significant in the mesencephalon ($p < 0.05$), thalamus ($p < 0.01$), and parietal cortex ($p < 0.01$) of clinical scrapie sheep (Figures 8 and 9), and in the mesencephalon ($p < 0.05$), obex ($p < 0.05$), thalamus ($p < 0.05$), and parietal cortex ($p < 0.01$) of preclinical animals (Figures 8 and 9).

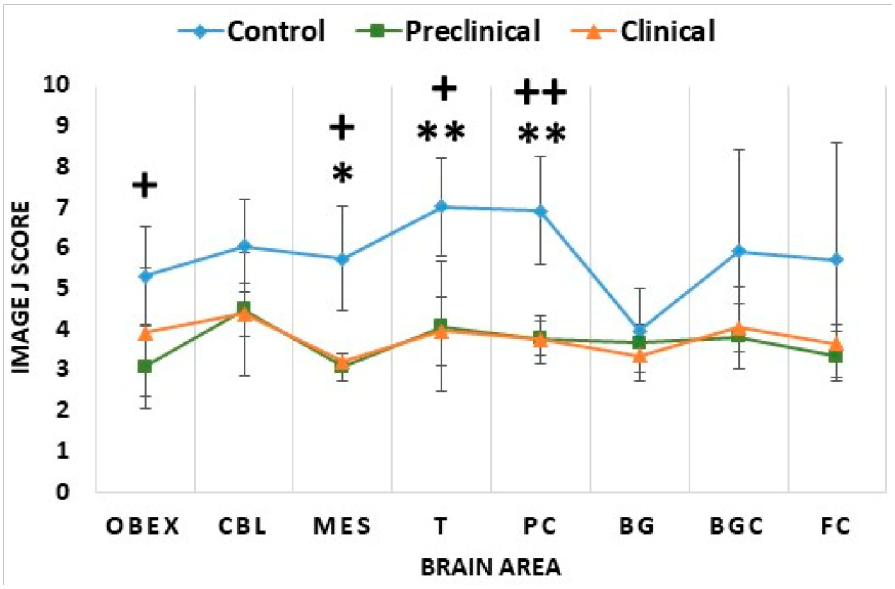

Figure 8. Comparison of 5mC Image J scores in the three sheep groups: control, preclinical, and clinical. The analyzed brain areas were the obex, cerebellum (CBL), mesencephalon (MES), thalamus (T), parietal cortex (PC), basal ganglia (BG), basal ganglia cortex (BGC), and frontal cortex (FC). The data are presented as mean values ± SEM. * Significant difference between control and clinical sheep ($p < 0.05$); ** significant difference between control and clinical sheep ($p < 0.01$); + significant difference between control and preclinical sheep ($p < 0.05$); ++ significant difference between control and preclinical sheep ($p < 0.01$).

Interestingly, 5hmC displayed the same pattern as 5mC. Contrary to the changes found in mice, no differences were observed in the levels of 5hmC between clinical and preclinical sheep (Figure 10), and lower levels of 5hmC were found in both clinical and preclinical sheep in comparison to healthy animals (Figure 10). This decrease in 5hmC levels was significant in the mesencephalon ($p < 0.01$), obex ($p < 0.05$), thalamus ($p < 0.01$), and parietal cortex ($p < 0.01$) of clinical animals (Figures 10 and 11), and also in the mesencephalon ($p < 0.001$), obex ($p < 0.01$), thalamus ($p < 0.01$), and parietal cortex ($p < 0.01$) of preclinical animals (Figures 10 and 11).

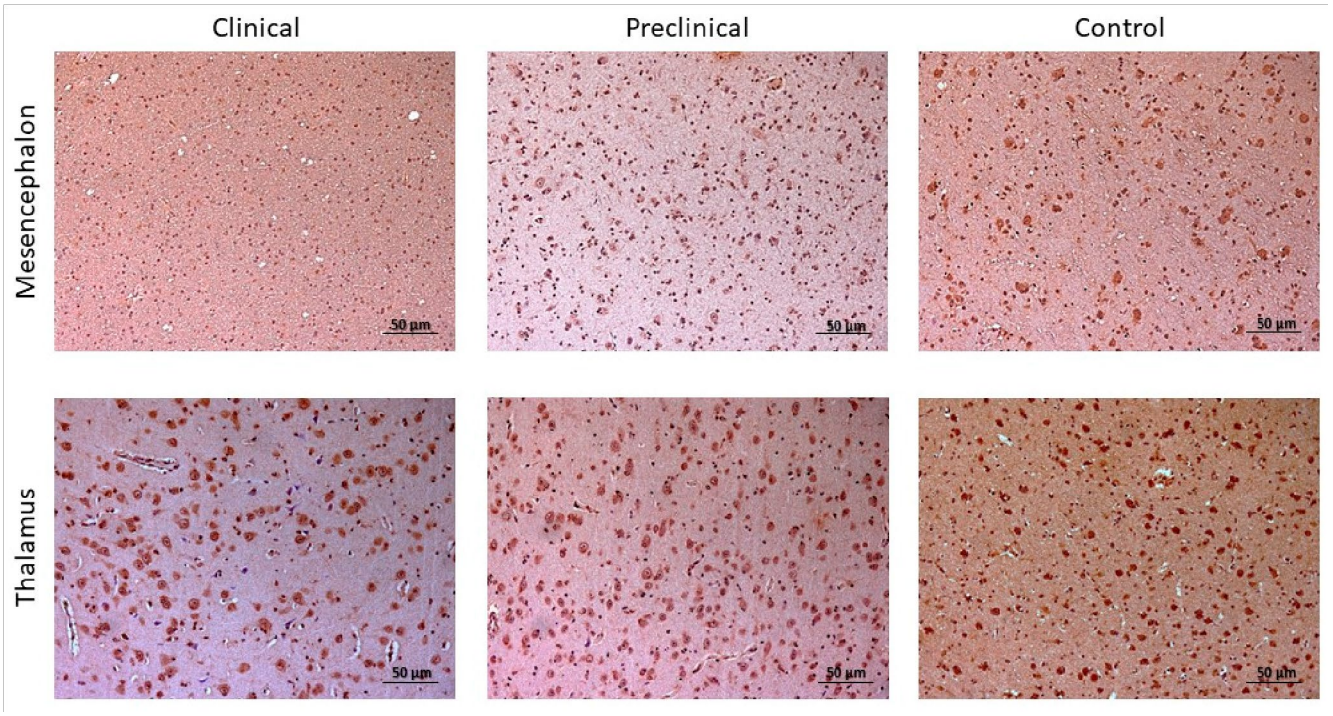

Figure 9. Immunostaining determination of 5mC in mesencephalon and thalamus of preclinical, clinical, and control sheep.

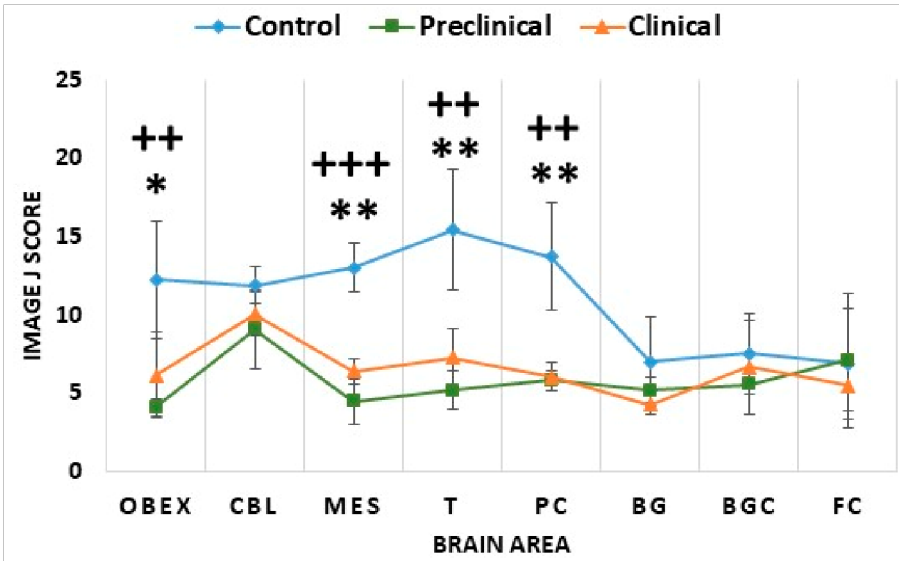

Figure 10. Comparison of 5hmC Image J scores in the three sheep groups: control, preclinical, and clinical. The analyzed brain areas were the obex, cerebellum (CBL), mesencephalon (MES), thalamus (T), parietal cortex (PC), basal ganglia (BG), basal ganglia cortex (BGC), and frontal cortex (FC). The data are presented as mean values ± SEM. * Significant difference between control and clinical sheep ($p < 0.05$); ** significant difference between control and clinical sheep ($p < 0.01$); ++ significant difference between control and preclinical sheep ($p < 0.01$); +++ significant difference between control and preclinical sheep ($p < 0.001$).

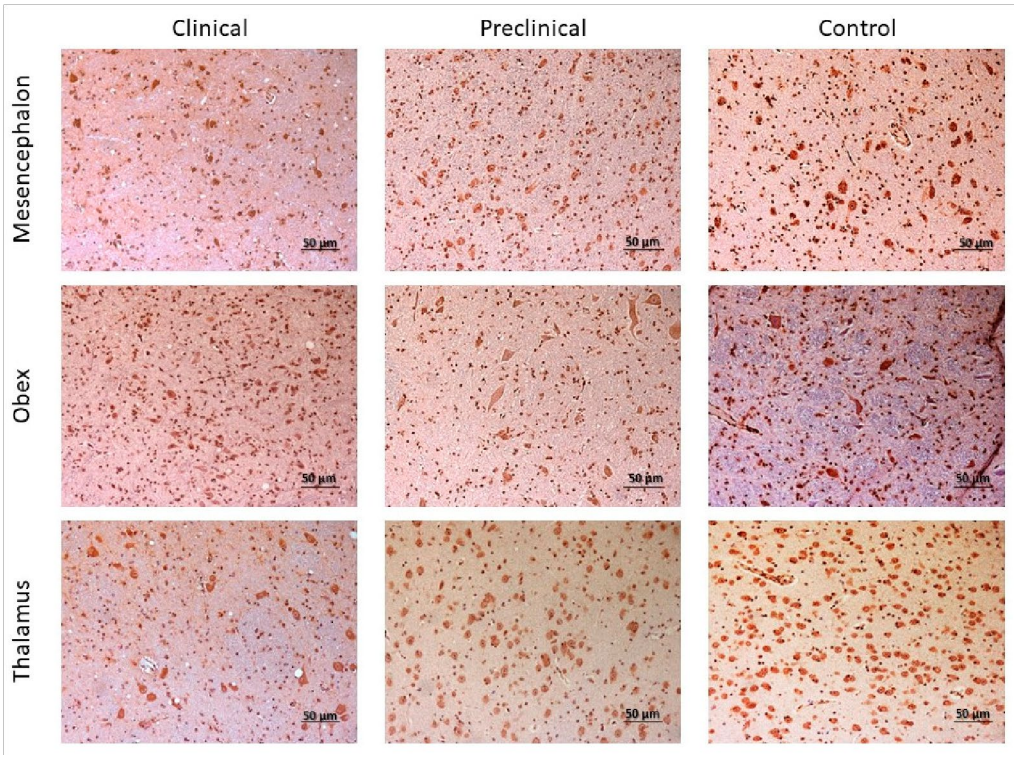

Figure 11. Immunostaining patterns of 5hmC in the mesencephalon, obex, and thalamus of preclinical, clinical, and control sheep.

2.4. Correlation between 5mC and 5hmC Levels

Pearson's correlation was used to evaluate the relationship between 5mC and 5hmC. Comparing all the analyzed brain areas, 5mC and 5hmC displayed a weak but significant positive

correlation in Tg338 mice (r = 0.1432, p = 0.0459) and a stronger correlation in sheep (r = 0.6136, $p = 1.023 \times 10^{-12}$), as shown in Figure 12a,b, respectively.

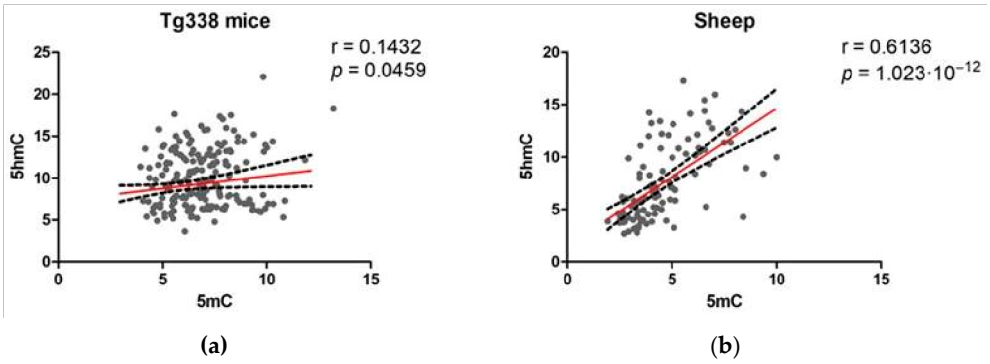

(**a**) (**b**)

Figure 12. Pearson's correlation between 5mC and 5hmC in (**a**) Tg338 mice and (**b**) sheep.

2.5. Correlation between the Levels of 5mC and 5hmC and the Expression Levels of Epigenetic Regulatory Genes in Tg338 Mice and Sheep

In the thalamus region of Tg338 mice and sheep brains, some associations were observed between 5mC and 5hmC levels, and several genes were implicated in epigenetic regulation using Pearson's correlation. Most of these associations were related to 5hmC levels.

In Tg338 mice, significant positive correlations were observed between 5hmC and *Dnmt1* (r = 0.5559, p = 0.0166) (Figure 13a), *Dnmt3a* (r = 0.6579, p = 0.0016) (Figure 13b), *Tet1* (r = 0.6479, p = 0.0027) (Figure 13c), *Tet2* (r = 0.5290, p = 0.0199) (Figure 13d), and *Hdac1* (r = 0.5861, p = 0.0066) (Figure 13e).

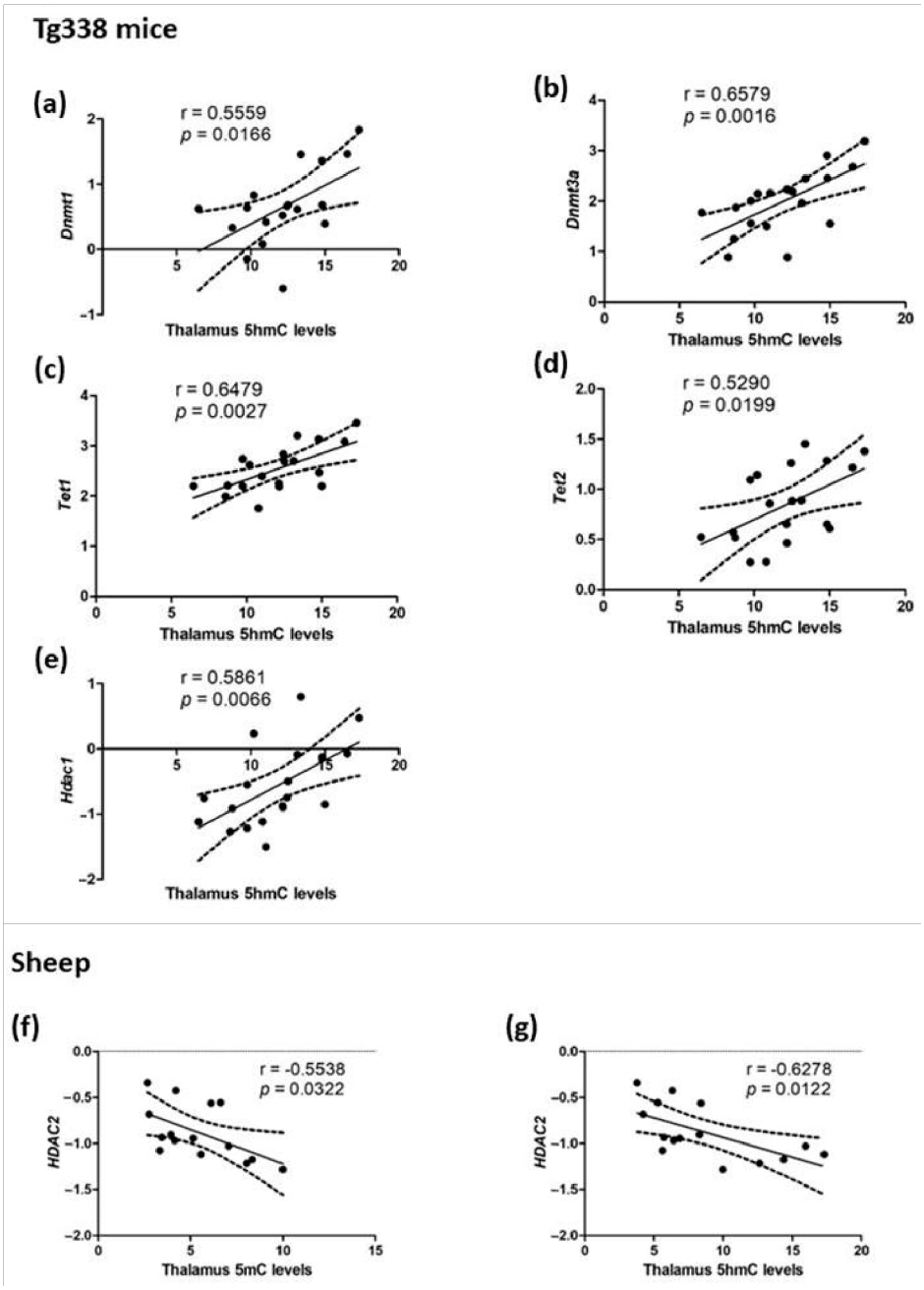

Figure 13. Correlations in the thalamus region of 5mC and 5hmC with the expression levels of some genes involved in epigenetic regulation. 5hmC positively correlated with (**a**) *Dnmt1*, (**b**) *Dnmt3a*, (**c**) *Tet1*, (**d**) *Tet2*, and (**e**) *Hdac1* in Tg338 mice, and 5mC (**f**) and 5hmC (**g**) negatively correlated with *HDAC2* in sheep.

On the contrary, significant negative correlations between *HDAC2*, 5mC (r = −0.5538, p = 0.0322) (Figure 13f), and 5hmC levels (r = −0.6278, p = 0.0122) (Figure 13g) were observed in sheep.

2.6. Correlation of 5mC and 5hmC Levels with Prion-Related Lesions

Spearman's correlation revealed some associations between 5mC, 5hmC, and prionrelated lesions when comparing all the analyzed brain areas in the full set of animals, especially in sheep.

Vacuolation was negatively correlated with 5mC in Tg338 mice (ρ = −0.1528, p = 0.0295). In sheep, 5mC displayed a negative correlation with PrP^{Sc} deposition (ρ = −0.3082, p = 0.0015) and vacuolation (ρ = −0.4369, p = 0.000002). 5hmC was also negatively correlated with vacuolation (ρ = −0.4167, p = 0.000006) and PrP^{Sc} accumulation (ρ = −0.3731, p = 0.00006). However, these significant correlations were lost when this parameter was calculated using only the set of scrapie-infected animals.

3. Discussion

Although recent evidence suggests an involvement of DNA methylation in prion disease pathology, the knowledge about its specific functions and roles is still limited. In the current study, we assessed the 5mC and 5hmC immunohistochemical brain profiles and the expression levels of genes encoding DNA methylation enzymes in a murine model of scrapie disease (Tg338 mice) and sheep naturally infected with scrapie. Moreover, we analyzed possible associations between the 5mC and 5hmC levels with prion-related lesions and with the expression levels of the DNA methylation-related genes.

The levels of 5mC have been studied in other neurodegenerative diseases, such as AD. In the brain of a triple-transgenic mouse model of AD (3xTg-AD) [37] and the brain of preclinical AD patients [38], a decrease in this epigenetic modification was reported. Similar results have been observed in our study, where scrapie-infected sheep and mice showed similar patterns. Clinical and preclinical animals displayed comparable brain levels of 5mC, which were significantly lower in the obex of clinical mice and the mesencephalon, thalamus, parietal cortex, and obex of clinical and preclinical sheep. Furthermore, a negative association of 5mC levels with prion-related lesions was observed in mice and especially in sheep, in which a negative correlation of 5mC with PrP^{Sc} accumulation and vacuolation was found, although the statistical significance of this correlation was lost when considering only the set of scrapie animals. This decrease in 5mC immunostaining is not related with the loss of cells due to prion toxicity and the consequent loss of nuclei because immunoreactivity was normalized taking into account the number of nuclei in each area. As a result, the decrease must be due to a real decrease in immunostaining inside the nucleus of the different cell populations. Although experimental animals used here displayed a similar age, small age differences at animal sacrifice could possibly have an effect on DNA methylation. Within the control group, age variability was found significantly correlated with 5mC in the thalamus of the control sheep. Nevertheless, the reduction in 5mC was still significant in the scrapie thalamus. In control mice, 5mC correlated with age in hypothalamus and cerebellum. We cannot discard the possibility that significant differences in these two specific areas of CNS between control and scrapie mice could have been observed in more homogenous groups. If the decline observed in 5mC levels is a trigger of the disease or a consequence of the disease-related neurodegenerative lesions, it is still unclear and warrants further investigation.

Several reports have shown distinctive levels of 5hmC in Alzheimer's and Parkinson's diseases with different trends between studies. In preclinical and clinical AD patients, different brain regions have been shown to display higher levels of 5hmC [20,38,39]. This increment was also observed in 3xTg-AD [37] and amyloid precursor protein (APP)/presenilin 1 (PS1) [40] AD mouse models and in the cerebellum of PD patients [22,41]. However, other studies point to a decrease in 5hmC in the entorhinal cortex and cerebellum of AD patients [42] and the brain of 3xTg-AD [43] and APP/PS1 [44] mice. In the present study, contrarily to 5mC, 5hmC levels displayed opposite results between sheep and mice. An increase in 5hmC levels was found in preclinical mice, whereas in clinical and preclinical sheep, 5hmC levels decreased in different CNS areas. Differences between the experimental and the natural model may be due to differences in the stage of disease in preclinical animals, whereas a controlled scrapie inoculation in mice allows sacrificing animals in a true preclinical stage clearly distinct from the clinical phase; preclinical sheep can be detected in a late stage, closer to the onset of symptoms.

Although no association was found between prion lesions and 5hmC in mice, in sheep, both 5mC and 5hmC correlated negatively with PrP^{Sc} deposits and vacuolation. Similarly, these correlations were not observed in the set of scrapie animals, suggesting that the correlation is linked to the course of the disease but not to the degree of the lesion. In the natural model, 5hmC follows the same decrease trend as 5mC. This positive correlation between 5mC and 5hmC has been reported in other studies of patients with autism [45] and AD [20]. As opposed to a negative correlation that could be related to the increment of 5hmC as a consequence of the decline in 5mC levels, the concurrent decrease in 5mC and 5hmC suggests that 5hmC could have

a specific role in prion disease pathology and not only act as a demethylation intermediate of 5mC.

Differential expression of genes encoding epigenetic regulatory enzymes was also observed. *Dnmt3b* interacts with *Hdac1* during the establishment of DNA methylation patterns [46]. Moreover, along with its role in de novo DNA methylation, *Dnmt3b* also functions as a DNA dehydroxymethylase, able to directly convert 5hmC to an unmethylated cytosine (C) [47]. In our study, preclinical mice displayed downregulation of *Dnmt3b* whereas, in clinical mice, *Dnmt3b* expression returns to normal levels. This early downregulation was not associated with a decrease in 5mC in the thalamus. In sheep, neither *DNMT3B* expression nor the levels of 5mC were modified significantly between preclinical and clinical animals. These expression changes are neither related to an increase in 5hmC, on the contrary, a significant decrease in 5hmC was observed in both, mice and sheep infected with scrapie. Modification in gene expression could be related with other biological processes. In the adult brain, *Dnmt3b* is required for neurogenesis, facilitating the neuronal maturation in the hippocampus of adult mice [48], and it also plays a role in regulating object-place recognition memory [49]. *Hdac1* is needed as well for neuronal differentiation of murine hippocampal neural stem cells [50] and is involved in DNA damage repair pathways and cognitive function [51], including fear extinction learning [52]. This latter brain function is compromised in schizophrenia patients [52]. Upregulation of *HDAC1* has been found in the prefrontal cortex of patients with schizophrenia [53] and overexpression of this enzyme seems to ameliorate the fear extinction learning cognitive function in mice [52]. The upregulation of *Hdac1* observed in clinical mice could be a compensatory mechanism trying to maintain balanced levels of 5mC and 5hmC, and at the same time, counteract the neurodegenerative effects produced by scrapie disease.

A recent study in mouse embryos showed that *Hdac1* and *Hdac2* were essential for maintaining correct DNA methylation patterns during preimplantation development. Deficiency of *Hdac1* and *Hdac2* in these embryos caused an increase in both forms of DNA methylation, 5mC and 5hmC [54]. Therefore, the upregulation of *HDAC2* observed in clinical scrapie sheep could contribute to the decrease in 5mC and 5hmC levels. Upregulation of *HDAC2* has also been observed in the brain of patients with AD [55] and PD [56] and Swiss albino old mice, and *HDAC2* overexpression has been correlated with reduced recognition memory [57,58]. Inhibition of *HDAC2*, conversely, slows down AD progression through ameliorating amyloid beta-induced neuronal impairments in APP/PS1 mice [59], enhancing mitochondrial respiration and reducing the levels of neurotoxic amyloid beta peptides in induced pluripotent stem cell-derived neurons [60]. These findings suggest that upregulation of *HDAC2*, in addition to contributing to the decline of 5mC and 5hmC, may also be entailed in aggravating the neurodegenerative process. Further studies are essential for delving into the specific role of this enzyme in prion diseases and studying its potential as a therapeutic target.

On the other hand, *Tet1*, which was downregulated in preclinical mice and preclinical and clinical sheep, is one of the enzymes capable of the conversion of 5mC to 5hmC, as well as its further oxidation to 5fC and 5caC intermediates [61]. The relationship between *Tet1* expression and 5hmC levels is somewhat controversial. Decreased levels of *TET1* accompanied by increased levels of 5hmC have been observed in chondrocytes from patients suffering osteoarthritis due to the minor conversion of 5hmC to 5fC or 5caC [62]. Cancer-related studies, however, show an association between reduced *TET1* expression levels and a decrease in 5hmC [63,64]. In addition, this enzyme has important functions in the adult brain beyond its role in DNA demethylation, being necessary for a functional axonmyelinic interface and a successful myelin repair [65] and also critical in the regulation of the neuroinflammation process, associating a downregulation of *Tet1* with aberrant activation of inflammatory response pathways [66]. Interestingly, neuroinflammation is increased during the course of scrapie disease [67–70]. In addition, *Tet1* knock-out mice show a deficiency in adult neurogenesis, spatial learning, and memory [71]. The downregulation of *Tet1* during scrapie disease could have different functional implications regarding the regulation of 5hmC levels, which are positively correlated with the levels of *Tet1*

in mice and decrease when the expression of this gene is downregulated and could also be involved in the impairment of the myelin repair and neuroinflammation pathways and the disruption of the neurogenesis process, contributing altogether to the disease progression.

In conclusion, our results show that DNA methylation and its regulating enzymes are involved in scrapie disease pathology, although there are differences in the epigenetic regulation between the natural model of the disease and the transgenic model. Both methylation forms, 5mC and especially 5hmC, were altered across different brain regions in the two models. 5mC diminished in infected mice and sheep and opposite trends were found for 5hmC, which increased in preclinical mice but diminished in preclinical and clinical sheep. The correlation found between 5mC and 5hmC suggests that the latter could have a relevant role in prion pathogenesis, not only as the intermediate derivative of 5mC. Differential expression of genes encoding epigenetic enzymes was also observed and related mainly to 5hmC patterns. Further studies are warranted to uncover the roles of 5mC and especially 5hmC in prion pathology. Oxidative bisulfite sequencing approaches would be necessary in order to quantify exactly the brain levels of 5hmC and 5mC and to identify specific genes with differential methylation or hydroxymethylation. More research is also indispensable to unravel the exact functions of the different enzymes of the epigenetic machinery in the disease progression and their potential for therapeutic interventions.

4. Materials and Methods

4.1. Animals

4.1.1. Tg338 mice

Tg338 mice (*n* = 24), which express a transgenic VRQ allele of the ovine *PRNP* gene under the ovine PrP promoter [35,36], were used in this study. The mice were divided into four groups: clinical mice (*n* = 6), preclinical mice (*n* = 6), clinical control (*n* = 6), and preclinical control (*n* = 6). Clinical and preclinical mice were intracerebrally inoculated with Tg338-adapted classical scrapie CNS homogenate, originally derived from ARQ/ARQ scrapie sheep, while preclinical and clinical controls were mock inoculated with noninoculated Tg338 CNS homogenate, using the procedure described earlier [72].

The animals included in the preclinical group were sacrificed before showing symptoms associated with scrapie and the clinical ones once they already showed these symptoms. At the same time, the control animals of each group were sacrificed at similar times. Animals in the preclinical groups were inoculated approximately 6 weeks later than the clinical groups in order to sacrifice all animals at similar ages and avoid a possible effect of age in the observed epigenetic modifications [73,74]. In an attempt to achieve homogeneous groups, controls and preclinical mice were sacrificed at different times corresponding to the days on which the animals in the clinical group were sacrificed, when each of them showed clear symptoms of prion disease. The characteristics of the Tg338 mice are summarized in Table 1.

Table 1. Characteristics of the Tg338 mice whose samples were used in this study. ID = mouse identification code and DPI = days post-inoculation at which they were sacrificed.

Group	ID	Gender	Age of Inoculation (Days)	Age of Sacrifice (Days)	DPI
Clinical control	7854-O	Male	42	216	174
	7850-O	Male	42	196	154
	6797-O	Male	42	190	148
	8756-O	Male	42	210	168
	8916-O	Male	42	212	170
	8258-O	Male	35	214	179
Clinical mice	7741-O	Male	35	189	154

	8562-O	Male	35	203	168
	7840-O	Male	35	209	174
	5720-O	Male	35	214	179
	0445-O	Male	35	205	170
	0527-O	Male	35	183	148
Preclinical control	6404-O	Male	77	214	137
	8373-O	Male	84	219	135
	8508-O	Male	84	196	112
	5997-O	Male	84	212	128
	6768-O	Male	84	212	128
	7038-O	Male	84	196	112
Preclinical mice	7731-O	Male	79	191	112
	6775-O	Male	79	214	135
	7000-O	Male	79	216	137
	7457-O	Male	79	207	128
	6248-O	Male	79	207	128
	6500-O	Male	79	191	112

4.1.2. Sheep

A total of 15 female Rasa Aragonesa sheep, aged between 4 and 6 years and carrying the ARQ/ARQ genotype for the ovine *PRNP* gene, were included in this study. They were divided into three groups depending on their clinical status: clinical sheep (n = 5), preclinical sheep (n = 5), and control sheep (n = 5). All selected animals had similar ages in order to exclude a possible influence of age in the observed epigenetic modifications [73,74]. Sheep in the preclinical stage were identified by immunohistochemical analysis of rectal mucosa biopsies and sacrificed before clinical signs were detectable by pentobarbital overdose, whereas animals in the clinical stage were identified by the observation of scrapie-related symptoms. These animals correspond to those used previously in an assessment study of neurogranin and neurofilament light chain as preclinical biomarkers in scrapie [34].

4.2. Tissue Collection

After the euthanasia of Tg338 mice, the brain of each mouse was harvested and divided sagittally. One hemisphere was fixed by immersion in 10% formalin for up to 48 h for further histopathological and immunohistochemical analyses. The other hemisphere was frozen immediately in dry ice and conserved at −80 °C. From this hemisphere, the thalamus region was used for gene expression studies.

Regarding ovine samples, after sheep were sacrificed, samples from eight areas of the CNS (the frontal cortex, basal ganglia cortex, basal ganglia, parietal cortex, thalamus, hippocampus, mesencephalon, and obex) were collected and fixed in 10% formaldehyde for further use in histopathological and immunohistochemical analyses. In addition, thalamus samples from each sheep were preserved in RNAlater™ solution (Thermo Fisher Scientific, Waltham, MA, USA) for gene expression analyses.

4.3. Neuropathological Evaluation of Tg338 Mice and Scrapie Sheep

Tg338 brains fixed previously in formalin were embedded in paraffin wax, cut into 4-µm-thick sections, and mounted on glass slides for evaluation of vacuolation, a prionrelated lesion, using hematoxylin and eosin (H-E) staining. PrP^{Sc} deposition analysis was carried out using the paraffin-embedded tissue (PET) blot method previously described [75]. Briefly, paraffin-embedded sections were collected onto nitrocellulose membranes (0.45 µm pore size; Bio-Rad, Hercules, CA, USA) and digested with 250 µg/mL of proteinase K for 2 h at 56 °C. Proteins adhered to the membrane were denatured with 3 M guanidine thiocyanate (Sigma-Aldrich, St. Louis, MO, USA) and PrP^{Sc} was detected using Sha31 mouse monoclonal antibody (SPI-Bio, Montigny le Bretonneux, France) at 1:8000 dilution for 1 h. Sections were then incubated for 1 h with an alkaline phosphatase-coupled goat anti-mouse antibody (Dako, St. Clara, CA, USA) at 1:500 dilution. Enzymatic activity was visualized using NBT/BCIP chromogen (Sigma-Aldrich, St. Louis, MO, USA). Vacuolation and PrP^{Sc} deposition were semiquantitatively evaluated per area with a scale score, being 0 for lack of vacuoles/PrP^{Sc} deposit and 5 for very intense vacuolation/PrP^{Sc} deposit, following the standard method to assess these features [76]. The histopathological data of PrP^{Sc} deposition and vacuolation are shown in Figure 1 and Supplementary Table S3. In scrapie sheep, paraffin-embedded 4 µm-thick sections from the eight previously mentioned areas were used for histopathological evaluation of vacuolation by H-E staining. PrP^{Sc} was detected by immunohistochemistry using the monoclonal primary antibody L42 (RBiopharm, Darmstadt, Germany) at 1:500 dilution for 30 min after formic acid treatment and proteinase K digestion, as previously described [77]. The histopathological evaluation of these sheep was performed in a previous study [34].

4.4. Expression Analysis of Genes Involved in Epigenetic Regulation

4.4.1. Gene Expression Analysis in Tg338 Mice

Seven genes, described to be involved in epigenetic regulation, were selected for the analysis of their expression profile in the thalamus of Tg338 mice: *Dnmt1*, *Dnmt3a*, *Dnmt3b*, *Hdac1*, *Hdac2*, *Tet1*, and *Tet2*. Table 2 shows TaqMan assays (Thermo Fisher Scientific) used for the amplification of the genes of interest.

Table 2. References of the probes used for the RT-qPCR TaqMan amplification assay in Tg338 mice. ID = identification of the commercial company (Thermo Fisher Scientific, Waltham, MA, USA).

Gene	ID
Dnmt1	Mm01151063_m1
Dnmt3a	Mm00432881_m1
Dnmt3b	Mm01240113_m1
Tet1	Mm01169087_m1
Tet2	Mm00524395_m1
Hdac1	Mm02745760_g1
Hdac2	Mm00515108_m1
Sdha	Mm01352366_m1
H6pd	Mm00557617_m1

Total RNA was isolated using the RNeasy Lipid Tissue Mini kit (Qiagen, Valencia, CA, USA). The quality and quantity of RNA were determined using a NanoDrop instrument (Thermo Fisher Scientific, Waltham, MA, USA). An amount of 200 ng of total RNA was used for retrotranscription with qScript™ cDNA Supermix (Quanta Biosciences™, Gaithersburg, MD, USA), according to the manufacturer's instructions. The resulting complementary DNA (cDNA) was diluted 1:5 in water and gene expression was quantified by RT-qPCR using the TaqMan universal PCR master mix

assays (Thermo Fisher Scientific) in a StepOne Plus Real-Time PCR instrument (Applied Biosystems, Waltham, MA, USA). All reactions were run in triplicate. The comparative quantification of the results was standardized by the $2^{-\Delta\Delta Ct}$ method [78], using the geometric mean of *Sdha* and *H6pd* housekeeping genes (Table 2) as a normalizer. Student's *t*-test was applied to identify differences between groups, which were considered significant at $p < 0.05$.

4.4.2. Gene Expression Analysis in Sheep

The expression profile of six genes (*DNMT1*, *DNMT3A*, *DNMT3B*, *HDAC1*, *HDAC2*, and *TET1*) was assessed in sheep thalamus samples. The primers used for the RT-qPCR assay are listed in Table 3.

Table 3. Sequences of primers used in the RT-qPCR assay in sheep. Fw = Forward primer and Rv = Reverse primer.

Gene	Primer Sequences
DNMT1	Fw: 5′-CCCAGGAGAAGCAAGTCTGATG-3′ Rv: 5′-TGATGGTGGTCTGCCTGGTAGT-3′
DNMT3A	Fw: 5′-GGGACCCCTACTACATCAGCAA-3′ Rv: 5′-GCATTCATTACTGCGATCACCTT-3′
DNMT3B	Fw: 5′-TGGTTTGGTGATGGCAAGTTC-3′ Rv: 5′-TGAAGGTCGCCAGGTTAAAGTG-3′
HDAC1	Fw: 5′-CCTCTCCGAGATGGGATTGA-3′ Rv: 5′-CTGCACTGGGCTGGAACAT-3’
HDAC2	Fw: 5′-GGAGCCCATGGCGTACAGT-3′ Rv: 5′-ACCCTGTCCGTAGTAATAATTTCCA-3′
TET1	Fw: 5′-GAAATGCAATAAGGATAGAAATAGTAGTGTACA-3′ Rv: 5′-TCTTCGTCGCTGCTTCTTCTT-3′

Total RNA isolation and retrotranscription were performed following identical procedures to the ones used with murine samples. The resulting cDNA was diluted 1:5 in water and gene expression was quantified by RT-qPCR using the Fast SYBR™ Green Master Mix (Applied Biosystems, Thermo Fisher Scientific) in a StepOne Plus Real-Time PCR instrument (Applied Biosystems). Each PCR was performed in triplicate. The results were standardized by the $2^{-\Delta\Delta Ct}$ method [78], using the geometric mean of *SDHA* and *G6PDH* housekeeping genes [79] as a normalizer. To identify differences between groups, Student's *t*-test was performed, and significant differences were considered at $p < 0.05$.

4.5. Immunohistochemical Analysis of 5-Methylcytosine and 5-Hydroxymethylcytosine Levels in Tg338 Mice and Sheep

Immunohistochemistry for the detection of 5mC and 5hmC was performed in paraffinembedded CNS tissue sections from Tg338 mice and sheep. In Tg338 mice, nine brain areas were studied: the frontal cortex, parietal cortex, thalamus, hypothalamus, hippocampus, mesencephalon, cerebellum, obex, and septal area/striatum. In sheep, a total of eight brain areas were analyzed: the frontal cortex, basal ganglia cortex, basal ganglia, parietal cortex, thalamus, hippocampus, mesencephalon, and obex.

After deparaffination and rehydration, tissue sections were subjected to antigen retrieval with citrate buffer (pH 6.0) for 20 min at 85 °C in a PTLink (Dako). Afterward, endogenous peroxidase activity was blocked using a precast solution (Dako Agilent, Glostrup, Denmark). Sections were then incubated overnight at 4 °C with the primary antibodies 5mC (Thermo Fisher Scientific, AB_2787107) at 1:100 dilution in Tg338 mice and 1:75 in sheep and 5hmC (Thermo Fisher Scientific, AB_2610634) at 1:200 dilution in Tg338 mice and 1:75 in sheep. The omission

of the primary antibody served as a background control for the nonspecific binding of the secondary antibody. Subsequently, the sections were incubated with an anti-mouse enzyme-conjugated EnVision polymer (Dako Agilent, Glostrup, Denmark) for 30 min at room temperature. Diaminobenzidine (DAB, Dako Agilent, Glostrup, Denmark) was used as the chromogen.

CNS sections were assessed and photographed using a Zeiss Axioskop 40 optical microscope (Zeiss, Jena, Germany). 5mC and 5hmC immunostaining levels were evaluated using Image J software and following the semi-quantification analysis method [80], in which for each image, the DAB staining intensity is normalized by the number of nuclei. Afterward, the normalized DAB staining intensity mean and its standard deviation were calculated for each group of animals (clinical, preclinical, and control) in both Tg338 mice and sheep. Student's *t*-test was applied to identify differences between scrapie-infected and control groups, which were considered significant at $p < 0.05$.

4.6. Correlation between 5mC and 5hmC Levels, Age, Gene Expression, and Prion-Associated Features

Pearson's and Spearman's correlations calculated with GraphPad Prism software v.5 were used to evaluate possible relationships between 5mC and 5hmC intensities and the expression levels of epigenetic regulatory genes in the thalamic region, and between 5mC and 5hmC levels and prion-related lesions in both Tg338 mice and sheep. Correlations were considered significant at $p < 0.05$. Correlations between the different methylation parameters and age were also calculated in control groups of mice and sheep in order to evaluate if age differences within groups could affect the obtained results.

Supplementary Materials: The following supporting information can be downloaded at https://www.mdpi.com/article/10.3390/ijms24021621/s1.

Author Contributions: Conceptualization, I.M.-B.; investigation, A.H., S.S., M.B., Ó.L.-P., M.S.-P. and J.M.T.; writing—original draft preparation, A.H.; writing—review and editing, I.M-B. and J.M.T.; visualization, A.H.; supervision, I.M.-B. and R.B.; project administration, I.M.-B., R.B. and J.M.T.; funding acquisition, I.M.-B., J.M.T., R.B., J.J.B. and P.Z. All authors have read and agreed to the published version of the manuscript.

Funding: This research was funded by Gobierno de Aragón and the European Social Fund cofinanced predoctoral grant Order IIU/2023/2017, the research project AGL2015-67945-P financed by the Spanish Ministry of Economy and Competitiveness, Feder funds, and the 19-20R-LAGENBIO Consolidated Group of the Gobierno de Aragón.

Institutional Review Board Statement: The animal study protocol was approved by the Ethics Committee for Animal Experimentation of the University of Zaragoza (PI40/15, PI138/15).

Informed Consent Statement: Not applicable.

Data Availability Statement: The data presented in this study are available within the article text, figures, and Supplementary Materials.

Acknowledgments: We are grateful to Vincent Béringue (UMR Virologie Immunologie Moléculaires (VIM-UR892), INRAE, Université Paris-Saclay) for providing us with the Tg338 mice.

Conflicts of Interest: The authors declare no conflict of interest.

References

1. Moore, L.D.; Le, T.; Fan, G. DNA Methylation and Its Basic Function. *Neuropsychopharmacology* **2013**, *38*, 23–38. [CrossRef]
2. Kulis, M.; Esteller, M. DNA Methylation and Cancer. *Adv. Genet.* **2010**, *70*, 27–56. [CrossRef]
3. Bestor, T.H. The DNA Methyltransferases of Mammals. *Hum. Mol. Genet.* **2000**, *9*, 2395–2402. [CrossRef]
4. Meng, H.; Meng, H.; Cao, Y.; Qin, J.; Song, X.; Zhang, Q.; Shi, Y.; Cao, L. DNA Methylation, Its Mediators and Genome Integrity. *Int. J. Biol. Sci.* **2015**, *11*, 604–617. [CrossRef] [PubMed]
5. Wu, S.C.; Zhang, Y. Active DNA Demethylation: Many Roads Lead to Rome. *Nat. Rev. Mol. Cell Biol.* **2010**, *11*, 607–620. [CrossRef] [PubMed]

6. Maiti, A.; Drohat, A.C. Thymine DNA Glycosylase Can Rapidly Excise 5-Formylcytosine and 5-Carboxylcytosine: Potential Implications for Active Demethylation of CpG Sites. *J. Biol. Chem.* **2011**, *286*, 35334–35338. [CrossRef] [PubMed]
7. Okano, M.; Bell, D.W.; Haber, D.A.; Li, E. DNA Methyltransferases Dnmt3a and Dnmt3b Are Essential for de Novo Methylation and Mammalian Development. *Cell* **1999**, *99*, 247–257. [CrossRef]
8. Goll, M.G.; Bestor, T.H. Eukaryotic Cytosine Methyltransferases. *Annu. Rev. Biochem.* **2005**, *74*, 481–514. [CrossRef]
9. Li, E. Chromatin Modification and Epigenetic Reprogramming in Mammalian Development. *Nat. Rev. Genet.* **2002**, *3*, 662–673. [CrossRef]
10. Rountree, M.R.; Bachman, K.E.; Herman, J.G.; Baylin, S.B. DNA Methylation, Chromatin Inheritance, and Cancer. *Oncogene* **2001**, *20*, 3156–3165. [CrossRef]
11. Tahiliani, M.; Koh, K.P.; Shen, Y.; Pastor, W.A.; Bandukwala, H.; Brudno, Y.; Agarwal, S.; Iyer, L.M.; Liu, D.R.; Aravind, L.; et al. Conversion of 5-Methylcytosine to 5-Hydroxymethylcytosine in Mammalian DNA by MLL Partner TET1. *Science* **2009**, *324*, 930–935. [CrossRef] [PubMed]
12. Münzel, M.; Lercher, L.; Müller, M.; Carell, T. Chemical Discrimination between DC and 5MedC via Their Hydroxylamine Adducts. *Nucleic Acids Res.* **2010**, *38*, e192. [CrossRef] [PubMed]
13. Song, C.X.; Szulwach, K.E.; Fu, Y.; Dai, Q.; Yi, C.; Li, X.; Li, Y.; Chen, C.H.; Zhang, W.; Jian, X.; et al. Selective Chemical Labeling Reveals the Genome-Wide Distribution of 5-Hydroxymethylcytosine. *Nat. Biotechnol.* **2011**, *29*, 68–75. [CrossRef]
14. Yu, M.; Hon, G.C.; Szulwach, K.E.; Song, C.X.; Zhang, L.; Kim, A.; Li, X.; Dai, Q.; Shen, Y.; Park, B.; et al. Base-Resolution Analysis of 5-Hydroxymethylcytosine in the Mammalian Genome. *Cell* **2012**, *149*, 1368–1380. [CrossRef] [PubMed]
15. Fan, G.; Martinowich, K.; Chin, M.H.; He, F.; Fouse, S.D.; Hutnick, L.; Hattori, D.; Ge, W.; Shen, Y.; Wu, H.; et al. DNA Methylation

Controls the Timing of Astrogliogenesis through Regulation of JAK-STAT Signaling. *Development* **2005**, *132*, 3345–3356. [CrossRef]

16. Feng, J.; Zhou, Y.; Campbell, S.L.; Le, T.; Li, E.; Sweatt, J.D.; Silva, A.J.; Fan, G. Dnmt1 and Dnmt3a Maintain DNA Methylation and Regulate Synaptic Function in Adult Forebrain Neurons. *Nat. Neurosci.* **2010**, *13*, 423–430. [CrossRef]
17. Globisch, D.; Münzel, M.; Müller, M.; Michalakis, S.; Wagner, M.; Koch, S.; Brückl, T.; Biel, M.; Carell, T. Tissue Distribution of 5-Hydroxymethylcytosine and Search for Active Demethylation Intermediates. *PLoS ONE* **2010**, *5*, e15367. [CrossRef]
18. Cheng, Y.; Bernstein, A.; Chen, D.; Jin, P. 5-Hydroxymethylcytosine: A New Player in Brain Disorders? *Exp. Neurol.* **2015**, *268*, 3–9. [CrossRef] [PubMed]
19. Szulwach, K.E.; Li, X.; Li, Y.; Song, C.X.; Wu, H.; Dai, Q.; Irier, H.; Upadhyay, A.K.; Gearing, M.; Levey, A.I.; et al. 5-HmC-Mediated Epigenetic Dynamics during Postnatal Neurodevelopment and Aging. *Nat. Neurosci.* **2011**, *14*, 1607–1616. [CrossRef]
20. Coppieters, N.; Dieriks, B.V.; Lill, C.; Faull, R.L.M.; Curtis, M.A.; Dragunow, M. Global Changes in DNA Methylation and Hydroxymethylation in Alzheimer's Disease Human Brain. *Neurobiol. Aging* **2014**, *35*, 1334–1344. [CrossRef]
21. Gao, Z.; Fu, H.J.; Zhao, L.B.; Sun, Z.Y.; Yang, Y.F.; Zhu, H.Y. Aberrant DNA Methylation Associated with Alzheimer's Disease in the Superior Temporal Gyrus. *Exp. Ther. Med.* **2018**, *15*, 103–108. [CrossRef] [PubMed]
22. Kaut, O.; Kuchelmeister, K.; Moehl, C.; Wüllner, U. 5-Methylcytosine and 5-Hydroxymethylcytosine in Brains of Patients with Multiple System Atrophy and Patients with Parkinson's Disease. *J. Chem. Neuroanat.* **2019**, *96*, 41–48. [CrossRef] [PubMed]
23. Young, J.I.; Sivasankaran, S.K.; Wang, L.; Ali, A.; Mehta, A.; Davis, D.A.; Dykxhoorn, D.M.; Petito, C.K.; Beecham, G.W.; Martin, E.R.; et al. Genome-Wide Brain DNA Methylation Analysis Suggests Epigenetic Reprogramming in Parkinson Disease. *Neurol. Genet.* **2019**, *5*, e342. [CrossRef] [PubMed]
24. Dabin, L.C.; Guntoro, F.; Campbell, T.; Bélicard, T.; Smith, A.R.; Smith, R.G.; Raybould, R.; Schott, J.M.; Lunnon, K.; Sarkies, P.; et al. Altered DNA Methylation Profiles in Blood from Patients with Sporadic Creutzfeldt–Jakob Disease. *Acta Neuropathol.* **2020**, *140*, 863–879. [CrossRef]
25. Hernaiz, A.; Sanz, A.; Sentre, S.; Ranera, B.; Lopez-Pérez, O.; Zaragoza, P.; Badiola, J.J.; Filali, H.; Bolea, R.; Toivonen, J.M.; et al. Genome-Wide Methylation Profiling in the Thalamus of Scrapie Sheep. *Front. Vet. Sci.* **2022**, *9*, 29. [CrossRef]
26. Ma, J.; Wang, F. Prion Disease and the "Protein-Only Hypothesis". *Essays Biochem.* **2014**, *56*, 181–191. [CrossRef]
27. Prusiner, S.B. Novel Proteinaceous Infectious Particles Cause Scrapie. *Science* **1982**, *216*, 136–144. [CrossRef]

28. Bell, J.E.; Ironside, J.W. Neuropathology of Spongiform Encephalopathies in Humans. *Br. Med. Bull.* **1993**, *49*, 738–777. [CrossRef]
29. Pattison, I.H.; Jones, K.M. The Astrocytic Reaction in Experimental Scrapie in the Rat. *Res. Vet. Sci.* **1967**, *8*, 160–165. [CrossRef]
30. Hope, J. The Biology and Molecular Biology of Scrapie-like Diseases. *Arch. Virol. Suppl.* **1993**, *7*, 201–214. [CrossRef]
31. Guntoro, F.; Viré, E.; Giordani, C.; Darwent, L.; Hummerich, H.; Linehan, J.; Sinka, K.; Jaunmuktane, Z.; Brandner, S.; Collinge, J.; et al. DNA Methylation Analysis of Archival Lymphoreticular Tissues in Creutzfeldt-Jakob Disease. *Acta Neuropathol.* **2022**, *144*, 785–787. [CrossRef]
32. Hernaiz, A.; Toivonen, J.M.; Bolea, R.; Martín-Burriel, I. Epigenetic Changes in Prion and Prion-like Neurodegenerative Diseases: Recent Advances, Potential as Biomarkers, and Future Perspectives. *Int. J. Mol. Sci.* **2022**, *23*, 12609. [CrossRef] [PubMed]
33. Viré, E.A.; Mead, S. Gene Expression and Epigenetic Markers of Prion Diseases. *Cell Tissue Res.* **2022**. [CrossRef] [PubMed] 34. Betancor, M.; Pérez-Lázaro, S.; Otero, A.; Marín, B.; Martín-Burriel, I.; Blennow, K.; Badiola, J.J.; Zetterberg, H.; Bolea, R.
Neurogranin and Neurofilament Light Chain as Preclinical Biomarkers in Scrapie. *Int. J. Mol. Sci.* **2022**, *23*, 7182. [CrossRef]
35. Laude, H.; Vilette, D.; Le Dur, A.; Archer, F.; Soulier, S.; Besnard, N.; Essalmani, R.; Vilotte, J.L. New in Vivo and Ex Vivo Models for the Experimental Study of Sheep Scrapie: Development and Perspectives. *C. R. Biol.* **2002**, *325*, 49–57. [CrossRef]
36. Vilotte, J.-L.; Soulier, S.; Essalmani, R.; Stinnakre, M.-G.; Vaiman, D.; Lepourry, L.; Da Silva, J.C.; Besnard, N.; Dawson, M.; Buschmann, A.; et al. Markedly Increased Susceptibility to Natural Sheep Scrapie of Transgenic Mice Expressing Ovine Prp. *J. Virol.* **2001**, *75*, 5977–5984. [CrossRef] [PubMed]
37. Cadena-Del-Castillo, C.; Valdes-Quezada, C.; Carmona-Aldana, F.; Arias, C.; Bermúdez-Rattoni, F.; Recillas-Targa, F. AgeDependent Increment of Hydroxymethylation in the Brain Cortex in the Triple-Transgenic Mouse Model of Alzheimer's Disease.
J. Alzheimer's Dis. **2014**, *41*, 845–854. [CrossRef]
38. Ellison, E.M.; Abner, E.L.; Lovell, M.A. Multiregional Analysis of Global 5-Methylcytosine and 5-Hydroxymethylcytosine throughout the Progression of Alzheimer's Disease. *J. Neurochem.* **2017**, *140*, 383–394. [CrossRef]
39. Bradley-Whitman, M.A.; Lovell, M.A. Epigenetic Changes in the Progression of Alzheimer's Disease. *Mech. Ageing Dev.* **2013**, *134*, 486–495. [CrossRef]
40. Huang, Q.; Xu, S.; Mo, M.; Yang, Q.; Li, J.; Zhong, Y.; Zhang, J.; Zhang, L.; Ye, X.; Liu, Z.; et al. Quantification of DNA Methylation and Hydroxymethylation in Alzheimer's Disease Mouse Model Using LC-MS/MS. *J. Mass Spectrom.* **2018**, *53*, 590–594. [CrossRef]
41. Stöger, R.; Scaife, P.J.; Shephard, F.; Chakrabarti, L. Elevated 5hmC Levels Characterize DNA of the Cerebellum in Parkinson's Disease. *NPJ Park. Dis.* **2017**, *3*, 6. [CrossRef]
42. Condliffe, D.; Wong, A.; Troakes, C.; Proitsi, P.; Patel, Y.; Chouliaras, L.; Fernandes, C.; Cooper, J.; Lovestone, S.; Schalkwyk, L.; et al. Cross-Region Reduction in 5-Hydroxymethylcytosine in Alzheimer's Disease Brain. *Neurobiol. Aging* **2014**, *35*, 1850–1854. [CrossRef] [PubMed]
43. Zhang, Y.; Zhang, Z.; Li, L.; Xu, K.; Ma, Z.; Chow, H.M.; Herrup, K.; Li, J. Selective Loss of 5hmC Promotes Neurodegeneration in the Mouse Model of Alzheimer's Disease. *FASEB J.* **2020**, *34*, 16364–16382. [CrossRef] [PubMed]
44. Shu, L.; Sun, W.; Li, L.; Xu, Z.; Lin, L.; Xie, P.; Shen, H.; Huang, L.; Xu, Q.; Jin, P.; et al. Genome-Wide Alteration of 5Hydroxymenthylcytosine in a Mouse Model of Alzheimer's Disease. *BMC Genom.* **2016**, *17*, 381. [CrossRef]
45. James, S.J.; Shpyleva, S.; Melnyk, S.; Pavliv, O.; Pogribny, I.P. Elevated 5-Hydroxymethylcytosine in the Engrailed-2 (EN-2) Promoter Is Associated with Increased Gene Expression and Decreased MeCP2 Binding in Autism Cerebellum. *Transl. Psychiatry* **2014**, *4*, e460. [CrossRef] [PubMed]
46. Geiman, T.M.; Sankpal, U.T.; Robertson, A.K.; Zhao, Y.; Zhao, Y.; Robertson, K.D. DNMT3B Interacts with HSNF2H Chromatin Remodeling Enzyme, HDACs 1 and 2, and Components of the Histone Methylation System. *Biochem. Biophys. Res. Commun.* **2004**, *318*, 544–555. [CrossRef] [PubMed]
47. Chen, C.C.; Wang, K.Y.; Shen, C.K.J. The Mammalian de Novo DNA Methyltransferases DNMT3A and DNMT3B Are Also DNA 5-Hydroxymethylcytosine Dehydroxymethylases. *J. Biol. Chem.* **2012**, *287*, 33116–33121. [CrossRef] [PubMed]

48. Zocher, S.; Overall, R.W.; Berdugo-Vega, G.; Rund, N.; Karasinsky, A.; Adusumilli, V.S.; Steinhauer, C.; Scheibenstock, S.; Händler, K.; Schultze, J.L.; et al. De Novo DNA Methylation Controls Neuronal Maturation during Adult Hippocampal Neurogenesis. *EMBO J.* **2021**, *40*, e107100. [CrossRef]
49. Kong, Q.; Yu, M.; Zhang, M.; Wei, C.; Gu, H.; Yu, S.; Sun, W.; Li, N.; Zhou, Y. Conditional Dnmt3b Deletion in Hippocampal DCA1 Impairs Recognition Memory. *Mol. Brain* **2020**, *13*, 42. [CrossRef]
50. Nieto-Estevez, V.; Changarathil, G.; Adeyeye, A.O.; Coppin, M.O.; Kassim, R.S.; Zhu, J.; Hsieh, J. HDAC1 Regulates Neuronal Differentiation. *Front. Mol. Neurosci.* **2022**, *14*, 815808. [CrossRef]
51. Pao, P.C.; Patnaik, D.; Watson, L.A.; Gao, F.; Pan, L.; Wang, J.; Adaikkan, C.; Penney, J.; Cam, H.P.; Huang, W.C.; et al. HDAC1 Modulates OGG1-Initiated Oxidative DNA Damage Repair in the Aging Brain and Alzheimer's Disease. *Nat. Commun.* **2020**, *11*, 2484. [CrossRef] [PubMed]
52. Bahari-Javan, S.; Maddalena, A.; Kerimoglu, C.; Wittnam, J.; Held, T.; Bähr, M.; Burkhardt, S.; Delalle, I.; Kügler, S.; Fischer, A.; et al. HDAC1 Regulates Fear Extinction in Mice. *J. Neurosci.* **2012**, *32*, 5062–5073. [CrossRef] [PubMed]
53. Sharma, R.P.; Grayson, D.R.; Gavin, D.P. Histone Deactylase 1 Expression Is Increased in the Prefrontal Cortex of Schizophrenia
    Subjects: Analysis of the National Brain Databank Microarray Collection. *Schizophr. Res.* **2008**, *98*, 111–117. [CrossRef] [PubMed]
54. Zhao, P.; Wang, H.; Wang, H.; Dang, Y.; Luo, L.; Li, S.; Shi, Y.; Wang, L.; Wang, S.; Mager, J.; et al. Essential Roles of HDAC1 and 2 in Lineage Development and Genome-Wide DNA Methylation during Mouse Preimplantation Development. *Epigenetics* **2020**, *15*, 369–385. [CrossRef] [PubMed]
55. Gräff, J.; Rei, D.; Guan, J.S.; Wang, W.Y.; Seo, J.; Hennig, K.M.; Nieland, T.J.F.; Fass, D.M.; Kao, P.F.; Kahn, M.; et al. An Epigenetic Blockade of Cognitive Functions in the Neurodegenerating Brain. *Nature* **2012**, *483*, 222–226. [CrossRef] [PubMed]
56. Tan, Y.; Delvaux, E.; Nolz, J.; Coleman, P.D.; Chen, S.; Mastroeni, D. Upregulation of Histone Deacetylase 2 in Laser Capture Nigral Microglia in Parkinson's Disease. *Neurobiol. Aging* **2018**, *68*, 134–141. [CrossRef]
57. Singh, P.; Thakur, M.K. Reduced Recognition Memory Is Correlated with Decrease in DNA Methyltransferase1 and Increase in Histone Deacetylase2 Protein Expression in Old Male Mice. *Biogerontology* **2014**, *15*, 339–346. [CrossRef]
58. Singh, P.; Thakur, M.K. Histone Deacetylase 2 Inhibition Attenuates Downregulation of Hippocampal Plasticity Gene Expression during Aging. *Mol. Neurobiol.* **2018**, *55*, 2432–2442. [CrossRef]
59. Nakatsuka, D.; Izumi, T.; Tsukamoto, T.; Oyama, M.; Nishitomi, K.; Deguchi, Y.; Niidome, K.; Yamakawa, H.; Ito, H.; Ogawa, K. Histone Deacetylase 2 Knockdown Ameliorates Morphological Abnormalities of Dendritic Branches and Spines to Improve
    Synaptic Plasticity in an APP/PS1 Transgenic Mouse Model. *Front. Mol. Neurosci.* **2021**, *14*, 297. [CrossRef]
60. Frankowski, H.; Yeboah, F.; Berry, B.J.; Kinoshita, C.; Lee, M.; Evitts, K.; Davis, J.; Kinoshita, Y.; Morrison, R.S.; Young, J.E.
    Knock-Down of HDAC2 in Human Induced Pluripotent Stem Cell Derived Neurons Improves Neuronal Mitochondrial Dynamics,
    Neuronal Maturation and Reduces Amyloid Beta Peptides. *Int. J. Mol. Sci.* **2021**, *22*, 2526. [CrossRef]
61. Ito, S.; Shen, L.; Dai, Q.; Wu, S.C.; Collins, L.B.; Swenberg, J.A.; He, C.; Zhang, Y. Tet Proteins Can Convert 5-Methylcytosine to 5-Formylcytosine and 5-Carboxylcytosine. *Science* **2011**, *333*, 1300–1303. [CrossRef]
62. Taylor, S.E.B.; Smeriglio, P.; Dhulipala, L.; Rath, M.; Bhutani, N. A Global Increase in 5-Hydroxymethylcytosine Levels Marks Osteoarthritic Chondrocytes. *Arthritis Rheumatol.* **2014**, *66*, 90–100. [CrossRef] [PubMed]
63. Park, J.-L.; Kim, H.-J.; Seo, E.-H.; Kwon, O.-H.; Lim, B.; Kim, M.; Kim, S.-Y.; Song, K.-S.; Kang, G.H.; Kim, H.J.; et al. Decrease of
    5hmC in Gastric Cancers Is Associated with TET1 Silencing Due to with DNA Methylation and Bivalent Histone Marks at TET1 CpG Island 3^0-Shore. *Oncotarget* **2015**, *6*, 37647–37662. [CrossRef] [PubMed]
64. Wang, K.C.; Kang, C.H.; Tsai, C.Y.; Chou, N.H.; Tu, Y.T.; Li, G.C.; Lam, H.C.; Liu, S.I.; Chang, P.M.; Lin, Y.H.; et al. Ten-Eleven Translocation 1 Dysfunction Reduces 5-Hydroxymethylcytosine Expression Levels in Gastric Cancer Cells. *Oncol. Lett.* **2018**, *15*, 278–284. [CrossRef] [PubMed]
65. Moyon, S.; Frawley, R.; Marechal, D.; Huang, D.; Marshall-Phelps, K.L.H.; Kegel, L.; Bøstrand, S.M.K.; Sadowski, B.; Jiang, Y.H.; Lyons, D.A.; et al. TET1-Mediated DNA Hydroxymethylation Regulates Adult Remyelination in Mice. *Nat. Commun.* **2021**, *12*, 3359. [CrossRef] [PubMed]
66. Greer, C.B.; Wright, J.; Weiss, J.D.; Lazarenko, R.M.; Moran, S.P.; Zhu, J.; Chronister, K.S.; Jin, A.Y.; Kennedy, A.J.; Sweatt, J.D.; et al. Tet1 Isoforms Differentially Regulate Gene Expression, Synaptic Transmission, and Memory in the Mammalian Brain. *J. Neurosci.* **2021**, *41*, 578–593. [CrossRef]

67. Carroll, J.A.; Striebel, J.F.; Race, B.; Phillips, K.; Chesebro, B. Prion Infection of Mouse Brain Reveals Multiple New Upregulated Genes Involved in Neuroinflammation or Signal Transduction. *J. Virol.* **2015**, *89*, 2388–2404. [CrossRef]
68. Guijarro, I.M.; Garcés, M.; Andrés-Benito, P.; Marín, B.; Otero, A.; Barrio, T.; Carmona, M.; Ferrer, I.; Badiola, J.J.; Monzón, M. Neuroimmune Response Mediated by Cytokines in Natural Scrapie after Chronic Dexamethasone Treatment. *Biomolecules* **2021**, *11*, 204. [CrossRef]
69. López-Pérez, Ó.; Bernal-Martín, M.; Hernaiz, A.; Llorens, F.; Betancor, M.; Otero, A.; Toivonen, J.M.; Zaragoza, P.; Zerr, I.; Badiola, J.J.; et al. BAMBI and CHGA in Prion Diseases: Neuropathological Assessment and Potential Role as Disease Biomarkers. *Biomolecules* **2020**, *10*, 706. [CrossRef]
70. Marcos-Carcavilla, A.; Calvo, J.H.; González, C.; Moazami-Goudarzi, K.; Laurent, P.; Bertaud, M.; Hayes, H.; Beattie, A.E.; Serrano, C.; Lyahyai, J.; et al. IL-1 Family Members as Candidate Genes Modulating Scrapie Susceptibility in Sheep: Localization, Partial Characterization, and Expression. *Mamm. Genome* **2007**, *18*, 53–63. [CrossRef]
71. Zhang, R.R.; Cui, Q.Y.; Murai, K.; Lim, Y.C.; Smith, Z.D.; Jin, S.; Ye, P.; Rosa, L.; Lee, Y.K.; Wu, H.P.; et al. Tet1 Regulates Adult Hippocampal Neurogenesis and Cognition. *Cell Stem Cell* **2013**, *13*, 237–245. [CrossRef]
72. López-Pérez, Ó.; Toivonen, J.M.; Otero, A.; Solanas, L.; Zaragoza, P.; Badiola, J.J.; Osta, R.; Bolea, R.; Martín-Burriel, I. Impairment of Autophagy in Scrapie-Infected Transgenic Mice at the Clinical Stage. *Lab. Investig.* **2020**, *100*, 52–63. [CrossRef] [PubMed]
73. Wagner, M.; Steinbacher, J.; Kraus, T.F.J.; Michalakis, S.; Hackner, B.; Pfaffeneder, T.; Perera, A.; Müller, M.; Giese, A.; Kretzschmar, H.A.; et al. Age-Dependent Levels of 5-Methyl-, 5-Hydroxymethyl-, and 5-Formylcytosine in Human and Mouse Brain Tissues. *Angew. Chem. Int. Ed. Engl.* **2015**, *54*, 12511–12514. [CrossRef] [PubMed]
74. Jung, M.; Pfeifer, G.P. Aging and DNA Methylation. *BMC Biol.* **2015**, *13*, 7. [CrossRef] [PubMed]
75. Schulz-Schaeffer, W.J.; Tschöke, S.; Kranefuss, N.; Dröse, W.; Hause-Reitner, D.; Giese, A.; Groschup, M.H.; Kretzschmar, H.A. The Paraffin-Embedded Tissue Blot Detects PrP(Sc) Early in the Incubation Time in Prion Diseases. *Am. J. Pathol.* **2000**, *156*, 51–56. [CrossRef]
76. Fraser, H.; Dickinson, A.G. Scrapie in Mice. Agent-Strain Differences in the Distribution and Intensity of Grey Matter Vacuolation. *J. Comp. Pathol.* **1973**, *83*, 29–40. [CrossRef]
77. Monleón, E.; Monzón, M.; Hortells, P.; Vargas, A.; Acín, C.; Badiola, J.J. Detection of PrPsc on Lymphoid Tissues from Naturally Affected Scrapie Animals: Comparison of Three Visualization Systems. *J. Histochem. Cytochem.* **2004**, *52*, 145–151. [CrossRef]
78. Livak, K.J.; Schmittgen, T.D. Analysis of Relative Gene Expression Data Using Real-Time Quantitative PCR and the $2^{-\Delta\Delta CT}$ Method. *Methods* **2001**, *25*, 402–408. [CrossRef]
79. Lyahyai, J.; Serrano, C.; Ranera, B.; Badiola, J.J.; Zaragoza, P.; Martin-Burriel, I. Effect of Scrapie on the Stability of Housekeeping Genes. *Anim. Biotechnol.* **2010**, *21*, 1–13. [CrossRef]
80. Crowe, A.; Yue, W. Semi-Quantitative Determination of Protein Expression Using Immunohistochemistry Staining and Analysis: An Integrated Protocol. *Bio Protocol* **2019**, *9*, e3465. [CrossRef]

MANUSCRITO IV

Effect of Scrapie Prion Infection in Ovine Bone Marrow-Derived Mesenchymal Stem Cells and Ovine Mesenchymal Stem Cell-Derived Neurons.

García-mendívil, Laura; Mediano, Diego Rubén; Hernaiz, Adelaida; Sanz-rubio, David; Vázquez, Francisco José; Marín, Belén; López-pérez, Óscar; Otero, Alicia; Badiola, Juan José; Zaragoza, Pilar; Ordovás, Laura; Bolea, Rosa; Martín-Burriel, Inmaculada.

Animals. Vol. 11, pág. 1137, 2021. doi:10.3390/ANI11041137.

animals

MDPI

Article

Effect of Scrapie Prion Infection in Ovine Bone Marrow-Derived Mesenchymal Stem Cells and Ovine Mesenchymal Stem Cell-Derived Neurons

Laura García-Mendívil, [1,2] Diego R. Mediano [1], Adelaida Hernaiz [1], David Sanz-Rubio [1,3], Francisco J. Vázquez [1,4], Belén Marín [5], Óscar López-Pérez [1,5,6], Alicia Otero [5], Juan J. Badiola [5], Pilar Zaragoza [1,6], Laura Ordovás [2], Rosa Bolea [5] and Inmaculada Martín-Burriel [1,5,6,*]

[1] Laboratorio de Genética Bioquímica (LAGENBIO), Instituto Agroalimentario de Aragón (IA2), Instituto de Investigación Sanitaria de Aragón (IISAragón), Universidad de Zaragoza, Miguel Servet 177, 50013 Zaragoza, Spain; lgmendivil@unizar.es (L.G.-M.); drmediano@gmail.com (D.R.M.); ahernaiz@unizar.es (A.H.); dsanz@iisaragon.es (D.S.-R.); pvazquez@unizar.es (F.J.V.); oscar.lopez@irta.cat (Ó.L.-P.); pilarzar@unizar.es (P.Z.)

[2] Biomedical Signal Interpretation and Computational Simulation (BSICoS), Institute of Engineering Research (I3A), University of Zaragoza & Instituto de Investigación Sanitaria (IIS), 50018 Zaragoza, Spain; lordovas@unizar.es

[3] Translational Research Unit, Instituto de Investigación Sanitaria de Aragón (IISAragón), Hospital Universitario Miguel Servet, 50009 Zaragoza, Spain

[4] Departamento de Patología Animal, Facultad de Veterinaria, Universidad de Zaragoza, Miguel Servet 177, 50013 Zaragoza, Spain

[5] Centro de Investigación en Encefalopatías y Enfermedades Transmisibles Emergentes, Instituto Agroalimentario de Aragón (IA2), Instituto de Investigación Sanitaria de Aragón (IISAragón), Universidad de Zaragoza, Miguel Servet 177, 50013 Zaragoza, Spain; belenm@unizar.es (B.M.); aliciaogar@unizar.es (A.O.); badiola@unizar.es (J.J.B.); rbolea@unizar.es (R.B.)

[6] Centro de Investigación Biomédica en Red de Enfermedades Neurodegenerativas (CIBERNED), Instituto Carlos III, 28031 Madrid, Spain

* Correspondence: minma@unizar.es; Tel.: +34-976-761-662

Citation: García-Mendívil, L.; Mediano, D.R.; Hernaiz, A.; Sanz-Rubio, D.; Vázquez, F.J.; Marín, B.; López-Pérez, Ó.; Otero, A.; Badiola, J.J.; Zaragoza, P.; et al. Effect of Scrapie Prion Infection in Ovine Bone Marrow-Derived Mesenchymal Stem Cells and Ovine Mesenchymal Stem Cell-Derived Neurons. *Animals* **2021**, *11*, 1137. https://doi.org/10.3390/ani11041137

Academic Editors: Eleonora Iacono and Barbara Merlo

Received: 2 March 2021
Accepted: 12 April 2021
Published: 15 April 2021

Simple Summary: Prion diseases are neurodegenerative disorders affecting humans and animals. The development of in vitro cellular models from naturally susceptible species like humans or ruminants can potentially make a great contribution to the study of many aspects of these diseases, including the ability of prions to infect and replicate in cells and therapeutics. Our study shows for the first time how ovine mesenchymal stem cells derived from bone marrow and their neural-like progeny are able to react to scrapie prion infection in vitro and assesses the effects of this infection on cell viability and proliferation. Finally, we observe that the differentiation of ovine mesenchymal stem cells into neuron-like cells makes them more permissive to prion infection.

Abstract: Scrapie is a prion disease affecting sheep and goats and it is considered a prototype of transmissible spongiform encephalopathies (TSEs). Mesenchymal stem cells (MSCs) have been proposed as candidates for developing in vitro models of prion diseases. Murine MSCs are able to propagate prions after previous mouse-adaptation of prion strains and, although ovine MSCs express the cellular prion protein (PrP^{C}), their susceptibility to prion infection has never been investigated. Here, we analyze the potential of ovine bone marrow-derived MSCs (oBM-MSCs), in growth and neurogenic conditions, to be infected by natural scrapie and propagate prion particles (PrP^{Sc}) in vitro, as well as the effect of this infection on cell viability and proliferation. Cultures were kept for 48–72 h in contact with homogenates of central nervous system (CNS) samples from scrapie or control sheep. In growth conditions, oBM-MSCs initially maintained detectable levels of PrP^{Sc} post-inoculation, as determined by Western blotting and ELISA. However, the PrP^{Sc} signal weakened and was lost over time. oBM-MSCs infected with scrapie displayed lower cell doubling and higher doubling times than those infected with control inocula. On the other hand, in neurogenic conditions, oBM-MSCs not only maintained detectable levels of PrP^{Sc} post-inoculation, as determined by ELISA, but this PrP^{Sc} signal also increased progressively over time. Finally, inoculation with CNS extracts seems to induce

the proliferation of oBM-MSCs in both growth and neurogenic conditions. Our results suggest that oBM-MSCs respond to prion infection by decreasing their proliferation capacity and thus might not be permissive to prion replication, whereas ovine MSC-derived neuron-like cells seem to maintain and replicate PrP^{Sc}.

Keywords: scrapie; prion; sheep; infection; mesenchymal stem cell; in vitro model

1. Introduction

Transmissible spongiform encephalopathies (TSEs) or prion diseases are fatal neurodegenerative disorders that affect humans and animals [1]. These diseases are caused by the conformational conversion of the cellular prion protein (PrP^{C}) to an infectious isoform that is partially resistant to proteases and prone to forming aggregates called PrP^{Sc} [2]. The accumulation of this isoform in the central nervous system (CNS) causes spongiform neuronal degeneration, activation of glial cells and neuronal loss [3]. Scrapie, which affects sheep and goats, was the first reported TSE [4] and it is considered the prototype of these diseases [5].

Cell culture systems are useful tools to study prion protein propagation in TSEs and to identify new prion therapeutics [6]. However, only a few cell lines can be infected and display PrP^{Sc} accumulation and/or infectious capacity [7]. In most cases, murine cell lines are used, requiring a previous mouse-adaptation of the prion strain to eliminate the problem of the species barrier [8].

Mesenchymal stem cells (MSCs) are fibroblast-like cells characterized by their capacity for both self-renewal and differentiation in mesodermal tissues (osteoblasts, adipocytes, chondrocytes and myocytes) [9]. These cells can also transdifferentiate in vitro into neuronlike cells [10,11] and undifferentiated cells expressing PrP^{C} [12], which seems to play a key role in the neuronal differentiation process of MSCs [13–15].

Murine compact bone-derived MSCs (CB-MSCs) are able to migrate to brain extracts from prion-infected mice in vitro and significantly prolong the survival of mice infected with the Chandler prion strain when injected in vivo [16]. Furthermore, murine bone marrow-derived mesenchymal stem cells (BM-MSCs) can be infected with a Gerstmann– Sträussler–Scheinker strain adapted in mice ex vivo [17] and maintain the infectivity along passages. The susceptibility of these cells to prion infection makes them good candidates for use in developing in vitro models for prion research [18]. Therefore, the development of in vitro models from naturally prion-susceptible species like humans or ruminants, which would avoid the adaptation process, would be very useful for cutting-edge prion research. Although in recent studies, human cerebral organoids [19] and astrocytes [20], both derived from human induced pluripotent stem cells (iPSCs), have been described to maintain and propagate prion infectivity in vitro, in domestic species like sheep, the reprogramming of somatic cells to iPSCs might require adjustments of standard protocols.

We have previously described the isolation of ovine MSCs from peripheral blood (oPB-MSCs), which express PrP^{C} at the transcript level [21]. Our group also reported the presence of PrP^{C} in ovine bone marrow-derived MSCs (oBM-MSCs) at both transcript and protein levels [18]. However, in contrast to BM-MSCs obtained from individuals with sporadic Creutzfeldt-Jakob disease (CJD), who are positive to PrP^{Sc} [12], the pathogenic prion protein was not detected in oBM-MSCs isolated from scrapie sheep [18]. In addition to the lack of PrP^{Sc}, these cells displayed diminished proliferation potential compared to oBM-MSCs derived from healthy sheep. To the best of our knowledge, the susceptibility of oBM-MSCs to scrapie infection in vitro and their potential to replicate prions have never been investigated. The aim of the present study was to

assess the susceptibility of oBMMSCs and their derivative neuron-like cells to scrapie prion infection in vitro, their potential to replicate prions and the effects of this infection on cell viability and proliferation.

2. Materials and Methods

2.1. Animals and Sample Collection

Bone marrow samples were obtained from 11 adult female (*n* = 7) and male (*n* = 4) sheep, aged from 1 to 7 years and carrying different genotypes for the *PRNP* gene (Table 1). After animal sedation (Xylazine) and local anesthesia (Lidocaine), bone marrow aspirates were harvested from the humeral head using a 13 G Jamshidi needle and 10-mL syringes previously loaded with 0.5 mL of sodium heparin. All procedures were carried out under Project Licence PI06/12, approved by the Ethical Committee for Animal Experiments from the University of Zaragoza. The care and use of animals were performed in accordance with the Spanish Policy for Animal Protection, RD53/2013, which meets European Union Directive 2010/63 on the protection of animals used for experimental and other scientific purposes.

Table 1. Characteristics of the animals selected to obtain bone marrow mesenchymal stem cells. The different assays in which the ovine bone marrow-derived mesenchymal stem cells (oBM-MSCs) were used, are also shown—Western blotting assay (WB), proliferation assay (PA), cell viability assay (MTT) and ELISA.

Sheep	Genotype	Sex	Age (Years)	Scrapie Status	Breed	Assay
BMO1	ARQ/ARQ	Female	7	Exposed, not detected	Rasa Aragonesa	WB, PA
BMO2	ARQ/ARQ	Female	4	Exposed, not detected	Rasa Aragonesa	WB, PA
BMO3	ARQ/ARQ	Female	4	Exposed, not detected	Rasa Aragonesa	WB, PA
BMO4	ARQ/ARQ	Male	1	Exposed, not detected	Rasa Aragonesa	MTT, ELISA
BMO5	ARQ/ARQ	Male	2	Preclinical	Crossbreed	MTT, ELISA
BMO6	ARQ/ARQ	Female	6	Exposed, not detected	Ojinegra	MTT, ELISA
BMO7	ARQ/ARQ	Male	3	Exposed, not detected	Crossbreed	MTT, ELISA
BMO8	ARQ/ARQ	Female	7	Exposed, not detected	Rasa Aragonesa	MTT
BMO9	ARR/ARQ	Female	5	Exposed, not detected	Rasa Aragonesa	MTT
BMO10	ARQ/VRQ	Female	4	Exposed, not detected	Crossbreed	MTT
BMO11	ARQ/VRQ	Male	2	Preclinical	Crossbreed	MTT, ELISA

The animals used in this study were maintained in an experimental flock in which the prevalence of scrapie was high. Although none of the animals displayed clinical signs compatible with scrapie, an in vivo test for PrP^{Sc} determination using third-eyelid biopsies was performed as previously described [22,23] to identify any scrapie-infected preclinical sheep. Two males were positive to scrapie but their cultures were maintained in the study to evaluate if these cultures could react differently to those obtained from negative sheep, although in previous studies infectivity was not detected in oBM-MSCs derived from scrapie sheep [18]. Negative animals were those that did not show scrapie compatible symptoms and were negative to PrP^{Sc} based on a third-eyelid biopsy.

2.2. Ovine Mesenchymal Stem Cell Isolation and Culture

MSC isolation from bone marrow aspirates (3–5 mL) was performed following the previously described protocol [18,21,24]. This protocol is based on the separation of the mononuclear fraction after density gradient centrifugation in Lymphoprep (Atom) and further isolation thanks to the ability of MSCs to adhere to plastic. After isolation, cells were expanded up to passage 3 in basal medium, consisting of low glucose Dulbecco's modified Eagle's medium (DMEM, Sigma-Aldrich, St. Louis, MO, USA) supplemented with 10% fetal bovine serum (FBS), 1% L-glutamine (Sigma-Aldrich) and 1% streptomycin/penicillin (Sigma-Aldrich).

In addition to plastic-adherence in standard culture conditions, the minimal criteria to define MSCs are the expression of certain cell surface markers and the ability to differentiate into

adipocytes, osteoblasts and chondroblasts in vitro [25]. The ability to differentiate to mesodermal lineages and the expression of mesenchymal and hematopoietic markers of these cultures have been evaluated previously [18]. After characterization, the expression of PrP^C in oBM-MSCs was confirmed by RT-qPCR and dot blotting [18].

2.3. Neurogenic Differentiation

To study whether neural differentiation increased the susceptibility to prion infection, oBM-MSC cultures were seeded at 1500 cells/cm^2 and differentiated into neuron-like cells using HyClone neurogenic medium (Thermo Scientific, Waltham, MA, USA) according to the manufacturer's instructions. The differentiation process lasted three days. Neural differentiation was monitored and confirmed by observing the cultures through an inverted optical microscope. The formation of neuron-like cells was seen within 24 h, peaking at 72 h (Figure 1a,b), as previously described [18].

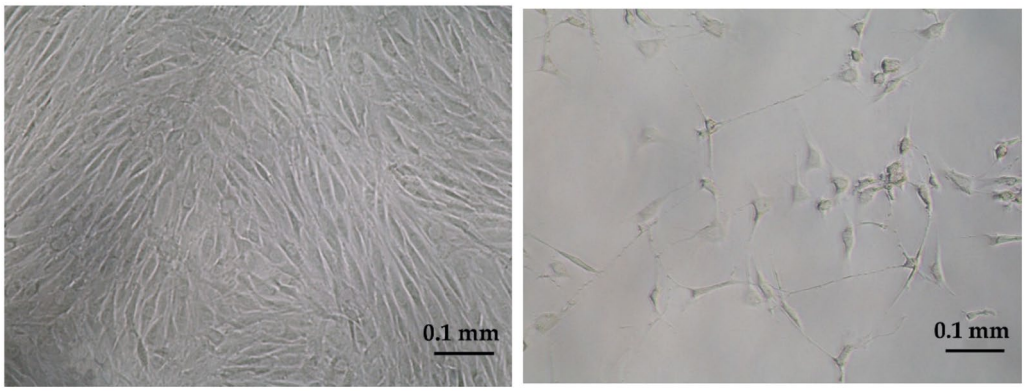

Figure 1. oBM-MSC differentiation into neuron-like cells 3 days after neurogenic induction with HyClone neurogenic medium: (**a**) oBM-MSCs in growth conditions and (**b**) oBM-MSCs in neurogenic differentiation.

2.4. Scrapie Inocula and Infection of oBM-MSC and Neuron-Like Cultures

Inocula were prepared using CNS samples from one healthy (negative controls) and one classical scrapie-infected sheep carrying the ARQ/ARQ genotype and preserved at the tissue bank of the Center of Encephalopathies and Emerging Transmissible Diseases (CEETE; University of Zaragoza). The presence/absence of PrP^{Sc} in the tissues was confirmed following protocols reported in other works [26], using two rapid diagnostic tests (Prionics-Check Western blotting; ThermoFisher Scientific and Idexx HerdChek; IDEXX, Westbrook, ME, USA) and confirmation by immunohistochemical examination of CNS tissue. CNS samples were homogenized and diluted 1:10 (g/mL) in physiological saline solution (Braun). Afterwards, samples were treated at 70 °C for 10 min before adding streptomycin sulphate (100 µg/mL) and benzylpenicillin (100 µg/mL). In order to check the safety of the inocula once generated, samples were incubated in blood agar plates, and the absence of any bacterial growth was confirmed.

To determine the effect of prion infection on the proliferation potential and the ability of prion replication, oBM-MSCs cultures were seeded at 5000 cells/cm^2 for proliferation conditions and at 1500 cells/cm^2 for neurogenic conditions. In both cases, three groups were established: positive, negative and control cultures. Positive cultures were infected with inocula from a scrapie-infected sheep, negative cultures with inocula from a healthy sheep and control cultures were kept in standard conditions. After adhesion for 24 h, basal media was substituted by inocula diluted 1:10 in DMEM media (10% FBS, 1% L-glutamine and 1% streptomycin/penicillin) for the oBM-MSC cultures and in HyClone media for the oBM-MSC cultures in neurogenic

differentiation. Cells were maintained in this medium for 48 h to analyze the proliferation potential and cell viability and for 72 h for the MTT/ELISA assays. Afterwards, the medium was changed twice a week.

2.5. Proliferation Potential and Cell Viability

To determine the effect of prion infection on oBM-MSC proliferation potential, cultures from three different donors (biological replicates) were seeded in 6-well plates at 5000 cells/cm^2, inoculated with scrapie and control inocula and maintained until passage 3 post-infection; every passage was performed at around 80% confluence. Adherent cells were counted every passage and the cell doubling number (CD) and cell doubling time (DT), used to determine the time it takes for a population of cells to double in size, were calculated as previously described [21,24]. The results were evaluated using the paired Student's *t*-test.

To assess early prion toxicity, cell viability was also evaluated using MTT in oBM-MSC from 8 donors at 3, 7 and 10 days post-inoculation (dpi), seeding 4 technical replicates for each culture. oBM-MSC cultures were seeded in 96-well plates at 5000 cells/cm^2 in growth conditions and at 1500 cells/cm^2 in neurogenic differentiation conditions. Briefly, the MTT assay was performed by adding 25 µL of MTT solution (2 mg/mL) per well. Then, the plates were incubated at 37 °C for 4 h. Afterwards, the content of each well was removed and was substituted with 150 µL of HCl solution (HCl 40 mM in isopropanol) per well. Plates were then incubated for 1 h at room temperature protected from light. The absorbance was measured at 570 nm in an Infinite F200 microplate reader (Tecan Ibérica Instrumentación, Barcelona, Spain). A calibration curve was prepared with different amounts of cells. Since oBM-MSCs in growth conditions are seeded in a higher density than the ones in neurogenic differentiation conditions, two calibration curves were prepared: a more concentrated one to compare oBM-MSCs in growth conditions (Figure S1a) and a more diluted one to compare cultures in neurogenic conditions (Figure S1b). In both cases, the calibration curve enabled us to establish the relationship between absorbance and the amount of cultured cells. The toxicity of the prion was studied in three conditions (inoculated with scrapie-positive brain homogenates, negative brain inoculum and noninoculated controls) and at three different stages (3, 7 and 10 dpi). As cells were kept in contact with the inoculum for 72 h, the stage 3 dpi corresponds to the moment just after inoculum removal. The moment of the infection with the inocula was considered as day 0. The normality of the results was evaluated with Shapiro–Wilk and D'Agostino–Pearson tests. Differences in cell viability and proliferation were evaluated with Student's *t*-test. Statistical significance was defined as $p < 0.05$.

2.6. PrP^{Sc} Detection

Cells from the three biological replicates analyzed in the proliferation assay were used to evaluate if PrP^{Sc} was increased or maintained along the passages in MSC cultures infected with scrapie and maintained under grown conditions. Approximately 10^6 cells of passages 1, 2 and 3 post-infection were frozen at −80 °C for further PrP^{Sc} determination by Western blotting. Pellets of frozen cells were homogenized in 100 µL of PBS. Afterwards, samples were analyzed using the BSE Scrapie Discriminatory Kit (Bio-Rad Laboratories, Hercules, CA, USA) and treated following the manufacturer's recommendations. Electrophoresis was developed in 12% SDS-PAGE gels. Protein was then transferred to a 0.20-µm nitrocellulose membrane (Bio-Rad). CDP-Star substrate (ThermoFisher Scientific, Westbrook, ME, USA) was used to determine chemiluminescence in a Versa-Doc Imaging System (Bio-Rad Laboratories). Chemiluminescence signals were evaluated using ImageJ 1.4.3.67 (Psion Image), as described previously [27].

Neurogenic differentiation of MSCs requires seeding cells at low density and differentiated cells cannot be maintained along passages. To test the ability of these cells to replicate PrP^{Sc}, we quantified the amount of the pathogenic protein soon after prion infection at three different stages (3 dpi, which corresponds to inoculum removal, 7 and 10 dpi) in oBM-MSCs in growth and neurogenic differentiation conditions. We used a more sensitive test, the ELISA kit EEB-Scrapie HerdCheck kit (IDEXX), following the manufacturer's recommendations. oBM-MSCs cultures from 5 donors were seeded in 6-well plates and the retrieval of the cells was performed by means of trypsinization and subsequent centrifugation. To quantify the PrP^{Sc} detection range of the ELISA kit, a calibration curve was performed using different concentrations of scrapie inocula (Figure S2). PrP^{Sc} was detected in all inoculum concentrations, showing that this kit is suitable to detect PrP^{Sc} in oBM-MSC cultures, as the amount of inocula used in oBM-MSC infection was higher than the most diluted concentration of the calibration curve. The inoculum used in the calibration curve was the same used to infect oBM-MSCs in growth and neurogenic conditions. For infection, a volume of 100 µL of scrapie inoculum per well was employed, which would correspond to >3 units of absorbance.

3. Results

3.1. Proliferation Potential of Infected oBM-MSC

The effect of scrapie infection on the proliferation capacity was analyzed in oBM-MSCs, calculating the CD and DT. Significant differences between cultures infected with scrapie and control inocula were found for both CD and DT at the first passage post-infection. CD was higher and DT was lower in the cultures treated with control inocula compared to those inoculated with scrapie brain cells (Table 2).

Table 2. Cell doubling number (CD) and cell doubling time (DT) of oBM-MSCs from 3 donors through passages 1 to 3 post-inoculation with 1% brain homogenates obtained from healthy and scrapie sheep and the average value for the three passages (Av).

Passage		Inocula	
		Healthy	**Scrapie**
1	**CD**	3.150 ± 0.286 *	2.949 ± 0.219 *
	DT (days)	1.714 ± 0.355 **	1.825 ± 0.343 **
2	**CD**	3.22 ± 0.651	2.870 ± 0.531
	DT (days)	2.054 ± 0.653	2.291 ± 0.681
3	**CD**	1.93 ± 0.390	1.807 ± 0.027
	DT (days)	2.116 ± 0.428	2.214 ± 0.033
Av	**CD**	2.871 ± 0.711 *	2.634 ± 0.597 *
	DT (days)	1.942 ± 0.469	2.097 ± 0.469

Significant differences were calculated using Student's *t*-test (* $p < 0.05$, ** $p < 0.01$).

3.2. Cell Viability of Infected Cultures

The effect of prion infection on cell viability was studied in three conditions (scrapie positive inoculum, healthy/negative inoculum and control without inoculum) and at three different stages (3, 7 and 10 dpi) in oBM-MSCs in growth conditions and in neurogenic differentiation.

Proliferation was evidenced in oBM-MSC cultures maintained in growth medium under the three conditions. Inoculated cultures displayed higher number of cells than controls at the three stages (3, 7 and 10 dpi). Proliferation was significantly lower in scrapie infected cells than in cultures treated with negative inocula at 3 dpi but, in subsequent stages (7 and 10 dpi), the positive cultures displayed significantly more cells than the negative cultures (Figure 2a).

In neurogenic differentiation conditions, the number of cells also increased over time in the three conditions, whereas inoculated cultures showed a higher growth than controls. Comparing between the inoculated cultures, the number of cells was significantly higher in cultures that were in contact with negative inoculum than the ones infected with scrapie, and this difference was statistically significant at 10 dpi (Figure 2b).

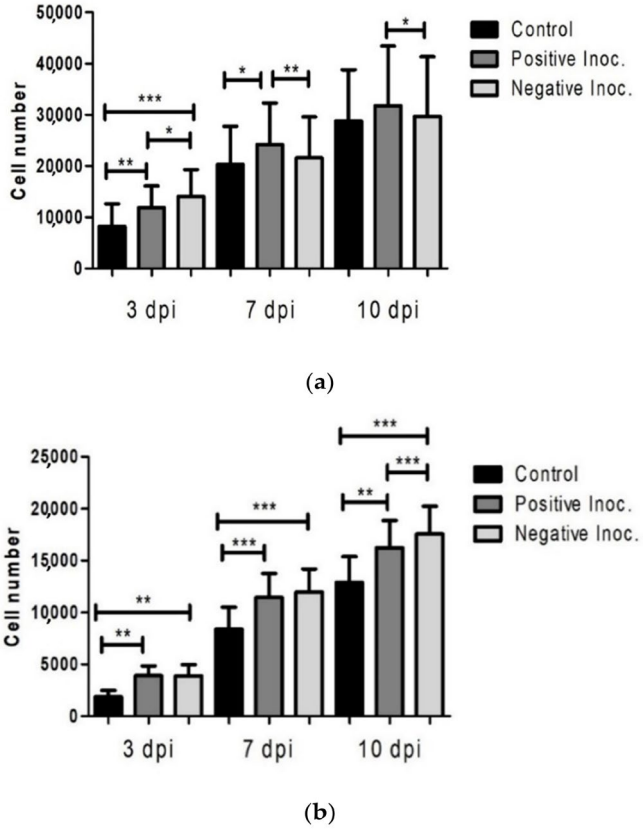

Figure 2. Cell viability study by MTT in infected oBM-MSC cultures in growth conditions (**a**) and neurogenic differentiation (**b**) 3, 7 and 10 days post-inoculation (dpi). oBM-MSCs were from 8 different donors and 4 technical replicates per culture were seeded. Significant differences were calculated using the Student *t*-test (* $p < 0.05$, ** $p < 0.01$, *** $p < 0.001$).

3.3. PrP^{Sc} Detection in Infected oBM-MSCs, Analyzed by Western Blotting

After inoculation of oBM-MSCs in growth conditions, surviving cells retained their ability to proliferate and were expanded until passage 3 post-infection. Western blotting analysis revealed the presence of PrP^{Sc} in the cultures during these three passages although the intensity of bands decreased with the number of passages (Figures 3 and S3) and was lost in further subcultures.

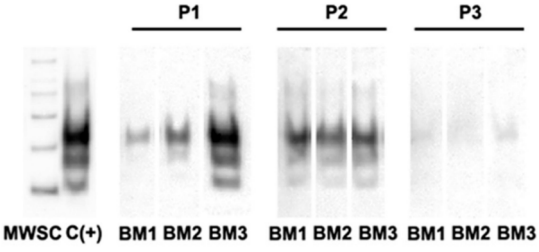

Figure 3. Determination of PrP^{Sc} by Western blotting in oBM-MSCs (BM1, BM2, BM3) infected with scrapie inocula at passages 1 to 3 (P1, P2, P3). MWSC = molecular weight marker; C (+) = positive control.

3.4. Prion Detection by ELISA in oBM-MSC and Neuron-Like Cultures Infected with Scrapie

To test the ability of MSC-derived neuron-like cells to replicate prions, the presence of PrP^{Sc} was studied by means of ELISA immediately after infection at three different stages (3, 7 and 10 dpi) in oBM-MSCs infected with positive inocula in growth and neurogenic differentiation conditions.

In oBM-MSCs maintained under growth conditions, a decrease in ELISA absorbance was observed, which could be associated with a loss of the PrP^{Sc} signal. Significant differences were found between 3 dpi and 7 dpi ($p < 0.05$) and 3 dpi and 10 dpi ($p < 0.01$) (Figure 4a).

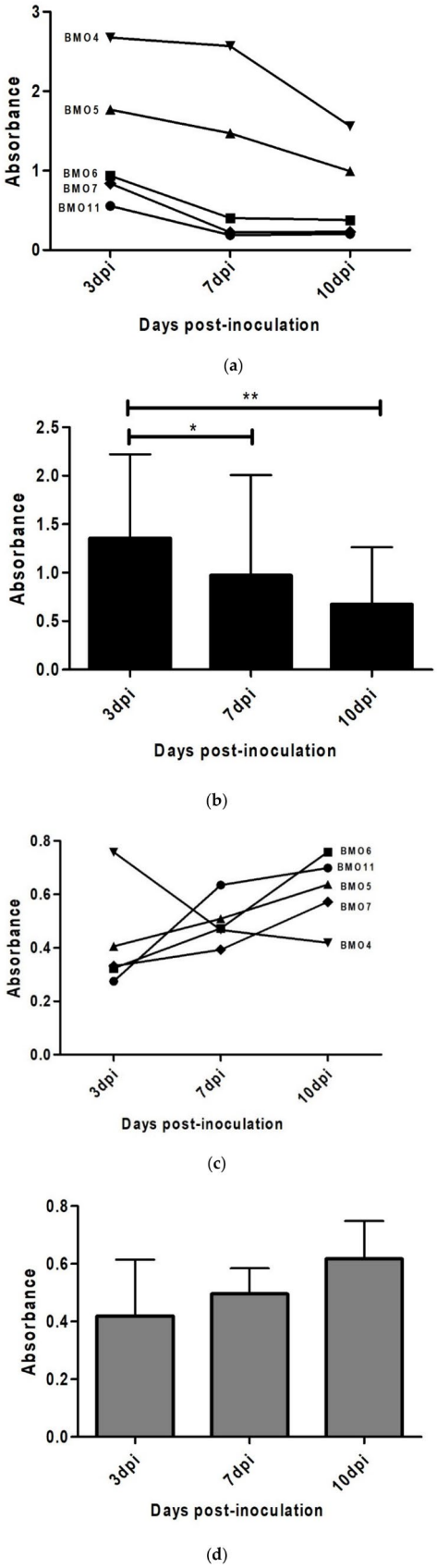

Figure 4. PrP^{Sc} detection via ELISA in infected oBM-MSC cultures from 5 donors in growth (**a**,**b**) and neurogenic differentiation (**c**,**d**) conditions 3, 7 and 10 days post-inoculation (dpi). Significant differences were calculated using Student's *t*-test (* $p < 0.05$, ** $p < 0.01$).

In contrast, the majority (four out of five) of neuron-like differentiated cultures showed an increase in absorbance over time, which could be associated with a progressive increase in the PrP^{Sc} signal. Even though most of the cultures had an increasing signal pattern, as one of them (BMO4) displayed decreased absorbance over time, no significant differences were found between any of the three stages (Figure 4b).

Although we used the same inoculum in all cultures, the initial amount of PrP^{Sc} was different in each culture at 3 dpi, suggesting a heterogeneity in the ability to retain prions. Higher cellular density under growth conditions would explain the higher absorbance observed in this condition, compared to neurogenic conditions.

4. Discussion

Prion diseases are fatal neurodegenerative disorders affecting humans and animals. Over the years, a substantial effort has been made to develop in vitro models for the study of these pathologies. Most of the cellular models are based on the culturing of murine cell lines [8] and require a previous adaptation of the strain to mice, due to the well-known phenomenon of the species barrier. Therefore, in vitro models with a natural host background would be very useful tools for research into many prion topics, e.g., prion replication, toxicity, genetic susceptibility, differences in strain susceptibility, early mechanisms of infection and new treatment testing.

MSCs can be easily collected from several accessible adult tissues like bone marrow or peripheral blood [8,28] and they show the ability to transdifferentiate into neuronal elements in vitro [10,29]. Several works have described the ability of murine stromal cells to propagate prion infectivity [12,17,30,31] and expanded MSCs obtained from sporadic Creutzfeldt-Jakob disease CJD patients have been shown to be positive for PrP^{Sc} [12]. The infectivity of MSCs obtained from sick individuals does not seem to be a pan-species characteristic, as oBM-MSCs from scrapie infected sheep did not show PrP^{Sc} [18]. Although MSCs derived from human, cattle and sheep express PrP^{C} [12,18] to the best of our knowledge, the potential of MSCs derived from these naturally susceptible species to propagate prion infection in vitro has never been investigated. In the present work, we infected ovine bone marrow-derived MSCs and their neuron-like derivatives with scrapie-infected sheep isolates to study the response of these cells to prion infection during a certain period of time.

MSCs can migrate to prion-affected neurological tissues as a response to secreting trophic factors that activate endogenous restorative reactions in the injured brain [32–34]. In our study, cell viability was higher in both oBM-MSCs and neural-differentiated cultures after inoculation compared with non-inoculated control cultures in the three monitored stages (3, 7 and 10 dpi), which suggests that brain inocula, independently of their origin, may contain factors that stimulate oBM-MSC proliferation.

Murine stromal cells are able to propagate prions for many passages [17,30]. On the contrary, oBM-MSCs do not seem to be permissive to PrP^{Sc} infection. The loss of PrP^{Sc} signal over time detected by ELISA in oBM-MSC cultures soon after infection with positive inocula suggests that these cells, if infected, are unable to replicate the prions, unlike what happens in mice. Similarly, Western blotting revealed the presence of PrP^{Sc} in scrapie-infected oBM-MSC cultures three passages after inoculation, but the presence of the pathologic protein seemed also to be weakened between passages 2 and 3, suggesting that PrP^{Sc} may be taken up by oBM-MSCs without leading to a successful prion infection. In some works, murine BM-MSCs infected with prions in vitro showed few or no PrP^{Sc} production during the first 10 or even 50 passages [12,31] and stable and detectable (by Western blotting) production of PrP^{Sc} afterwards. We could not

explore this possibility because, contrary to murine cells, MSCs obtained from humans or unconventional model organisms including sheep are able to be maintained in culture for far fewer passages [35,36].

Moreover, after inoculation with scrapie, oBM-MSC cultures displayed a high proliferation rate, with an average doubling time during the three passages that was lower than the DT described previously for BM-MSC cultures derived from scrapie and healthy sheep [18]. Cell division modulates prion accumulation in cultured cells [37] and direct proximity between donor and recipient cells increases the infection in other cell culture models [38]. The high proliferation rate observed in oBM-MSCs could help to avoid the transmission of PrP^{Sc} from infected cells to non-infected ones because the cells are not in contact for a long enough time. Therefore, only the cells infected during the inoculation process and their daughters would show infection and this would be diluted in successive passages. Changes in culture conditions focused on slowing down the proliferation rate or increasing their contact in spheroid cultures could facilitate the propagation.

On the other hand, we cannot discard the possibility that infection with scrapieinfected brain cells could be toxic for the oBM-MSC cultures. Even though no toxicity was observed in murine MSCs infected with the CJD agent [12], we have to take into account that our cells come from a naturally susceptible host. In our study, CD was significantly higher in cells infected with healthy brain extracts and, accordingly, DT was higher in cells infected with scrapie inocula. Therefore, those cells exposed to scrapie prions showed lower proliferation potential, similar to the findings observed in MSCs obtained from scrapie sheep [18]. This could be a consequence of the loss of infected cells due to prion toxicity. In the MTT assay, the effect of prion infection on cell viability was evaluated during the first passage after prion infection. Toxicity seems to be an early effect of prion infection, as 3 days after inoculation, viability was lower in scrapie cultures than in healthy infected cultures. In contrast with the first assay, at the end of this passage (10 dpi), the number of cells in scrapie-infected cultures was higher than that in the cultures inoculated with control brain cells. This could be a consequence of differences in the inocula, as brain tissues used in the different experiments were different and could have contained different amounts of PrP^{Sc} and therefore exhibited different degrees of toxicity. Nevertheless, throughout all passages, CD and DT differences were lower and, similarly, the number of cells in scrapie-infected cultures increased after early toxicity. In both cases, this increase in proliferation and viability was accompanied by the loss of PrP^{Sc} detection, which might indicate a recovery of the cell culture conditions after the elimination of PrP^{Sc} infected cells, increasing the proportion of non-infected cells, which display higher proliferation potential.

Regarding the differentiation of oBM-MSC cultures into neuron-like cells, although certain toxicity was also observed 3 days after prion infection, four out of the five cultures analyzed seemed to be infected and possibly displayed the ability to replicate the pathological prion protein. Although we did not obtain statistical support for this observation, the ELISA assay showed that these cells maintained the PrP^{Sc} signal and this signal increased progressively over time. Similarly, astrocytes derived from human induced pluripotent stem cells are capable of replicating prions from brain samples of CJD patients, generating prion infectivity in vitro [20]. Taking this into account and knowing that cells from the central nervous system are the target of the pathological prion protein, oBM-MSC-derived neuron-like cells may have a greater ability to capture and replicate PrP^{Sc} than oBM-MSCs in growth conditions. The lack of statistical significance in our results was due to the existence of variability in prion replication, as one

culture (BMO4) failed to replicate prions. This culture displayed a *PRNP* genotype identical to other three cultures (ARQ/ARQ), suggesting that, in addition to the *PRNP* genotype, other factors influence prion replication. Despite all the cultures being infected with the same amount of inoculum, BMO4 was the one that showed the highest absorbance for PrP^{Sc} under both growth and differentiation conditions. Differences in the ability to access prions could explain differences in toxicity and prion replication.

The observed differences in undifferentiated and differentiated oBM-MSCs suggest that the latter possess a competence for infection that it is not present at the MSC stage, even though they share a genetic background for each given animal. This system, using oBM-MSC-neuron-like derivates, could serve for the investigation (in an isogenic context) of the molecular trigger that sustains scrapie infection in vitro, specifically in the neural lineage. In addition, differences between cultures harboring the same *PRNP* genotype could help in the identification of other factors related to prion susceptibility.

5. Conclusions

This work describes for the first time the infection with scrapie agents of bone marrow-derived MSCs obtained from sheep, which is a natural host of prion diseases. Culturing ovine MSCs with CNS extracts in growth and neurogenic conditions induced cell proliferation, although some toxicity was observed in scrapie-infected cultures. Inoculated oBM-MSCs in growth conditions were not permissive to prion infection, whereas most cultures under neurogenic differentiation conditions seemed to retain and replicate the pathological prion protein. oBM-MSC-derived neuron-like cells could be a good candidate for developing in vitro studies in species for which iPSC reprogramming is not standardized, like sheep. Further studies focusing on elucidating the molecular mechanisms implicated in retaining prion infectivity and inducing prion toxicity in mesenchymal stem cells and MSC-derived neuron-like cells are warranted.

Supplementary Materials: The following are available online at https://www.mdpi.com/article/10.3390/ani11041137/s1, Figure S1: Calibration curves used in the MTT assay: (a) calibration curve used to establish the relationship between absorbance and the amount of MSCs in growth conditions (r^2 = 0.96) and (b) calibration curve used to establish the relationship between absorbance and the amount of MSCs in neurogenic conditions (r^2 = 0.98). Figure S2: Calibration logarithmic curve used to evaluate the sensitivity of PrPSc detection of the EEB-Scrapie HerdCheck kit, where y = 0.626ln(x) + 0.4023 and r^2 = 0.9911. Figure S3: Full Western blotting membranes used for PrP^{Sc} determination in oBM-MSCs (BM1, BM2, BM3) infected with scrapie inocula at passages 1 to 3 (P1, P2, P3). MWSC = molecular weight marker; C (+) = positive control.

Author Contributions: Conceptualization, I.M.-B.; methodology, I.M.-B.; formal analysis, L.G.-M. and D.R.M.; investigation, L.G.-M., D.R.M., A.H., D.S.-R., Ó.L.-P. and A.O.; animal handling and surgical treatment, B.M. and F.J.V.; writing—original draft preparation, A.H. and L.G.-M.; writing— review and editing, I.M.-B. and L.O.; visualization, A.H.; supervision, I.M.-B., R.B. and L.O.; project administration, I.M.-B., P.Z., R.B. and J.J.B.; funding acquisition, I.M.-B., R.B., P.Z. and J.J.B. All authors have read and agreed to the published version of the manuscript.

Funding: This work was performed as part of the RTI2018-098711-B-I00 project financed by Ministerio de Ciencia, Innovación y Universidades, Agencia Estatal de Investigación and Fondo Europeo de Desarrollo Regional and by REDPRION, 65% co-financed by the European Regional Development Fund (ERDF) through the Interreg V-A Spain-France-Andorra program (POCTEFA 2014-2020). POCTEFA aims to reinforce the economic and social integration of the French–Spanish–Andorran border. Its support is focused on developing economic, social and environmental cross-border activities through joint strategies, favoring sustainable territorial development.

Institutional Review Board Statement: The study was conducted under Project License PI06/12 approved by the Ethical Committee for Animal Experiments from the University of Zaragoza. The care and use of animals were performed in accordance with the Spanish Policy for Animal Protection RD53/2013, which meets the European Union Directive 2010/63 on the protection of animals used for experimental and other scientific purposes.

Data Availability Statement: The raw data of the results presented in this study are available on request from the corresponding author.

Acknowledgments: We thank the staff of the Large Animal section of the Veterinary Hospital of the University of Zaragoza, co-financed by the Cátedra Ruralia-Bantierra, for their assistance in sheep management and sedation for bone marrow sampling. This publication uses extracts from Diego Rubén Mediano Martín-Maestro's PhD thesis [39] and the University of Zaragoza does not reserve any right of exclusive publication.

Conflicts of Interest: The authors declare no conflict of interest.

References

1. Prusiner, S.B. The prion diseases. *Brain Pathol.* **1998**, *8*, 499–513. [CrossRef]
2. Prusiner, S.B. Novel proteinaceous infectious particles cause scrapie. *Science* **1982**, *216*, 136–144. [CrossRef]
3. Bell, J.E.; Ironside, J.W. Neuropathology of spongiform encephalopathies in humans. *Br. Med. Bull.* **1993**, *49*, 738–777. [CrossRef] [PubMed]
4. Pattison, I.H.; Jones, K.M. The astrocytic reaction in experimental scrapie in the rat. *Res. Vet. Sci.* **1967**, *8*, 160–165. [CrossRef]
5. Zabel, M.D.; Reid, C. A brief history of prions. *Pathog. Dis.* **2015**, *73*. [CrossRef] [PubMed]
6. McMahon, H.E. Cell culture methods for screening of prion therapeutics. In *Methods in Molecular Biology*; Humana Press Inc.: Totowa, NJ, USA, 2017; Volume 1658, pp. 295–304.
7. Bedecs, K. Cell culture models to unravel prion protein function and aberrancies in prion diseases. *Methods Mol. Biol.* **2008**, *459*, 1–20. [CrossRef] [PubMed]
8. Solassol, J.; Crozet, C.; Lehmann, S. Prion propagation in cultured cells. *Br. Med. Bull.* **2003**, *66*, 87–97. [CrossRef] [PubMed]
9. Pittenger, M.F.; Mackay, A.M.; Beck, S.C.; Jaiswal, R.K.; Douglas, R.; Mosca, J.D.; Moorman, M.A.; Simonetti, D.W.; Craig, S.; Marshak, D.R. Multilineage potential of adult human mesenchymal stem cells. *Science* **1999**, *284*, 143–147. [CrossRef]
10. Woodbury, D.; Reynolds, K.; Black, I.B. Adult bone marrow stromal stem cells express germline, ectodermal, endodermal, and mesodermal genes prior to neurogenesis. *J. Neurosci. Res.* **2002**, *69*, 908–917. [CrossRef] [PubMed]
11. Zhao, L.R.; Duan, W.M.; Reyes, M.; Keene, C.D.; Verfaillie, C.M.; Low, W.C. Human bone marrow stem cells exhibit neural phenotypes and ameliorate neurological deficits after grafting into the ischemic brain of rats. *Exp. Neurol.* **2002**, *174*, 11–20. [CrossRef]
12. Takakura, Y.; Yamaguchi, N.; Nakagaki, T.; Satoh, K.; Kira, J.; Nishida, N. Bone marrow stroma cells are susceptible to prion infection. *Biochem. Biophys. Res. Commun.* **2008**, *377*, 957–961. [CrossRef]
13. Shi, F.; Yang, Y.; Wang, T.; Kouadir, M.; Zhao, D.; Hu, S. Cellular Prion Protein Promotes Neuronal Differentiation of AdiposeDerived Stem Cells by Upregulating miRNA-124. *J. Mol. Neurosci.* **2016**, *59*, 48–55. [CrossRef]
14. Martellucci, S.; Santacroce, C.; Manganelli, V.; Santilli, F.; Piccoli, L.; Cassetta, M.; Misasi, R.; Sorice, M.; Mattei, V. Isolation, propagation, and prion protein expression during neuronal differentiation of human dental pulp stem cells. *J. Vis. Exp.* **2019**, *2019*, e59282. [CrossRef]
15. Martellucci, S.; Santacroce, C.; Santilli, F.; Piccoli, L.; Monache, S.D.; Angelucci, A.; Misasi, R.; Sorice, M.; Mattei, V. Cellular and molecular mechanisms mediated by recPrP C involved in the neuronal differentiation process of mesenchymal stem cells. *Int. J. Mol. Sci.* **2019**, *20*, 345. [CrossRef] [PubMed]
16. Shan, Z.; Hirai, Y.; Nakayama, M.; Hayashi, R.; Yamasaki, T.; Hasebe, R.; Song, C.H.; Horiuchi, M. Therapeutic effect of autologous compact bone-derived mesenchymal stem cell transplantation on prion disease. *J. Gen. Virol.* **2017**, *98*, 2615–2627. [CrossRef] [PubMed]
17. Akimov, S.; Vasilyeva, I.; Yakovleva, O.; McKenzie, C.; Cervenakova, L. Murine bone marrow stromal cell culture with features of mesenchymal stem cells susceptible to mouse-adapted human TSE agent, Fukuoka-1. *Folia Neuropathol.* **2009**, *47*, 205–214. [PubMed]
18. Mediano, D.R.; Sanz-Rubio, D.; Bolea, R.; Marín, B.; Vázquez, F.J.; Remacha, A.R.; López-Pérez, Ó.; Fernández-Borges, N.; Castilla, J.; Zaragoza, P.; et al. Characterization of mesenchymal stem cells in sheep naturally infected with scrapie. *J. Gen. Virol.* **2015**, *96*, 3715–3726. [CrossRef] [PubMed]
19. Groveman, B.R.; Foliaki, S.T.; Orru, C.D.; Zanusso, G.; Carroll, J.A.; Race, B.; Haigh, C.L. Sporadic Creutzfeldt-Jakob disease prion infection of human cerebral organoids. *Acta Neuropathol. Commun.* **2019**, *7*, 90. [CrossRef]
20. Krejciova, Z.; Alibhai, J.; Zhao, C.; Krencik, R.; Rzechorzek, N.M.; Ullian, E.M.; Manson, J.; Ironside, J.W.; Head, M.W.; Chandran, S. Human stem cell-derived astrocytes replicate human prions in a PRNP genotype-dependent manner. *J. Exp. Med.* **2017**, *214*, 3481–3495. [CrossRef]

21. Lyahyai, J.; Mediano, D.R.; Ranera, B.; Sanz, A.; Remacha, A.R.; Bolea, R.; Zaragoza, P.; Rodellar, C.; Martín-Burriel, I. Isolation and characterization of ovine mesenchymal stem cells derived from peripheral blood. *BMC Vet. Res.* **2012**, *8*, 169. [CrossRef]
22. Hortells, P.; Monzón, M.; Monleón, E.; Acín, C.; Vargas, A.; Bolea, R.; Luján, L.; Badiola, J.J. Pathological findings in retina and visual pathways associated to natural Scrapie in sheep. *Brain Res.* **2006**, *1108*, 188–194. [CrossRef]
23. O'Rourke, K.I.; Baszler, T.V.; Besser, T.E.; Miller, J.M.; Cutlip, R.C.; Wells, G.A.H.; Ryder, S.J.; Parish, S.M.; Hamir, A.N.; Cockett, N.E.; et al. Preclinical diagnosis of scrapie by immunohistochemistry of third eyelid lymphoid tissue. *J. Clin. Microbiol.* **2000**, *38*, 3254–3259. [CrossRef] [PubMed]
24. Ranera, B.; Ordovás, L.; Lyahyai, J.; Bernal, M.L.; Fernandes, F.; Remacha, A.R.; Romero, A.; Vázquez, F.J.; Osta, R.; Cons, C.; et al. Comparative study of equine bone marrow and adipose tissue-derived mesenchymal stromal cells. *Equine Vet. J.* **2012**, *44*, 33–42. [CrossRef] [PubMed]
25. Dominici, M.; Le Blanc, K.; Mueller, I.; Slaper-Cortenbach, I.; Marini, F.C.; Krause, D.S.; Deans, R.J.; Keating, A.; Prockop, D.J.; Horwitz, E.M. Minimal criteria for defining multipotent mesenchymal stromal cells. The International Society for Cellular Therapy position statement. *Cytotherapy* **2006**, *8*, 315–317. [CrossRef]
26. Bolea, R.; Monleón, E.; Schiller, I.; Raeber, A.J.; Acín, C.; Monzón, M.; Martín-Burriel, I.; Struckmeyer, T.; Oesch, B.; Badiola, J.J. Comparison of immunohistochemistry and two rapid tests for detection of abnormal prion protein in different brain regions of sheep with typical scrapie. *J. Vet. Diagn. Investig.* **2005**, *17*, 467–469. [CrossRef]
27. Filali, H.; Vidal, E.; Bolea, R.; Márquez, M.; Marco, P.; Vargas, A.; Pumarola, M.; Martin-Burriel, I.; Badiola, J.J. Gene and protein patterns of potential prion-related markers in the central nervous system of clinical and preclinical infected sheep. *Vet. Res.* **2013**, *44*, 14. [CrossRef] [PubMed]
28. Zvaifler, N.J.; Marinova-Mutafchieva, L.; Adams, G.; Edwards, C.J.; Moss, J.; Burger, J.A.; Maini, R.N. Mesenchymal precursor cells in the blood of normal individuals. *Arthritis Res.* **2000**, *2*, 477–488. [CrossRef]
29. Sanchez-Ramos, J.; Song, S.; Cardozo-Pelaez, F.; Hazzi, C.; Stedeford, T.; Willing, A.; Freeman, T.B.; Saporta, S.; Janssen, W.; Patel, N.; et al. Adult bone marrow stromal cells differentiate into neural cells in vitro. *Exp. Neurol.* **2000**, *164*, 247–256. [CrossRef]
30. Akimov, S.; Yakovleva, O.; Vasilyeva, I.; McKenzie, C.; Cervenakova, L. Persistent Propagation of Variant Creutzfeldt-Jakob Disease Agent in Murine Spleen Stromal Cell Culture with Features of Mesenchymal Stem Cells. *J. Virol.* **2008**, *82*, 10959–10962. [CrossRef] [PubMed]
31. Cervenakova, L.; Akimov, S.; Vasilyeva, I.; Yakovleva, O.; McKenzie, C.; Cervenak, J.; Piccardo, P.; Asher, D.M. Fukuoka-1 strain of transmissible spongiform encephalopathy agent infects murine bone marrow-derived cells with features of mesenchymal stem cells. *Transfusion* **2011**, *51*, 1755–1768. [CrossRef]
32. Song, C.-H.; Honmou, O.; Ohsawa, N.; Nakamura, K.; Hamada, H.; Furuoka, H.; Hasebe, R.; Horiuchi, M. Effect of Transplantation of Bone Marrow-Derived Mesenchymal Stem Cells on Mice Infected with Prions. *J. Virol.* **2009**, *83*, 5918–5927. [CrossRef] [PubMed] 33. Chopp, M.; Li, Y. Treatment of neural injury with marrow stromal cells. *Lancet Neurol.* **2002**, *1*, 92–100. [CrossRef]
34. Song, C.-H.; Honmou, O.; Furuoka, H.; Horiuchi, M. Identification of Chemoattractive Factors Involved in the Migration of Bone Marrow-Derived Mesenchymal Stem Cells to Brain Lesions Caused by Prions. *J. Virol.* **2011**, *85*, 11069–11078. [CrossRef] [PubMed]
35. Bonab, M.M.; Alimoghaddam, K.; Talebian, F.; Ghaffari, S.H.; Ghavamzadeh, A.; Nikbin, B. Aging of mesenchymal stem cell in vitro. *BMC Cell Biol.* **2006**, *7*, 14. [CrossRef]
36. Calloni, R.; Viegas, G.S.; Türck, P.; Bonatto, D.; Henriques, J.A.P. Mesenchymal stromal cells from unconventional model organisms. *Cytotherapy* **2014**, *16*, 3–16. [CrossRef] [PubMed]
37. Ghaemmaghami, S.; Phuan, P.W.; Perkins, B.; Ullman, J.; May, B.C.H.; Cohen, F.E.; Prusiner, S.B. Cell division modulates prion accumulation in cultured cells. *Proc. Natl. Acad. Sci. USA* **2007**, *104*, 17971–17976. [CrossRef] [PubMed]
38. Kanu, N.; Imokawa, Y.; Drechsel, D.N.; Williamson, R.A.; Birkett, C.R.; Bostock, C.J.; Brockes, J.P. Transfer of scrapie prion infectivity by cell contact in culture. *Curr. Biol.* **2002**, *12*, 523–530. [CrossRef]
39. Mediano, D.R. *Caracterización de Células Madre Mesenquimales Ovinas Infectadas Por Scrapie*; University of Zaragoza: Zaragoza, Spain, 2016. (In Spanish)

MANUSCRITO V

Susceptibility of ovine bone marrow-derived mesenchymal stem cell spheroids to scrapie prion infection.

Hernaiz, Adelaida; Cobeta, Paula; Marín, Belén; Vázquez, Francisco José; Badiola, Juan José; Zaragoza, Pilar; Bolea, Rosa; Martín-Burriel, Inmaculada.

En revisión

Susceptibility of ovine bone marrow-derived mesenchymal stem cell spheroids to scrapie prion infection

Adelaida Hernaiz [1], Paula Cobeta [1], Belén Marín [2], Francisco J. Vázquez [1,3], Juan J. Badiola [2], Pilar Zaragoza [1,4], Rosa Bolea [2], Inmaculada Martín-Burriel [1,2,4,*]

[1] Laboratorio de Genética Bioquímica (LAGENBIO), Facultad de Veterinaria, Universidad de Zaragoza, IA2, IIS-Aragón, Zaragoza, Spain

[2] Centro de Encefalopatías y Enfermedades Transmisibles Emergentes (CEETE), Facultad de Veterinaria, Universidad de Zaragoza, IA2, IIS-Aragón, Zaragoza, Spain

[3] Departamento de Patología Animal, Facultad de Veterinaria, Universidad de Zaragoza, Zaragoza, Spain

[4] Centro de Investigación Biomédica en Red de Enfermedades Neurodegenerativas (CIBERNED), Instituto de Salud Carlos III, Madrid, Spain

* Correspondence: minma@unizar.es; Tel.: +34 976761662

Abstract

In neurodegenerative diseases, including prion diseases, cellular in vitro models appear as fundamental tools for the study of pathogenic mechanisms and potential therapeutic compounds. Two-dimensional (2D) monolayer cell culture systems are the most used cell-based assays, but these platforms are not able to reproduce the microenvironment of in vivo cells. This limitation can be surpassed using three-dimensional (3D) culture systems such as spheroids, that mimic better the in vivo cell interactions. Here, we evaluated the effect of scrapie prion infection in monolayer-cultured ovine bone marrow-derived mesenchymal stem cells (oBM-MSCs) and oBM-MSC-derived spheroids in growth and neurogenic conditions, analysing their cell viability and the ability to maintain prion infection. MTT assay was performed in oBM-MSCs and spheroids subjected to three conditions: inoculated with brain homogenate from scrapie-infected sheep, inoculated with brain homogenate from healthy sheep and non-inoculated controls. The 3D conditions improved the cell viability in most cases, although in scrapie-infected spheroids in growth conditions a decrease in cell viability was observed. The levels of pathological prion protein (PrP^{Sc}) in scrapie-infected oBM-MSCs and spheroids were measured by ELISA. In neurogenic conditions, monolayer cells and spheroids maintained the levels of PrP^{Sc} over time. In growth conditions, however, oBM-MSCs showed decreasing levels of PrP^{Sc} throughout time, whereas spheroids were able to maintain stable PrP^{Sc} levels. The presence of PrP^{Sc} in spheroids was also confirmed by immunocytochemistry. Altogether, these results show that 3D culture microenvironment improves the permissiveness of oBM-MSCs to scrapie infection in growth conditions and maintains the infection ability in neurogenic conditions, making this model of potential use for prion studies.

Keywords: 3D culture; Spheroids; Mesenchymal stem cells; Scrapie; Prion

1. Introduction

Cell cultures have proven to be useful tools for a variety of applications in research. There are currently many established cell lines and primary cultures available and widely used for different purposes. Two-dimensional (2D) platforms in which flat monolayer cells are cultured are the most commonly used for research in cell-based assays [1]. These 2D cell culture systems are accessible, convenient and cost-effective [1]. However, various limitations are still of concern, including the failure to imitate the in vivo architecture and microenvironments. Compared with in vivo cells, 2D-cultured cells possess many different features such as morphological characteristics, proliferation and differentiation potentials, interactions of cell-cell and cell-surrounding matrix, and signal transduction [1–3].

To overcome these drawbacks, three-dimensional (3D) cell culture platforms emerge as a promising approach. Although the optimal 3D condition requirements vary between cell types and the characteristic features of cells in 3D cultures differ in accordance with their types, these 3D culture systems have proven to be more realistic for translating cell-based assay findings to in vivo applications due to their ability to closely mimic the behaviour of in vivo cells [4]. There are different 3D culture systems including spheroids, organoids, hydrogel embedding, bioreactors, scaffolds and bioprinting [1,5], that have potential applications in drug discovery, disease modelling and tissue engineering [6–8].

Spheroids are multicellular aggregates with spherical shape that can be formed from several types of cells including mesenchymal stem cells (MSCs) [9]. They are able to better mimic cell-cell and cell-matrix interactions than 2D cultures, but they lack the capacity to recapitulate the tissue organization exhibited in vivo [10]. In MSCs, spheroid formation enhances the characteristics of these cells by improving their stemness, facilitating the differentiation to multiple lineages and delaying the in vitro replicative senescent processes [11–13].

In the field of neurodegenerative diseases, 3D cell culture platforms appear as good models to reproduce different features of neurodegeneration link to these diseases. In Alzheimer's disease (AD), 3D hydrogel embedded human neural stem cells [14,15] and neural progenitor cells [16,17], and scaffold-encapsulated induced pluripotent stem cell (iPSC)-derived neural progenitor cells [18] can recapitulate amyloid-beta aggregation and accumulation of hyperphosphorylated tau, which are key hallmarks in this disease. Furthermore, a triculture model using neurons, astrocytes and microglia constructed in a microfluidic platform also showed these AD hallmarks and allowed the study of microglia recruitment, neuroinflammatory response and neuron/astrocyte damage [19]. Human iPSC-derived hippocampal spheroids [20] and brain organoids [21–23] have also been developed, having as well

the ability to mimic AD pathology and the potential to be used for screening therapeutic strategies. In Parkinson's disease (PD), dopaminergic neurons [24,25] and SH-SY5Y neuroblastoma cells [26,27] cultured in matrigel-based platforms can model several PD features such as α-synuclein accumulation and Lewy body-like inclusions. Midbrain organoids carrying *LRRK2* G2019S mutation have also been created to successfully model *LRRK2*-associated sporadic PD [28].

Prion diseases or Transmissible Spongiform Encephalopathies (TSEs) are neurodegenerative disorders caused by a pathological misfolded protein derived from the innocuous cellular prion protein (PrP^{C}) called PrP^{Sc} [29]. These diseases occur in humans and animals and among the various types of TSEs, the one affecting sheep and goats, known as scrapie, was the first discovered and is considered a good model for studying different disease aspects in these pathologies [30–32]. Regarding 3D culture methods, only two studies using human cerebral organoids have been reported. In these studies, iPSC-derived human cerebral organoids were able to uptake and propagate sporadic Creutzfeldt Jakob disease (sCJD) prions [33] and also responded to an anti-prion compound by showing delayed prion propagation [34].

A previous study of our group evaluated the effect of scrapie prion infection in ovine bone marrow-derived mesenchymal stem cells (oBM-MSCs) cultured in growth conditions and subjected to neurogenic differentiation [35]. In this study, oBM-MSCs initially took up PrP^{Sc} but they were not able to maintain it over time. MSC-derived neuron-like cells, on the contrary, absorbed and maintained stable PrP^{Sc} levels throughout the culture time [35]. These results were obtained using a 2D culture system approach that may not exactly mimic the physiological response of these cells to prion infection. Therefore, in the current study, we decided to assess the effect of scrapie prion infection in oBM-MSCs-derived spheroids cultured in growth and neurogenic conditions, analysing their ability to maintain prion infection and the impact of this infection in cell viability.

2. Materials and methods

2.1. Bone marrow extraction and ovine mesenchymal stem cell isolation and culture

A bone marrow sample was obtained from an adult female rasa aragonesa sheep of two years of age and carrying the ARQ/ARQ genotype for the *PRNP* gene. After the sedation with xylazine and the local anaesthesia with lidocaine, bone marrow aspirate was harvested from the humeral head using a 13 G Jamshidi needle and a 10 mL syringe previously loaded with 0.5 mL of sodium heparin. All procedures were carried out under project licence PI44/18, approved by the Ethical Committee for

Animal Experiments from the University of Zaragoza. The care and use of animals were performed in accordance with the Spanish Policy for Animal Protection, RD53/2013, which meets European Union Directive 2010/63 on the protection of animals used for experimental and other scientific purposes.

MSC isolation from the bone marrow aspirate (3 mL) was performed following the previously described protocol [36–38]. This protocol is based on the separation of the mononuclear fraction after density gradient centrifugation in Lymphoprep (Atom) and further isolation thanks to the ability of MSCs to adhere to plastic. After isolation, cells were expanded up to passage 2 in basal medium, consisting of low glucose Dulbecco's modified Eagle's medium (DMEM, Sigma-Aldrich, St. Louis, MO, USA) supplemented with 10 % fetal bovine serum (FBS), 1 % L-glutamine (Sigma-Aldrich) and 1 % streptomycin/penicillin (Sigma-Aldrich).

2.2. Ovine mesenchymal stem cell characterization

The minimal criteria to characterise MSCs are their plastic-adherence capacity in standard culture conditions and their ability to differentiate to mesodermal lineages (adipocytes, osteoblasts and chondroblasts) in vitro [39].

Adipogenic, osteogenic and chondrogenic differentiation was evaluated in vitro. The differentiation into mesodermal lineages was performed using specific commercial differentiation kits for osteogenic (StemPro® Osteogenesis Differentiation Kit, Gibco, Life Technologies) and chondrogenic (StemPro® Chondrogenesis Differentiation Kit, Gibco, Life Technologies) differentiation and for adipogenic differentiation basal medium supplemented with 1 µM dexamethasone, 500 µM 3-Isobutyl-1-methylxanthine (IBMX), 200 µM indomethacin and 15 % of rabbit serum was used [38,40]. Subsequently, adipogenic differentiation was confirmed using a 0.3 % Oil Red O (Sigma-Aldrich) specific stain at day 8 of differentiation; chondrogenic differentiation was identified by Alcian Blue G dye (1 : 1 in methanol) (Sigma-Aldrich) after 15 days of chondrogenic culture and osteogenic differentiation was confirmed by 2 % Alizarin Red S staining (Sigma-Aldrich) at 21 days of culture.

2.3. Formation and culture of ovine mesenchymal stem cell spheroids

For spheroid formation, 96-well Nuclon Sphera low-attachment plates (ThermoFisher Scientific) were used. In each well, 45,000 cells were seeded to form a unique spheroid per well. The cells were seeded in droplets and afterwards 200 µL of basal medium was added in each well. To ensure a correct formation of the spheroids, the plates were incubated during 5 days at 37 °C with 5 % of CO_2 without

changing the medium. Afterwards, the medium was changed every 48-72 h. After 7 days of formation, the spheroids were stabilized and ready to perform the subsequent assays.

2.4. Neurogenic differentiation of ovine mesenchymal stem cells and spheroids

2.4.1. Neurogenic differentiation

Ovine BM-MSCs were seeded at 5,000 cells/cm^2 and differentiated into neuron-like cells using HyClone AdvanceSTEM™ Neural Differentiation Kit (ThermoFisher Scientific) according to the manufacturer's instructions. The differentiation process lasted three days. Neural differentiation was monitored by observing the cells through an inverted optical microscope. The formation of neuron-like cells was seen within 24 h, peaking at 72 h, as previously described [36]. To maintain the cells in the differentiation state, the medium was changed every 48 h.

For the neurogenic differentiation of spheroids, after they were stabilized, the same neural induction kit as 2D cultures was used, following the same guidelines for medium change.

2.4.2. Nissl bodies staining

To verify the correct neurogenic differentiation, neuron-like cells and spheroids were stained with 1 % Cresyl Violet Solution (abcam) to detect Nissl bodies, which are granular structures present in neuronal cell bodies and composed of rough endoplasmic reticulum rich in RNA [41]. The staining was performed after 3 days of neurogenic differentiation.

2.4.3. Expression analysis of neuronal markers

The expression of a set of neuronal markers was assessed by real-time quantitative PCR (RT-qPCR) in both neuron-like cells and spheroids. These markers were *NEFM* (Neurofilament medium chain), *MAP2* (Microtubule-associated protein 2) and *TUBB3* (Tubulin beta 3 class III) [37]. *HPRT* (Hypoxanthine phosphoribosyltransferase) and *G6PDH* (Glucose-6-phosphate dehydrogenase) were used as housekeeping genes [37].

For total RNA extraction from 2D neuron-like cell cultures and further retrotranscription to cDNA, the Cells-to-cDNA™ II kit (ThermoFisher Scientific) was used. For spheroids, RNA was extracted using the Direct-zol™ RNA Miniprep kit (Zymo Research). cDNA was then obtained using the qScript™

cDNA SuperMix (QuantaBio). All procedures were performed following the manufacturer's instructions.

Gene expression was quantified by RT-qPCR using the Fast SYBR^{TM} Green Master Mix (Applied Biosystems, ThermoFisher Scientific) in a QuantStudio 3 Real-Time PCR instrument (Applied Biosystems). The comparative quantification of the results was standardized by the $2^{-\Delta\Delta Ct}$ method [42], using the geometric mean of *HPRT* and *G6PDH* housekeeping genes as a normalizer.

2.5. Scrapie inocula and infection of 2D ovine mesenchymal stem cell cultures and spheroids in growth and neurogenic conditions

Two different inocula were prepared using central nervous system (CNS) samples: one from a healthy sheep (negative control) and one from a classical scrapie-infected sheep, both carrying the ARQ/ARQ genotype. The inocula were preserved at the tissue bank of the Center of Encephalopathies and Emerging Transmissible Diseases (CEETE; University of Zaragoza). The presence/absence of PrP^{Sc} in the CNS tissues was confirmed following the protocols used in previous works [43], which consisted of two rapid diagnostic tests (Prionics-CheckWestern blotting; ThermoFisher Scientific and Idexx HerdChek; IDEXX, Westbrook, ME, USA) and confirmation by immunohistochemical examination of the CNS tissue. CNS samples were homogenized and diluted 1:10 (g/mL) in physiological saline solution (Braun). Afterwards, samples were treated at 70 °C for 10 min before adding streptomycin sulphate (100 µg/mL) and benzylpenicillin (100 µg/mL). To check the safety of the inocula once generated, samples were incubated in blood agar plates, and the absence of any bacterial growth was confirmed.

To assess the effect of prion infection in cell viability of 2D oBM-MSC cultures and spheroids in growth and neurogenic conditions and their ability to replicate prions, oBM-MSCs were seeded at 5,000 cells/cm^2 and spheroids were generated from 45,000 cells each. For each condition, three groups were established: positive, negative and control. Positive cells and spheroids were infected with inoculum from a scrapie-infected sheep, negative with inoculum from a healthy sheep and control cells and spheroids were kept in standard conditions. For infection, basal medium was substituted by inocula diluted 1:10 in DMEM medium (10 % FBS, 1 % L-glutamine and 1 % streptomycin/penicillin) for the 2D oBM-MSCs and spheroids in growth conditions, and in HyClone medium for the 2D oBM-MSCs and spheroids subjected to neurogenic differentiation. Cells and spheroids were maintained in this

medium for 48 h to analyse the cell viability and prion replication ability. Afterwards, the medium was changed twice a week.

2.6. PrP^{Sc} detection

2.6.1. ELISA (Enzyme-linked immunosorbent assay)

To test the ability to replicate PrP^{Sc} of 2D oBM-MSCs and spheroids inoculated with scrapie-infected brain homogenate, in growth and neurogenic conditions, the amount of the pathogenic protein was quantified at three different stages (2 dpi, corresponding to the inoculum removal, 5 and 8 dpi) with the ELISA kit EEB-Scrapie HerdCheck kit (IDEXX), following the manufacturer's recommendations. A previous study of our group showed that this kit was suitable for a sensitive detection of PrP^{Sc} in oBM-MSC cultures [35]. oBM-MSCs were seeded at 5,000 cells/cm^2 in 6-well plates and the retrieval of the cells was performed by means of trypsinization and subsequent centrifugation to obtain 3 technical replicates per condition and time (dpi). Spheroids formed from 45,000 cells were also collected and 3 spheroids/technical replicates were analysed per condition and time (dpi).

2.6.2. Immunocytochemistry of infected spheroids

The presence of PrP^{Sc} in spheroids was also confirmed by immunocytochemistry at 5 dpi. Spheroids in growth and neurogenic conditions were fixed in 4 % paraformaldehyde and stained with 0.2 % eosin. Each spheroid was then included in a 1 % agarose matrix and subsequently the matrices containing the spheroids were embedded in paraffin. Afterwards, paraffin-embedded spheroids were cut obtaining 3 µm-thick-slices. Hematoxylin-eosin staining was performed to evaluate the integrity of the spheroids after the inclusion in paraffin.

For immunocytochemistry, after deparaffination and rehydration, spheroids sections were subjected to antigen retrieval with citrate buffer (pH 6.0) for 10 min at 96 °C in a PTLink (Dako). Afterwards, endogenous peroxidase activity was blocked using a precast solution (Dako Agilent, Glostrup, Denmark). Sections were then incubated 30 min at room temperature with the primary antibodies L42 (1:500, R-Biopharm, Darmstadt, Germany) and F89 (1:2000, R-Biopharm, Darmstadt, Germany). Omission of the primary antibody served as a background control for nonspecific binding of the secondary antibody. Subsequently, the sections were incubated with an anti-mouse enzyme-

conjugated EnVision polymer (Dako Agilent, Glostrup, Denmark) for 30 min at room temperature. Diaminobenzidine (DAB, Dako Agilent, Glostrup, Denmark) was used as the chromogen. Spheroids sections were assessed and photographed using a Zeiss Axioskop 40 optical microscope (Zeiss, Jena, Germany) and the software AxioVision Rel.4.7.

2.7. Cell viability assay

MTT assay was performed to evaluate cell viability and early prion toxicity in oBM-MSCs and neuron-like cells at 2, 5 and 8 days post-inoculation (dpi). Time 2 dpi corresponded to the one of inoculum removal, considering the moment of the infection with the inocula as day 0. The toxicity of the prion in oBM-MSCs and neuron-like cells was studied in three conditions (inoculated with scrapie-positive brain homogenates, negative brain inoculum and non-inoculated controls) and at three different stages (2, 5 and 8 dpi). Cells were seeded in 96-well plates at 5,000 cells/cm^2 and 8 technical replicates were analysed for each condition per time (dpi). Briefly, the MTT assay was performed by adding 25 µL of MTT solution (2 mg/mL) per well. Then, the plates were incubated at 37 °C for 4 h. Afterwards, the content of each well was removed and was substituted with 150 µL of HCl solution (HCl 40 mM in isopropanol) per well. Plates were then incubated for 1 h at room temperature protected from light. The absorbance was measured at 570 nm in an Infinite F200 microplate reader (Tecan Ibérica Instrumentación, Barcelona, Spain). Differences in cell viability were evaluated with Student's t-test. Statistical significance was defined as $p < 0.05$.

The viability after prion infection was also analysed in spheroids at both growth and neurogenic conditions by MTT assay at 2, 5 and 8 dpi and as well in three conditions (inoculated with scrapie-positive brain homogenates, negative brain inoculum and non-inoculated controls). Spheroids were formed from 45,000 cells per spheroid in 96-well Nuclon Sphera low-attachment plates (ThermoFisher Scientific) and 4 technical replicates were analysed for each condition per time (dpi). The MTT assay was performed using the same reagents as in oBM-MSCs and neuron-like cells, but the incubation times were different: spheroids were incubated at 37 °C for 24 h with MTT solution and 4 h at room temperature protected from light with HCl solution [44]. Differences in cell viability were also evaluated with Student's t-test and statistical significance was defined as well as $p < 0.05$.

3. Results

3.1. Ovine mesenchymal stem cell differentiation into mesodermal lineages

To characterise oBM-MSCs, their ability to differentiate into adipocytes, chondrocytes and osteocytes was assessed.

Cells under adipogenic conditions presented red cytoplasmatic lipid droplets (Figure 1a and b). In chondrogenic conditions, cells aggregated in nodule-like formations (Figure 1c and d) and red-stained calcium deposits were found in osteogenic conditions (Figure 1e and f).

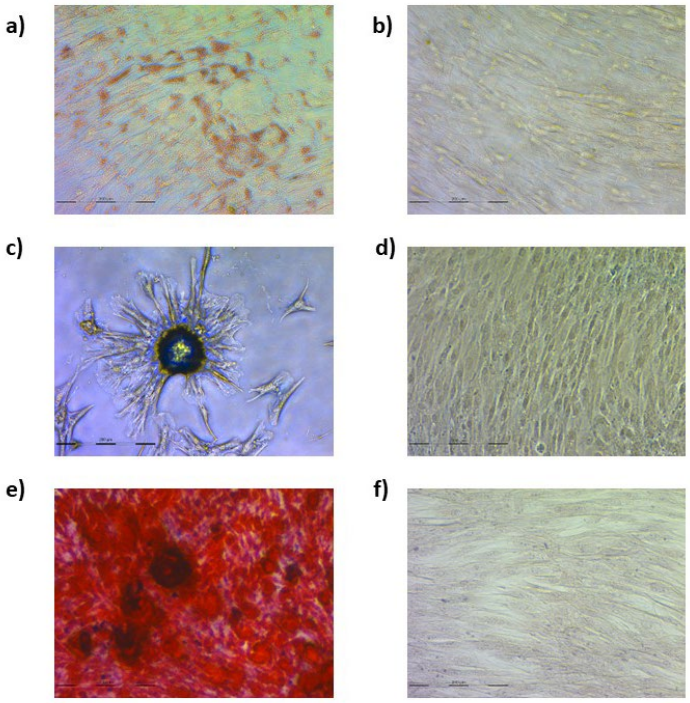

Figure 1. oBM-MSC staining for adipogenic, chondrogenic and osteogenic differentiation. Oil red O staining of cells cultured for 8 days in adipogenic differentiation medium **(a)** and basal medium **(b)**; alcian blue staining of cells cultured for 15 days in chondrogenic **(c)** and basal medium **(d)** and alizarin red staining of cells cultured for 21 days in osteogenic differentiation medium **(e)** and basal medium **(f)**.

3.2. Spheroid formation

As shown in Figures 2 and 3, after 7 days of culture, the size of the spheroids was stabilized and one spheroid per well was formed. Size of final spheroids ranged between 392 and 427 μm.

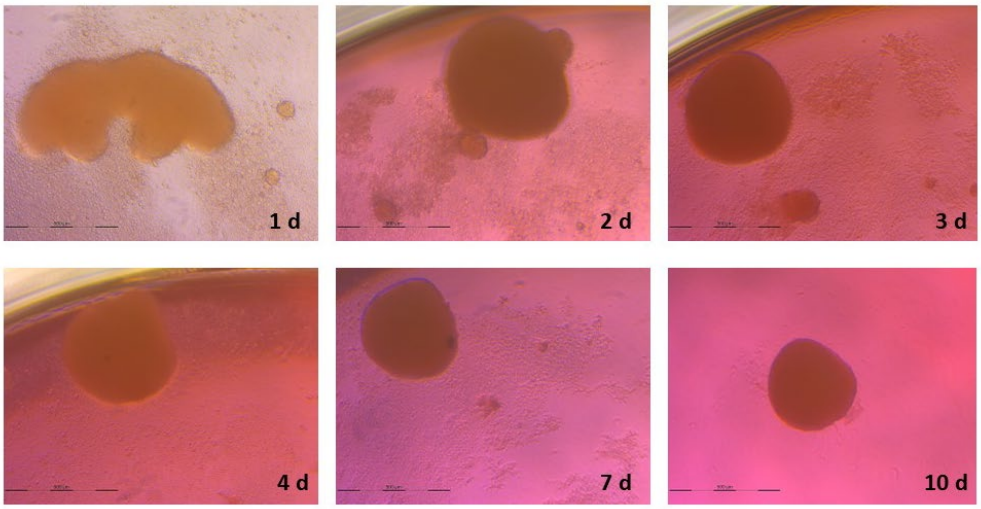

Figure 2. Timeline images of spheroid formation from 1 day to 10 days of culture in basal conditions.

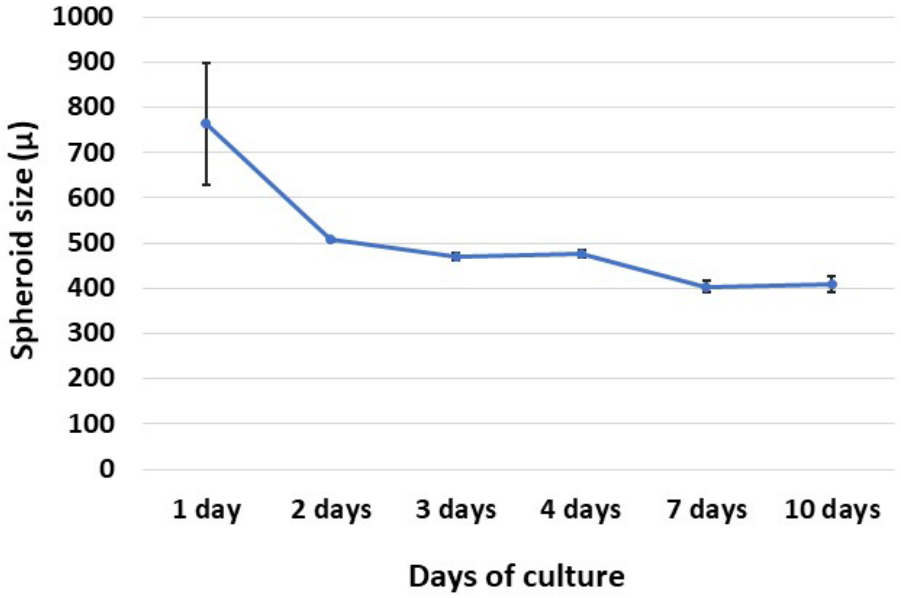

Figure 3. Line chart showing the size of the spheroids (µ) throughout 10 days of culture in basal conditions. The data are presented as mean values ± SEM (n = 4).

3.3. Neurogenic differentiation

3.3.1. Ovine mesenchymal stem cell 2D cultures

The differentiation of oBM-MSCs into neuron-like cells was assessed by Nissl bodies staining in cells subjected to neurogenic differentiation and by analysing the expression of three neuronal markers: *NEFM*, *MAP2* and *TUBB3*.

The presence of Nissl bodies in the soma of neuron-like cells was confirmed using Cresyl Violet staining (Figure 4). Regarding the expression of neuronal markers, *TUBB3* and *MAP2* displayed higher expression levels in neuron-like

cells in comparison to the cells in growth conditions. *NEFM*, conversely, showed lower expression levels in cells subjected to neurogenic differentiation (Table 1). Overall, the presence of Nissl bodies and the increased expression of two neuronal markers confirmed the neurogenic differentiation of oBM-MSCs.

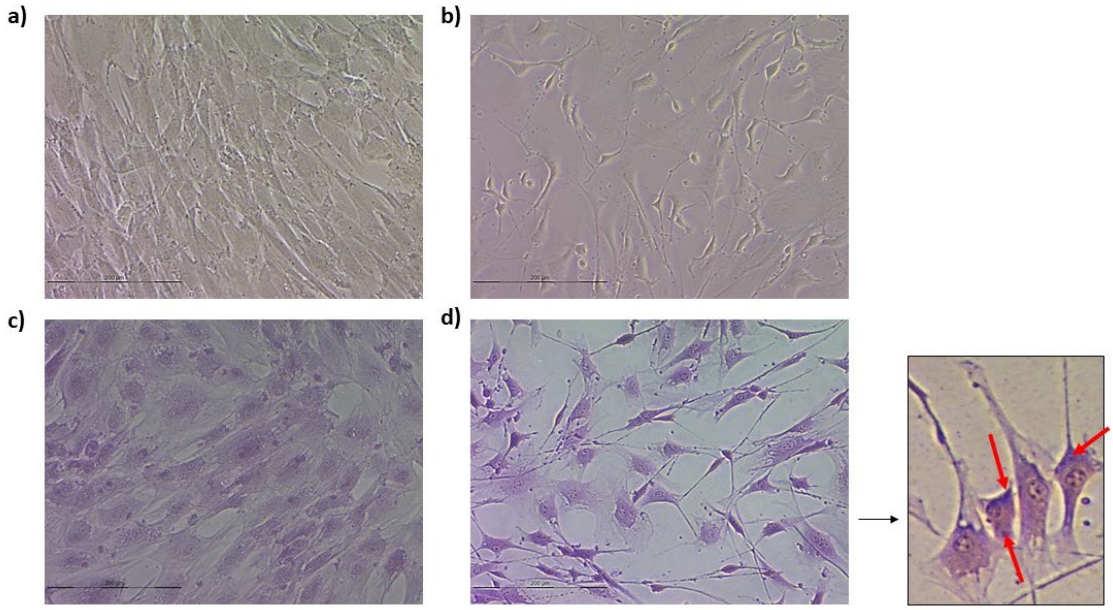

Figure 4. oBM-MSCs in basal **(a)** and neurogenic differentiation **(b)** conditions. Cresyl Violet staining of oBM-MSCs in basal medium **(c)** and oBM-MSC derived neuron-like cells **(d)** 3 days after neurogenic induction. Nissl bodies present in neuron-like cells are marked with red arrows.

Table 1. Expression levels of neuronal markers *NEFM*, *MAP2* and *TUBB3* in oBM-MSCs and neuron-like cells 3 days after neurogenic induction. Relative expression levels are shown in terms of $2^{-\Delta\Delta Ct}$.

Gene	**Expression levels ($2^{-\Delta\Delta Ct}$) in oBM-MSCs**	**Expression levels ($2^{-\Delta\Delta Ct}$) in neuron-like cells**
TUBB3	1	1.46
NEFM	1	0.50
MAP2	1	321.63

3.3.2. Spheroids

The evaluation of neurogenic differentiation in spheroids was carried out in the same way as in oBM-MSCs: Cresyl Violet staining was performed along with the expression analysis of *NEFM*, *TUBB3* and *MAP2* neuronal markers.

Together with the presence of Nissl bodies, spheroids under neurogenic differentiation conditions displayed a kind of prolongations on its contour that could be associated with neuronal morphology (Figure 5). Moreover, in neuron-like differentiated spheroids, the expression of the three neuronal markers, although slightly, was increased compared to the spheroids in basal conditions (Table 2). Therefore, the neurogenic differentiation of spheroids was also confirmed.

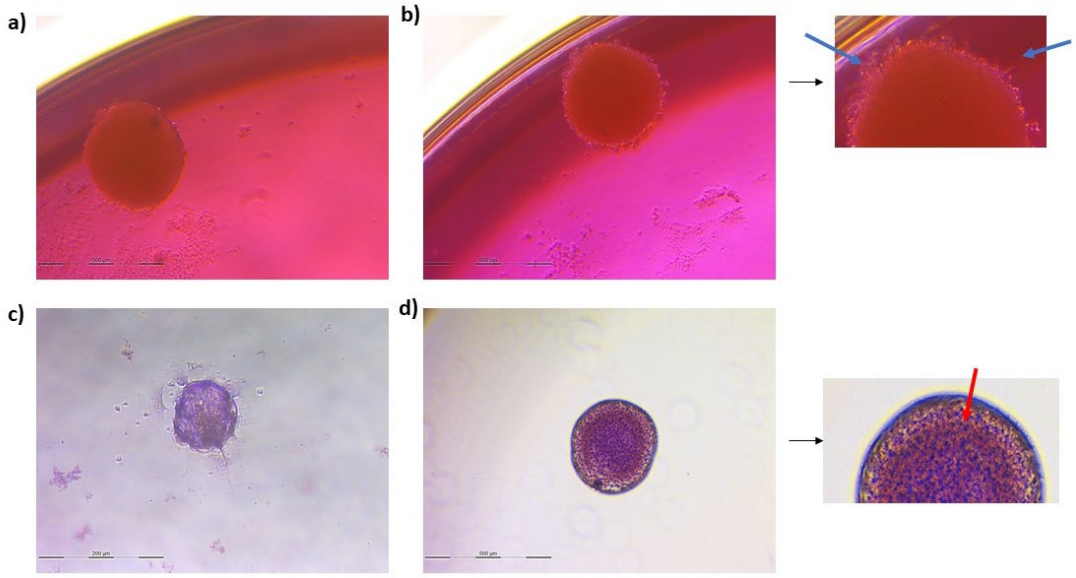

Figure 5. Spheroids in basal **(a)** and neurogenic differentiation **(b)** conditions. Cresyl Violet staining of spheroids in basal **(c)** and neurogenic **(d)** conditions 3 days after neuronal induction. Blue arrows indicate the prolongations formed on the contour of the spheroid and the red arrow marks the Nissl bodies.

Table 2. Expression levels of neuronal markers *NEFM*, *MAP2* and *TUBB3* in spheroids in basal and neurogenic differentiation conditions 3 days after neurogenic induction. Relative expression levels are shown in terms of $2^{-\Delta\Delta Ct}$.

Gene	**Expression levels ($2^{-\Delta\Delta Ct}$) in spheroids in basal conditions**	**Expression levels ($2^{-\Delta\Delta Ct}$) in spheroids in neurogenic differentiation conditions**
TUBB3	1	1.21
NEFM	1	1.13
MAP2	1	2.24

3.4. Levels of PrP^{Sc} after prion infection

3.4.1. Ovine mesenchymal stem cells and neuron-like cells infected with scrapie

PrP^{Sc} signal was measured after the infection with scrapie brain homogenate in oBM-MSCs and neuron-like cells at 2, 5 and 8 days' post-inoculation. As shown in Figure 6, the levels of PrP^{Sc} in oBM-MSCs cultured in 2D decreased over time, whereas in neuron-like cells the levels were maintained stable throughout the time, with a slight decrease at 8 dpi.

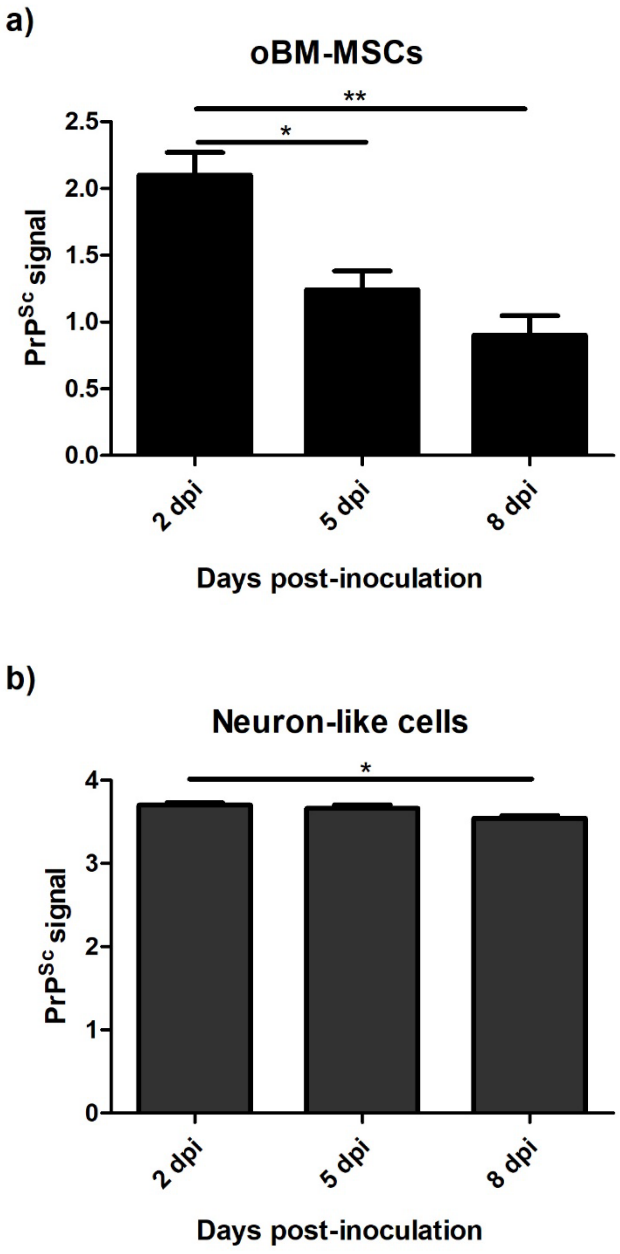

Figure 6. PrP^{Sc} levels measured by ELISA in oBM-MSCs **(a)** and neuron-like cells **(b)** 2, 5 and 8 days after prion infection. Data are shown as mean values ± SEM. * $p < 0.05$; ** $p < 0.01$

3.4.2. Spheroids in growth and neurogenic conditions infected with scrapie

The levels of PrP^{Sc} detected by ELISA were also analysed in scrapie-infected spheroids in growth and neurogenic conditions. Unlike 2D oBM-MSCs, spheroids in growth conditions showed stable levels of PrP^{Sc} over time (Figure 7a). In spheroids cultured in neurogenic conditions, a slightly decrease of PrP^{Sc} signal was found at 5 dpi, but later PrP^{Sc} levels were recovered at 8 dpi (Figure 7b). The presence of PrP^{Sc} in scrapie-infected spheroids was as well confirmed by immunocytochemistry (Figure 8).

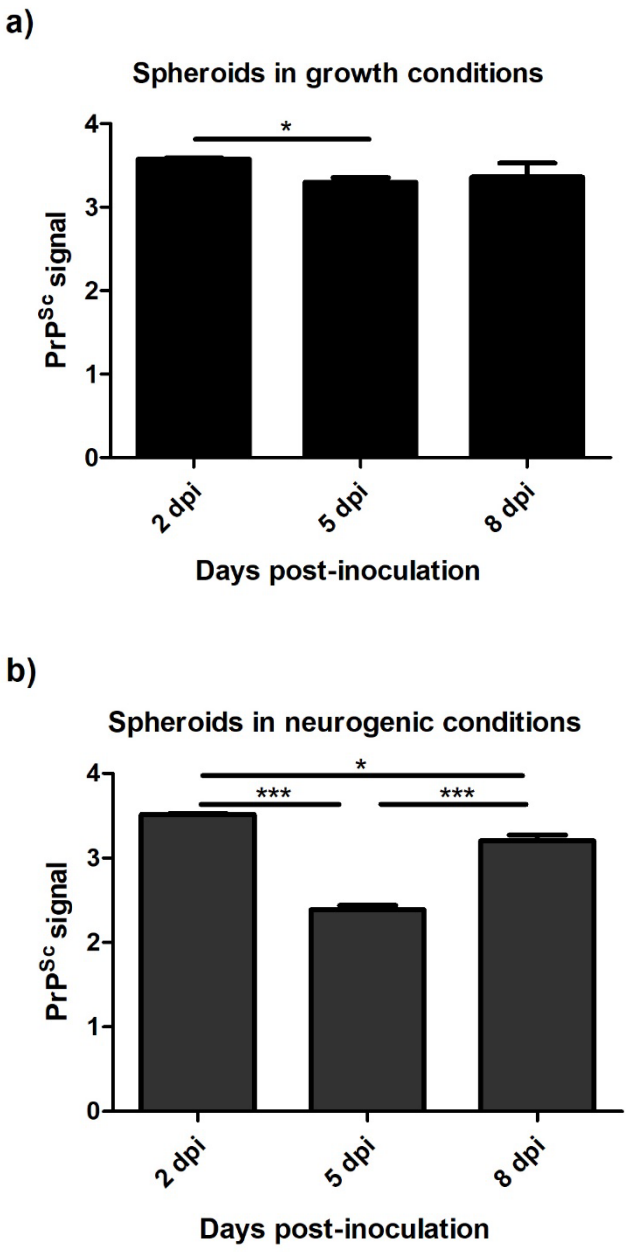

Figure 7. PrP^{Sc} levels detected by ELISA in spheroids in growth **(a)** and neurogenic **(b)** conditions 2, 5 and 8 days after prion infection. Data are shown as mean values ± SEM. * $p < 0.05$; *** $p < 0.001$

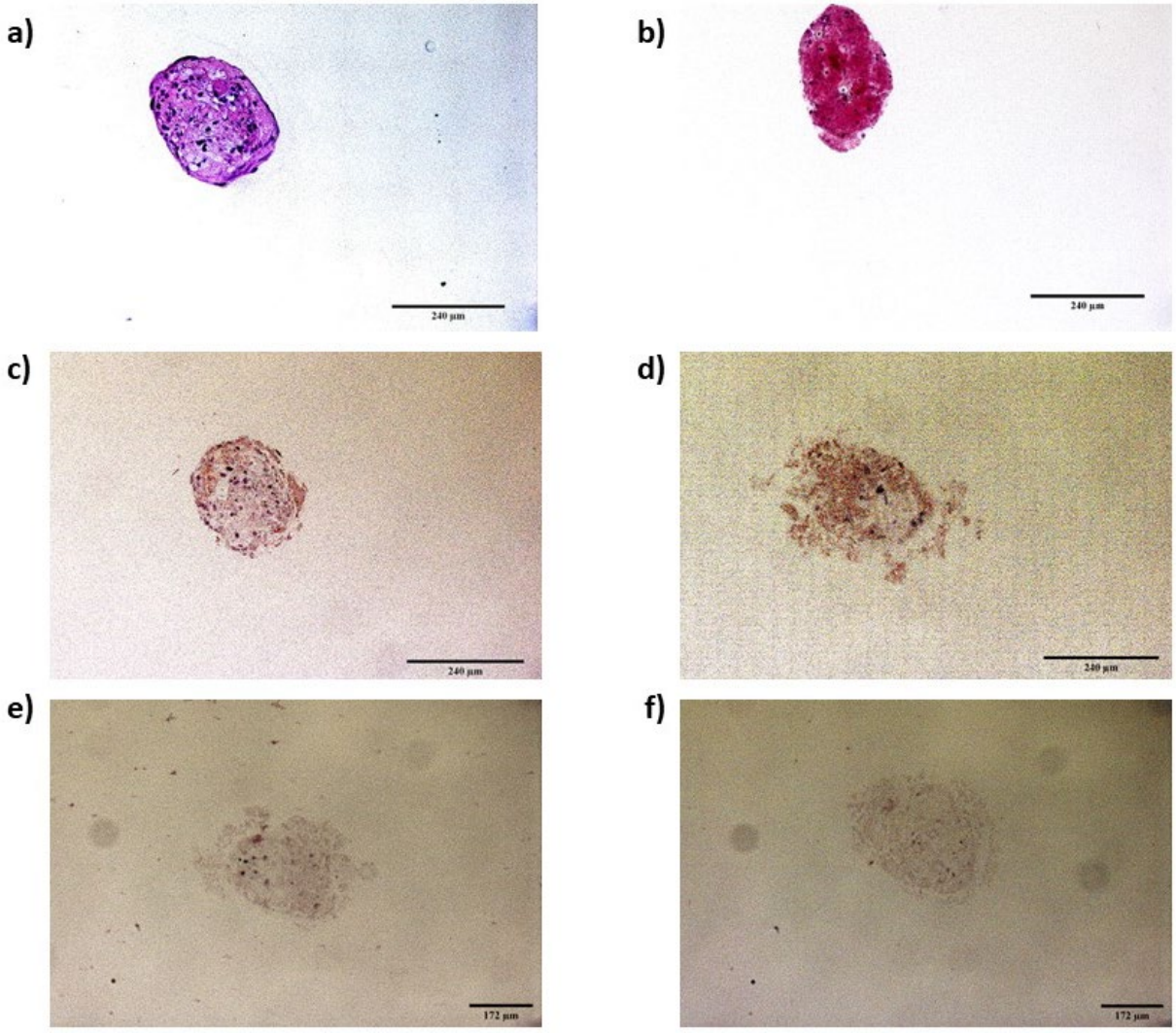

Figure 8. Hematoxylin-Eosin staining of spheroids in growth **(a)** and neurogenic **(b)** conditions. PrP^{Sc} immunostaining (brown deposits) of scrapie-infected spheroids in growth **(c)** and neurogenic differentiation **(d)** conditions, and their respective background controls with omission of the primary antibody **(e)**, **(f)**.

3.5. Viability after prion infection

3.5.1. oBM-MSC and neuron-like cell 2D cultures

The effect of prion infection in cell viability was assessed in three infection times. oBM-MSCs infected with scrapie-positive inoculum showed increased viability compared to the cells infected with negative inoculum and non-inoculated controls at 2 dpi, whereas, at 5 dpi a significant decrease in viability was observed in scrapie and negative-infected cells compared to the controls.

At 8 dpi, the levels of viability in cells infected with positive and negative inocula were recovered, being similar to the non-inoculated controls (Figure 9a).

In neuron-like cells, an initial increase in cell viability was also observed in scrapie-infected cells along with a significant decrease at 5 dpi. Conversely to oBM-MSCs, this decrease was maintained at 8 dpi (Figure 9b).

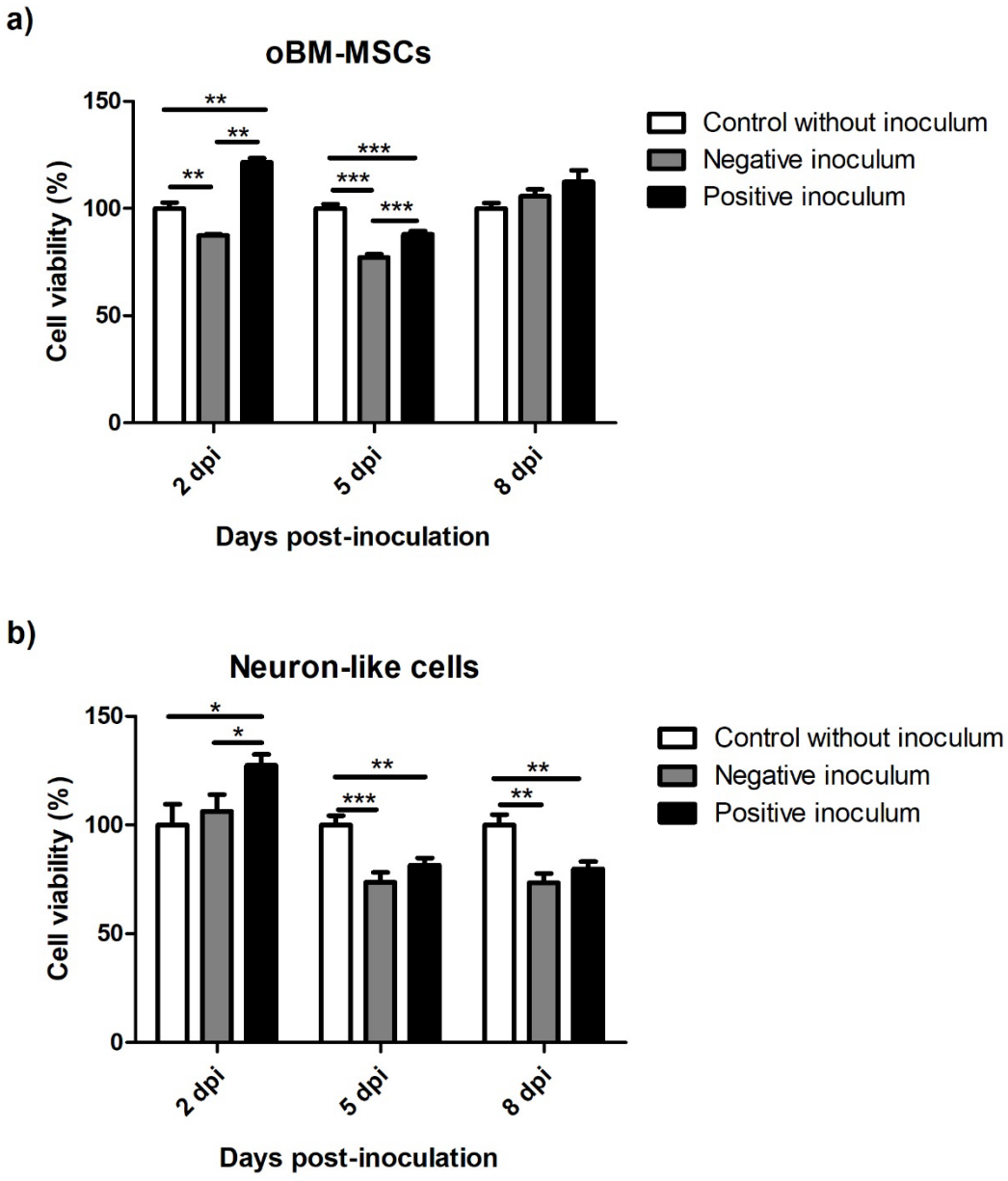

Figure 9. Cell viability of oBM-MSCs **(a)** and neuron-like cells **(b)** 2, 5 and 8 days after prion infection. The viability values are presented as percentages (%), considering the viability of the controls without inoculum as 100 % in all the infection times. Data are shown as mean values ± SEM. * $p < 0.05$; ** $p < 0.01$; *** $p < 0.001$

3.5.2. Spheroids in growth and neurogenic conditions

Cell viability was also assessed in spheroids in both growth and neurogenic differentiation conditions.

In growth conditions, spheroids infected with negative inoculum displayed increasing cell viability over time. The ones infected with positive inoculum, otherwise, showed an increased cell viability at 5 dpi but, afterwards, the viability decreased greatly at 8 dpi (Figure 10a).

In neurogenic conditions, spheroids infected with negative inoculum showed as well high levels of cell viability during the three infection times. Contrary to the observed in spheroids in growth conditions, spheroids infected with scrapie-positive inoculum displayed an increment in cell viability over time (Figure 10b).

a)

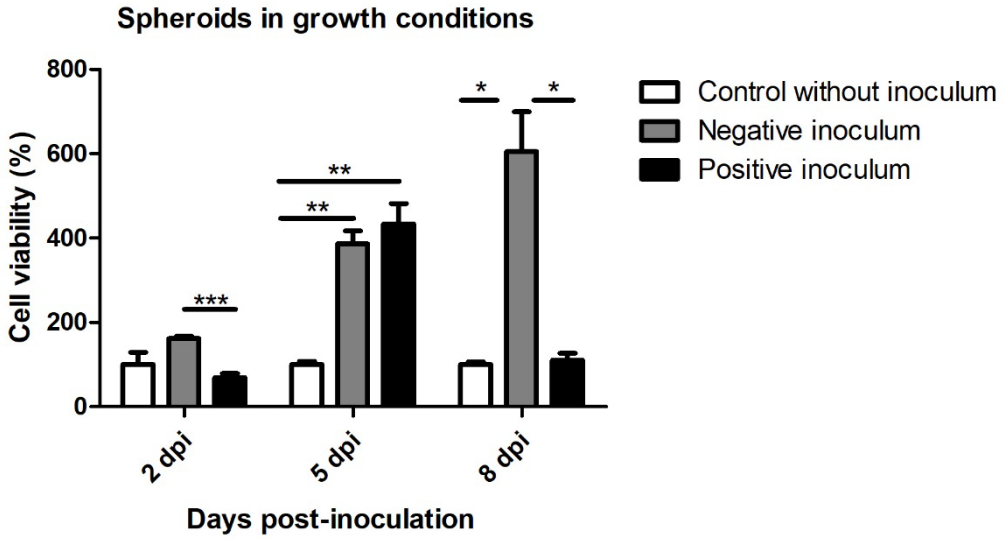

b)

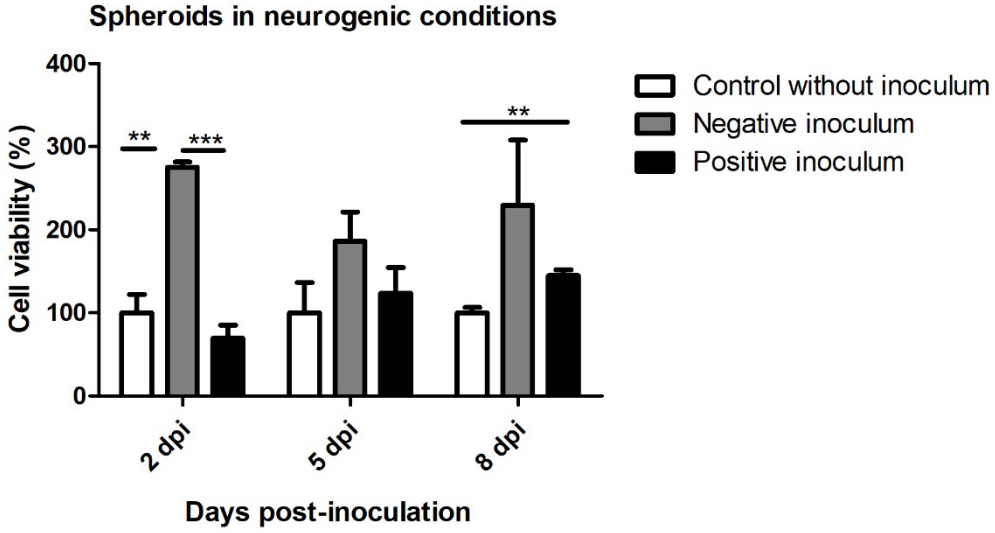

Figure 10. Cell viability of spheroids in growth **(a)** and neurogenic **(b)** conditions 2, 5 and 8 days post-inoculation. The viability values are presented as percentages (%), considering the viability of the controls without inoculum as 100 % in all the infection times. Data are shown as mean values ± SEM. * $p < 0.05$; ** $p < 0.01$; *** $p < 0.001$

4. Discussion

Three-dimensional in vitro culture systems have arisen as a novel approach for cell culture. These systems are able to better mirror the microenvironment and interactions of the cells in vivo, making them useful tools for creating in vitro disease models that reliably reproduce disease inherent characteristics. Our group previously evaluated the effect of scrapie prion infection in oBM-MSCs cultured in 2D in basal and neurogenic conditions [35]. In order to determine if the three-dimensional conditions induce changes in the way these cells react to prion infection, in the present study, we assessed the effect of scrapie prion infection in oBM-MSCs and oBM-MSC-derived neuron-like cells, cultured in two-dimensional monolayer conditions and as spheroids, analysing the ability to maintain or propagate PrP^{Sc} and a possible prion toxicity that could affect cell viability.

Mesenchymal stem cells were first characterised. The ability to plastic adhesion and the tri-lineage differentiation confirmed the nature of these cells [37,39].

Murine bone marrow-derived MSCs can be infected and propagate Fukuoka-1 human prion strain [45,46], and a persistent propagation of mouse-adapted variant CJD and Fukuoka-1 strain has been described in spleen-derived murine stromal cells [47]. In accordance with our previous study [35], we have observed a decline in PrP^{Sc} levels in 2D cultures of oBM-MSCs infected with scrapie throughout the culture time, whereas neuron-like cells displayed steady PrP^{Sc} levels over time. These results confirm that oBM-MSCs cultured in two-dimensional conditions are less permissive to scrapie infection compared to neuron-like cells that seem to be able to uptake and maintain scrapie infection over time.

Regarding 3D in vitro models for prion diseases, only human cerebral organoids have been described to uptake and propagate sCJD prions [33]. Within MSC-derived spheroids, a specific microenvironment more similar to in vivo conditions is formed, in which the diffusion inwards of nutrients and gases, and outwards of metabolic wastes is limited [48,49]. Moreover, a decreased cell size, cell cycle quiescence and reduced energy metabolism have been found in MSC-spheroids compared with MSCs in monolayer conditions [48,50,51]. The differences in the microenvironment of MSCs in 2D and 3D conditions could explain the distinct results observed between oBM-MSCs infected with scrapie on a culture plate and scrapie-infected

spheroids in growth conditions. Contrary to 2D cultures, spheroids in growth conditions were able to maintain stable levels of PrP^{Sc} over time. On the other hand, like neuron-like cells, spheroids in neurogenic conditions also took up and maintained PrP^{Sc} levels. These results indicate that the 3D microenvironment makes oBM-MSCs more permissive to prion infection when cultured in growth conditions and maintains the ability of neuron-like cells to absorb and retain scrapie prions.

Although primary neuronal cultures show toxicity after prion propagation in vitro that varies in a strain- and neuronal type-specific manner [52,53], murine MSCs are able to propagate prions in growth conditions without signs of toxicity [45–47]. In our previous study, oBM-MSCs and their derivative neuron-like cells infected with brain homogenates of healthy and scrapie-infected sheep displayed increasing levels of cell viability throughout the culture time in comparison to non-inoculated cells, suggesting that brain inocula may contain factors that stimulate oBM-MSC proliferation [35]. Similarly, in the present study, scrapie-infected oBM-MSCs showed higher cell viability levels than non-inoculated controls just after removing the inocula (2 dpi), however we did not observe this increase in cells inoculated with negative inoculum. It seems that MSC division is more stimulated with scrapie brains. In fact, it has been described that MSCs can migrate to brain lesions caused by prions, being this migration mediated by different chemoattractive factors [54–56]. Similarly, neuron-like cells infected with scrapie displayed an increase in cell viability only after being in contact with the inocula, confirming our previous data, however, in this study toxicity was observed afterwards. Therefore, the effect of brain inocula in oBM-MSC proliferation seems to vary between cultures. This variation could be explained by the cellular heterogeneity found in MSCs in which donor, tissue source, culture environment, isolation methods, and passage can affect the phenotype [57,58], making distinct cultures react slightly different to CNS homogenates. However, we have to keep in mind that inocula of both negative and positive brains are also different. Amounts of initial PrP^{Sc} could be different, which would affect MSC reaction to infection. Nevertheless, the early response to scrapie infection was the same in both studies, an increment of cell viability, which means a higher proliferation potential either in growth or neurogenic conditions when cultured on plates after being in contact with scrapie tissues. The decrease of cell viability observed afterwards could be a consequence of prion toxicity.

Ovine MSC spheroids inoculated with brain homogenates of healthy and scrapie-infected sheep displayed different viability patterns than the monolayer-cultured cells. Negative inoculum increases the viability of spheroids in both growth and neurogenic conditions, however this increase was not observed in spheroids infected with scrapie, which remained

at viability levels similar to controls. Compared to monolayer-cultured MSCs, human MSC spheroids show higher cell survival and enhanced cell yield and stemness [59–61]. This enhanced cell viability of spheroids seems to be mediated by the induction of autophagy and the suppression of reactive oxygen species (ROS) [61]. Remarkably, an impairment of the autophagy process has been described in scrapie disease [62,63]. The decreased viability observed in scrapie-infected spheroids in growth conditions with respect to those inoculated with negative brain could be due to a dysfunction of the autophagy mechanism caused by prion infection that could counteract the positive effect exerted by neurotrophic factors in the brain. These results suggest that 3D conditions improve in most cases the viability of inoculated oBM-MSCs, as infected spheroids at least maintain the viability observed in controls, but prions exert their toxicity by limiting the growth potential of spheroids stimulated with neurotrophic factors.

5. Conclusions

In conclusion, oBM-MSC-derived spheroids in growth and neurogenic conditions are able to uptake and maintain scrapie prions and mimic prion toxicity, making this three-dimensional approach a potential in vitro model to study prion disease mechanisms and therapeutics in a more in vivo-like environment.

6. Supplementary Materials

Not applicable.

7. Author Contributions

Conceptualization, I.M-B.; methodology, I.M-B. and A.H.; investigation, A.H., P.C., B.M. and F.J.V.; writing—original draft preparation, A.H. and P.C.; writing—review and editing, I.M-B., R.B., P.Z., J.J.B., B.M. and F.J.V.; supervision, I.M-B; project administration, I.M-B. and R.B.; funding acquisition, I.M-B., R.B., P.Z. and J.J.B. All authors have read and agreed to the published version of the manuscript.

8. Funding

This research was funded by the Agencia Estatal de Investigación and Fondos FEDER grant RTI2018-098711-B-100, the Gobierno de Aragón consolidated research group A19-20R, and the Gobierno de Aragón and the European Social Fund co-financed predoctoral grant Order IIU/2023/2017.

9. Institutional Review Board Statement

The animal procedures were carried out under project licence PI44/18, approved by the Ethical Committee for Animal Experiments from the University of Zaragoza.

10. Acknowledgments

We thank Sandra Felices Mayordomo and Daniel Romanos Lizano for the technical support received during the preparation of microtome spheroid sections.

11. Conflicts of Interest

The authors declare no conflict of interest.

12. References

1. Chaicharoenaudomrung, N., Kunhorm, P. & Noisa, P. Three-dimensional cell culture systems as an in vitro platform for cancer and stem cell modeling. *World J. Stem Cells* **11**, 1065–1083 (2019).

2. Lv, D., Hu, Z., Lu, L., Lu, H. & Xu, X. Three-dimensional cell culture: A powerful tool in tumor research and drug discovery. *Oncol. Lett.* **14**, 6999–7010 (2017).

3. Weigelt, B., Ghajar, C. M. & Bissell, M. J. The need for complex 3D culture models to unravel novel pathways and identify accurate biomarkers in breast cancer. *Adv. Drug Deliv. Rev.* **69**–**70**, 42–51 (2014).

4. Ravi, M., Paramesh, V., Kaviya, S. R., Anuradha, E. & Paul Solomon, F. D. 3D cell culture systems: advantages and applications. *J. Cell. Physiol.* **230**, 16–26 (2015).

5. Suarez-Martinez, E., Suazo-Sanchez, I., Celis-Romero, M. & Carnero, A. 3D and organoid culture in research: physiology, hereditary genetic diseases and cancer. *Cell Biosci.* **12**, (2022).

6. Imamura, Y. *et al.* Comparison of 2D- and 3D-culture models as drug-testing platforms in breast cancer. *Oncol. Rep.* **33**, 1837–1843 (2015).

7. Tekin, H. *et al.* Effects of 3D culturing conditions on the transcriptomic profile of stem-cell-derived neurons. *Nat. Biomed. Eng.* **2**, 540–554 (2018).

8. Zhang, Y. S. *et al.* Bioprinting 3D microfibrous scaffolds for engineering endothelialized myocardium and heart-on-a-chip. *Biomaterials* **110**, 45–59 (2016).

9. Cesarz, Z. & Tamama, K. Spheroid Culture of Mesenchymal Stem Cells. *Stem Cells Int.* **2016**, (2016).

10. Bates, R. C., Edwards, N. S. & Yates, J. D. Spheroids and cell survival. *Crit. Rev. Oncol. Hematol.* **36**, 61–74 (2000).

11. Cheng, N.-C., Chen, S.-Y., Li, J.-R. & Young, T.-H. Short-term spheroid formation enhances the regenerative capacity of adipose-derived stem cells by promoting stemness, angiogenesis, and chemotaxis. *Stem Cells Transl. Med.* **2**, 584–594 (2013).

12. Frith, J. E., Thomson, B. & Genever, P. G. Dynamic three-dimensional culture methods enhance mesenchymal stem cell properties and increase therapeutic potential. *Tissue Eng. Part C. Methods* **16**, 735–749 (2010).

13. Wang, W. *et al.* 3D spheroid culture system on micropatterned substrates for improved differentiation efficiency of multipotent mesenchymal stem cells. *Biomaterials* **30**, 2705–2715 (2009).

14. Choi, S. H. *et al.* A three-dimensional human neural cell culture model of Alzheimer's disease. *Nature* **515**, 274–278 (2014).

15. Papadimitriou, C. *et al.* 3D Culture Method for Alzheimer's Disease Modeling Reveals Interleukin-4 Rescues Aβ42-Induced Loss of Human Neural Stem Cell Plasticity. *Dev. Cell* **46**, 85-101.e8 (2018).

16. Kim, Y. H. *et al.* A 3D human neural cell culture system for modeling Alzheimer's disease. *Nat. Protoc.* **10**, 985–1006 (2015).

17. Kwak, S. S. *et al.* Amyloid-β42/40 ratio drives tau pathology in 3D human neural cell culture models of Alzheimer's disease. *Nat. Commun.* **11**, (2020).

18. Ranjan, V. D. *et al.* A microfiber scaffold-based 3D in vitro human neuronal culture model of Alzheimer's disease. *Biomater. Sci.* **8**, 4861–4874 (2020).

19. Park, J. *et al.* A 3D human triculture system modeling neurodegeneration and neuroinflammation in Alzheimer's disease. *Nat. Neurosci.* **21**, 941–951 (2018).

20. Pomeshchik, Y. *et al.* Human iPSC-Derived Hippocampal Spheroids: An Innovative Tool for Stratifying Alzheimer Disease Patient-Specific Cellular Phenotypes and Developing Therapies. *Stem cell reports* **15**, 256–273 (2020).

21. Chen, X. *et al.* Modeling Sporadic Alzheimer's Disease in Human Brain Organoids under Serum Exposure. *Adv. Sci. (Weinheim, Baden-Wurttemberg, Ger.* **8**, (2021).

22. Park, J. C. *et al.* A logical network-based drug-screening platform for Alzheimer's disease representing pathological features of human brain organoids. *Nat. Commun.* **12**, (2021).

23. Zhao, J. *et al.* APOE4 exacerbates synapse loss and neurodegeneration in Alzheimer's disease patient iPSC-derived cerebral organoids. *Nat. Commun.* **11**, (2020).

24. Fiore, N. J., Tamer-Mahoney, J. D., Beheshti, A., Nieland, T. J. F. & Kaplan, D. L. 3D biocomposite culture enhances differentiation of dopamine-like neurons from SH-SY5Y cells: A model for studying Parkinson's disease phenotypes. *Biomaterials* **290**, (2022).

25. Gilmozzi, V. *et al.* Generation of hiPSC-Derived Functional Dopaminergic Neurons in Alginate-Based 3D Culture. *Front. cell Dev. Biol.* **9**, (2021).

26. Li, Z. F. *et al.* A Matrigel-based 3D construct of SH-SY5Y cells models the α-synuclein pathologies of Parkinson's disease. *Dis. Model. Mech.* **15**, (2022).

27. Taylor-Whiteley, T. R., Le Maitre, C. L., Duce, J. A., Dalton, C. F. & Smith, D. P. Recapitulating Parkinson's disease pathology in a three-dimensional human neural cell culture model. *Dis. Model. Mech.* **12**, (2019).

28. Kim, H. *et al.* Modeling G2019S-LRRK2 Sporadic Parkinson's Disease in 3D Midbrain Organoids. *Stem cell reports* **12**, 518–531 (2019).

29. Ma, J. & Wang, F. Prion disease and the 'protein-only hypothesis'. *Essays Biochem.* **56**, 181–91 (2014).

30. Pattison, I. H. & Jones, K. M. The astrocytic reaction in experimental scrapie in the rat. *Res. Vet. Sci.* **8**, 160–5 (1967).

31. Prusiner, S. B. Novel proteinaceous infectious particles cause scrapie. *Science* **216**, 136–44 (1982).

32. Hope, J. The biology and molecular biology of scrapie-like diseases. *Arch. Virol. Suppl.* **7**, 201–214 (1993).

33. Groveman, B. R. *et al.* Sporadic Creutzfeldt-Jakob disease prion infection of human cerebral organoids. *Acta Neuropathol. Commun.* **7**, 90 (2019).

34. Groveman, B. R. *et al.* Human cerebral organoids as a therapeutic drug screening model for Creutzfeldt-Jakob disease. *Sci. Rep.* **11**, (2021).

35. García-mendívil, L. *et al.* Effect of Scrapie Prion Infection in Ovine Bone Marrow-Derived Mesenchymal Stem Cells and Ovine Mesenchymal Stem Cell-Derived Neurons. *Anim. an open access J. from MDPI* **11**, (2021).

36. Mediano, D. R. *et al.* Characterization of mesenchymal stem cells in sheep naturally infected with scrapie. *J. Gen. Virol.* **96**, 3715–3726 (2015).

37. Lyahyai, J. *et al.* Isolation and characterization of ovine mesenchymal stem cells derived from peripheral blood. *BMC Vet. Res.* **8**, (2012).

38. Ranera, B. *et al.* Comparative study of equine bone marrow and adipose tissue-derived mesenchymal stromal cells. *Equine Vet. J.* **44**, 33–42 (2012).

39. Dominici, M. *et al.* Minimal criteria for defining multipotent mesenchymal stromal cells. The International Society for Cellular Therapy position statement. *Cytotherapy* **8**, 315–317 (2006).

40. Jäger, M., Bachmann, R., Scharfstädt, A. & Krauspe, R. Ovine Cord Blood Accommodates Multipotent Mesenchymal Progenitor Cells. *In Vivo (Brooklyn).* **20**, 205–214 (2006).

41. Palay, S. L. & Palade, G. E. The fine structure of neurons. *J. Biophys. Biochem. Cytol.* **1**, 69–88 (1955).

42. Livak, K. J. & Schmittgen, T. D. Analysis of relative gene expression data using real-time quantitative PCR and the 2-ΔΔCT method. *Methods* **25**, 402–408 (2001).

43. Bolea, R. *et al.* Comparison of immunohistochemistry and two rapid tests for detection of abnormal prion protein in different brain regions of sheep with typical scrapie. *J. Vet. Diagn. Invest.* **17**, 467–469 (2005).

44. Bresciani, G. *et al.* Evaluation of Spheroid 3D Culture Methods to Study a Pancreatic Neuroendocrine Neoplasm Cell Line. *Front. Endocrinol. (Lausanne).* **10**, (2019).

45. Akimov, S., Vasilyeva, I., Yakovleva, O., McKenzie, C. & Cervenakova, L. Murine bone marrow stromal cell culture with features of mesenchymal stem cells susceptible to mouse-adapted human TSE agent, Fukuoka-1. *Folia Neuropathol.* **47**, 205–14 (2009).

46. Cervenakova, L. *et al.* Fukuoka-1 strain of transmissible spongiform encephalopathy agent infects murine bone marrow-derived cells with features of mesenchymal stem cells. *Transfusion* **51**, 1755–1768 (2011).

47. Akimov, S., Yakovleva, O., Vasilyeva, I., McKenzie, C. & Cervenakova, L. Persistent Propagation of Variant Creutzfeldt-Jakob Disease Agent in Murine Spleen Stromal Cell Culture with Features of Mesenchymal Stem Cells. *J. Virol.* **82**, 10959–10962 (2008).

48. Jauković, A. *et al.* Specificity of 3D MSC Spheroids Microenvironment: Impact on MSC

Behavior and Properties. *Stem cell Rev. reports* **16**, 853–875 (2020).

49. Sart, S., Tsai, A. C., Li, Y. & Ma, T. Three-Dimensional Aggregates of Mesenchymal Stem Cells: Cellular Mechanisms, Biological Properties, and Applications. *https://home.liebertpub.com/teb* **20**, 365–380 (2013).

50. Liu, Y., Muñoz, N., Tsai, A. C., Logan, T. M. & Ma, T. Metabolic Reconfiguration Supports Reacquisition of Primitive Phenotype in Human Mesenchymal Stem Cell Aggregates. *Stem Cells* **35**, 398–410 (2017).

51. Zhang, Q. *et al.* Three-dimensional spheroid culture of human gingiva-derived mesenchymal stem cells enhances mitigation of chemotherapy-induced oral mucositis. *Stem Cells Dev.* **21**, 937–947 (2012).

52. Cronier, S., Laude, H. & Peyrin, J. M. Prions can infect primary cultured neurons and astrocytes and promote neuronal cell death. *Proc. Natl. Acad. Sci. U. S. A.* **101**, 12271–12276 (2004).

53. Hannaoui, S. *et al.* Prion propagation and toxicity occur in vitro with two-phase kinetics specific to strain and neuronal type. *J. Virol.* **87**, 2535–2548 (2013).

54. Shan, Z. *et al.* Therapeutic effect of autologous compact bone-derived mesenchymal stem cell transplantation on prion disease. *J. Gen. Virol.* **98**, 2615–2627 (2017).

55. Song, C.-H., Honmou, O., Furuoka, H. & Horiuchi, M. Identification of Chemoattractive Factors Involved in the Migration of Bone Marrow-Derived Mesenchymal Stem Cells to Brain Lesions Caused by Prions. *J. Virol.* **85**, 11069–11078 (2011).

56. Song, C.-H. *et al.* Effect of Transplantation of Bone Marrow-Derived Mesenchymal Stem Cells on Mice Infected with Prions. *J. Virol.* **83**, 5918–5927 (2009).

57. Wang, Z. *et al.* Single-cell transcriptome atlas of human mesenchymal stem cells exploring cellular heterogeneity. *Clin. Transl. Med.* **11**, (2021).

58. Yin, J. Q., Zhu, J. & Ankrum, J. A. Manufacturing of primed mesenchymal stromal cells for therapy. *Nat. Biomed. Eng.* **3**, 90–104 (2019).

59. Jiang, B. *et al.* Spheroidal formation preserves human stem cells for prolonged time under ambient conditions for facile storage and transportation. *Biomaterials* **133**, 275–286 (2017).

60. Li, Y. *et al.* Three-dimensional spheroid culture of human umbilical cord mesenchymal

stem cells promotes cell yield and stemness maintenance. *Cell Tissue Res.* **360**, 297–307 (2015).

61. Regmi, S. *et al.* Enhanced viability and function of mesenchymal stromal cell spheroids is mediated via autophagy induction. *Autophagy* **17**, 2991–3010 (2021).

62. López-Pérez, Ó. *et al.* Dysregulation of autophagy in the central nervous system of sheep naturally infected with classical scrapie. *Sci. Rep.* **9**, 1911 (2019).

63. López-Pérez, Ó. *et al.* Impairment of autophagy in scrapie-infected transgenic mice at the clinical stage. *Lab. Invest.* **100**, 52–63 (2020).

MANUSCRITO VI

RNA-sequencing transcriptomic analysis of scrapie-infected ovine mesenchymal stem cells.

Hernaiz, Adelaida; Marín, Belén; Vázquez, Francisco José; Badiola, Juan José; Zaragoza, Pilar; Bolea, Rosa; Martín-Burriel, Inmaculada.

En revisión

RNA-sequencing transcriptomic analysis of scrapie-infected ovine mesenchymal stem cells

Adelaida Hernaiz [1], Belén Marín [2], Francisco J. Vázquez [1,3], Juan J. Badiola [2], Pilar Zaragoza [1,4], Rosa Bolea [2], Inmaculada Martín-Burriel [1,2,4,*]

[1] Laboratorio de Genética Bioquímica (LAGENBIO), Facultad de Veterinaria, Universidad de Zaragoza, IA2, IIS-Aragón, Zaragoza, Spain

[2] Centro de Encefalopatías y Enfermedades Transmisibles Emergentes (CEETE), Facultad de Veterinaria, Universidad de Zaragoza, IA2, IIS-Aragón, Zaragoza, Spain

[3] Departamento de Patología Animal, Facultad de Veterinaria, Universidad de Zaragoza, Zaragoza, Spain

[4] Centro de Investigación Biomédica en Red de Enfermedades Neurodegenerativas (CIBERNED), Instituto de Salud Carlos III, Madrid, Spain

* Correspondence: minma@unizar.es; Tel.: +34 976761662

Abstract

In neurodegenerative diseases, including prion diseases, cellular models arise as useful tools to study the pathogenic mechanisms occurring in these diseases and to assess the efficacy of potential therapeutic compounds. In the present study, a RNA-sequencing analysis of bone marrow-derived ovine mesenchymal stem cells (oBM-MSCs) infected with scrapie was performed to try to unravel genes and pathways potentially involved with prion disease mechanisms and to assess the potential of these cells to act as in vitro models of prion toxicity. oBM-MSCs were cultured in three different conditions: inoculated with brain homogenate of scrapie-infected sheep, with brain homogenate of healthy sheep and in standard growth conditions without inoculum. The cell viability and presence of prions was determined. In the transcriptomic analysis the three conditions were analysed in two infection times: 2 and 4 days' post-inoculation (dpi). Differentially expressed genes in scrapie-infected oBM-MSCs were found in the two infection times finding the higher number at 2 dpi. These genes were also enriched in multiple pathways and biological functions related with prion replication and toxicity. Moreover, a set of 11 genes was selected for a validation study, having 7 of these genes significant expression changes in scrapie-infected cells and functions related with prion propagation and its associated toxicity. These results indicate that ovine mesenchymal stem cells infected with scrapie could be useful in vitro models to study prion toxicity mechanisms and to test anti-prion compounds.

Keywords: Mesenchymal stem cells; in vitro model; RNA-sequencing; scrapie; prion; toxicity.

1. Introduction

Neurodegenerative diseases, including Alzheimer's, Parkinson's and Huntington's diseases, Amyotrophic lateral sclerosis and prion diseases, are a group of disorders characterized by a chronic progressive degeneration of the structure and function of the central nervous system (CNS). The aggregation and accumulation of misfolded proteins in the CNS leading to cellular dysfunction, loss of synaptic connections, and brain damage is a hallmark event in these pathologies [1]. Unfortunately, the exact pathogenic mechanisms occurring in these diseases are not fully understood, and there are no current effective treatments to stop the disease progression [2]. In this regard, cellular in vitro models appear as useful tools to investigate underlying molecular mechanisms in these diseases and specific roles of certain molecules and compounds, and to screen potential pharmacological targets [2].

In prion diseases or transmissible spongiform encephalopathies (TSEs), there are various murine cell lines that can replicate mouse-adapted prion strains [3–6]. These strains are not naturally occurring, and they may not accurately express the characteristics of the original disease-causing strains [7]. Therefore, it is critical to use cell models from natural susceptible species that replicate natural strains in order to reliably study disease characteristics and develop potential therapies [7]. Several cellular models from naturally infected animals and humans have been developed. MDBK bovine-derived kidney cells [8] and MDB cells derived from mule deer brain [9] are able to replicate BSE (Bovine spongiform encephalopathy) and CWD (Chronic wasting disease) prions, respectively. Two dimensional ovine mesenchymal stem cell (MSC) cultures also react to ovine scrapie prion infection showing early prion toxicity and decreased proliferation capacity, and ovine MSC-derived neuron-like cells can maintain and replicate the pathological prion protein (PrP^{Sc}) [10]. In addition, human-induced pluripotent stem cell-derived astrocytes [11] and human cerebral organoids [12] have been described to successfully propagate CJD (Creutzfeldt Jakob disease) prions.

MSCs express the cellular prion protein (PrP^{C}) [13,14] and murine MSCs can be infected with prions accumulating PrP^{Sc} [15–18]. A recent study of our group showed that ovine bone marrow-derived mesenchymal stem cells (oBM-MSCs) infected with ovine scrapie are able to uptake PrP^{Sc}, causing cell toxicity and a decline in the proliferation capacity [10]. As the exact molecular mechanisms of prion cell toxicity are still unclear, oBM-MSCs could be used as an in vitro model to study prion toxicity.

By comparing differences in gene expression patterns, transcriptomic analyses are helpful tools for studying cell biology and for understanding the physiological and pathological processes involved within a cell [19]. RNA-sequencing (RNA-seq) is a transcriptome profiling

technology that uses next-generation sequencing platforms, allowing the investigation of differential expression patterns between various conditions such as disease and healthy status [19–21]. This technology has been used to explore the transcriptome of several neurodegenerative diseases, including Alzheimer's and Parkinson's diseases, at tissue and cell level, in order to find genes and pathways altered or involved in these pathologies [22–25]. In prion diseases, such as CJD and scrapie, microarray and RNA-seq transcriptomic approaches have also been employed to uncover the underlying molecular mechanisms associated with TSEs [26–29].

In the present study, with the aim of assessing the potential of oBM-MSCs as in vitro models of prion toxicity and delve into the pathogenic mechanisms of prion infection, RNA-seq of ovine bone marrow-derived mesenchymal stem cells infected with scrapie was performed to identify differentially expressed genes and molecular routes potentially involved in prion toxicity and replication. After the transcriptomic analysis, a set of differentially expressed genes was selected for a validation study using quantitative real-time PCR to verify the results obtained in the RNA-seq analysis.

2. Materials and methods

2.1. Ovine mesenchymal stem cell culture

A bone marrow sample was obtained from a female rasa aragonesa sheep of one year of age and carrying the ARQ/ARQ genotype for the *PRNP* gene. After the sedation with xylazine and the local anaesthesia with lidocaine, bone marrow aspirate was harvested from the humeral head using a 13 G Jamshidi needle and a 10 mL syringe previously loaded with 0.5 mL of sodium heparin. All procedures were carried out under project licence PI44/18, approved by the Ethical Committee for Animal Experiments from the University of Zaragoza. The care and use of animals were performed in accordance with the Spanish Policy for Animal Protection, RD53/2013, which meets European Union Directive 2010/63 on the protection of animals used for experimental and other scientific purposes.

MSC isolation from the bone marrow aspirate (2-3 mL) was performed following the previously described protocol [14,30,31]. This protocol is based on the separation of the mononuclear fraction after density gradient centrifugation in Lymphoprep (Atom) and further isolation thanks to the ability of MSCs to adhere to plastic. After isolation, cells were expanded up to passage 2 in basal medium, consisting of low glucose Dulbecco's modified Eagle's medium

(DMEM, Sigma-Aldrich, St. Louis, MO, USA) supplemented with 10 % fetal bovine serum (FBS), 1 % L-glutamine (Sigma-Aldrich) and 1 % streptomycin/penicillin (Sigma-Aldrich).

2.2. Infection of ovine mesenchymal stem cells, cell viability assay and PrP^{Sc} detection

2.2.1. Infection with brain inoculum

To infect oBM-MSCs, two different inocula were prepared using CNS samples: one from a healthy sheep (negative control) and one from a classical scrapie-infected sheep, both carrying the ARQ/ARQ genotype. The inocula were preserved at the tissue bank of the Centre of Encephalopathies and Emerging Transmissible Diseases (CEETE; University of Zaragoza). The presence/absence of PrP^{Sc} in the CNS tissues was confirmed following the protocols used in previous studies [32], which consisted of two rapid diagnostic tests (Prionics-CheckWestern blotting; ThermoFisher Scientific and Idexx HerdChek; IDEXX, Westbrook, ME, USA) and confirmation by immunohistochemical examination of the CNS tissue. CNS samples were homogenized and diluted 1:10 (g/mL) in physiological saline solution (Braun). Afterwards, samples were treated at 70 °C for 10 min before adding streptomycin sulphate (100 µg/mL) and benzylpenicillin (100 µg/mL). To evaluate the safety of the inocula once generated, samples were incubated in blood agar plates, and the absence of any bacterial growth was confirmed.

For inoculation, basal medium was substituted by inocula diluted 1:10 in DMEM medium (10 % FBS, 1 % L-glutamine and 1 % streptomycin/penicillin). Cells were maintained in this medium for 48 h for the cell viability assay, the detection of PrP^{Sc} and the RNA-sequencing assay. Afterwards, the medium was changed twice a week.

2.2.2. Cell viability assay

The toxicity and cell viability were studied using the MTT assay in three conditions (inoculated with scrapie-positive brain homogenates, negative brain inoculum and non-inoculated controls) and at three different stages (2, 5 and 8 dpi), being 2 dpi the time of inoculum removal, considering the moment of the infection with the inocula as day 0. Cells were seeded in 96-well plates at 5,000 cells/cm^2 and 8 technical replicates were analysed for each condition per time (dpi). Briefly, the MTT assay was performed by adding 25 µL of MTT solution (2

mg/mL) per well. Then, the plates were incubated at 37 °C for 4 h. Afterwards, the content of each well was removed and was substituted with 150 µL of HCl solution (HCl 40 mM in isopropanol) per well. Plates were then incubated for 1 h at room temperature protected from light. The absorbance was measured at 570 nm in an Infinite F200 microplate reader (Tecan Ibérica Instrumentación, Barcelona, Spain). Differences in cell viability were evaluated with Student's t-test. Statistical significance was defined as $P < 0.05$. The viability values were represented as percentages (%), considering the viability of the non-inoculated controls as 100 % in all the infection times.

2.2.3. PrP^{Sc} detection

To test the ability of oBM-MSCs inoculated with scrapie-infected brain homogenate to replicate prions, the amount of PrP^{Sc} was quantified at three different stages (2 dpi, corresponding to the inoculum removal, 5 and 8 dpi) with the ELISA kit EEB-Scrapie HerdCheck kit (IDEXX), following the manufacturer's recommendations. A previous study of our group showed that this kit was suitable for a sensitive detection of PrP^{Sc} in oBM-MSC cultures [10]. Cells were seeded at 5,000 cells/cm^2 in 6-well plates and the retrieval of the cells was performed by means of trypsinization and subsequent centrifugation to obtain 3 technical replicates per condition and time (dpi).

2.3. RNA extraction of ovine mesenchymal stem cells

For the RNA-sequencing assay, cells were seeded at 9,000 cells/cm^2 in T25 flasks. Two infection times (2 dpi, corresponding to the inoculum removal, and 4 dpi) and three conditions were studied (cells inoculated with scrapie-infected brain homogenate, cells inoculated with negative brain inoculum and non-inoculated controls) with 3 technical replicates per condition and time (dpi).

Cells were retrieved by trypsinization and subsequent centrifugation. Afterwards, RNA was extracted using the Direct-zol RNA MiniPrep kit (Zymo Research) following the manufacturer´s instructions.

Before library preparation, the integrity of the RNA samples was checked with Agilent 2100 Bioanalyzer, RNA purity was evaluated with agarose gel electrophoresis and NanoDrop spectrophotometer (Thermo Fisher Scientific, Waltham, MA, USA), and the quantity of RNA was determined using NanoDrop spectrophotometer and Agilent 2100 Bioanalyzer. Approximately 2 µg of total RNA per sample were used for RNA sequencing.

2.4. RNA-sequencing and bioinformatic analysis

2.4.1. Library preparation, quality control, mapping, and quantification

The cDNA library construction was performed at Novogene in Cambridge (UK). Quantified libraries were pooled and sequenced on an Illumina platform, according to effective library concentration and data amount, and paired-end reads were generated. The quality control of raw reads was made using in-house perl scripts, and clean reads were obtained by removing reads containing adapters, reads containing ploy-N and low quality reads. Q20, Q30 and GC content of the clean data were then calculated. After the quality control, the paired-end clean reads were aligned to the ovine reference genome oar_rambouillet-v1.0 (Ensembl) using the software Hisat2 v2.0.5. The mapped reads of each sample were assembled by StringTie v1.3.3b [33] in a reference-based approach. For transcript quantification, the software FeatureCounts v1.5.0-p3 was used and FPKM (expected number of Fragments Per Kilobase of transcript sequence per Millions base pairs sequenced) of each gene was then calculated based on the length of the gene and read count mapped to this gene.

2.4.2. Differential expression analysis and GO, KEGG, and GSEA enrichment analyses

Differential expression analysis was performed using the DESeq2 R package v1.20.0. The resulting P-values were adjusted using the Benjamini and Hochberg's approach for controlling the false discovery rate (FDR). Genes with an adjusted P-value < 0.05 found by DESeq2 were assigned as differentially expressed.

Gene Ontology (GO) and Kyoto Encyclopedia of Genes and Genomes (KEGG) enrichment analyses of differentially expressed genes (DEGs) were implemented by the clusterProfiler R package v3.8.1. GO terms and KEGG pathways with adjusted P-value < 0.05 were considered significantly enriched. For the Gene Set Enrichment Analysis (GSEA), the GSEA analysis tool v3.0 was used.

2.5. Quantitative real-time PCR

To validate the results observed in the RNA-sequencing analysis, a set of 11 genes was selected among the significant DEGs which showed higher changes in expression (fold change) between scrapie-infected MSCs and MSCs infected with negative inoculum at 2 dpi.

Retrotranscription was performed from 200 ng of total RNA using qScript™ cDNA Supermix (Quanta Biosciences™), according to the manufacturer's instructions. Resulting cDNA was diluted 1:5 in water and gene expression was quantified by quantitative real-time PCR (RT-qPCR) using the Fast SYBR™ Green Master Mix (Applied Biosystems, Thermo Fisher Scientific) in a StepOne Plus Real-Time PCR instrument (Applied Biosystems). Each sample was amplified by triplicate. The comparative quantification of the results was standardized by the $2^{-\Delta\Delta Ct}$ method [34], using the geometric mean of *SDHA*, *G6PDH* and *GAPDH* housekeeping genes [35] as a normalizer. Student's t-test was applied to identify differences between groups, which were considered significant at $P < 0.05$. Table 1 lists the primers used for the RT-qPCR assay.

Table 1. Sequences of primers used in the RT-qPCR assay. Fw = Forward primer and Rv = Reverse primer.

Gene	Primer sequences
RPS15A	Fw: TGCTCCAAAGTCATCGTCAG Rv: CAAATCTGGGGCTGATCACT
MMP1	Fw: TGCTCATGCTTTTCAACCAG Rv: GAGCAAGCTGAACATCACCA
PGAP4	Fw: TGTAAAATGGGGACCGTGAT Rv: CAGCTGCTCCATAGGTGTCA
SERPINB2	Fw: GTTTGTGGCAGACCATCCTT Rv: GCCACACCATGTCTGTGTTC
PDK4	Fw: AGCTGACCCAGTCACCAATC Rv: ACTGCCACCACATCACAGTT
MMP12	Fw: TATGGCCTCGAGATGGAAAC Rv: ATTTTCAACATCCGGCACTC
PRR11	Fw: GAAAGCACTTCAGGCTGGAC Rv: CTTTGGACTTCGGTTTCAGG
SAA3	Fw: AGCCCTGTCATTCTTGGTTG Rv: TCCCTGGTCATACCCTTGAG
PTGS1	Fw: AAAGAAGCTGGTTTGCCTCA Rv: TCCACACTGATGCTCTCGAC
CYP1A1	Fw: GGGCACGTGCTGACCTT Rv: GTGAAGCTGTAGAGGTCGGG

F13A1	Fw: GACTGCATTGTGGGGAAGTT Rv: TGACCATAGCTCCAGCTCCT

3. Results

3.1. Viability of scrapie-infected ovine mesenchymal stem cells

After inoculation of oBM-MSCs with brain homogenates of scrapie-infected and healthy sheep, it was observed a significant increment in the growth of positive (Pos) and negative-infected (Neg) cells in comparison to the non-inoculated controls (Naif) (Figure 1). Moreover, although positive cells grew more than the negative and non-inoculated cells, their viability decreased over time indicating a possible early toxicity of prion infection. Negative cells showed as well a decline in cell viability throughout time (Figure 1).

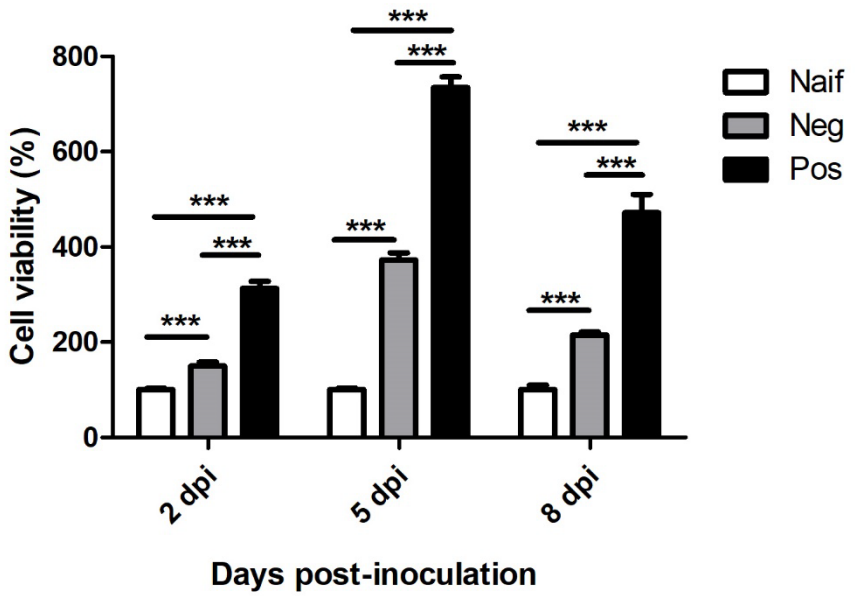

Figure 1. MTT assay showing the cell viability of scrapie-infected oBM-MSCs (Pos), cells inoculated with negative inoculum (Neg) and non-inoculated controls (Naif) at 2, 5 and 8 days post-inoculation (dpi). The viability values are presented as percentages (%), considering the viability of Naif cells as 100 % in all the infection times. Data are presented as mean values ± SEM. *** $P < 0.001$

3.2. PrP^{Sc} levels in scrapie-infected ovine mesenchymal stem cells

As it is shown in Figure 2, initially after prion infection (2 dpi), oBM-MSCs inoculated with scrapie-infected sheep brain homogenate maintained PrP^{Sc} levels, but afterwards PrP^{Sc} signal was lost over time. This reduction displayed a trend to signification ($P = 0.1$) in both 5 and 8 dpi comparted to 2 dpi.

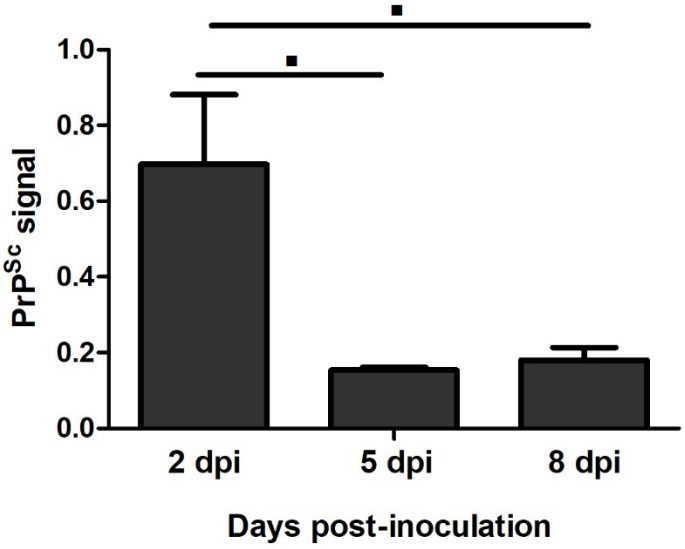

Figure 2. PrP^{Sc} levels in oBM-MSCs infected with scrapie quantified by ELISA at 2, 5 and 8 days post-inoculation (dpi). Data are shown as absorbance mean values ± SEM. ▪ P = 0.1

3.3. Clean data quality and mapping results

After filtering the raw reads, clean reads had an error rate lower than 1 % and GC content distribution was equal and stable in all sequenced samples. Around 98 % of the bases had a quality score greater than 20 and around 94 % greater than 30 (Supplementary Table S1).

Approximately 97 % of the clean reads were aligned to the reference sheep genome, being around the 87-89 % aligned to unique positions and 8-9 % to multiple locations in the genome (Supplementary Table S2). The majority of the reads were mapped in exon regions (67.04 % ± 0.68).

3.4. Distribution of gene expression levels

The distribution of gene expression levels among the different samples was similar (Supplementary Figure S1). The correlation coefficient of samples within groups was greater than 0.92 with a $R^2 > 0.8$, which showed close expression patterns (Supplementary Figure S2). Intergroup differences were evaluated by principal component analysis (PCA), being the samples between groups dispersed and the samples within groups gathered together (Figure 3). Moreover, a total of 11,926 genes were co-expressed in the three groups of samples (Naif, Pos and Neg) (Figure 4).

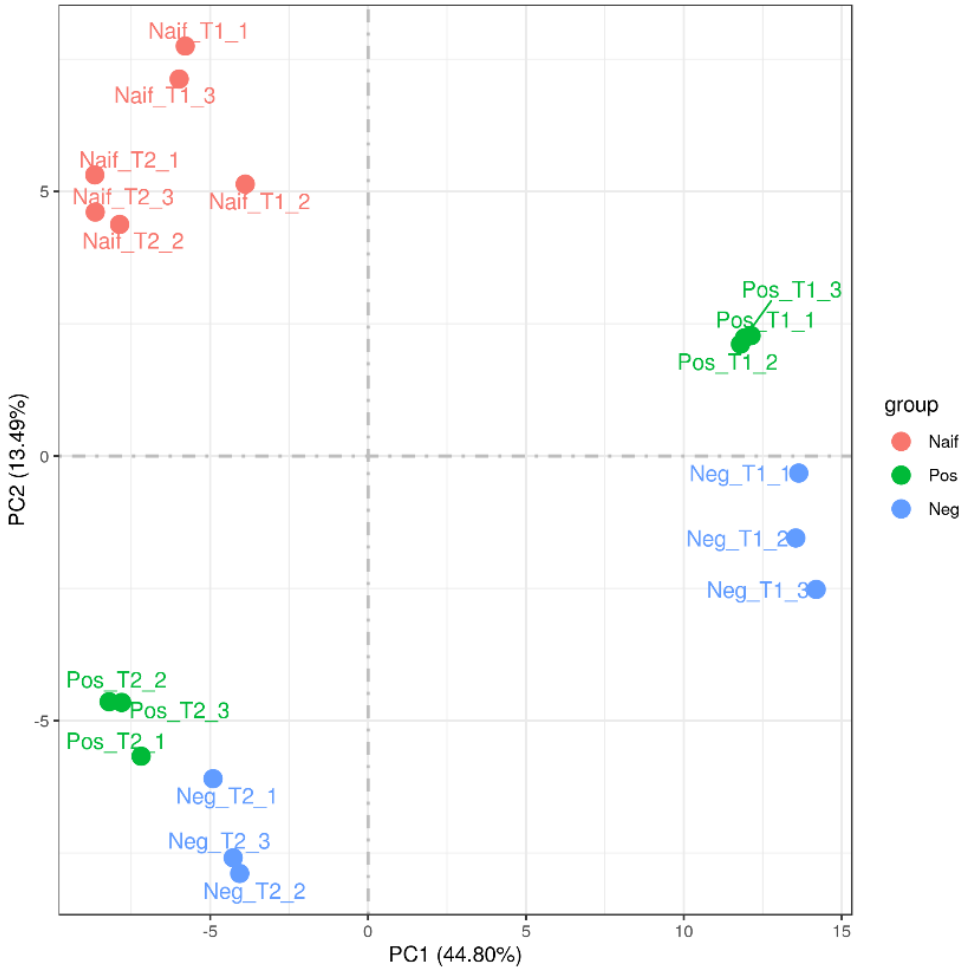

Figure 3. Principal component analysis showing the different sample groups (Naif_T1, Naif_T2, Pos_T1, Pos_T2, Neg_T1 and Neg_T2) clustered separately.

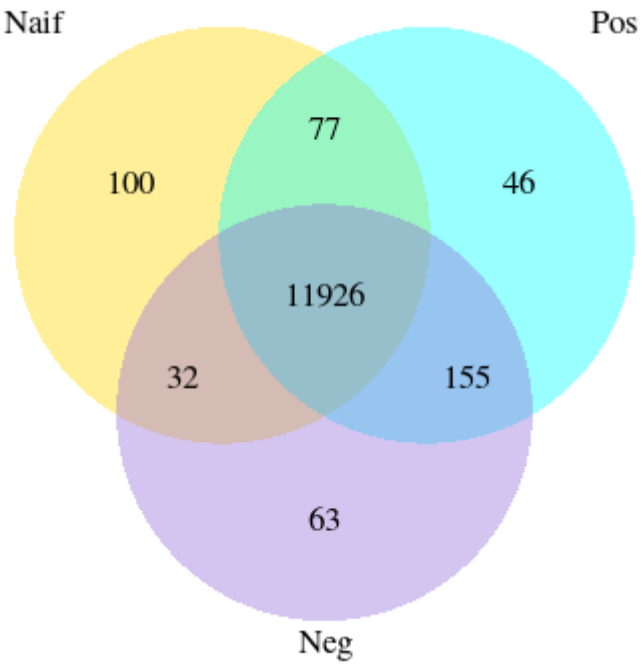

Figure 4. Venn diagram representing the number of co-expressed genes between Naif, Pos and Neg groups.

3.5. Differential gene expression analysis

Differentially expressed genes were found between the different groups at the two infection times T1 (2 dpi) and T2 (4 dpi). The higher number of DEGs was observed early after prion infection (2 dpi). Between positive and negative-infected cells, a total of 2,777 genes were differentially expressed (1,390 up-regulated and 1,387 down-regulated) at 2 dpi (Table 2, Figure 5a, Supplementary Table S3), whereas only 469 DEGs (206 up-regulated and 263 down-regulated) were found at 4 dpi (Table 2, Figure 5b, Supplementary Table S4). Regarding the DEGs observed in positive-infected cells when compared with non-inoculated controls (Naif), 4,502 and 1,897 genes were differentially expressed at 2dpi (Table 2, Supplementary Table S5) and 4 dpi (Table 2, Supplementary Table S6) respectively. Between negative-infected and naif cells, 5,685 DEGs were found at 2 dpi (Table 2, Supplementary Table S7) and 3,197 at 4 dpi (Table 2, Supplementary Table S8). Hierarchical clustering analysis of DEGs was also carried out, showing genes and samples with similar expression patterns clustering together (Figure 6). All Naif cells clustered together whereas infected cells were grouped according to the analysis time.

Table 2. Number of differentially expressed genes found in all compared groups with a P-value < 0.05 and after correction with adjusted P-value < 0.05.

	P-value < 0.05			adjusted P-value < 0.05		
compared groups[1]	**all DEGs[2]**	**up DEGs[3]**	**down DEGs[4]**	**all DEGs[2]**	**up DEGs[3]**	**down DEGs[4]**
Pos_T1vsNeg_T1	4183	2112	2071	2777	1390	1387
Pos_T1vsNaif_T1	5685	2874	2811	4502	2294	2208
Neg_T1vsNaif_T1	6751	3360	3391	5685	2850	2835
Pos_T2vsNeg_T2	1665	826	839	469	206	263
Pos_T2vsNaif_T2	3323	1698	1625	1897	993	904
Neg_T2vsNaif_T2	4524	2287	2237	3197	1642	1555

[1] Compared groups: Compared group names.

[2] All DEGs: The total number of differential genes in the compared groups.

[3] Up DEGs: The up-regulated number of differential genes in the compared groups.

[4] Down DEGs: The down-regulated number of differential genes in the compared groups.

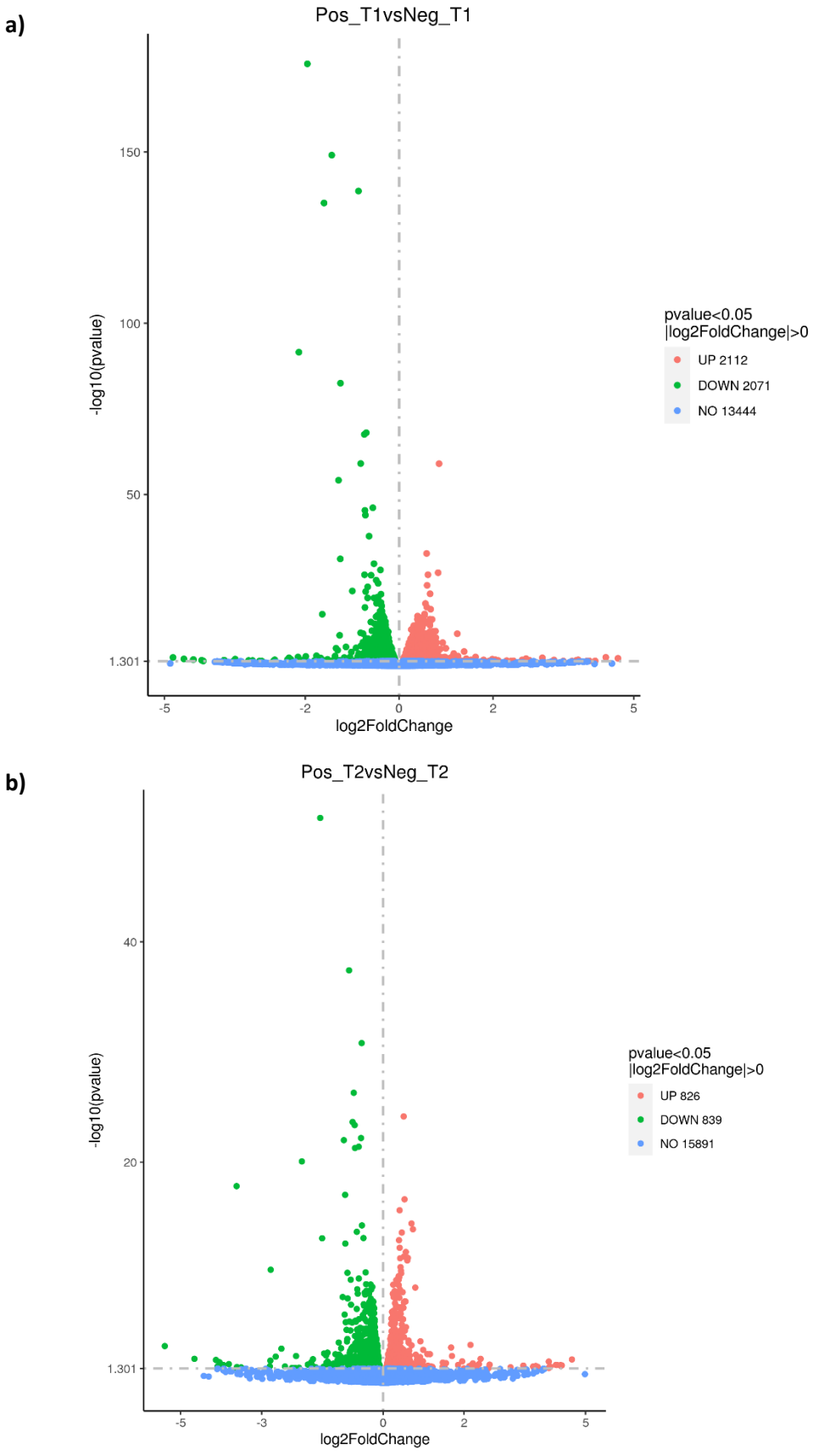

Figure 5. Volcano plots showing the overall distribution of differentially expressed genes between scrapie-infected cells (Pos) and cells infected with

negative-inoculum (Neg) at **(a)** 2 dpi (T1) and **(b)** 4 dpi (T2). The x-axis shows the fold change in gene expression (log2FoldChange), and the y-axis shows the statistical significance (-log10pvalue). Red dots represent up-regulated genes and green dots represent down-regulated genes. The blue dashed line indicates the threshold line for differential gene screening criteria.

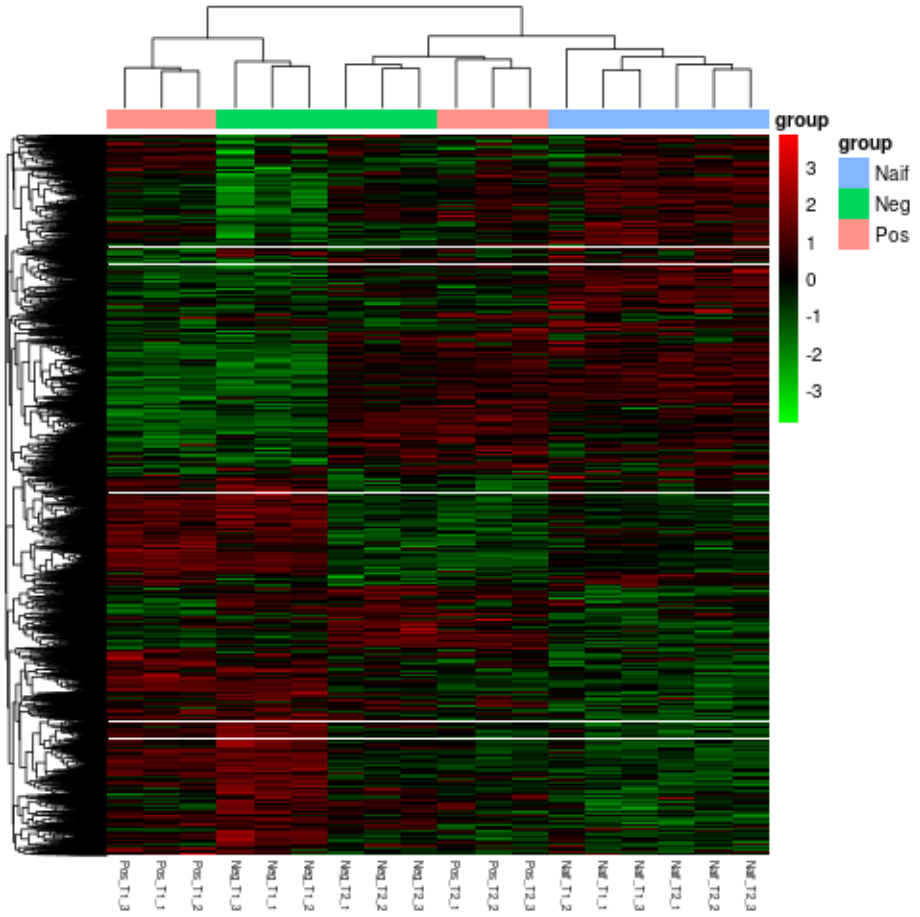

Figure 6. Differential expression gene clustering heatmap clustered using the log2(FPKM+1) value. Red colour indicates genes with high expression levels, and green colour indicates genes with low expression levels. The colour ranging from red to green indicates that log2(FPKM+1) values where from large to small.

3.6. Enrichment analysis of differentially expressed genes

GO and KEGG enrichment analysis were performed in order to find biological functions and pathways significantly associated with differentially expressed genes. DEGs identified between scrapie-infected cells (Pos) and cells infected with negative inoculum (Neg) at 2 dpi and 4 dpi were the most enriched in significant biological pathways and functions.

Regarding GO terms, at 2 dpi, up-regulated DEGs between positive and negative-infected cells were enriched in several molecular functions including GTPase binding, enzyme binding, microtubule motor activity and binding, tubulin binding, cytoskeletal protein binding and protein kinase activity. The cellular component nucleus and the biological process protein phosphorylation were also enriched (Supplementary Figure S3, Supplementary Table S9). Down-regulated DEGs were significantly associated with the molecular functions oxidoreductase activity, structural molecule activity and structural constituent of ribosome, the cellular components ribonucleoprotein complex and cytoplasmatic part, and the biological processes cellular amide metabolic process, translation and peptide biosynthetic and metabolic processes (Supplementary Figure S3, Supplementary Table S10).

On the other hand, at 4 dpi, up-regulated DEGs were enriched in the molecular functions actin binding, ligase and protein kinase activities, the biological processes protein phosphorylation and cell adhesion, and the cellular component extracellular matrix (Supplementary Figure S3, Supplementary Table S11). Down-regulated DEGs were also associated with different molecular functions including ferric and calcium ion binding, tubulin binding, nucleoside-triphosphatase activity, microtube binding, pyrophosphatase and hydrolase activities, and with the biological processes nucleotide catabolic process and pyruvate and ADP metabolic processes (Supplementary Figure S3, Supplementary Table S12).

DEGs were as well associated with several KEGG pathways and disease terms. At 2 dpi, up-regulated DEGs were enriched in various biological functions such as cell cycle, regulation of actin cytoskeleton, focal adhesion, foxO signalling pathway and cellular senescence (Figure 7a, Supplementary Table S13). Down-regulated DEGs were significantly associated with several disease terms including Parkinson's, Huntington's and Alzheimer's diseases, and with other biological functions and terms such as ribosome, lysosome, proteasome, oxidative phosphorylation, ferroptosis and protein processing in endoplasmic reticulum (Figure 7b, Supplementary Table S14).

a)

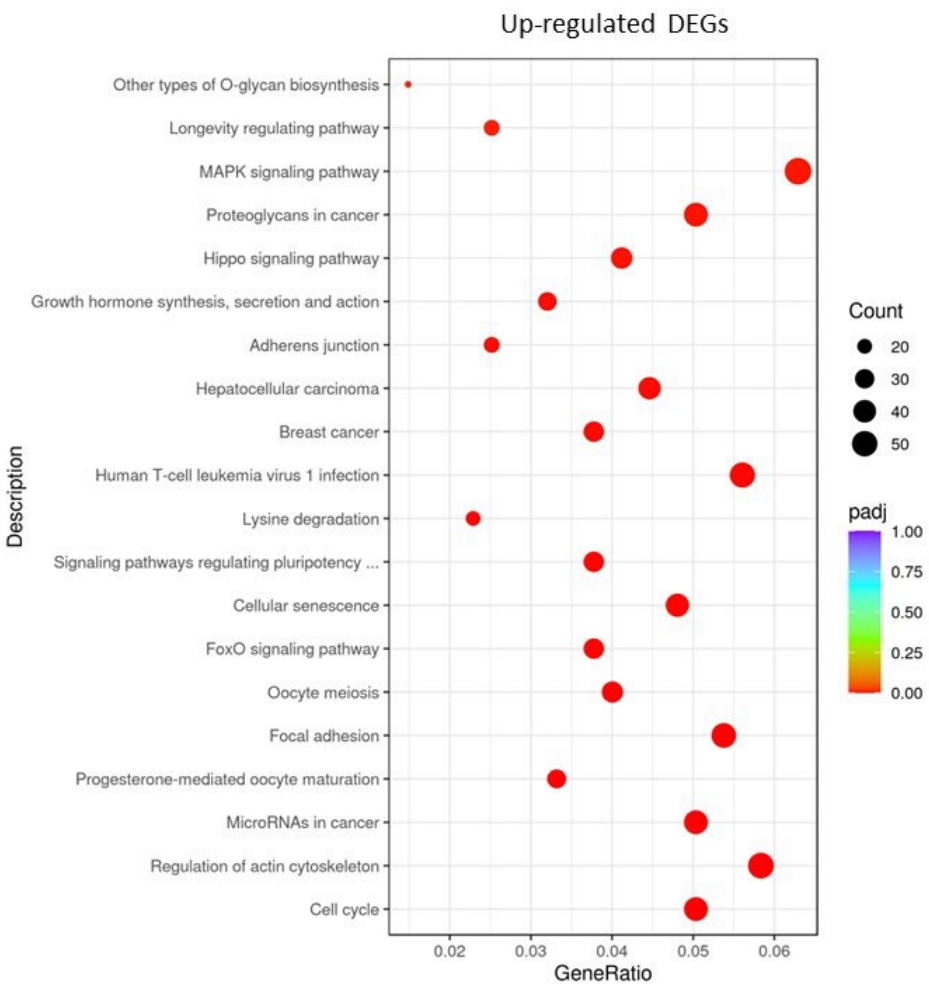
Up-regulated DEGs
Other types of O-glycan biosynthesis
Longevity regulating pathway
MAPK signaling pathway
Proteoglycans in cancer
Hippo signaling pathway
Growth hormone synthesis, secretion and action
Adherens junction
Hepatocellular carcinoma
Breast cancer
Human T-cell leukemia virus 1 infection
Lysine degradation
Signaling pathways regulating pluripotency ...
Cellular senescence
FoxO signaling pathway
Oocyte meiosis
Focal adhesion
Progesterone-mediated oocyte maturation
MicroRNAs in cancer
Regulation of actin cytoskeleton
Cell cycle
Description
0.02
0.03
0.04
0.05
0.06
GeneRatio
Count
20
30
40
50
padj
1.00
0.75
0.50
0.25
0.00

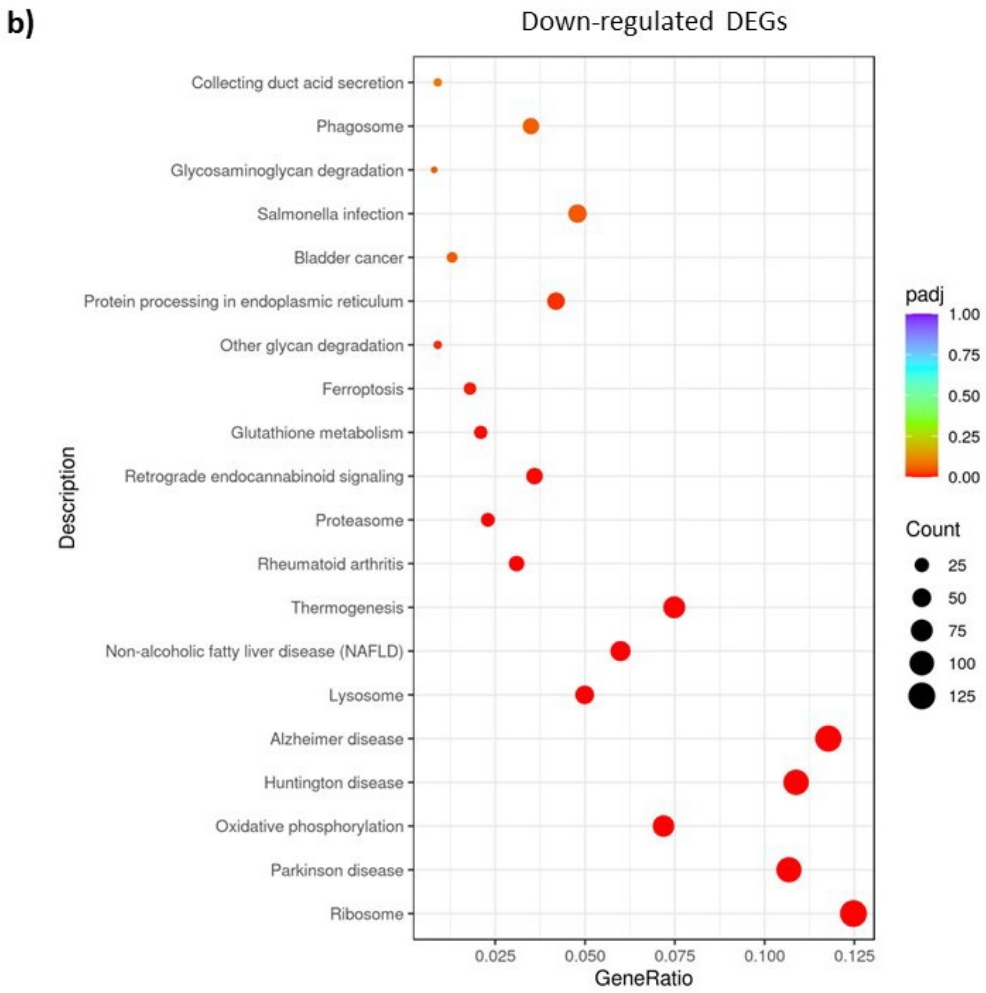

Figure 7. KEGG enrichment scatter plots of **(a)** up-regulated DEGs and **(b)** down-regulated DEGs in positive infected cultures (Pos) with respect to negative cultures (Neg) at 2 dpi (T1). The abscissa is the ratio of the number of differential genes linked with the KEGG pathway to the total number of differential genes. The ordinate is KEGG Pathway. The size of a point represents the number of genes annotated to a specific KEGG pathway. The colour from red to purple represents the significant level of the enrichment.

At 4 dpi, up-regulated DEGs were associated with wnt and TGF-beta signalling pathways, extracellular matrix-receptor interaction, protein digestion and absorption and axon guidance, whereas down-regulated DEGs were enriched in lysosome, glycolysis, ferroptosis, biosynthesis of amino acids and DNA replication pathways (Supplementary Tables S15 and S16).

3.7. RT-qPCR validation of RNA-sequencing analysis

The expression of 11 genes differentially expressed at 2 dpi between scrapie- and negative-infected cells was quantified with RT-qPCR to assess the validity of the results of the RNA-sequencing transcriptomic analysis.

Most of the analysed genes showed expression trends concordant with those observed in the RNA-sequencing analysis (Table 3). Three genes (*MMP1*, *SERPINB2* and *MMP12*) were significantly down-regulated in scrapie-infected cells compared to the cells inoculated with negative inoculum, whereas four genes (*PGAP4*, *PDK4*, *PRR11* and *F13A1*) were significantly up-regulated. The other four remaining genes (*RPS15A*, *SAA3*, *PTGS1* and *CYP1A1*) did not display significant expression changes.

Overall, the RT-qPCR results were congruent with the RNA-sequencing profiling, supporting the validity of the transcriptomic analysis.

Table 3. RT-qPCR validation results. Relative expression changes are expressed in terms of $2^{-\Delta\Delta Ct}$ in scrapie-infected cells (Pos) and negative inoculum-infected cells (Neg) at 2 dpi (T1). Significant changes are expressed as P-value. NS = non-significant.

Gene	$2^{-\Delta\Delta Ct}$ Pos_T1	$2^{-\Delta\Delta Ct}$ Neg_T1	RT-qPCR Pos_T1vsNeg_T1	RNAseq Pos_T1vsNeg_T1	Same expression trend	Validated gene (RT-qPCR P-value)
RPS15A	1.27	1	Up	Down	No	No (NS)
MMP1	0.27	1	Down	Down	Yes	Yes (p = 0.001)
PGAP4	1.37	1	Up	Up	Yes	Yes (p = 0.1)
SERPINB2	0.62	1	Down	Down	Yes	Yes (p = 0.08)
PDK4	1.45	1	Up	Up	Yes	Yes (p = 0.1)
MMP12	0.26	1	Down	Down	Yes	Yes (p = 0.001)
PRR11	1.63	1	Up	Up	Yes	Yes (p = 0.01)
Saa3	0.89	1	Down	Down	Yes	No (NS)
PTGS1	0.80	1	Down	Down	Yes	No (NS)
CYP1A1	0.85	1	Down	Up	No	No (NS)
F13A1	1.76	1	Up	Up	Yes	Yes (p = 0.008)

4. Discussion

In the current study, a RNA-seq transcriptomic analysis of ovine bone marrow-derived mesenchymal stem cells infected with scrapie was carried out to identify genes and biological pathways potentially involved in prion infection and its associated toxicity.

A previous study of our group reported that oBM-MSCs infected with scrapie were capable of uptaking PrP^{Sc} initially after prion infection, but they were unable to maintain PrP^{Sc} over time. The viability of oBM-MSCs after prion infection was also decreased indicating a toxic

effect of prion infection in these cells [10]. Similar results were observed in the oBM-MSC culture selected for the transcriptomic analysis in the present work. Interestingly, the higher number of differentially expressed genes was found early after prion infection (2 dpi) coinciding with the time when oBM-MSCs have been in contact with the different inocula and the amount of PrP^{Sc} is higher in positive cultures. This fact suggests that oBM-MSCs could react promptly to prion infection triggering different mechanisms that could lead to prion toxicity.

The DEGs found in scrapie-infected oBM-MSCs were enriched in several pathways and biological functions that are related to the known role of the cellular prion protein. This protein is implicated in a variety of biological processes including cell adhesion, calcium homeostasis and regulation of cytoskeletal components and extracellular matrix molecules [36–40]. Moreover, PrP^{C} interacts with GTPase proteins to regulate protein trafficking [39] and also protects cells from premature cellular senescence [41]. This protein takes part as well in different signalling routes such as TGF-beta [42] and Wnt pathways [43], being the latter impaired in the brain of scrapie-infected mice [44]. Another function impaired in prion diseases is iron homeostasis. PrP^{C} has a role in iron uptake [45] and an iron imbalance have been reported in brains of CJD patients probably due to a sequestration of iron in PrP^{Sc}-protein complexes that include ferritin [46,47]. These complexes are redox-active and can potentially create a cytotoxic environment [48]. All these mentioned cellular functions were enriched in oBM-MSCs infected with scrapie, which seem to mimic the dysregulation of different cellular processes regulated by PrP^{C} that may be disrupted after the conversion of PrP^{C} to PrP^{Sc} causing cell homeostasis imbalance and toxicity.

Ribosomes and ribonucleoprotein complex were terms also enriched in infected oBM-MSCs. Ribosomes are organelles involved in protein synthesis, but they are also implicated in protein folding [49]. The protein folding activity of the ribosome (PFAR) has been associated with the propagation of prions and other misfolded proteins and anti-PFAR drugs seem to reduce PrP^{Sc} propagation in vitro [50,51]. DEGs of positive-infected cells were associated as well with Alzheimer's, Parkinson's and Huntington's diseases, known as prion-like diseases because they share common pathogenic features with TSEs [1], and with ferroptosis which is a regulated lysosomal cell death process resulting from iron accumulation and lipid peroxidation [52] that has been associated with the pathophysiology of different diseases including cancer [53] and prion-like neurodegenerative diseases [54]. These mechanisms found in oBM-MSCs subjected to scrapie infection could contribute to PrP^{Sc} propagation and cell death.

On the other hand, changes in the expression of seven genes were validated by RT-qPCR. Two genes encoding two different matrix metalloproteinases were downregulated in scrapie-infected oBM-MSCs: *MMP1* (Matrix metalloproteinase 1) and *MMP12* (Matrix metalloproteinase 12). Matrix metalloproteinases (MMPs) are extracellular endopeptidases involved in extracellular matrix (ECM) turnover and degradation of its constituents [55,56]. The ECM is a dynamic structure undergoing controlled remodelling, and the balance between the synthesis, development and degradation of its components is essential to ensure a normal physiology [57]. Altered expression of matrix proteases can dysregulate this homeostatic balance leading to various pathological conditions [57]. Moreover, an excessive MMP proteolytic activity has been associated with the pathogenesis of several CNS diseases, such as cerebral ischemia, Parkinson's and Alzheimer's diseases, and traumatic injury [58]. The MMP1 and MMP12 enzymes are also implicated in the CNS inflammation process. *MMP12* is upregulated in aged brains of C57BL/6J mice enhancing neuroinflammation [59] and increased *MMP1* expression in rat microglia treated with synthetic prion peptide 106-126 is accompanied by an increment of several cytokines and inflammatory mediators [60]. Dysregulation of genes encoding proteins involved in ECM remodelling have also been described in other in vitro models where inhibition of metalloproteinases 2-9 was related with an increase of prion propagation [61]. The downregulation of these genes observed in oBM-MSCs could also be related to prion propagation as ECM components, including proteases, can interact with or process pathological misfolded proteins regulating their spreading capabilities [62] .

SERPINB2 (Serpin peptidase inhibitor clade B member 2), which was as well downregulated in oBM-MSCs, may function as a stress response protein with cytoprotective activity. In mouse embryonic fibroblasts transfected with mutant huntingtin, *SERPINB2* modulates protein degradation capacity and protein aggregation, and protects cells from the proteotoxicity associated with protein misfolding and proteostasis dysfunction [63]. Therefore, a downregulation of this gene during prion infection could be an indicator of cytotoxicity in oBM-MSC cultures.

PGAP4 is a gene encoding for post-GPI attachment to proteins GalNAc transferase 4, which is a GPI-specific GalNAc transferase that catalyses the first reaction for generating the GalNAc chain, a posttranslational modification found in different proteins including PrP^{C} [64]. This GPI-GalNAc side chain seems to be implicated in the conversion of PrP^{C} to PrP^{Sc} [65]. A recent study reported that prion-infected *PGAP4* knock-out mice displayed shorter disease incubation periods than the wild type ones, indicating a possible protective role of GPI-

GalNAc side chain and *PGAP4* against prion pathology [66]. The upregulation of *PGAP4* in oBM-MSCs could be a neuroprotective mechanism activated in response to scrapie infection.

Another upregulated gene in scrapie infected oBM-MSCs was *PDK4*. PrP^C is a regulator of glucose metabolism orientating the energetic metabolism towards mitochondria oxidative degradation of glucose. PrP^C exerts this action coupling to the cAMP/PKA (Protein kinase A) signalling pathway that attenuates *PDK4* (Pyruvate dehydrogenase kinase 4) expression. This preferential use of glucose limits fatty acids beta-oxidation and the onset of oxidative stress conditions [67]. In the hippocampus of prion-infected mice, an overexpression of *PDK4* has been described along with a decrease of glucose oxidative degradation and an increase in fatty acid-associated oxidative stress. Moreover, inhibition of *PDK4* extended the survival time of these mice [67]. The loss of PrP^C in oBM-MSCs during prion infection could provoke an upregulation of *PDK4* leading to oxidative stress conditions in these cells due to a deregulation of the glucose metabolism.

The upregulation of two more genes was also validated in scrapie infected oBM-MSCs: *PRR11* (Proline-rich protein 11) and *F13A1* (Coagulation factor XIII A chain). *PRR11* is a tumor-related gene involved in cell cycle, tumorigenesis and metastasis that is upregulated in different types of cancer including gastric and lung cancers [68–70]. In non-small-cell lung cancer cells, the silencing of *PRR11* induces autophagy and inhibits cell proliferation [69]. Interestingly, an impairment of the autophagy process has been described in sheep naturally infected with scrapie [71] and in scrapie-infected transgenic mice [72]. The upregulation of *PRR11* observed in our study could reduce the autophagic activity of the cells favouring PrP^{Sc} formation. *F13A1* expression, otherwise, has been associated with pro-inflammatory and cell stress pathways in adipose tissue [73,74]. As an upregulation of this gene was found in oBM-MSCs, it can be thought that the pathways found in adipose tissue could also be triggered in these cells as a consequence of the prion infection. These two genes have never been related to prion or other neurodegenerative diseases before. Further studies are necessary to elucidate their potential role in these diseases.

Altogether, our findings show that ovine mesenchymal stem cells infected with scrapie differentially express genes involved in pathways related with prion propagation and toxicity, making them a potential in vitro cellular model to study toxicity mechanisms and test anti-prion drugs.

5. Author Contributions

Conceptualization, I.M-B.; investigation, A.H., B.M. and F.J.V.; writing—original draft preparation, A.H.; writing—review and editing, I.M-B., R.B., P.Z., J.J.B., B.M. and F.J.V.;

supervision, I.M-B; project administration, I.M-B. and R.B.; funding acquisition, I.M-B., R.B., P.Z. and J.J.B.

6. Funding

Research was supported by the Agencia Estatal de Investigación and Fondos FEDER grant RTI2018-098711-B-100, the Gobierno de Aragón consolidated research group A19-20R, and the Gobierno de Aragón and the European Social Fund co-financed predoctoral grant Order IIU/2023/2017.

7. Data availability statement

The raw and processed transcriptomic data generated in this study will be deposited in NCBI's Gene Expression Omnibus [75].

8. Conflicts of interest

The authors declare no conflict of interest.

9. References

1. Soto, C. & Pritzkow, S. Protein misfolding, aggregation, and conformational strains in neurodegenerative diseases. *Nat. Neurosci.* **21**, 1332–1340 (2018).

2. Schlachetzki, J. C. M., Saliba, S. W. & de Oliveira, A. C. P. Studying neurodegenerative diseases in culture models. *Rev. Bras. Psiquiatr.* **35 Suppl 2**, (2013).

3. Butler, D. A. *et al.* Scrapie-infected murine neuroblastoma cells produce protease-resistant prion proteins. *J. Virol.* **62**, 1558–1564 (1988).

4. Klöhn, P. C., Stoltze, L., Flechsig, E., Enari, M. & Weissmann, C. A quantitative, highly sensitive cell-based infectivity assay for mouse scrapie prions. *Proc. Natl. Acad. Sci. U. S. A.* **100**, 11666–11671 (2003).

5. Mahal, S. P. *et al.* Prion strain discrimination in cell culture: the cell panel assay. *Proc. Natl. Acad. Sci. U. S. A.* **104**, 20908–20913 (2007).

6. Nishida, N. *et al.* Successful transmission of three mouse-adapted scrapie strains to murine neuroblastoma cell lines overexpressing wild-type mouse prion protein. *J. Virol.* **74**, 320–325 (2000).

7. Krance, S. H. *et al.* Cellular models for discovering prion disease therapeutics: Progress and challenges. *J. Neurochem.* **153**, 150–172 (2020).

8. Tark, D. *et al.* Generation of a persistently infected MDBK cell line with natural bovine

spongiform encephalopathy (BSE). *PLoS One* **10**, (2015).

9. Raymond, G. J. *et al.* Inhibition of protease-resistant prion protein formation in a transformed deer cell line infected with chronic wasting disease. *J. Virol.* **80**, 596–604 (2006).

10. García-mendívil, L. *et al.* Effect of Scrapie Prion Infection in Ovine Bone Marrow-Derived Mesenchymal Stem Cells and Ovine Mesenchymal Stem Cell-Derived Neurons. *Anim. an open access J. from MDPI* **11**, (2021).

11. Krejciova, Z. *et al.* Human stem cell-derived astrocytes replicate human prions in a PRNP genotype-dependent manner. *J. Exp. Med.* **214**, 3481–3495 (2017).

12. Groveman, B. R. *et al.* Sporadic Creutzfeldt-Jakob disease prion infection of human cerebral organoids. *Acta Neuropathol. Commun.* **7**, 90 (2019).

13. Zhang, C. C., Steele, A. D., Lindquist, S. & Lodish, H. F. Prion protein is expressed on long-term repopulating hematopoietic stem cells and is important for their self-renewal. *Proc. Natl. Acad. Sci. U. S. A.* **103**, 2184–2189 (2006).

14. Lyahyai, J. *et al.* Isolation and characterization of ovine mesenchymal stem cells derived from peripheral blood. *BMC Vet. Res.* **8**, (2012).

15. Akimov, S., Vasilyeva, I., Yakovleva, O., McKenzie, C. & Cervenakova, L. Murine bone marrow stromal cell culture with features of mesenchymal stem cells susceptible to mouse-adapted human TSE agent, Fukuoka-1. *Folia Neuropathol.* **47**, 205–14 (2009).

16. Akimov, S., Yakovleva, O., Vasilyeva, I., McKenzie, C. & Cervenakova, L. Persistent Propagation of Variant Creutzfeldt-Jakob Disease Agent in Murine Spleen Stromal Cell Culture with Features of Mesenchymal Stem Cells. *J. Virol.* **82**, 10959–10962 (2008).

17. Cervenakova, L. *et al.* Fukuoka-1 strain of transmissible spongiform encephalopathy agent infects murine bone marrow-derived cells with features of mesenchymal stem cells. *Transfusion* **51**, 1755–1768 (2011).

18. Takakura, Y. *et al.* Bone marrow stroma cells are susceptible to prion infection. *Biochem. Biophys. Res. Commun.* **377**, 957–961 (2008).

19. Chen, B. J., Mills, J. D., Janitz, C. & Janitz, M. RNA-Sequencing to Elucidate Early Patterns of Dysregulation Underlying the Onset of Alzheimer's Disease. *Methods Mol. Biol.* **1303**, 327–347 (2016).

20. Courtney, E., Kornfeld, S., Janitz, K. & Janitz, M. Transcriptome profiling in neurodegenerative disease. *J. Neurosci. Methods* **193**, 189–202 (2010).

21. Marguerat, S., Wilhelm, B. T. & Bähler, J. Next-generation sequencing: applications beyond genomes. *Biochem. Soc. Trans.* **36**, 1091–1096 (2008).

22. Guennewig, B. *et al.* Defining early changes in Alzheimer's disease from RNA sequencing of brain regions differentially affected by pathology. *Sci. Rep.* **11**, (2021).

23. Olah, M. *et al.* Single cell RNA sequencing of human microglia uncovers a subset associated with Alzheimer's disease. *Nat. Commun.* **11**, (2020).

24. Smajic, S. *et al.* Single-cell sequencing of human midbrain reveals glial activation and a Parkinson-specific neuronal state. *Brain* **145**, 964–978 (2022).

25. Soreq, L. *et al.* Whole transcriptome RNA sequencing data from blood leukocytes derived from Parkinson's disease patients prior to and following deep brain stimulation treatment. *Genomics data* **3**, 57–60 (2014).

26. Bartoletti-Stella, A. *et al.* Analysis of RNA Expression Profiles Identifies Dysregulated Vesicle Trafficking Pathways in Creutzfeldt-Jakob Disease. *Mol. Neurobiol.* **56**, 5009–5024 (2019).

27. Carroll, J. A., Race, B., Williams, K., Striebel, J. & Chesebro, B. RNA-seq and network analysis reveal unique glial gene expression signatures during prion infection. *Mol. Brain* **13**, (2020).

28. Filali, H. *et al.* Gene expression profiling and association with prion-related lesions in the medulla oblongata of symptomatic natural scrapie animals. *PLoS One* **6**, (2011).

29. Filali, H. *et al.* Medulla oblongata transcriptome changes during presymptomatic natural scrapie and their association with prion-related lesions. *BMC Genomics* **13**, (2012).

30. Mediano, D. R. *et al.* Characterization of mesenchymal stem cells in sheep naturally infected with scrapie. *J. Gen. Virol.* **96**, 3715–3726 (2015).

31. Ranera, B. *et al.* Comparative study of equine bone marrow and adipose tissue-derived mesenchymal stromal cells. *Equine Vet. J.* **44**, 33–42 (2012).

32. Bolea, R. *et al.* Comparison of immunohistochemistry and two rapid tests for detection of abnormal prion protein in different brain regions of sheep with typical scrapie. *J. Vet.*

Diagn. Invest. **17**, 467–469 (2005).

33. Pertea, M. *et al.* StringTie enables improved reconstruction of a transcriptome from RNA-seq reads. *Nat. Biotechnol.* **33**, 290–295 (2015).

34. Livak, K. J. & Schmittgen, T. D. Analysis of relative gene expression data using real-time quantitative PCR and the 2-ΔΔCT method. *Methods* **25**, 402–408 (2001).

35. Lyahyai, J. *et al.* Effect of scrapie on the stability of housekeeping genes. *Anim. Biotechnol.* **21**, (2010).

36. Beraldo, F. H. *et al.* Role of α7 nicotinic acetylcholine receptor in calcium signaling induced by prion protein interaction with stress-inducible protein. *J. Biol. Chem.* **285**, 36542–36550 (2010).

37. Hall, G. N. M. *et al.* Cellular prion protein interaction with vitronectin supports axonal growth and is compensated by integrins. *J. Cell Sci.* **120**, 1915–1926 (2007).

38. Head, B. P., Patel, H. H. & Insel, P. A. Interaction of membrane/lipid rafts with the cytoskeleton: Impact on signaling and function: Membrane/lipid rafts, mediators of cytoskeletal arrangement and cell signaling. *Biochim. Biophys. Acta - Biomembr.* **1838**, 532–545 (2014).

39. Hirsch, T. Z., Martin-Lannerée, S. & Mouillet-Richard, S. Functions of the Prion Protein. *Prog. Mol. Biol. Transl. Sci.* **150**, 1–34 (2017).

40. Málaga-Trillo, E. *et al.* Regulation of Embryonic Cell Adhesion by the Prion Protein. *PLOS Biol.* **7**, e1000055 (2009).

41. Boilan, E. *et al.* Role of Prion protein in premature senescence of human fibroblasts. *Mech. Ageing Dev.* **170**, 106–113 (2018).

42. Wurm, S. & Wechselberger, C. Prion protein modifies TGF-beta induced signal transduction. *Biochem. Biophys. Res. Commun.* **349**, 525–532 (2006).

43. Besnier, L. S. *et al.* The cellular prion protein PrPc is a partner of the Wnt pathway in intestinal epithelial cells. *Mol. Biol. Cell* **26**, 3313–3328 (2015).

44. Sun, J. *et al.* Remarkable impairment of Wnt/β-catenin signaling in the brains of the mice infected with scrapie agents. *J. Neurochem.* **136**, 731–740 (2016).

45. Singh, A. *et al.* Prion protein regulates iron transport by functioning as a ferrireductase.

J. Alzheimers. Dis. **35**, 541–552 (2013).

46. Singh, A. *et al.* Abnormal brain iron homeostasis in human and animal prion disorders. *PLoS Pathog.* **5**, (2009).

47. Singh, A., Qing, L., Kong, Q. & Singh, N. Change in the characteristics of ferritin induces iron imbalance in prion disease affected brains. *Neurobiol. Dis.* **45**, 930–938 (2012).

48. Basu, S. *et al.* Modulation of proteinase K-resistant prion protein in cells and infectious brain homogenate by redox iron: implications for prion replication and disease pathogenesis. *Mol. Biol. Cell* **18**, 3302–3312 (2007).

49. Voisset, C., Saupe, S. J. & Blondel, M. The various facets of the protein-folding activity of the ribosome. *Biotechnol. J.* **6**, 668–673 (2011).

50. Voisset, C. *et al.* The double life of the ribosome: When its protein folding activity supports prion propagation. *Prion* **11**, 89–97 (2017).

51. Bamia, A. *et al.* Anti-prion Drugs Targeting the Protein Folding Activity of the Ribosome Reduce PABPN1 Aggregation. *Neurotherapeutics* **18**, 1137–1150 (2021).

52. Gao, H. *et al.* Ferroptosis is a lysosomal cell death process. *Biochem. Biophys. Res. Commun.* **503**, 1550–1556 (2018).

53. Mou, Y. *et al.* Ferroptosis, a new form of cell death: opportunities and challenges in cancer. *J. Hematol. Oncol.* **12**, (2019).

54. Reichert, C. O. *et al.* Ferroptosis Mechanisms Involved in Neurodegenerative Diseases. *Int. J. Mol. Sci.* **21**, 1–27 (2020).

55. Khokha, R., Murthy, A. & Weiss, A. Metalloproteinases and their natural inhibitors in inflammation and immunity. *Nat. Rev. Immunol.* **13**, 649–665 (2013).

56. Minta, K. *et al.* Dynamics of cerebrospinal fluid levels of matrix metalloproteinases in human traumatic brain injury. *Sci. Rep.* **10**, (2020).

57. Cox, T. R. & Erler, J. T. Remodeling and homeostasis of the extracellular matrix: implications for fibrotic diseases and cancer. *Dis. Model. Mech.* **4**, 165–178 (2011).

58. Crocker, S. J., Pagenstecher, A. & Campbell, I. L. The TIMPs tango with MMPs and more in the central nervous system. *J. Neurosci. Res.* **75**, 1–11 (2004).

59. Liu, Y. *et al.* Matrix metalloproteinase-12 contributes to neuroinflammation in the aged

brain. *Neurobiol. Aging* **34**, 1231–1239 (2013).

60. Song, K. *et al.* Synthetic prion Peptide 106-126 resulted in an increase matrix metalloproteinases and inflammatory cytokines from rat astrocytes and microglial cells. *Toxicol. Res.* **28**, 5–9 (2012).

61. Marbiah, M. M. *et al.* Identification of a gene regulatory network associated with prion replication. *EMBO J.* **33**, 1527–1547 (2014).

62. Moretto, E., Stuart, S., Surana, S., Vargas, J. N. S. & Schiavo, G. The Role of Extracellular Matrix Components in the Spreading of Pathological Protein Aggregates. *Front. Cell. Neurosci.* **16**, (2022).

63. Lee, J. A. *et al.* SerpinB2 (PAI-2) Modulates Proteostasis via Binding Misfolded Proteins and Promotion of Cytoprotective Inclusion Formation. *PLoS One* **10**, (2015).

64. Hirata, T. *et al.* Identification of a Golgi GPI-N-acetylgalactosamine transferase with tandem transmembrane regions in the catalytic domain. *Nat. Commun.* **9**, (2018).

65. Bate, C., Nolan, W. & Williams, A. Sialic Acid on the Glycosylphosphatidylinositol Anchor Regulates PrP-mediated Cell Signaling and Prion Formation. *J. Biol. Chem.* **291**, 160–170 (2016).

66. Hirata, T. *et al.* Loss of the N-acetylgalactosamine side chain of the GPI-anchor impairs bone formation and brain functions and accelerates the prion disease pathology. *J. Biol. Chem.* **298**, (2022).

67. Arnould, H. *et al.* Loss of prion protein control of glucose metabolism promotes neurodegeneration in model of prion diseases. *PLoS Pathog.* **17**, (2021).

68. Hu, H. *et al.* Proline-Rich Protein 11 Regulates Self-Renewal and Tumorigenicity of Gastric Cancer Stem Cells. *Cell. Physiol. Biochem.* **47**, 1721–1728 (2018).

69. Zhang, L. *et al.* Silencing of PRR11 suppresses cell proliferation and induces autophagy in NSCLC cells. *Genes Dis.* **5**, 158–166 (2017).

70. Zhou, L. *et al.* Overexpression of PRR11 promotes tumorigenic capability and is associated with progression in esophageal squamous cell carcinoma. *Onco. Targets. Ther.* **12**, 2677–2693 (2019).

71. López-Pérez, Ó. *et al.* Dysregulation of autophagy in the central nervous system of sheep naturally infected with classical scrapie. *Sci. Rep.* **9**, 1911 (2019).

72. López-Pérez, Ó. *et al.* Impairment of autophagy in scrapie-infected transgenic mice at the clinical stage. *Lab. Investig.* **100**, 52–63 (2020).

73. Kaartinen, M. T. *et al.* Transglutaminases and Obesity in Humans: Association of F13A1 to Adipocyte Hypertrophy and Adipose Tissue Immune Response. *Int. J. Mol. Sci.* **21**, 1–20 (2020).

74. Kaartinen, M. T. *et al.* F13A1 transglutaminase expression in human adipose tissue increases in acquired excess weight and associates with inflammatory status of adipocytes. *Int. J. Obes. (Lond).* **45**, 577–587 (2021).

75. Edgar, R., Domrachev, M. & Lash, A. Gene Expression Omnibus: NCBI gene expression and hybridization array data repository. *Nucleic Acids Res.* **30**, 207–210 (2002).

Discusión global de los trabajos

Discusión global de los trabajos aportados

En este apartado, se van a enumerar y discutir los principales hallazgos y resultados de la investigación realizada en este trabajo de tesis doctoral, los cuales están recogidos en el compendio de publicaciones que acompaña la tesis y se engloban en dos grandes objetivos, el estudio de la metilación como mecanismo epigenético en el scrapie ovino y el desarrollo de modelos celulares de enfermedad priónica basados en el uso de células madre mesenquimales ovinas.

1. La metilación del DNA en el scrapie ovino

En el primer artículo titulado "*Epigenetic Changes in Prion and Prion-like Neurodegenerative Diseases: Recent Advances, Potential as Biomarkers, and Future Perspectives*", se realiza una revisión bibliográfica sobre la implicación de los principales mecanismos epigenéticos en las enfermedades neurodegenerativas priónicas y *prion-like*. Este trabajo de revisión muestra que, tanto la metilación del DNA, como las modificaciones postraduccionales de histonas y los microRNAs están involucrados en la fisiopatología de estas enfermedades neurodegenerativas de una manera específica, ya que hay pocos mecanismos comunes entre todas ellas.

Una vez revisados los conocimientos descubiertos hasta el momento sobre el papel de los mecanismos epigenéticos en las enfermedades priónicas, procedimos a plantear un primer estudio de la metilación del DNA en la enfermedad de scrapie, dando lugar al segundo artículo de esta tesis titulado "*Genome-Wide Methylation Profiling in the Thalamus of Scrapie Sheep*", donde presentamos el primer estudio realizado en enfermedades priónicas de secuenciación genómica de DNA transformado con bisulfito en el SNC. En este estudio, se analizó el perfil de metilación de muestras de tálamo de ovejas infectadas de manera natural con scrapie clásico en fase clínica.

A pesar de que los animales infectados y los animales sanos mostraran niveles globales de metilación similares, se consiguieron identificar genes que albergaban regiones con metilación diferencial (DMGs). Se identificaron un total de 8.907 regiones con metilación diferencial (DMRs) en las muestras de scrapie, de las cuales 4.630 estaban hipermetiladas y 4.277 hipometiladas. También se llevó a cabo un análisis para identificar promotores con metilación diferencial (DMPs), hallando un total de 39 DMPs, 15 hipermetilados y 24 hipometilados.

Los análisis de enriquecimiento de *Gene Ontology (GO)* y *Kyoto Encyclopedia of Genes and Genomes (KEGG)* revelaron que los DMGs identificados en los animales infectados estaban

implicados en distintas rutas moleculares y funciones biológicas, entre las que se pueden destacar, la transducción de señales intracelulares, el transporte transmembrana, la unión celular y de proteínas, vías de señalización del calcio, vías de señalización del AMP cíclico, la sinapsis colinérgica, el ritmo circadiano y los mecanismos de apoptosis. En la regulación de todos estos procesos interviene de una forma u otra la PrP^C. Varios estudios señalan que la PrP^C modula diversos componentes involucrados en la proliferación y adhesión celulares, en las vías de señalización y transporte transmembrana, y en la diferenciación celular [160]. Además, esta proteína regula el funcionamiento correcto de las sinapsis y el mantenimiento de la plasticidad sináptica e interviene en el ritmo circadiano regulando la homeostasis del sueño [161]. Mediante la activación de la vía de señalización del AMP cíclico, la PrP^C promueve la supervivencia neuronal, el crecimiento de las neuritas [162] y el mantenimiento de la mielina [161]. En cuanto a las vías de señalización del calcio y los mecanismos de apoptosis, esta proteína también regula la homeostasis intracelular del calcio y ejerce control sobre algunas vías de señalización de apoptosis [162]. Por tanto, el enriquecimiento en genes con cambios de metilación involucrados en estas funciones en la enfermedad de scrapie, donde la PrP^C pierde su función por su conversión a PrP^{Sc}, sugiere una regulación epigenética de estos procesos.

Dado que la metilación del DNA participa en la regulación de la expresión génica, decidimos evaluar el efecto de dicha metilación sobre la expresión de genes diferencialmente metilados en scrapie. Para ello, de todos los DMGs identificados, seleccionamos un conjunto de genes con funciones en el sistema nervioso conocidas y/o asociados con otras enfermedades neurodegenerativas. La evaluación de la expresión se llevó a cabo mediante PCR a tiempo real (RT-qPCR), encontrando cambios significativos en la expresión de cinco genes: *PCDH19*, *SNCG*, *WDR45B*, *PEX1* y *CABIN1*.

A la hora de analizar el efecto de la metilación sobre la expresión de los genes, es importante tener en cuenta que la posición de la metilación en la unidad de transcripción determina su control sobre la expresión génica [163], es decir, dependiendo de si la metilación se encuentra en regiones promotoras, en exones o intrones, el efecto sobre la expresión génica es diferente. La metilación en promotores se asocia normalmente con represión de la expresión génica, mientras que la metilación en exones se asocia con activación de la expresión [163]. En cuanto a los intrones, existe una relación inversa entre la metilación del primer intrón de un gen y su expresión, que podría ser debida a la presencia de potenciadores o *enhancers* intrónicos que interactuasen con el promotor o promotores del gen [164].

De los cinco genes validados, *SNCG* y *WDR45B* podrían tener un papel neuroprotector frente a la enfermedad de scrapie. El gen *SNCG* codifica la proteína neuronal sinucleína γ, la cual está involucrada en los mecanismos patogénicos de la neurodegeneración y el cáncer [165]. En condiciones fisiológicas, los astrocitos expresan esta proteína estimulando el ciclo celular y participando en la expresión y liberación extracelular del factor neurotrófico derivado del cerebro (BNDF) [166]. Por otro lado, esta sinucleína es capaz de inhibir la agregación de la sinucleína α, proteína presente en los cuerpos de Lewy cuya agregación anómala tiene lugar en la enfermedad de Parkinson [167]. En neuronas de ratones transgénicos, la sobreexpresión de la sinucleína γ produce una patología neurodegenerativa severa con depleción de neurofilamentos y muerte de neuronas motoras [168]. En pacientes con Alzheimer, también se ha descrito un aumento de la expresión de esta proteína en el cerebro y en el líquido cefalorraquídeo [166], considerándose este aumento un marcador pronóstico de condiciones neurodegenerativas [168]. Considerando todos estos hallazgos, la expresión disminuida de *SNCG*, acompañada de una hipermetilación en la región promotora, observada en los animales infectados con scrapie sugiere una función neuroprotectora de este gen probablemente a nivel de los astrocitos, los cuales están implicados en el proceso de replicación y propagación del prion.

El gen *WDR45B* codifica la proteína WIPI3. Las proteínas WIPI (WIPI1, WIPI2, WIPI3 y WIPI4) participan en el control de la autofagia. La proteína WIPI3, en concreto, interviene en la formación de autofagosomas [169]. La autofagia es un mecanismo que regula la degradación de orgánulos dañados y proteínas mal plegadas, desempeñando un papel importante en el mantenimiento de la homeostasis neuronal [170]. En las enfermedades priónicas [171–174] y en otras enfermedades neurodegenerativas [175] se ha descrito una desregulación de este proceso. Como la homeostasis neuronal y la autofagia se encuentran alteradas en la enfermedad de scrapie, el aumento de expresión de *WDR45B* observado en los animales afectados podría ser una respuesta del organismo para intentar mantener la homeostasis neuronal y un correcto funcionamiento del proceso de autofagia.

Los genes *PCDH19*, *PEX1* y *CABIN1*, en cambio, podrían contribuir a la progresión de la enfermedad. El gen *PCDH19* codifica una proteína perteneciente a la familia de las protocadherinas, proteínas que regulan la transducción de señales en las sinapsis y el establecimiento de las conexiones neuronales. Estas proteínas se expresan principalmente en el SNC y participan en el desarrollo neuronal, la migración, la segregación y la plasticidad sináptica. Los niveles de expresión más elevados de *PCDH19* se encuentran en el sistema nervioso, aunque también se expresa en otros tejidos [176]. Este gen regula la proliferación de progenitores neuronales, la formación de circuitos y la actividad neuronal [177], así como la

neurotransmisión GABA y la maduración de neuronas [178]. En el autismo, se han descrito alteraciones de la expresión de protocadherinas y se han asociado mutaciones en el gen *PCDH19* con la encefalopatía epiléptica infantil [176]. La metilación de este gen solo se ha estudiado en el carcinoma hepatocelular, donde se halló una hipermetilación en la región promotora junto con una disminución de la expresión génica [179]. En el caso de los animales con scrapie, también se observó una disminución de la expresión y una hipermetilación de la región promotora. Dada la importancia de este gen en el mantenimiento de la homeostasis neuronal, su expresión disminuida podría asociarse o contribuir a la progresión de la enfermedad.

El gen *PEX1* codifica la proteína peroxina 1, la cual interviene en la biogénesis de peroxisomas, concretamente en la importación de proteínas de la matriz peroxisomal [180]. Los peroxisomas son orgánulos que contribuyen en el metabolismo lipídico celular y en el equilibrio redox [181]. En el SNC, la función de estos orgánulos está centrada en la síntesis de éter fosfolípidos, que son componentes importantes de la mielina para la síntesis de ácido docosahexaenoico (DHA), el cual interviene en la señalización del sistema nervioso y en la degradación de componentes tóxicos y D-aminoácidos, protegiendo las estructuras cerebrales y modulando la señalización sináptica [182]. En las enfermedades de Alzheimer y Parkinson, en la esclerosis lateral amiotrófica y en el autismo existe una disfunción de los peroxisomas y/o una alteración de sus metabolitos [181,182]. Como ejemplo, los pacientes con Alzheimer muestran un transporte peroxisomal ineficiente entre las neuritas y el soma, y una desregulación del metabolismo lipídico peroxisomal. Estas alteraciones contribuyen a la patología del Alzheimer agravando la progresión de la enfermedad [181]. En los animales infectados con scrapie, se observó un aumento de expresión en este gen que se correlacionaba con la espongiosis y con la acumulación de PrP^{Sc}, lo que sugiere que la función de los peroxisomas también podría estar comprometida en la enfermedad de scrapie.

En el SNC, el gen *CABIN1* codifica una proteína de unión a la calcineurina que actúa como un represor de la misma dependiente del calcio [183]. La calcineurina es una enzima fosfatasa expresada en distintos tipos celulares incluidas las neuronas, donde está implicada en la transmisión sináptica y en la liberación de neurotransmisores [184]. En la enfermedad de Alzheimer, la activación crónica y anómala de esta proteína en las neuronas causa disfunción sináptica, mientras que su inhibición mejora la morfología sináptica [185]. En las enfermedades priónicas, también se produce una disfunción y pérdida de las sinapsis [161]. Además, se ha descrito que la activación de la calcineurina mediada por el péptido sintético PrP 106-126 desencadena la muerte de células neuronales [186]. Todos estos datos sugieren que la

disminución de la expresión de *CABIN1* observada en los animales afectados podría desencadenar la activación de la calcineurina contribuyendo de esta forma a la disfunción sináptica y la muerte neuronal.

Además de realizar este estudio de expresión, también comparamos nuestro set de DMGs con otro estudio que previamente había identificado genes con expresión diferencial en scrapie [187]. Tras esta comparación, identificamos 21 genes comunes entre ambos estudios que albergaban regiones con metilación diferencial, sugiriendo que la metilación del DNA también podría estar implicada en la regulación de la expresión de estos genes previamente descritos.

Este primer estudio de metilación del DNA en el tálamo de ovejas con scrapie nos permitió evidenciar la implicación de este mecanismo epigenético en la patogenia de la enfermedad. Hay que tener en cuenta que los resultados obtenidos solo eran de una zona concreta del SNC en animales en fase clínica. Por otro lado, la técnica de secuenciación de DNA transformado con bisulfito tiene la limitación de que no permite distinguir entre las distintas formas de metilación del DNA, concretamente entre 5mC y 5hmC, que son las formas más abundantes. Por todo ello, decidimos plantear el tercer trabajo de esta tesis que dio lugar al artículo titulado "*5-methylcytosine and 5-hydroxymethylcytosine in scrapie-infected sheep and mouse brain tissues*". En este estudio, realizamos un análisis inmunohistoquímico de los niveles de 5mC y 5hmC en distintas regiones del SNC en ovejas infectadas de manera natural con scrapie clásico y en un modelo murino transgénico de scrapie (ratones Tg338), tanto en fase clínica como preclínica. Para profundizar más en el mecanismo de metilación del DNA en scrapie, también analizamos en la región del tálamo mediante RT-qPCR la expresión de genes que codifican enzimas reguladoras del proceso de metilación (*DNMT1*, *DNMT3A*, *DNMT3B*, *TET1* y *TET2*) junto con la expresión de dos genes que codifican dos enzimas HDAC (*HDAC1* y *HDAC2*), las cuales se asocian con las enzimas DNMTs para regular la expresión génica [188]. Por último, evaluamos la posible correlación entre los niveles de 5mC y 5hmC con los niveles de expresión génica y con las lesiones asociadas a la patología priónica.

Las áreas anatómicas del SNC analizadas en ovejas fueron las siguientes: obex, cerebelo, mesencéfalo, tálamo, corteza parietal, ganglios basales, corteza de los ganglios basales y corteza frontal. En los ratones Tg338, se analizaron las siguientes áreas: obex, cerebelo, mesencéfalo, hipocampo, tálamo, hipotálamo, corteza parietal, área septal y corteza frontal.

Los perfiles de 5mC también se han estudiado en otras enfermedades neurodegenerativas como el Alzheimer. Se ha descrito una disminución de esta biomolécula en el cerebro de pacientes preclínicos [189] y en un modelo murino transgénico de Alzheimer [190]. De manera

similar, en nuestro estudio, se observó una disminución de los niveles de 5mC en las ovejas y ratones infectados con scrapie. Los animales clínicos y preclínicos mostraban niveles cerebrales de 5mC parecidos, siendo significativamente más bajos que los niveles observados en los controles en el obex de los ratones clínicos y en el mesencéfalo, tálamo, corteza parietal y obex de las ovejas clínicas y preclínicas. Además, se observó una asociación negativa de los niveles de 5mC con las lesiones relacionadas con priones en ratones y sobre todo en ovejas, en las que se encontró una correlación negativa de 5mC con la acumulación de PrP^{Sc} y la vacuolización, aunque la significación estadística de esta correlación se perdió al considerar solo el conjunto de animales con scrapie. Esta disminución de la inmunotinción de 5mC no está relacionada con la pérdida de células debida a la toxicidad priónica y la consiguiente pérdida de núcleos, ya que la inmunorreactividad se normalizó teniendo en cuenta el número de núcleos en cada zona. Por tanto, se trata de una disminución real de la inmunotinción dentro del núcleo de las diferentes poblaciones celulares.

En el caso de los perfiles de 5hmC, existen discrepancias entre diversos estudios realizados en Alzheimer y Parkinson. En pacientes clínicos y preclínicos de Alzheimer, varias regiones cerebrales muestran niveles elevados de 5hmC [189,191,192]. Este incremento también se ha observado en modelos murinos de Alzheimer [190,193] y en el cerebelo de pacientes con Parkinson [194,195]. Sin embargo, otros estudios muestran una disminución de 5hmC en la corteza entorrinal y en el cerebelo de pacientes con Alzheimer [196] y en el cerebro de ratones transgénicos de Alzheimer [197,198]. En nuestro estudio, a diferencia de la 5mC, los niveles de 5hmC mostraron resultados opuestos entre ovejas y ratones. Se encontró un aumento de los niveles de 5hmC en ratones preclínicos, mientras que en ovejas clínicas y preclínicas los niveles de 5hmC disminuyeron en diferentes áreas del SNC. Las diferencias entre el modelo experimental y el natural pueden deberse a diferencias en el estadio de la enfermedad en los animales preclínicos: una inoculación controlada de scrapie en ratones permite sacrificar los animales en un verdadero estadio preclínico claramente distinto de la fase clínica, mientras que las ovejas preclínicas pueden detectarse en un estadio tardío, más cercano al inicio de los síntomas.

No se encontró ninguna asociación entre las lesiones priónicas y los niveles de 5hmC en ratones. En ovejas, en cambio, al igual que la 5mC, los niveles de 5hmC se correlacionaron negativamente con los depósitos de PrP^{Sc} y la vacuolización, aunque también se perdió la significación estadística de esta correlación al considerar solo el conjunto de animales con scrapie, lo que sugiere que dicha correlación está ligada al curso de la enfermedad, pero no al grado de lesión. En el modelo natural, la 5hmC sigue la misma tendencia de disminución

que la 5mC. Esta correlación positiva entre 5mC y 5hmC se ha descrito en otros estudios de pacientes con autismo [199] y Alzheimer [191]. Esta disminución concurrente de 5mC y 5hmC, en lugar de una correlación negativa que podría relacionarse con el incremento de 5hmC como consecuencia de la disminución de los niveles de 5mC, sugiere que 5hmC podría tener un papel específico en la patología de las enfermedades priónicas y no solo actuar como un intermediario de desmetilación de 5mC.

En cuanto a los análisis de expresión de genes codificantes de proteínas involucradas en la regulación epigenética en la región del tálamo, encontramos algunos cambios de expresión significativos en los animales con scrapie. Durante el establecimiento de los patrones de metilación del DNA, Dnmt3b interactúa con Hdac1 [200]. Además, esta enzima, junto con su papel en la metilación de novo del DNA, también funciona como una deshidroximetilasa del DNA capaz de convertir directamente la forma 5hmC en una citosina (C) no metilada [201]. En los ratones preclínicos, observamos una disminución de la expresión de *Dnmt3b*, mientras que en los ratones clínicos esta disminución se recuperaba aumentando la expresión de *Dnmt3b* hasta niveles normales. Este descenso temprano de la expresión no se correlacionó con los niveles de 5mC ni 5hmC en el tálamo. En ovejas, no se observaron cambios significativos en la expresión del gen *DNMT3B* ni tampoco una asociación con los niveles de 5mC y 5hmC. Por tanto, esta modificación de la expresión génica podría estar relacionada con otros procesos biológicos. En el cerebro adulto, Dnmt3b es necesaria para la neurogénesis, facilitando la maduración neuronal en el hipocampo de ratones adultos [202] e interviene en la regulación de la memoria de reconocimiento de objetos y lugares [203]. Hdac1 también es necesaria para la diferenciación neuronal de las células madre neurales del hipocampo murino [204] y está implicada en las vías de reparación del DNA y en la función cognitiva [205], incluido el condicionamiento del miedo [206]. Esta última función cerebral está comprometida en pacientes con esquizofrenia [206]. Se ha detectado un aumento de *HDAC1* en la corteza prefrontal de pacientes con esquizofrenia [207] y la sobreexpresión de esta enzima parece mejorar la función cognitiva de condicionamiento del miedo en ratones [206]. El aumento de expresión de *Hdac1* observado en ratones Tg338 clínicos podría ser un mecanismo compensatorio para intentar mantener niveles equilibrados de 5mC y 5hmC y, al mismo tiempo, contrarrestar los efectos neurodegenerativos producidos por la enfermedad de scrapie.

En ovejas clínicas, se observó un aumento de la expresión de *HDAC2*. Las enzimas Hdac1 y Hdac2 son esenciales para mantener patrones correctos de metilación del DNA durante el desarrollo preimplantacional en embriones de ratón. Una deficiencia de estas enzimas en los embriones murinos provoca un aumento de las formas de metilación del DNA 5mC y

5hmC [208]. Por tanto, el aumento de *HDAC2* observado en ovejas clínicas podría contribuir a la disminución de los niveles de 5mC y 5hmC. El aumento de expresión de *HDAC2* también se ha observado en el cerebro de pacientes con Alzheimer [209] y Parkinson [210], y la sobreexpresión de esta enzima se ha correlacionado con una reducción de la memoria de reconocimiento [211,212]. En un modelo murino de Alzheimer, la inhibición de *HDAC2* ralentiza la progresión de la enfermedad mejorando las alteraciones neuronales inducidas por el amiloide beta [213] y en neuronas derivadas de iPSCs, mejora la respiración mitocondrial y reduce los niveles de péptidos beta amiloides neurotóxicos [214]. Estos hallazgos sugieren que el aumento de expresión de *HDAC2*, además de contribuir a la disminución de 5mC y 5hmC, también podría estar implicado en el agravamiento del proceso neurodegenerativo.

De las dos enzimas TET estudiadas, el gen *Tet1* mostró una expresión disminuida en ratones preclínicos y en ovejas clínicas y preclínicas. La enzima Tet1 es una de las enzimas encargadas de la conversión de 5mC a 5hmC, así como de su posterior oxidación a los intermediarios 5fC y 5caC [215]. La relación entre la expresión de *Tet1* y los niveles de 5hmC es controvertida. En condrocitos de pacientes con osteoartritis, se han observado niveles disminuidos de *TET1* acompañados de niveles aumentados de 5hmC debido a una menor conversión de 5hmC a 5fC o 5caC [216]. Por el contrario, estudios realizados en cáncer muestran una asociación de los niveles de expresión reducidos de TET1 con una disminución de 5hmC [217,218]. Esta enzima también desempeña funciones en el cerebro adulto más allá de su papel en la desmetilación del DNA, siendo necesaria en los procesos de reparación de la mielina [219] y en la regulación del proceso de neuroinflamación, asociándose una disminución de su expresión con una activación anómala de las vías de respuesta inflamatoria [220]. Durante el transcurso de la enfermedad de scrapie, se produce un aumento de la neuroinflamación [221–224]. Además, en ratones *knock-out* de *Tet1* se produce una deficiencia en la neurogénesis adulta y en el aprendizaje espacial y la memoria [225]. La disminución de la expresión de *Tet1* durante la enfermedad de scrapie podría tener diferentes implicaciones funcionales: con respecto a la regulación de los niveles de 5hmC, éstos están positivamente correlacionados con los niveles de *Tet1* en el tálamo de los ratones y descienden cuando la expresión de este gen está disminuida. Por otro lado, la disminución de este gen también podría estar implicada en el deterioro de la reparación de la mielina y las vías de neuroinflamación, y en la interrupción del proceso de neurogénesis, contribuyendo en conjunto a la progresión de la enfermedad.

Tras estos dos estudios de metilación del DNA en la enfermedad de scrapie, se puede concluir que este mecanismo epigenético está involucrado en la patogenia de la enfermedad. En los animales infectados con scrapie, existen cambios globales de metilación

en distintas zonas del SNC, así como en genes concretos, que podrían tener funciones neuroprotectoras o contribuir al desarrollo de la enfermedad. Las formas de metilación 5mC y 5hmC podrían desempeñar cada una un papel concreto en la enfermedad de scrapie. Además, distintas enzimas reguladoras epigenéticas también muestran una expresión diferencial en los animales afectados. Se necesitan más estudios para determinar si estos cambios detectados son causa o consecuencia de los fenómenos neurodegenerativos producidos en la enfermedad de scrapie. Realizar estudios de secuenciación genómica oxidativa con bisulfito también serían de gran ayuda, ya que esta tecnología permite diferenciar entre las formas 5mC y 5hmC, por lo que se podrían obtener perfiles genómicos de cada una de las formas, así como detectar cambios de metilación e hidroximetilación en genes concretos, pudiendo evaluar posteriormente su efecto en la expresión. Por último, también sería indispensable investigar sobre las funciones exactas de las distintas enzimas epigenéticas en la progresión de la enfermedad y evaluar su posible potencial terapéutico.

2. Las células madre mesenquimales como modelo celular de scrapie ovino

En el trabajo que da lugar al cuarto artículo de esta tesis titulado "*Effect of Scrapie Prion Infection in Ovine Bone Marrow-Derived Mesenchymal Stem Cells and Ovine Mesenchymal Stem Cell-Derived Neurons*", procedimos a infectar con inóculo cerebral de ovejas con scrapie células madre mesenquimales ovinas derivadas de médula ósea cultivadas en monocapa en condiciones de crecimiento y diferenciación neurogénica. Posteriormente, evaluamos el efecto de la infección sobre la proliferación y viabilidad celulares y la capacidad de estas células para infectarse y replicar el prion.

Las MSCs son capaces de migrar a tejidos cerebrales afectados por priones. Esta migración parece estar mediada por la secreción de distintos factores tróficos y quimiotácticos, que activan mecanismos reparadores en el cerebro lesionado [141,142,226]. En nuestro estudio, tras la inoculación, la viabilidad celular fue mayor tanto en los cultivos de MSCs en condiciones de crecimiento como en los de diferenciación neurogénica en comparación con los cultivos control no inoculados, sugiriendo que los inóculos cerebrales, independientemente de su origen, pueden contener factores que estimulen la proliferación de las MSCs. Este efecto se observó inmediatamente después de poner en contacto las células con los priones en un único pase y también a más largo plazo. Tras la inoculación con scrapie, los cultivos de MSCs en crecimiento mostraron una alta tasa de proliferación, con un tiempo medio de duplicación (DT, en inglés *cell doubling time*) durante los tres pases inferior al DT descrito previamente para cultivos de MSCs derivados de ovejas con scrapie y ovejas sanas [119].

Por otra parte, a diferencia de las MSCs murinas que son capaces de mantener y propagar la infección priónica durante muchos pases sucesivos [143,144], las MSCs ovinas, en cambio, no

parecen ser permisivas a la infección con scrapie. La pérdida de señal de PrP^{Sc} detectada por ELISA a lo largo del tiempo (dentro de un mismo pase) en los cultivos en condiciones de crecimiento poco después de la infección con inóculos positivos sugiere que estas células se infectan, pero son incapaces de mantener y replicar el prion, a diferencia de lo que ocurre en ratones. Del mismo modo, cuando se analizó mediante Western blot la presencia de PrP^{Sc} en cultivos en crecimiento infectados con scrapie en tres pases sucesivos tras la inoculación, la señal de PrP^{Sc} también se debilitó entre los pases 2 y 3, indicando que las MSCs captan la PrP^{Sc} pero no mantienen la infección. En otros trabajos con MSCs murinas, se ha descrito que tras la infección *in vitro* con priones, estas células muestran una producción escasa o nula de PrP^{Sc} durante los 10 o incluso 50 primeros pases [136,145], pero posteriormente la producción de esta proteína se estabiliza. En nuestro caso, no pudimos explorar esta posibilidad porque, a diferencia de las células murinas, las MSCs obtenidas de humanos o de organismos modelo no convencionales como las ovejas, pueden mantenerse en cultivo durante muchos menos pases [227,228].

La división celular limita la acumulación de priones en las células en cultivo [229] y la proximidad directa entre células donantes y receptoras facilita la infección en otros modelos de cultivo celular [230]. La alta tasa de proliferación observada en las MSCs ovinas inoculadas con scrapie podría dificultar la transmisión de PrP^{Sc} de las células infectadas a las no infectadas, debido a que las células no estén en contacto durante un tiempo suficiente. De esta forma, solo las células infectadas durante el proceso de inoculación y sus hijas mostrarían infección y ésta se diluiría en pases sucesivos.

Por otro lado, tampoco podemos descartar la posibilidad de que la infección con scrapie pueda ser tóxica para los cultivos de MSCs ovinas. Aunque no se ha observado toxicidad en las MSCs murinas infectadas con CJD [136], hay que tener en cuenta que nuestras células proceden de una especie naturalmente susceptible a la enfermedad. En nuestro estudio, el número de duplicación celular (CD, en inglés *cell doubling number*) fue significativamente mayor en las células infectadas con extractos de cerebro sano y, en consecuencia, el DT fue mayor en las células infectadas con inóculos positivos. Por lo tanto, de manera similar a los hallazgos observados en MSCs obtenidas de ovejas con scrapie respecto a ovejas control [119], las células infectadas con scrapie mostraron un potencial de proliferación menor que las células infectadas con inóculo negativo. No obstante, a lo largo de los pases, las diferencias de CD y DT entre los cultivos infectados con inóculo de ovejas con scrapie y ovejas sanas fueron reduciéndose. En el mismo pase tras la infección, 3 días después de la inoculación la viabilidad era menor en los cultivos con scrapie que en los cultivos con inóculo negativo, sin embargo, a los 10 días tras la inoculación el número de células en los cultivos infectados con

scrapie era superior al de los cultivos infectados con inóculo negativo. La disminución temprana de la proliferación y la viabilidad de los cultivos infectados con scrapie podría ser consecuencia de la pérdida de células infectadas debido a la toxicidad ejercida por los priones. El aumento posterior de ambos parámetros coincidió con la pérdida de detección de PrP^{Sc}, lo que podría indicar una recuperación de las condiciones de cultivo celular tras la eliminación de las células infectadas, aumentando la proporción de células no infectadas, las cuales muestran un mayor potencial de proliferación.

En cuanto a las MSCs ovinas en condiciones de diferenciación neurogénica, aunque también se observó cierta toxicidad 3 días después de la infección con scrapie, cuatro de los cinco cultivos analizados parecían haberse infectado y el ensayo ELISA mostró que la señal de PrP^{Sc} en estas células aumentaba progresivamente con el tiempo. De forma similar, los astrocitos derivados de iPSCs humanas son capaces de replicar priones de muestras cerebrales de pacientes con CJD, generando infectividad priónica *in vitro* [231]. Teniendo esto en cuenta y sabiendo que las células del SNC son la diana de la PrP^{Sc}, las MSCs ovinas en condiciones de diferenciación neurogénica podrían tener una mayor capacidad de capturar y replicar el prion que las MSCs en condiciones de crecimiento.

Teniendo en cuenta que las células en condiciones de crecimiento y diferenciadas tenían un mismo fondo genético, las diferencias observadas en cuanto a la capacidad para multiplicar el prion sugieren que las células en condiciones neurogénicas poseen alguna característica que las hace más aptas para la infección que no está presente en las MSCs indiferenciadas.

En este trabajo, se muestra por primera vez el efecto que tiene la infección de scrapie sobre las células madre mesenquimales ovinas tanto en condiciones de crecimiento como en condiciones de diferenciación neurogénica. Hay que tener en cuenta que este estudio se ha realizado en células cultivadas en monocapa, es decir, en un sistema en dos dimensiones. Estos sistemas no son capaces de mimetizar el ambiente ni las interacciones de las células en condiciones *in vivo* y, por tanto, su capacidad para modelar una enfermedad es más limitada. Esta limitación se puede solventar mediante el uso de sistemas de cultivo en tres dimensiones. Uno de estos sistemas es el cultivo en esferoides celulares, el cual permite mejorar la interacción entre las células aumentando el contacto entre ellas y creando un ambiente más similar a las condiciones *in vivo*. Por ello, el cultivo en 3D podría facilitar la propagación de priones en las MSCs ovinas. Teniendo en cuenta este nuevo enfoque, decidimos plantear el quinto trabajo de esta tesis que se presenta en el artículo titulado "*Susceptibility of ovine bone marrow-derived mesenchymal stem cell spheroids to scrapie prion infection*", donde evaluamos cómo afectan las condiciones 3D a las células madre mesenquimales ovinas en cuanto a su respuesta a la infección con scrapie tanto en

condiciones de crecimiento como de diferenciación neurogénica. Al igual que en el estudio anterior, analizamos su capacidad de captación del prion, así como el efecto de dicha infección sobre la viabilidad celular.

En este estudio, partimos de un único cultivo celular cultivado en monocapa y en forma de esferoides para analizar las posibles diferencias entre el sistema 2D y 3D.

En cuanto al cultivo en monocapa, al igual que en el estudio anterior, observamos un descenso en los niveles de PrP^{Sc} en las MSCs ovinas infectadas con scrapie a lo largo del tiempo de cultivo, mientras que en condiciones de diferenciación neurogénica los niveles de PrP^{Sc} se mantuvieron estables.

En las enfermedades priónicas, la infección de un modelo celular 3D solo se ha descrito en organoides cerebrales formados a partir de iPSCs humanas, los cuales son capaces de captar y propagar priones de sCJD [158]. En nuestro estudio, a diferencia de los cultivos 2D, los esferoides en condiciones de crecimiento fueron capaces de mantener niveles estables de PrP^{Sc} a lo largo del tiempo. Por otra parte, al igual que las células cultivadas en monocapa, los esferoides en condiciones neurogénicas también captaron y mantuvieron los niveles de PrP^{Sc}. Las diferencias en el microambiente de las MSCs en condiciones 2D y 3D podrían explicar los distintos resultados observados entre las MSCs infectadas con scrapie cultivadas en monocapa y los esferoides infectados con scrapie en condiciones de crecimiento. Se ha descrito que dentro de los esferoides derivados de MSCs se forma un microambiente específico más similar a las condiciones *in vivo*, en el que la difusión de nutrientes y gases hacia el interior y de desechos metabólicos hacia el exterior está limitada [232,233]. Además, en esferoides derivados de MSCs, se ha observado una disminución del tamaño celular, así como quiescencia del ciclo celular y reducción del metabolismo energético en comparación con las MSCs cultivadas en monocapa [232,234,235], factores que contribuyen al desarrollo de la enfermedad priónica. Nuestros resultados sugieren que el microambiente 3D hace que las MSCs ovinas sean más permisivas a la infección con priones cuando se cultivan en condiciones de crecimiento, a la vez que mantiene la capacidad para absorber y retener el prion en condiciones neurogénicas.

En este segundo estudio con MSCs, hemos encontrado algunas diferencias con el trabajo anterior respecto al efecto de la inoculación con scrapie en la viabilidad celular de las MSCs cultivas en 2D. En el estudio anterior, las MSCs infectadas con extractos cerebrales de ovejas sanas e infectadas con scrapie en condiciones de crecimiento y diferenciación neurogénica mostraban niveles crecientes de viabilidad celular a lo largo del tiempo de cultivo en comparación con las células no inoculadas, sugiriendo que los inóculos cerebrales pueden contener factores que estimulen la proliferación de las MSCs. De manera similar, en este

estudio, las MSCs infectadas con scrapie en condiciones de crecimiento mostraron niveles de viabilidad celular superiores a los controles no inoculados justo después de retirar el inóculo. Sin embargo, no observamos este aumento en las células inoculadas con inóculo negativo. Las MSCs en condiciones de diferenciación neurogénica infectadas con scrapie también mostraron un aumento de la viabilidad celular inmediatamente después de estar en contacto con el inóculo, pero posteriormente se observó toxicidad con una consecuente disminución de la viabilidad. Por tanto, el efecto de los inóculos cerebrales sobre la proliferación de las MSCs parece variar entre cultivos. Esta variación podría explicarse por la heterogeneidad celular encontrada en las MSCs, en las que el donante, el tipo de tejido de procedencia, el entorno de cultivo, los métodos de aislamiento y el pase celular pueden afectar al fenotipo [236,237], haciendo que los distintos cultivos reaccionen de forma ligeramente diferente a los homogeneizados cerebrales. Por otro lado, también hay que tener en cuenta que los inóculos cerebrales utilizados son diferentes a los del primer estudio. Las cantidades de PrP^{Sc} iniciales podrían ser diferentes, lo que afectaría a la reacción de las MSCs a la infección. No obstante, la respuesta temprana a la infección con scrapie fue la misma en ambos estudios: un incremento de la viabilidad celular, lo que implica un mayor potencial de proliferación tanto en condiciones de crecimiento como neurogénicas en el cultivo en monocapa.

Los esferoides de MSCs ovinas inoculados con inóculo positivo y negativo mostraron patrones de viabilidad diferentes a los de las células cultivadas en monocapa tanto en condiciones de crecimiento como de diferenciación. El inóculo negativo aumentó la viabilidad de los esferoides tanto en condiciones de crecimiento como neurogénicas. Sin embargo, este aumento no se observó en los esferoides infectados con scrapie, que se mantuvieron en niveles de viabilidad similares a los esferoides control no inoculados. En comparación con las MSCs cultivadas en monocapa, los esferoides de MSCs humanas muestran una mayor supervivencia celular y un mayor rendimiento y capacidad de crecimiento celulares [238–240]. Esta mayor viabilidad de los esferoides parece estar mediada por la inducción de la autofagia y la supresión de las especies reactivas de oxígeno (ROS) [240]. En la enfermedad de scrapie, se ha descrito una alteración del proceso de autofagia en el SNC de ovino infectado con scrapie [173,174] y en modelos murinos de la enfermedad [172]. La menor viabilidad observada en los esferoides infectados con scrapie, sobre todo en condiciones de crecimiento, respecto a los inoculados con inóculo negativo podría deberse a una disfunción en el mecanismo de autofagia causada por la infección priónica que podría contrarrestar el efecto positivo ejercido por los factores neurotróficos del cerebro. Estos resultados sugieren que las condiciones 3D mejoran en la mayoría de los casos la viabilidad

de las MSCs inoculadas, ya que los esferoides infectados mantienen niveles de viabilidad similares o superiores a los de los esferoides control no inoculados. Es probable que los priones ejerzan su toxicidad sobre los esferoides infectados con scrapie limitando su potencial de crecimiento y contrarrestando la estimulación ejercida por los factores neurotróficos cerebrales.

Los análisis de infección y viabilidad celular demuestran que los esferoides derivados de MSCs ovinas en condiciones de crecimiento y neurogénicas son capaces de captar y mantener los niveles de PrP^{Sc} e imitar la toxicidad priónica, lo que convierte a este enfoque tridimensional en un posible modelo *in vitro* para estudiar la enfermedad de scrapie en un entorno más parecido al *in vivo*.

En condiciones de crecimiento, tanto en el primer estudio de MSCs cultivadas en dos dimensiones como en el segundo estudio de esferoides celulares, pudimos observar cierto grado de toxicidad celular inmediatamente después de la infección con inóculos cerebrales de scrapie, lo que sugería un efecto tóxico de la infección priónica en las MSCs ovinas. Con el objetivo de profundizar en los posibles mecanismos implicados en esta toxicidad y en la capacidad de infección de las MSCs ovinas, planteamos el último estudio de esta tesis doctoral titulado "*RNA-sequencing transcriptomic analysis of scrapie-infected ovine mesenchymal stem cells*", en el cual realizamos un análisis transcriptómico de células madre mesenquimales ovinas infectadas con scrapie mediante la tecnología de secuenciación de RNA de nueva generación *RNA-seq*, para identificar genes diferencialmente expresados (DEGs) en estas células, así como posibles rutas y funciones biológicas alteradas. Tras el análisis transcriptómico y la identificación de DEGs, evaluamos mediante RT-qPCR la expresión de 11 genes seleccionados del conjunto de DEGs identificados con el objetivo de validar los resultados obtenidos en el *RNA-seq*.

En este estudio, también partimos de un único cultivo de MSCs ovinas cultivadas en monocapa en condiciones de crecimiento, analizando tres condiciones distintas en dos tiempos de infección. Las condiciones fueron: MSCs infectadas con homogeneizado cerebral de ovejas con scrapie, MSCs inoculadas con homogeneizado cerebral de ovejas sanas y MSCs sin inocular. Las células se mantuvieron en contacto con los inóculos 2 días y los tiempos de infección seleccionados para el análisis transcriptómico fueron 2 días (inmediatamente después de eliminar el inóculo) y 4 días después de la inoculación. Para comprobar la viabilidad de las MSCs en las tres condiciones de estudio, así como los niveles de PrP^{Sc} en los distintos tiempos de infección en las MSCs infectadas, realizamos respectivamente un ensayo MTT y un ELISA. Los resultados obtenidos en ambos ensayos fueron similares a los del primer estudio en MSCs ovinas cultivadas en monocapa: la señal de PrP^{Sc} fue mermando

a lo largo del tiempo y la viabilidad celular disminuyó poco después de la inoculación debido a la toxicidad ejercida por los priones.

En los dos tiempos de infección, se identificaron DEGs entre los distintos grupos, detectándose el mayor número de DEGs en el primer tiempo de infección (2 días tras la inoculación). En este tiempo, se encontraron un total de 2.777 genes entre las MSCs infectadas con scrapie y las MSCs con inóculo negativo, 4.502 genes entre las MSCs infectadas con scrapie y las no inoculadas, y 5.685 genes entre las MSCs con inóculo negativo y las no inoculadas. Por otro lado, en el segundo tiempo de infección, se identificaron 469 genes con expresión diferencial entre las MSCs infectadas con scrapie y las MSCs con inóculo negativo, 1.897 genes entre las MSCs infectadas con scrapie y las no inoculadas, y 3.197 genes entre las MSCs con inóculo negativo y las no inoculadas. El mayor número de DEGs detectado coincidió con el momento en el que las MSCs ovinas habían estado en contacto con los diferentes inóculos y la cantidad de PrP^{Sc} era mayor en los cultivos positivos, indicando que estas células reaccionan de manera temprana a la infección priónica pudiendo desencadenar mecanismos que podrían contribuir a la toxicidad priónica.

En cuanto a los análisis de enriquecimiento de GO y KEGG, los DEGs identificados entre las MSCs infectadas con scrapie y las MSCs infectadas con inóculo negativo en los dos tiempos de infección fueron los que mostraron un mayor enriquecimiento en distintas rutas y funciones biológicas, de las cuales se pueden destacar: unión a GTPasas, componente estructural del ribosoma, complejo ribonucleoproteico, procesos metabólicos, unión a proteínas del citoesqueleto, fosforilación proteica, actividad oxidorreductasa, adhesión celular, componentes de la matriz extracelular (ECM), unión a iones de calcio y hierro, senescencia celular, ferroptosis, procesamiento de proteínas en el retículo endoplasmático, glicólisis, vías de señalización de wnt y TGF-beta, y los términos de enfermedades neurodegenerativas *prion-like* Alzheimer, Parkinson y Huntington.

Algunas de estas funciones enriquecidas en los genes que muestran expresión alterada en las MSCs infectadas con scrapie estaban asociadas con las funciones conocidas de la PrP^{C}, la cual está implicada en varios procesos biológicos como la adhesión celular, la homeostasis del calcio y la regulación de componentes del citoesqueleto y de la matriz extracelular [241–245]. Además de interactuar con proteínas de la ECM, esta proteína también interacciona con GTPasas para regular el tráfico de proteínas [244] y protege a las células de la senescencia celular prematura [246]. La PrP^{C} también participa en diferentes vías de señalización, como las vías TGF-beta [247] y Wnt [248], estando esta última alterada en el cerebro de ratones infectados con scrapie [249]. Otra función alterada en las enfermedades priónicas es la homeostasis del hierro, pues la PrP^{C} participa en la captación de hierro [250]. En el cerebro de pacientes con

CJD, se ha descrito un desequilibrio en los niveles de hierro, probablemente debido a un secuestro del hierro en complejos proteicos de PrP^{Sc} que incluyen ferritina [251,252]. Estos complejos son redox activos y pueden crear un entorno citotóxico [253]. Por tanto, el enriquecimiento de genes implicados en estas funciones en las MSCs ovinas infectadas con scrapie indica que estas células parecen ser capaces de reproducir la disfunción de distintos procesos regulados por la PrP^{C} cuando se produce la conversión de PrP^{C} a PrP^{Sc} causando un desequilibrio de la homeostasis celular y toxicidad.

Otros términos enriquecidos en las células infectadas fueron los ribosomas y el complejo ribonucleoproteico. Los ribosomas son orgánulos que participan en la síntesis de proteínas, pero también están implicados en el plegamiento de proteínas [254]. La actividad de plegamiento de proteínas del ribosoma (PFAR) se ha asociado con la propagación de priones y otras proteínas mal plegadas, y los fármacos anti-PFAR parecen reducir la propagación de la PrP^{Sc} *in vitro* [255,256]. Por otro lado, los DEGs de las células infectadas se asociaron con las enfermedades de Alzheimer, Parkinson y Huntington, enfermedades *prion-like* que comparten características patogénicas con las enfermedades priónicas, y con la ferroptosis, que es un tipo de muerte celular programada resultante de la acumulación de hierro y la peroxidación lipídica [257] que se ha asociado con la fisiopatología de diferentes enfermedades, incluyendo el cáncer [258] y las enfermedades *prion-like* [259]. Estos mecanismos enriquecidos en las MSCs infectadas con scrapie podrían contribuir a la propagación de la PrP^{Sc} y a la muerte celular.

Del conjunto de DEGs identificados en el primer tiempo de infección entre las MSCs infectadas con scrapie y las MSCs inoculadas con inóculo negativo, analizamos la expresión de once genes mediante RT-qPCR con la finalidad de validar los datos de expresión obtenidos mediante el *RNA-seq*. Se validó la expresión de siete de los once genes. La mayoría de los genes analizados mostraron un perfil de expresión acorde con el observado en el análisis transcriptómico. Tres genes (*MMP1*, *MMP12* y *SERPINB2*) estaban significativamente disminuidos en las células infectadas con scrapie en comparación con las células inoculadas con inóculo negativo, mientras que cuatro genes (*PGAP4*, *PDK4*, *PRR11* y *F13A1*) estaban significativamente aumentados. Los otros cuatro genes restantes (*RPS15A*, *SAA3*, *PTGS1* y *CYP1A1*) no mostraron cambios de expresión significativos. En general, los resultados de RT-qPCR concordaron con el perfil de secuenciación, respaldando la validez de los resultados transcriptómicos.

Los genes *MMP1* y *MMP12* codifican dos metaloproteinasas de la matriz (MMPs). Las MMPs son endopeptidasas extracelulares implicadas en la remodelación de la ECM y en la degradación de sus constituyentes [260,261]. La ECM es una estructura dinámica sometida a una

remodelación controlada, y el equilibrio entre la síntesis, el desarrollo y la degradación de sus componentes es esencial para garantizar una correcta fisiología [262]. La expresión alterada de las MMPs puede alterar este equilibrio homeostático y dar lugar a diversas condiciones patológicas [262]. Además, una actividad proteolítica excesiva de las MMPs se ha asociado con la patogénesis de varias enfermedades del SNC, como la isquemia cerebral, las enfermedades de Parkinson y Alzheimer, y los traumatismos cerebrales [263]. Las enzimas MMP1 y MMP12 también están implicadas en el proceso de inflamación del SNC. La expresión de *MMP12* está aumentada en cerebros envejecidos de ratones potenciando la neuroinflamación [264], y el aumento de expresión de *MMP1* en la microglía de ratas tratada con el péptido priónico sintético 106-126 se acompaña de un incremento de varias citoquinas y mediadores inflamatorios [265]. La desregulación de genes que codifican proteínas implicadas en la remodelación de la ECM también se ha descrito en otros modelos *in vitro* en los que la inhibición de las MMPs 2-9 se ha relacionado con un aumento de la propagación del prion [266]. La disminución de la expresión de estos dos genes en las MSCs infectadas con scrapie también podría estar relacionada con la propagación del prion, ya que los componentes de la ECM, incluidas las proteasas, pueden interactuar con proteínas patológicas mal plegadas regulando su capacidad de propagación [267].

La proteína codificada por el gen *SERPINB2* funciona como una proteína de respuesta al estrés con actividad citoprotectora. En fibroblastos murinos embrionarios transfectados con huntingtina mutada, *SERPINB2* modula la capacidad de degradación y la agregación de proteínas, y protege a las células de la proteotoxicidad asociada al mal plegamiento de proteínas y a la disfunción de la proteostasis [268]. Por tanto, la disminución de la expresión de este gen durante la infección con priones podría ser un indicador de citotoxicidad en las MSCs ovinas.

PGAP4 es un gen que codifica la proteína GalNAc transferasa 4, una GalNAc transferasa GPI-específica que cataliza la primera reacción para generar la cadena GalNAc, una modificación postraduccional que se encuentra en diferentes proteínas, incluida la PrP^{C} [269]. Esta cadena lateral GPI-GalNAc parece estar implicada en la conversión de PrP^{C} a PrP^{Sc} [270]. En un estudio en ratones *knock-out* de *PGAP4* infectados con priones, se observó que estos ratones mostraban periodos de incubación más cortos que los ratones de tipo salvaje o *wild type*, indicando un posible papel protector del gen *PGAP4* y de la cadena lateral GPI-GalNAc frente a la patología priónica [271]. El aumento de expresión del gen *PGAP4* en las MSCs ovinas podría ser un mecanismo neuroprotector activado en respuesta a la infección con scrapie.

El gen *PDK4* codifica la enzima piruvato deshidrogenasa quinasa 4. La PrP^{C} es un regulador del metabolismo de la glucosa que orienta el metabolismo energético hacia la degradación

oxidativa mitocondrial de la glucosa. Esta regulación la realiza acoplándose a la vía de señalización del AMP cíclico y la proteína quinasa A, la cual atenúa la expresión de *PDK4*. Esta utilización preferente de la glucosa limita la beta oxidación de los ácidos grasos y la aparición de condiciones de estrés oxidativo [272]. En el hipocampo de ratones infectados con priones, se ha observado una sobreexpresión de *PDK4* junto con una disminución de la degradación oxidativa de la glucosa y un aumento del estrés oxidativo asociado al catabolismo de los ácidos grasos. Además, la inhibición de *PDK4* prolongó el tiempo de supervivencia de estos ratones [272]. La pérdida de PrP^{C} durante la infección con scrapie en las MSCs ovinas podría provocar un aumento de expresión de *PDK4* que condujera a condiciones de estrés oxidativo en estas células debido a una desregulación del metabolismo de la glucosa.

PRR11 es un gen asociado a tumores que interviene en el ciclo celular, la tumorigénesis y la metástasis, cuya expresión está aumentada en diferentes tipos de cáncer, como el cáncer gástrico y el pulmonar [273–275]. En las células de cáncer pulmonar no microcítico, el silenciamiento de *PRR11* induce la autofagia e inhibe la proliferación celular [274]. Como ya se ha mencionado, existe una alteración del proceso de autofagia en la enfermedad de scrapie [172,174]. El aumento de *PRR11* observado en nuestro estudio podría reducir la actividad autofágica de las células favoreciendo la formación de PrP^{Sc}. Por último, la expresión de *F13A1* se ha asociado con vías proinflamatorias y de estrés celular en el tejido adiposo [276,277]. Dado que observamos un aumento de expresión de este gen en las MSCs ovinas, cabe suponer que las vías descritas en el tejido adiposo también podrían activarse en las MSCs como consecuencia de la infección priónica.

Este estudio transcriptómico muestra, por tanto, que las células madre mesenquimales ovinas infectadas con scrapie expresan de forma diferencial genes involucrados en distintas vías relacionadas con la propagación y la toxicidad priónicas. Además, la validación de una batería de genes que podrían desempeñar un papel en la neuropatología de las enfermedades priónicas abre un nuevo campo de estudio para la investigación del comportamiento y la función de estos genes en condiciones *in vivo*, pudiendo analizar también su potencial uso como biomarcadores o dianas terapéuticas.

Tras estudiar la capacidad de infección de las MSCs ovinas en condiciones 2D y 3D, analizar el efecto de dicha infección sobre su proliferación y viabilidad, y profundizar a nivel transcriptómico en los mecanismos de infección y toxicidad priónicas, se puede concluir que estas células son un modelo *in vitro* capaz de infectarse y de reproducir la toxicidad ejercida por los priones tanto cultivadas en monocapa como en un entorno más similar al *in vivo* en forma de esferoides, siendo unas candidatas óptimas para ahondar en el estudio de los

mecanismos patogénicos de las enfermedades priónicas y para el desarrollo de futuras terapias.

Conclusiones/Conclusions

Conclusiones

Los resultados obtenidos en la presente tesis doctoral han permitido llegar a las siguientes conclusiones:

1. En tálamo de ovino con scrapie, la metilación diferencial de genes involucrados en distintas funciones biológicas reguladas por la proteína prion celular, la validación *de novo* de cambios de expresión de genes con metilación diferencial e *in silico* de genes con expresión diferencial previamente descritos en scrapie indican que este mecanismo epigenético está involucrado en la neuropatología asociada a la enfermedad.
2. Las funciones de los genes que muestran metilación diferencial podrían tener un papel neuroprotector y/o intervenir en la progresión de la enfermedad.
3. Los perfiles inmunohistoquímicos de 5mC y 5hmC en el SNC de ovejas infectadas con scrapie de manera natural y de un modelo murino transgénico de scrapie muestran cambios en ambas formas de metilación del DNA desde la fase preclínica de la enfermedad, sugiriendo que tanto 5mC como 5hmC podrían desempeñar una función concreta en la enfermedad de scrapie.
4. La expresión diferencial de genes que intervienen en la regulación de los niveles de 5mC y 5hmC y en distintas funciones cerebrales detectada en ovejas infectadas con scrapie y en el modelo murino indican su posible implicación en la patología de la enfermedad y su potencial uso como dianas terapéuticas.
5. Las MSCs ovinas cultivadas en condiciones de crecimiento son más permisivas a la infección con scrapie cuando se encuentran en forma de esferoides tridimensionales y no en monocapa, siendo capaces de mantener los niveles de PrP^{Sc} a lo largo del tiempo de cultivo, lo que indica que el microambiente generado en los esferoides fomenta la captación del prion.
6. Las MSCs ovinas en condiciones de diferenciación neurogénica son capaces de mantener la infección con scrapie de manera estable a lo largo del tiempo de cultivo tanto en forma de esferoides como cultivadas en monocapa, siendo ambos sistemas de cultivo celular permisivos a la infección priónica y útiles como modelo celular para la replicación del prion.
7. La infección con scrapie de las MSCs ovinas en condiciones de crecimiento y diferenciación neurogénica, tanto cultivadas en monocapa como en esferoides, afecta a la viabilidad y proliferación celular confirmando la idoneidad del modelo para el estudio de la toxicidad de la infección priónica.

8. El estudio transcriptómico de MSCs ovinas infectadas con scrapie en condiciones de crecimiento identificó genes con expresión diferencial involucrados en funciones relacionadas con la propagación y la toxicidad priónicas, corroborando que las MSCs ovinas, además de ser capaces de infectarse con scrapie, también reproducen la toxicidad ejercida por el agente priónico, postulándose como un modelo *in vitro* óptimo para el estudio de las enfermedades priónicas.

Conclusions

The results obtained in this doctoral thesis have led to the following conclusions:

1. In the thalamus of scrapie sheep, the differential methylation of genes involved in different biological functions regulated by the cellular prion protein, the *de novo* validation of expression changes in genes with differential methylation and *in silico* of differentially expressed genes previously described in scrapie indicate that this epigenetic mechanism is involved in the neuropathology associated with the disease.
2. The functions of genes showing differential methylation could have a neuroprotective role and/or intervene in disease progression.
3. Immunohistochemical profiles of 5mC and 5hmC in the CNS of naturally scrapie-infected sheep and a transgenic murine model of scrapie show changes in both forms of DNA methylation since the preclinical phase of the disease, suggesting that both 5mC and 5hmC could play a specific role in scrapie disease.
4. The differential expression of genes involved in the regulation of 5mC and 5hmC levels and in different brain functions detected in scrapie-infected sheep and in the murine model indicate their possible involvement in the pathogenesis of the disease and their potential use as therapeutic targets.
5. Ovine MSCs cultured under growth conditions are more permissive to scrapie infection in the form of three-dimensional spheroids than in monolayer, being able to maintain PrP^{Sc} levels throughout the culture time, indicating that the microenvironment generated in the spheroids promotes prion uptake.
6. Ovine MSCs under neurogenic differentiation conditions are able to maintain scrapie infection stably throughout the culture time as spheroids and cultured in monolayer, being both cell culture systems permissive to prion infection and useful as a cell model for prion replication.
7. Scrapie infection of ovine MSCs under growth and neurogenic conditions, in both monolayer and spheroid culture, affects cell viability and proliferation, confirming the suitability of the model for the study of prion toxicity.
8. The transcriptomic study of ovine MSCs infected with scrapie under growth conditions identified differentially expressed genes involved in functions related to prion propagation and toxicity, corroborating that ovine MSCs, in addition to their ability to be infected with scrapie, also reproduce the toxicity exerted by the prion agent, becoming an optimal *in vitro* model for the study of prion diseases.

Apéndices

APÉNDICE 1: Factor de impacto de las revistas y áreas temáticas correspondientes a las publicaciones que se recogen en la tesis.

Factor de impacto de las revistas y áreas temáticas correspondientes a las publicaciones que se recogen en la tesis

1. **International Journal of Molecular Sciences**
   - Artículos:
     I. Hernaiz, Adelaida; Toivonen, Janne Markus; Bolea, Rosa; Martín-Burriel, Inmaculada. **Epigenetic Changes in Prion and Prion-like Neurodegenerative Diseases: Recent Advances, Potential as Biomarkers, and Future Perspectives.** *International Journal of Molecular Sciences. Vol. 23, pág. 12609, 2022.* doi:10.3390/IJMS232012609.
     II. Hernaiz, Adelaida; Sentre, Sara; Betancor, Marina; López-Pérez, Óscar; Salinas-Pena, Mónica; Zaragoza, Pilar; Badiola, Juan José; Toivonen, Janne Markus; Bolea, Rosa; Martín-Burriel, Inmaculada. **5-Methylcytosine and 5-Hydroxymethylcytosine in Scrapie-Infected Sheep and Mouse Brain Tissues.** *International Journal of Molecular Sciences. Vol. 24, pág. 1621, 2023.* doi:10.3390/IJMS24021621.
   - Factor de impacto JCR: 6,208
   - Áreas temáticas: Biochemistry and Molecular Biology (Q1)
2. **Frontiers in Veterinary Science**
   - Artículo:
     Hernaiz, Adelaida; Sanz, Arianne; Sentre, Sara; Ranera, Beatriz; Lopez-Pérez, Óscar; Zaragoza, Pilar; Badiola, Juan José; Filali, Hicham; Bolea, Rosa; Toivonen, Janne Markus; Martín-Burriel, Inmaculada. **Genome-Wide Methylation Profiling in the Thalamus of Scrapie Sheep.** *Frontiers in Veterinary Science. Vol. 0, pág. 29, 2022.* doi:10.3389/FVETS.2022.824677.
   - Factor de impacto JCR: 3,471
   - Áreas temáticas: Veterinary Sciences (Q1)
3. **Animals**
   - Artículo:
     García-mendívil, Laura; Mediano, Diego Rubén; Hernaiz, Adelaida; Sanz-rubio, David; Vázquez, Francisco José; Marín, Belén; López-pérez, Óscar; Otero, Alicia; Badiola, Juan José; Zaragoza, Pilar; Ordovás, Laura; Bolea, Rosa; Martín-Burriel, Inmaculada. **Effect of Scrapie Prion Infection in Ovine Bone Marrow-Derived Mesenchymal Stem Cells and Ovine Mesenchymal Stem Cell-Derived Neurons.** *Animals. Vol. 11, pág. 1137, 2021.* doi:10.3390/ANI11041137.

- Factor de impacto JCR: 3,231
- Áreas temáticas: Veterinary Sciences (Q1); Agriculture, Dairy and Animal Science (Q1)

APÉNDICE 2: Contribución del doctorando.

Departamento de Anatomía, Embriología y Genética Animal
Universidad Zaragoza

Departamento de Patología Animal
Universidad Zaragoza

Dra. Inmaculada Martín Burriel, Catedrática del Departamento de Anatomía, Embriología y Genética Animal, y Dra. Rosa María Bolea Bailo, Vicerrectora de Política Científica y Catedrática del Departamento de Patología Animal de la Facultad de Veterinaria (Universidad de Zaragoza), como directoras de la presente memoria presentada por Adelaida Hernaiz Martorell para optar al grado de Doctor,

CERTIFICAN:

Que Doña Adelaida Hernaiz Martorell ha participado activamente como ejecutora principal en todos los trabajos incluidos en esta tesis doctoral, tanto en la realización de las tareas laboratoriales, como en el análisis de los resultados y la elaboración de las conclusiones y escritura de los manuscritos.

Y para que conste, firmamos el presente documento en Zaragoza, a 17 de enero de 2023.

MARTIN BURRIEL INMACULADA - DNI 25446478Z
Firmado digitalmente por MARTIN BURRIEL INMACULADA - DNI 25446478Z
Fecha: 2023.01.18 11:58:17 +01'00'

Fdo.: Inmaculada Martín Burriel

BOLEA BAILO ROSA MARIA - DNI 72964847S
Firmado digitalmente por BOLEA BAILO ROSA MARIA - DNI 72964847S
Fecha: 2023.01.22 17:42:48 +01'00'

Fdo.: Rosa M.ª Bolea Bailo

APÉNDICE 3: Renuncia de los coautores no doctores de las publicaciones a presentar en otra tesis doctoral los trabajos incluidos en la presente tesis.

Escuela de Doctorado
Universidad Zaragoza

RENUNCIA DE LOS COAUTORES DE LOS TRABAJOS PRESENTADOS COMO PARTE DE UNA TESIS DOCTORAL EN LA MODALIDAD DE COMPENDIO DE PUBLICACIONES

1.- Datos personales del coautor		
Apellidos: Sentre Domingo	Nombre: Sara	
DNI/Pasaporte/NIE: 25200117Y	Teléfono 680109607	Correo electrónico sarasentre@gmail.com

2.- Tesis Doctoral
Título: Biomarcadores epigenéticos y desarrollo de modelos celulares en scrapie ovino
Autor: Adelaida Hernaiz Martorell
Programa de doctorado: Ciencias Biomédicas y Biotecnológicas

3.- Publicaciones que formarán parte de la tesis y de las que el firmante es coautor

Hernaiz, Adelaida; Sanz, Arianne; Sentre, Sara; Ranera, Beatriz; Lopez-Pérez, Óscar; Zaragoza, Pilar; Badiola, Juan José; Filali, Hicham; Bolea, Rosa; Toivonen, Janne Markus; Martín-Burriel, Inmaculada. Genome-Wide Methylation Profiling in the Thalamus of Scrapie Sheep. Frontiers in Veterinary Science. Vol. 0, pág. 29, 2022. doi:10.3389/FVETS.2022.824677.

Hernaiz, Adelaida; Sentre, Sara; Betancor, Marina; López-Pérez, Óscar; Salinas-Pena, Mónica; Zaragoza, Pilar; Badiola, Juan José; Toivonen, Janne Markus; Bolea, Rosa; Martín-Burriel, Inmaculada. 5-Methylcytosine and 5-Hydroxymethylcytosine in Scrapie-Infected Sheep and Mouse Brain Tissues. International Journal of Molecular Sciences. Vol. 24, pág. 1621, 2023. doi:10.3390/IJMS24021621.

RENUNCIA:

Renuncio a que las publicaciones anteriores puedan ser presentadas como parte de otra tesis doctoral en la modalidad de compendio de publicaciones.

<lugar>,<fecha>

Zaragoza 17 de enero de 2023

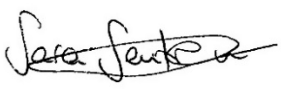

Firma: Sara Sentre Domingo

Escuela de Doctorado
Universidad Zaragoza

RENUNCIA DE LOS COAUTORES DE LOS TRABAJOS PRESENTADOS COMO PARTE DE UNA TESIS DOCTORAL EN LA MODALIDAD DE COMPENDIO DE PUBLICACIONES

1.- Datos personales del coautor		
Apellidos: Marín González	Nombre: Mª Belén	
DNI/Pasaporte/NIE: 09335522Y	Teléfono 976762945	Correo electrónico belenm@unizar.es

2.- Tesis Doctoral
Título: Biomarcadores epigenéticos y desarrollo de modelos celulares en scrapie ovino
Autor: Adelaida Hernaiz Martorell
Programa de doctorado: Ciencias Biomédicas y Biotecnológicas

3.- Publicaciones que formarán parte de la tesis y de las que el firmante es coautor

García-mendívil, Laura; Mediano, Diego Rubén; Hernaiz, Adelaida; Sanz-rubio, David; Vázquez, Francisco José; Marín, Belén; López-pérez, Óscar; Otero, Alicia; Badiola, Juan José; Zaragoza, Pilar; Ordovás, Laura; Bolea, Rosa; Martín-Burriel, Inmaculada. Effect of Scrapie Prion Infection in Ovine Bone Marrow-Derived Mesenchymal Stem Cells and Ovine Mesenchymal Stem Cell-Derived Neurons. Animals. Vol. 11, pág. 1137, 2021. doi:10.3390/ANI11041137.

RENUNCIA:

Renuncio a que las publicaciones anteriores puedan ser presentadas como parte de otra tesis doctoral en la modalidad de compendio de publicaciones.

<lugar>,<fecha>
Zaragoza 17 de enero de 2023

MARIN GONZALEZ MARIA BELEN - DNI 09335522Y
Firmado digitalmente por MARIN GONZALEZ MARIA BELEN - DNI 09335522Y
Fecha: 2023.01.17 13:11:24 +01'00'

Firma: Mª Belén Marín González

Escuela de Doctorado
Universidad Zaragoza

RENUNCIA DE LOS COAUTORES DE LOS TRABAJOS PRESENTADOS COMO PARTE DE UNA TESIS DOCTORAL EN LA MODALIDAD DE COMPENDIO DE PUBLICACIONES

1.- Datos personales del coautor		
Apellidos: Betancor Caro	Nombre: Marina	
DNI/Pasaporte/NIE: 43229927R	Teléfono 679543164	Correo electrónico mbetancorcaro@gmail.com

2.- Tesis Doctoral
Título: Biomarcadores epigenéticos y desarrollo de modelos celulares en scrapie ovino
Autor: Adelaida Hernaiz Martorell
Programa de doctorado: Ciencias Biomédicas y Biotecnológicas

3.- Publicaciones que formarán parte de la tesis y de las que el firmante es coautor

Hernaiz, Adelaida; Sentre, Sara; Betancor, Marina; López-Pérez, Óscar; Salinas-Pena, Mónica; Zaragoza, Pilar; Badiola, Juan José; Toivonen, Janne Markus; Bolea, Rosa; Martín-Burriel, Inmaculada. 5-Methylcytosine and 5-Hydroxymethylcytosine in Scrapie-Infected Sheep and Mouse Brain Tissues. International Journal of Molecular Sciences. Vol. 24, pág. 1621, 2023. doi:10.3390/IJMS24021621.

RENUNCIA:

Renuncio a que las publicaciones anteriores puedan ser presentadas como parte de otra tesis doctoral en la modalidad de compendio de publicaciones.

<lugar>,<fecha>

Zaragoza, 16 de enero de 2023

BETANCOR CARO MARINA - DNI 43229927R

Firmado digitalmente por BETANCOR CARO MARINA - DNI 43229927R
Fecha: 2023.01.16 20:58:17 +01'00'

Firma:

Conforme a lo dispuesto en la legislación vigente (Reglamento (UE) 2016/679, de 27 de abril), de protección de datos de carácter personal, le informamos que sus datos pasarán a ser tratados por la Universidad de Zaragoza con la finalidad de tramitar la gestión académica y administrativa de sus estudiantes, así como su participación en actividades y servicios universitarios. Puede ejercer sus derechos de acceso, rectificación, limitación, oposición o portabilidad ante el Gerente de la UZ

Escuela de Doctorado
Universidad Zaragoza

RENUNCIA DE LOS COAUTORES DE LOS TRABAJOS PRESENTADOS COMO PARTE DE UNA TESIS DOCTORAL EN LA MODALIDAD DE COMPENDIO DE PUBLICACIONES

1.- Datos personales del coautor		
Apellidos: SALINAS PENA	Nombre: MÓNICA	
DNI/Pasaporte/NIE: 73213941L	Teléfono 695364490	Correo electrónico monicasalinaspena@gmail.com

2.- Tesis Doctoral
Título: Biomarcadores epigenéticos y desarrollo de modelos celulares en scrapie ovino
Autor: Adelaida Hernaiz Martorell
Programa de doctorado: Ciencias Biomédicas y Biotecnológicas

3.- Publicaciones que formarán parte de la tesis y de las que el firmante es coautor

Hernaiz, Adelaida; Sentre, Sara; Betancor, Marina; López-Pérez, Óscar; Salinas-Pena, Mónica; Zaragoza, Pilar; Badiola, Juan José; Toivonen, Janne Markus; Bolea, Rosa; Martín-Burriel, Inmaculada. 5-Methylcytosine and 5-Hydroxymethylcytosine in Scrapie-Infected Sheep and Mouse Brain Tissues. International Journal of Molecular Sciences. Vol. 24, pág. 1621, 2023. doi:10.3390/IJMS24021621.

RENUNCIA:

Renuncio a que las publicaciones anteriores puedan ser presentadas como parte de otra tesis doctoral en la modalidad de compendio de publicaciones.

<lugar>,<fecha>
Barcelona, 17 Enero

Firma: Firmado por SALINAS PENA, MONICA (FIRMA) el día 17/01/2023 con

Conforme a lo dispuesto en la legislación vigente (Reglamento (UE) 2016/679, de 27 de abril), de protección de datos de carácter personal, le informamos que sus datos pasarán a ser tratados por la Universidad de Zaragoza con la finalidad de tramitar la gestión académica y administrativa de sus estudiantes, así como su participación en actividades y servicios universitarios. Puede ejercer sus derechos de acceso, rectificación, limitación, oposición o portabilidad ante el Gerente de la UZ

Referencias bibliográficas

1. Johnson, R. T. Prion diseases. *Lancet. Neurol.* **4**, 635–642 (2005).

2. Wang, H., Rhoads, D. D. & Appleby, B. S. Human prion diseases. *Curr. Opin. Infect. Dis.* **32**, 272–276 (2019).

3. Knight, R. Infectious and Sporadic Prion Diseases. *Prog. Mol. Biol. Transl. Sci.* **150**, 293–318 (2017).

4. Capellari, S., Strammiello, R., Saverioni, D., Kretzschmar, H. & Parchi, P. Genetic Creutzfeldt-Jakob disease and fatal familial insomnia: insights into phenotypic variability and disease pathogenesis. *Acta Neuropathol.* **121**, 21–37 (2011).

5. Liberski, P. P. Gerstmann-Sträussler-Scheinker disease. *Adv. Exp. Med. Biol.* **724**, 128–137 (2012).

6. Liberski, P. P., Sikorska, B. & Brown, P. Kuru: the first prion disease. *Adv. Exp. Med. Biol.* **724**, 143–153 (2012).

7. Will, R. G. Acquired prion disease: iatrogenic CJD, variant CJD, kuru. *Br. Med. Bull.* **66**, 255–265 (2003).

8. Imran, M. & Mahmood, S. An overview of animal prion diseases. *Virol. J.* **8**, (2011).

9. Jeffrey, M. & González, L. Classical sheep transmissible spongiform encephalopathies: pathogenesis, pathological phenotypes and clinical disease. *Neuropathol. Appl. Neurobiol.* **33**, 373–394 (2007).

10. Healy, A. M. *et al.* The clinical neurology of scrapie in Irish sheep. *J. Vet. Intern. Med.* **17**, 908–916 (2003).

11. Benestad, S. L. *et al.* Cases of scrapie with unusual features in Norway and designation of a new type, Nor98. *Vet. Rec.* **153**, 202–208 (2003).

12. Hunter, N. PrP genetics in sheep and the implications for scrapie and BSE. *Trends Microbiol.* **5**, 331–334 (1997).

13. Moum, T. *et al.* Polymorphisms at codons 141 and 154 in the ovine prion protein gene are associated with scrapie Nor98 cases. *J. Gen. Virol.* **86**, 231–235 (2005).

14. Acín, C. *et al.* Classical and Atypical Scrapie in Sheep and Goats. Review on the Etiology, Genetic Factors, Pathogenesis, Diagnosis, and Control Measures of Both Diseases. *Anim. an open access J. from MDPI* **11**, 1–20 (2021).

15. Ricketts, M. N. Public health and the BSE epidemic. *Curr. Top. Microbiol. Immunol.* **284**, 99–119 (2004).

16. Ducrot, C., Arnold, M., Koeijer, A. De, Heim, D. & Calavas, D. Review on the epidemiology and dynamics of BSE epidemics. *Vet. Res.* **39**, (2008).

17. Otero, A., Velásquez, C. D., Aiken, J. & McKenzie, D. Chronic wasting disease: a cervid prion infection looming to spillover. *Vet. Res.* **52**, 115 (2021).

18. Williams, E. S. & Young, S. Chronic wasting disease of captive mule deer: a spongiform encephalopathy. *J. Wildl. Dis.* **16**, 89–98 (1980).

19. Uehlinger, F. D., Johnston, A. C., Bollinger, T. K. & Waldner, C. L. Systematic review of management strategies to control chronic wasting disease in wild deer populations in North America. *BMC Vet. Res.* **12**, (2016).

20. Gill, A. C. & Castle, A. R. The cellular and pathologic prion protein. *Handb. Clin. Neurol.* **153**, 21–44 (2018).

21. Wopfner, F. *et al.* Analysis of 27 mammalian and 9 avian PrPs reveals high conservation of flexible regions of the prion protein. *J. Mol. Biol.* **289**, 1163–1178 (1999).

22. Mahal, S. P., Asante, E. A., Antoniou, M. & Collinge, J. Isolation and functional characterisation of the promoter region of the human prion protein gene. *Gene* **268**, 105–114 (2001).

23. Castle, A. R. & Gill, A. C. Physiological Functions of the Cellular Prion Protein. *Front. Mol. Biosci.* **4**, (2017).

24. Adle-Biassette, H. *et al.* Immunohistochemical Expression of Prion Protein (PrPC) in the Human Forebrain During Development. *J. Neuropathol. Exp. Neurol.* **65**, 698–706 (2006).

25. Lima, F. R. S. *et al.* Cellular prion protein expression in astrocytes modulates neuronal survival and differentiation. *J. Neurochem.* **103**, 2164–2176 (2007).

26. Moser, M., Colello, R. J., Pott, U. & Oesch, B. Developmental expression of the prion protein gene in glial cells. *Neuron* **14**, 509–517 (1995).

27. Dürig, J. *et al.* Differential constitutive and activation-dependent expression of prion protein in human peripheral blood leucocytes. *Br. J. Haematol.* **108**, 488–495 (2000).

28. Ganley, R. P. *et al.* Inhibitory Interneurons That Express GFP in the PrP-GFP Mouse Spinal

Cord Are Morphologically Heterogeneous, Innervated by Several Classes of Primary Afferent and Include Lamina I Projection Neurons among Their Postsynaptic Targets. *J. Neurosci.* **35**, 7626–7642 (2015).

29. Peralta, O. A. & Eyestone, W. H. Quantitative and qualitative analysis of cellular prion protein (PrPC) expression in bovine somatic tissues. *http://dx.doi.org/10.4161/pri.3.3.9772* **3**, 161–170 (2009).

30. Prusiner, S. B. Prions. *Proc. Natl. Acad. Sci. U. S. A.* **95**, 13363–13383 (1998).

31. Caughey, B. W. *et al.* Secondary Structure Analysis of the Scrapie-Associated Protein PrP 27–30 in Water by Infrared Spectroscopy. *Biochemistry* **30**, 7672–7680 (1991).

32. McCutcheon, S. *et al.* All Clinically-Relevant Blood Components Transmit Prion Disease following a Single Blood Transfusion: A Sheep Model of vCJD. *PLoS One* **6**, e23169 (2011).

33. Haley, N. J. *et al.* Detection of chronic wasting disease prions in salivary, urinary, and intestinal tissues of deer: potential mechanisms of prion shedding and transmission. *J. Virol.* **85**, 6309–6318 (2011).

34. Shaked, G. M. *et al.* A Protease-resistant Prion Protein Isoform Is Present in Urine of Animals and Humans Affected with Prion Diseases. *J. Biol. Chem.* **276**, 31479–31482 (2001).

35. Da Costa Dias, B., Jovanovic, K. & Weiss, S. F. T. Alimentary prion infections: Touchdown in the intestine. *Prion* **5**, 6–9 (2011).

36. Donaldson, D. S., Else, K. J. & Mabbott, N. A. The Gut-Associated Lymphoid Tissues in the Small Intestine, Not the Large Intestine, Play a Major Role in Oral Prion Disease Pathogenesis. *J. Virol.* **89**, 9532–9547 (2015).

37. Clark, A. M. & Moar, J. A. Scrapie: a clinical assessment. *Vet. Rec.* **130**, 377–378 (1992).

38. Barnett, K. C. & Palmer, A. C. Retinopathy in sheep affected with natural scrapie. *Res. Vet. Sci.* **12**, 383–385 (1971).

39. Sharp, M. W. & Collings, D. F. Ovine abomasal enlargement and scrapie. *Vet. Rec.* **120**, 215 (1987).

40. Vargas, F. *et al.* Clinical characterisation of natural scrapie in a native Spanish breed of sheep. *Vet. Rec.* **156**, 318–320 (2005).

41. Detwiler, L. A. Scrapie. *Rev. Sci. Tech.* **11**, 491–537 (1992).

42. Wood, J. L., McGill, I. S., Done, S. H. & Bradley, R. Neuropathology of scrapie: a study of the distribution patterns of brain lesions in 222 cases of natural scrapie in sheep, 1982-1991. *Vet. Rec.* **140**, 167–174 (1997).

43. Lazarini, F., Boussin, F., Deslys, J. P., Tardy, M. & Dormont, D. Astrocyte gene expression in experimental mouse scrapie. *J. Comp. Pathol.* **111**, 87–98 (1994).

44. Rezaie, P. & Lantos, P. L. Microglia and the pathogenesis of spongiform encephalopathies. *Brain Res. Rev.* **35**, 55–72 (2001).

45. Ye, X., Scallet, A. C., Kascsak, R. J. & Carp, R. I. Astrocytosis and amyloid deposition in scrapie-infected hamsters. *Brain Res.* **809**, 277–287 (1998).

46. Houston, F. *et al.* Comparative Susceptibility of Sheep of Different Origins, Breeds and PRNP Genotypes to Challenge with Bovine Spongiform Encephalopathy and Scrapie. *PLoS One* **10**, (2015).

47. Thorgeirsdottir, S., Sigurdarson, S., Thorisson, H. M., Georgsson, G. & Palsdottir, A. PrP gene polymorphism and natural scrapie in Icelandic sheep. *J. Gen. Virol.* **80 (Pt 9)**, 2527–2534 (1999).

48. Dawson, M., Hoinville, L. J., Hosie, B. D. & Hunter, N. Guidance on the use of PrP genotyping as an aid to the control of clinical scrapie. Scrapie Information Group. *Vet. Rec.* **142**, 623–625 (1998).

49. Hoinville, L. J. A review of the epidemiology of scrapie in sheep. *Rev. Sci. Tech.* **15**, 827–852 (1996).

50. Bruce, M. E. TSE strain variation. *Br. Med. Bull.* **66**, 99–108 (2003).

51. Unterberger, U., Voigtländer, T. & Budka, H. Pathogenesis of prion diseases. *Acta Neuropathol.* **109**, 32–48 (2005).

52. Hamir, A. N. *et al.* Experimental transmission of scrapie agent to susceptible sheep by intralingual or intracerebral inoculation. *Can. J. Vet. Res.* **72**, 63 (2008).

53. Maignien, T., Lasmézas, C. I., Beringue, V., Dormont, D. & Deslys, J. P. Pathogenesis of the oral route of infection of mice with scrapie and bovine spongiform encephalopathy agents. *J. Gen. Virol.* **80 (Pt 11**, 3035–3042 (1999).

54. Mabbott, N. A. & Bruce, M. E. The immunobiology of TSE diseases. *J. Gen. Virol.* **82**, 2307–2318 (2001).

55. St. Rose, S. G. *et al.* Comparative evidence for a link between Peyer's patch development and susceptibility to transmissible spongiform encephalopathies. *BMC Infect. Dis.* **6**, (2006).

56. Van Keulen, L. J. M., Vromans, M. E. W. & Van Zijderveld, F. G. Early and late pathogenesis of natural scrapie infection in sheep. *APMIS* **110**, 23–32 (2002).

57. Ryder, S. J., Spencer, Y. I., Bellerby, P. J. & March, S. A. Immunohistochemical detection of PrP in the medulla oblongata of sheep: the spectrum of staining in normal and scrapie-affected sheep. *Vet. Rec.* **148**, 7–13 (2001).

58. Cassmann, E. D. & Greenlee, J. J. Pathogenesis, detection, and control of scrapie in sheep. *Am. J. Vet. Res.* **81**, 600–614 (2020).

59. González, L., Martin, S. & Jeffrey, M. Distinct profiles of PrP(d) immunoreactivity in the brain of scrapie- and BSE-infected sheep: implications for differential cell targeting and PrP processing. *J. Gen. Virol.* **84**, 1339–1350 (2003).

60. Schreuder, B. E., Keulen, L. J. van & Vromans, M. E. Tonsillar biopsy and PrPSc detection in the preclinical diagnosis of scrapie. *Vet Rec* **142**, 564–568 (1998).

61. O'Rourke, K., Baszler, T. V & Besser, T. E. Preclinical diagnosis of scrapie by immunohistochemistry of third eyelid lymphoid tissue. *J Clin Microbiol* **38**, 3254–3259 (2000).

62. González, L., Dagleish, M. P. & Martin, S. Diagnosis of preclinical scrapie in live sheep by the immunohistochemical examination of rectal biopsies. *Vet Rec* **162**, 397–403 (2008).

63. Dassanayake, R. P. *et al.* Sensitive and specific detection of classical scrapie prions in the brains of goats by real-time quaking-induced conversion. *J. Gen. Virol.* **97**, 803–812 (2016).

64. Wilham, J. M. *et al.* Rapid end-point quantitation of prion seeding activity with sensitivity comparable to bioassays. *PLoS Pathog.* **6**, (2010).

65. Garza, M. C. *et al.* Protein misfolding cyclic amplification corroborates the absence of PrPSc accumulation in placenta from foetuses with the ARR/ARQ genotype in natural scrapie. *Vet. Microbiol.* **203**, 294–300 (2017).

66. Garza, M. C. *et al.* Detection of PrPres in genetically susceptible fetuses from sheep with natural scrapie. *PLoS One* **6**, (2011).

67. Saá, P., Castilla, J. & Soto, C. Ultra-efficient replication of infectious prions by automated protein misfolding cyclic amplification. *J. Biol. Chem.* **281**, 35245–35252 (2006).

68. Thorne, L. *et al.* In vitro amplification of ovine prions from scrapie-infected sheep from Great Britain reveals distinct patterns of propagation. *BMC Vet. Res.* **8**, (2012).

69. Windl, O. & Dawson, M. Animal prion diseases. *Subcell. Biochem.* **65**, 497–516 (2012).

70. Moore, L. D., Le, T. & Fan, G. DNA methylation and its basic function. *Neuropsychopharmacology* vol. 38 23–38 (2013).

71. Kulis, M. & Esteller, M. DNA methylation and cancer. *Adv. Genet.* **70**, 27–56 (2010).

72. Bestor, T. H. The DNA methyltransferases of mammals. *Hum. Mol. Genet.* **9**, 2395–2402 (2000).

73. Meng, H. *et al.* DNA methylation, its mediators and genome integrity. *Int. J. Biol. Sci.* **11**, 604–617 (2015).

74. Wu, S. C. & Zhang, Y. Active DNA demethylation: many roads lead to Rome. *Nat. Rev. Mol. Cell Biol.* **11**, 607–620 (2010).

75. Maiti, A. & Drohat, A. C. Thymine DNA glycosylase can rapidly excise 5-formylcytosine and 5-carboxylcytosine: potential implications for active demethylation of CpG sites. *J. Biol. Chem.* **286**, 35334–35338 (2011).

76. Li, E. Chromatin modification and epigenetic reprogramming in mammalian development. *Nat. Rev. Genet.* **3**, 662–673 (2002).

77. Song, C. X. *et al.* Selective chemical labeling reveals the genome-wide distribution of 5-hydroxymethylcytosine. *Nat. Biotechnol.* **29**, 68–75 (2011).

78. Yu, M. *et al.* Base-resolution analysis of 5-hydroxymethylcytosine in the mammalian genome. *Cell* **149**, 1368–1380 (2012).

79. Tahiliani, M. *et al.* Conversion of 5-methylcytosine to 5-hydroxymethylcytosine in mammalian DNA by MLL partner TET1. *Science* **324**, 930–935 (2009).

80. Okano, M., Bell, D. W., Haber, D. A. & Li, E. DNA methyltransferases Dnmt3a and Dnmt3b are essential for de novo methylation and mammalian development. *Cell* **99**, 247–257

(1999).

81. Goll, M. G. & Bestor, T. H. Eukaryotic cytosine methyltransferases. *Annu. Rev. Biochem.* **74**, 481–514 (2005).

82. Audia, J. E. & Campbell, R. M. Histone modifications and cancer. *Cold Spring Harb. Perspect. Biol.* **8**, (2016).

83. ALLFREY, V. G., FAULKNER, R. & MIRSKY, A. E. ACETYLATION AND METHYLATION OF HISTONES AND THEIR POSSIBLE ROLE IN THE REGULATION OF RNA SYNTHESIS. *Proc. Natl. Acad. Sci. U. S. A.* **51**, 786–794 (1964).

84. Bannister, A. J. & Kouzarides, T. Regulation of chromatin by histone modifications. *Cell Res.* **21**, 381–395 (2011).

85. Hodawadekar, S. C. & Marmorstein, R. Chemistry of acetyl transfer by histone modifying enzymes: structure, mechanism and implications for effector design. *Oncogene* **26**, 5528–5540 (2007).

86. Yang, X. J. & Seto, E. HATs and HDACs: from structure, function and regulation to novel strategies for therapy and prevention. *Oncogene* **26**, 5310–5318 (2007).

87. Oki, M., Aihara, H. & Ito, T. Role of histone phosphorylation in chromatin dynamics and its implications in diseases. *Subcell. Biochem.* **41**, 319–336 (2007).

88. Sugiyama, K. *et al.* Aurora-B associated protein phosphatases as negative regulators of kinase activation. *Oncogene* **21**, 3103–3111 (2002).

89. Ng, S. S., Yue, W. W., Oppermann, U. & Klose, R. J. Dynamic protein methylation in chromatin biology. *Cell. Mol. Life Sci.* **66**, 407–422 (2009).

90. Zhang, X. *et al.* Structural basis for the product specificity of histone lysine methyltransferases. *Mol. Cell* **12**, 177–185 (2003).

91. Wolf, S. S. The protein arginine methyltransferase family: an update about function, new perspectives and the physiological role in humans. *Cell. Mol. Life Sci.* **66**, 2109–2121 (2009).

92. Shi, Y. *et al.* Histone demethylation mediated by the nuclear amine oxidase homolog LSD1. *Cell* **119**, 941–953 (2004).

93. Black, J. C., Van Rechem, C. & Whetstine, J. R. Histone Lysine Methylation Dynamics:

Establishment, Regulation, and Biological Impact. *Mol. Cell* **48**, 491–507 (2012).

94. Hyun, K., Jeon, J., Park, K. & Kim, J. Writing, erasing and reading histone lysine methylations. *Exp. Mol. Med.* **49**, (2017).

95. Huang, W. MicroRNAs: Biomarkers, diagnostics, and therapeutics. *Methods Mol. Biol.* **1617**, 57–67 (2017).

96. Place, R. F., Li, L. C., Pookot, D., Noonan, E. J. & Dahiya, R. MicroRNA-373 induces expression of genes with complementary promoter sequences. *Proc. Natl. Acad. Sci. U. S. A.* **105**, 1608–1613 (2008).

97. Catalanotto, C., Cogoni, C. & Zardo, G. MicroRNA in Control of Gene Expression: An Overview of Nuclear Functions. *Int. J. Mol. Sci.* **17**, (2016).

98. Bottani, M., Banfi, G. & Lombardi, G. Perspectives on mirnas as epigenetic markers in osteoporosis and bone fracture risk: A step forward in personalized diagnosis. *Front. Genet.* **10**, 1044 (2019).

99. Hwang, J. Y., Aromolaran, K. A. & Zukin, R. S. The emerging field of epigenetics in neurodegeneration and neuroprotection. *Nat. Rev. Neurosci.* **18**, 347–361 (2017).

100. Miller, C. A. & Sweatt, J. D. Covalent modification of DNA regulates memory formation. *Neuron* **53**, 857–69 (2007).

101. Kaas, G. A. *et al.* TET1 controls CNS 5-methylcytosine hydroxylation, active DNA demethylation, gene transcription, and memory formation. *Neuron* **79**, 1086–1093 (2013).

102. Levenson, J. M. *et al.* Regulation of histone acetylation during memory formation in the hippocampus. *J. Biol. Chem.* **279**, 40545–40559 (2004).

103. Swank, M. W. & Sweatt, J. D. Increased histone acetyltransferase and lysine acetyltransferase activity and biphasic activation of the ERK/RSK cascade in insular cortex during novel taste learning. *J. Neurosci.* **21**, 3383–3391 (2001).

104. Schratt, G. microRNAs at the synapse. *Nat. Rev. Neurosci.* **10**, 842–849 (2009).

105. Woldemichael, B. T. & Mansuy, I. M. Micro-RNAs in cognition and cognitive disorders: Potential for novel biomarkers and therapeutics. *Biochemical Pharmacology* vol. 104 1–7 (2016).

106. Sun, J., Sun, J., Ming, G. L. & Song, H. Epigenetic regulation of neurogenesis in the adult mammalian brain. *Eur. J. Neurosci.* **33**, 1087–1093 (2011).

107. Fan, G. *et al.* DNA methylation controls the timing of astrogliogenesis through regulation of JAK-STAT signaling. *Development* **132**, 3345–3356 (2005).

108. Fasano, C. A. *et al.* shRNA knockdown of Bmi-1 reveals a critical role for p21-Rb pathway in NSC self-renewal during development. *Cell Stem Cell* **1**, 87–99 (2007).

109. Jawerka, M. *et al.* The specific role of histone deacetylase 2 in adult neurogenesis. *Neuron Glia Biol.* **6**, 93–107 (2010).

110. Kim, H. J., Leeds, P. & Chuang, D. M. The HDAC inhibitor, sodium butyrate, stimulates neurogenesis in the ischemic brain. *J. Neurochem.* **110**, 1226–1240 (2009).

111. Jaunmuktane, Z. & Brandner, S. Invited Review: The role of prion-like mechanisms in neurodegenerative diseases. *Neuropathology and Applied Neurobiology* (2019) doi:10.1111/nan.12592.

112. Masnata, M. *et al.* Demonstration of prion-like properties of mutant huntingtin fibrils in both in vitro and in vivo paradigms. *Acta Neuropathol.* **137**, 981–1001 (2019).

113. Krance, S. H. *et al.* Cellular models for discovering prion disease therapeutics: Progress and challenges. *J. Neurochem.* **153**, 150–172 (2020).

114. Vilette, D. Cell models of prion infection. *Vet. Res.* **39**, (2008).

115. Vorberg, I. & Chiesa, R. Experimental models to study prion disease pathogenesis and identify potential therapeutic compounds. *Curr. Opin. Pharmacol.* **44**, 28–38 (2019).

116. Bosque, P. J. & Prusiner, S. B. Cultured cell sublines highly susceptible to prion infection. *J. Virol.* **74**, 4377–4386 (2000).

117. Walia, R., Ho, C. C., Lee, C., Gilch, S. & Schatzl, H. M. Gene-edited murine cell lines for propagation of chronic wasting disease prions. *Sci. Rep.* **9**, 11151 (2019).

118. Lyon, A. *et al.* Application of PMCA to screen for prion infection in a human cell line used to produce biological therapeutics. *Sci. Rep.* **9**, (2019).

119. Mediano, D. R. *et al.* Characterization of mesenchymal stem cells in sheep naturally infected with scrapie. *J. Gen. Virol.* **96**, 3715–3726 (2015).

120. Takatsuki, H., Imamura, M., Mori, T. & Atarashi, R. Pentosan polysulfate induces low-level

persistent prion infection keeping measurable seeding activity without PrP-res detection in Fukuoka-1 infected cell cultures. *Sci. Rep.* **12**, (2022).

121. Chandler, R. L. ENCEPHALOPATHY IN MICE PRODUCED BY INOCULATION WITH SCRAPIE BRAIN MATERIAL. *Lancet* **277**, 1378–1379 (1961).

122. Butler, D. A. *et al.* Scrapie-infected murine neuroblastoma cells produce protease-resistant prion proteins. *J. Virol.* **62**, 1558–1564 (1988).

123. Schätzl, H. M. *et al.* A hypothalamic neuronal cell line persistently infected with scrapie prions exhibits apoptosis. *J. Virol.* **71**, 8821–8831 (1997).

124. Follet, J. *et al.* PrP expression and replication by Schwann cells: implications in prion spreading. *J. Virol.* **76**, 2434–2439 (2002).

125. Iwamaru, Y. *et al.* Microglial cell line established from prion protein-overexpressing mice is susceptible to various murine prion strains. *J. Virol.* **81**, 1524–1527 (2007).

126. Vorberg, I., Raines, A., Story, B. & Priola, S. A. Susceptibility of common fibroblast cell lines to transmissible spongiform encephalopathy agents. *J. Infect. Dis.* **189**, 431–439 (2004).

127. Dlakic, W. M., Grigg, E. & Bessen, R. A. Prion infection of muscle cells in vitro. *J. Virol.* **81**, 4615–4624 (2007).

128. Muñoz-Gutiérrez, J. F. *et al.* hTERT-immortalized ovine microglia propagate natural scrapie isolates. *Virus Res.* **198**, 35–43 (2015).

129. Tark, D. *et al.* Generation of a persistently infected MDBK cell line with natural bovine spongiform encephalopathy (BSE). *PLoS One* **10**, (2015).

130. Raymond, G. J. *et al.* Inhibition of protease-resistant prion protein formation in a transformed deer cell line infected with chronic wasting disease. *J. Virol.* **80**, 596–604 (2006).

131. Krejciova, Z. *et al.* Human stem cell-derived astrocytes replicate human prions in a PRNP genotype-dependent manner. *J. Exp. Med.* **214**, 3481–3495 (2017).

132. Pittenger, M. F. *et al.* Multilineage potential of adult human mesenchymal stem cells. *Science (80-.).* **284**, 143–147 (1999).

133. Woodbury, D., Reynolds, K. & Black, I. B. Adult bone marrow stromal stem cells express

germline, ectodermal, endodermal, and mesodermal genes prior to neurogenesis. *J. Neurosci. Res.* **69**, 908–917 (2002).

134. Zhao, L. R. *et al.* Human bone marrow stem cells exhibit neural phenotypes and ameliorate neurological deficits after grafting into the ischemic brain of rats. *Exp. Neurol.* **174**, 11–20 (2002).

135. Lyahyai, J. *et al.* Isolation and characterization of ovine mesenchymal stem cells derived from peripheral blood. *BMC Vet. Res.* **8**, (2012).

136. Takakura, Y. *et al.* Bone marrow stroma cells are susceptible to prion infection. *Biochem. Biophys. Res. Commun.* **377**, 957–961 (2008).

137. Martellucci, S. *et al.* Isolation, propagation, and prion protein expression during neuronal differentiation of human dental pulp stem cells. *J. Vis. Exp.* **2019**, (2019).

138. Martellucci, S. *et al.* Cellular and molecular mechanisms mediated by recPrP C involved in the neuronal differentiation process of mesenchymal stem cells. *Int. J. Mol. Sci.* **20**, (2019).

139. Shi, F. *et al.* Cellular Prion Protein Promotes Neuronal Differentiation of Adipose-Derived Stem Cells by Upregulating miRNA-124. *J. Mol. Neurosci.* **59**, 48–55 (2016).

140. Shan, Z. *et al.* Therapeutic effect of autologous compact bone-derived mesenchymal stem cell transplantation on prion disease. *J. Gen. Virol.* **98**, 2615–2627 (2017).

141. Song, C.-H., Honmou, O., Furuoka, H. & Horiuchi, M. Identification of Chemoattractive Factors Involved in the Migration of Bone Marrow-Derived Mesenchymal Stem Cells to Brain Lesions Caused by Prions. *J. Virol.* **85**, 11069–11078 (2011).

142. Song, C.-H. *et al.* Effect of Transplantation of Bone Marrow-Derived Mesenchymal Stem Cells on Mice Infected with Prions. *J. Virol.* **83**, 5918–5927 (2009).

143. Akimov, S., Vasilyeva, I., Yakovleva, O., McKenzie, C. & Cervenakova, L. Murine bone marrow stromal cell culture with features of mesenchymal stem cells susceptible to mouse-adapted human TSE agent, Fukuoka-1. *Folia Neuropathol.* **47**, 205–14 (2009).

144. Akimov, S., Yakovleva, O., Vasilyeva, I., McKenzie, C. & Cervenakova, L. Persistent Propagation of Variant Creutzfeldt-Jakob Disease Agent in Murine Spleen Stromal Cell Culture with Features of Mesenchymal Stem Cells. *J. Virol.* **82**, 10959–10962 (2008).

145. Cervenakova, L. *et al.* Fukuoka-1 strain of transmissible spongiform encephalopathy

agent infects murine bone marrow-derived cells with features of mesenchymal stem cells. *Transfusion* **51**, 1755–1768 (2011).

146. Chaicharoenaudomrung, N., Kunhorm, P. & Noisa, P. Three-dimensional cell culture systems as an in vitro platform for cancer and stem cell modeling. *World J. Stem Cells* **11**, 1065–1083 (2019).

147. Lv, D., Hu, Z., Lu, L., Lu, H. & Xu, X. Three-dimensional cell culture: A powerful tool in tumor research and drug discovery. *Oncol. Lett.* **14**, 6999–7010 (2017).

148. Ravi, M., Paramesh, V., Kaviya, S. R., Anuradha, E. & Paul Solomon, F. D. 3D cell culture systems: advantages and applications. *J. Cell. Physiol.* **230**, 16–26 (2015).

149. Suarez-Martinez, E., Suazo-Sanchez, I., Celis-Romero, M. & Carnero, A. 3D and organoid culture in research: physiology, hereditary genetic diseases and cancer. *Cell Biosci.* **12**, (2022).

150. Chen, X. *et al.* Modeling Sporadic Alzheimer's Disease in Human Brain Organoids under Serum Exposure. *Adv. Sci. (Weinheim, Baden-Wurttemberg, Ger.* **8**, (2021).

151. Park, J. C. *et al.* A logical network-based drug-screening platform for Alzheimer's disease representing pathological features of human brain organoids. *Nat. Commun.* **12**, (2021).

152. Pomeshchik, Y. *et al.* Human iPSC-Derived Hippocampal Spheroids: An Innovative Tool for Stratifying Alzheimer Disease Patient-Specific Cellular Phenotypes and Developing Therapies. *Stem cell reports* **15**, 256–273 (2020).

153. Zhao, J. *et al.* APOE4 exacerbates synapse loss and neurodegeneration in Alzheimer's disease patient iPSC-derived cerebral organoids. *Nat. Commun.* **11**, (2020).

154. Fiore, N. J., Tamer-Mahoney, J. D., Beheshti, A., Nieland, T. J. F. & Kaplan, D. L. 3D biocomposite culture enhances differentiation of dopamine-like neurons from SH-SY5Y cells: A model for studying Parkinson's disease phenotypes. *Biomaterials* **290**, (2022).

155. Gilmozzi, V. *et al.* Generation of hiPSC-Derived Functional Dopaminergic Neurons in Alginate-Based 3D Culture. *Front. cell Dev. Biol.* **9**, (2021).

156. Kim, H. *et al.* Modeling G2019S-LRRK2 Sporadic Parkinson's Disease in 3D Midbrain Organoids. *Stem cell reports* **12**, 518–531 (2019).

157. Li, Z. F. *et al.* A Matrigel-based 3D construct of SH-SY5Y cells models the α-synuclein pathologies of Parkinson's disease. *Dis. Model. Mech.* **15**, (2022).

158. Groveman, B. R. *et al.* Sporadic Creutzfeldt-Jakob disease prion infection of human cerebral organoids. *Acta Neuropathol. Commun.* **7**, 90 (2019).

159. Groveman, B. R. *et al.* Human cerebral organoids as a therapeutic drug screening model for Creutzfeldt-Jakob disease. *Sci. Rep.* **11**, (2021).

160. Atkinson, C. J., Zhang, K., Munn, A. L., Wiegmans, A. & Wei, M. Q. Prion protein scrapie and the normal cellular prion protein. *Prion* vol. 10 63–82 (2016).

161. Wulf, M. A., Senatore, A. & Aguzzi, A. The biological function of the cellular prion protein: An update. *BMC Biology* vol. 15 34 (2017).

162. Gavín, R., Lidón, L., Ferrer, I. & Río, J. A. del. The Quest for Cellular Prion Protein Functions in the Aged and Neurodegenerating Brain. *Cells* **9**, 591 (2020).

163. Jones, P. A. Functions of DNA methylation: Islands, start sites, gene bodies and beyond. *Nature Reviews Genetics* vol. 13 484–492 (2012).

164. Anastasiadi, D., Esteve-Codina, A. & Piferrer, F. Consistent inverse correlation between DNA methylation of the first intron and gene expression across tissues and species. *Epigenetics and Chromatin* **11**, 37 (2018).

165. Roy, S. & Bhat, R. Suppression, disaggregation, and modulation of γ-Synuclein fibrillation pathway by green tea polyphenol EGCG. *Protein Sci.* **28**, 382–402 (2019).

166. Winham, C. L. *et al.* γ-Synuclein Induces Human Cortical Astrocyte Proliferation and Subsequent BDNF Expression and Release. *Neuroscience* **410**, 41–54 (2019).

167. Sanjeev, A. & Mattaparthi, V. S. K. Computational Study on the Role of γ-Synuclein in Inhibiting the α-Synuclein Aggregation. *Cent. Nerv. Syst. Agents Med. Chem.* **19**, 24–30 (2018).

168. Ninkina, N. *et al.* Gamma-synucleinopathy: neurodegeneration associated with overexpression of the mouse protein. *Hum. Mol. Genet.* **18**, 1779–94 (2009).

169. Bakula, D. *et al.* WIPI3 and WIPI4 β-propellers are scaffolds for LKB1-AMPK-TSC signalling circuits in the control of autophagy. *Nat. Commun.* **8**, 15637 (2017).

170. Ji, C. *et al.* Role of Wdr45b in maintaining neural autophagy and cognitive function. *Autophagy* **16**, 615–625 (2019).

171. JW, B., W, S. & J, T. Neuronal autophagy in experimental Creutzfeldt-Jakob's disease. *Acta*

Neuropathol. **78**, 410–418 (1989).

172. López-Pérez, Ó. *et al.* Impairment of autophagy in scrapie-infected transgenic mice at the clinical stage. *Lab. Investig.* **100**, 52–63 (2020).

173. López-Pérez, Ó., Bolea, R., Marín, B., Badiola, J. J. & Martín-Burriel, I. Autophagy impairment in highly prion-affected brain areas of sheep experimentally infected with atypical scrapie. *Vet. Microbiol.* **233**, 78–84 (2019).

174. López-Pérez, Ó. *et al.* Dysregulation of autophagy in the central nervous system of sheep naturally infected with classical scrapie. *Sci. Rep.* **9**, 1911 (2019).

175. Martini-Stoica, H., Xu, Y., Ballabio, A. & Zheng, H. The Autophagy-Lysosomal Pathway in Neurodegeneration: A TFEB Perspective. *Trends in Neurosciences* vol. 39 221–234 (2016).

176. Gerosa, L., Francolini, M., Bassani, S. & Passafaro, M. The Role of Protocadherin 19 (PCDH19) in Neurodevelopment and in the Pathophysiology of Early Infantile Epileptic Encephalopathy-9 (EIEE9). *Developmental Neurobiology* vol. 79 75–84 (2019).

177. Fujitani, M., Zhang, S., Fujiki, R., Fujihara, Y. & Yamashita, T. A chromosome 16p13.11 microduplication causes hyperactivity through dysregulation of miR-484/protocadherin-19 signaling. *Mol. Psychiatry* **22**, 364–374 (2017).

178. Bassani, S. *et al.* The female epilepsy protein PCDH19 is a new GABAAR-binding partner that regulates GABAergic transmission as well as migration and morphological maturation of hippocampal neurons. *Hum. Mol. Genet.* **27**, 1027–1038 (2018).

179. Zhang, T. *et al.* Methylation of PCDH19 predicts poor prognosis of hepatocellular carcinoma. *Asia. Pac. J. Clin. Oncol.* **14**, e352–e358 (2018).

180. Waterham, H. R., Ferdinandusse, S. & Wanders, R. J. A. Human disorders of peroxisome metabolism and biogenesis. *Biochim. Biophys. Acta - Mol. Cell Res.* **1863**, 922–933 (2016).

181. Islinger, M., Voelkl, A., Fahimi, H. D. & Schrader, M. The peroxisome: an update on mysteries 2.0. *Histochemistry and Cell Biology* vol. 150 443–471 (2018).

182. Berger, J., Dorninger, F., Forss-Petter, S. & Kunze, M. Peroxisomes in brain development and function. *Biochim. Biophys. Acta - Mol. Cell Res.* **1863**, 934–955 (2016).

183. Hammond, D. R. & Udvadia, A. J. Cabin1 expression suggests roles in neuronal development. *Dev. Dyn.* **239**, 2443–2451 (2010).

184. Tarasova, E. O., Gaydukov, A. E. & Balezina, O. P. Calcineurin and Its Role in Synaptic Transmission. *Biochemistry (Moscow)* vol. 83 674–689 (2018).

185. Hopp, S. C. *et al.* Neuronal calcineurin transcriptional targets parallel changes observed in Alzheimer disease brain. *J. Neurochem.* **147**, 24–39 (2018).

186. Hong, J. M., Moon, J. H. & Park, S. Y. Human prion protein-mediated calcineurin activation induces neuron cell death via AMPK and autophagy pathway. *Int. J. Biochem. Cell Biol.* **119**, 105680 (2020).

187. Filali, H. *et al.* Gene expression profiling and association with prion-related lesions in the medulla oblongata of symptomatic natural scrapie animals. *PLoS One* **6**, (2011).

188. Rountree, M. R., Bachman, K. E., Herman, J. G. & Baylin, S. B. DNA methylation, chromatin inheritance, and cancer. *Oncogene 2001 2024* **20**, 3156–3165 (2001).

189. Ellison, E. M., Abner, E. L. & Lovell, M. A. Multiregional analysis of global 5-methylcytosine and 5-hydroxymethylcytosine throughout the progression of Alzheimer's disease. *J. Neurochem.* **140**, 383–394 (2017).

190. Cadena-Del-Castillo, C. *et al.* Age-dependent increment of hydroxymethylation in the brain cortex in the triple-transgenic mouse model of Alzheimer's disease. *J. Alzheimers. Dis.* **41**, 845–854 (2014).

191. Coppieters, N. *et al.* Global changes in DNA methylation and hydroxymethylation in Alzheimer's disease human brain. *Neurobiol. Aging* **35**, 1334–1344 (2014).

192. Bradley-Whitman, M. A. & Lovell, M. A. Epigenetic changes in the progression of Alzheimer's disease. *Mech. Ageing Dev.* **134**, 486–495 (2013).

193. Huang, Q. *et al.* Quantification of DNA methylation and hydroxymethylation in Alzheimer's disease mouse model using LC-MS/MS. *J. Mass Spectrom.* **53**, 590–594 (2018).

194. Kaut, O., Kuchelmeister, K., Moehl, C. & Wüllner, U. 5-methylcytosine and 5-hydroxymethylcytosine in brains of patients with multiple system atrophy and patients with Parkinson's disease. *J. Chem. Neuroanat.* **96**, 41–48 (2019).

195. Stöger, R., Scaife, P. J., Shephard, F. & Chakrabarti, L. Elevated 5hmC levels characterize DNA of the cerebellum in Parkinson's disease. *NPJ Park. Dis.* **3**, (2017).

196. Condliffe, D. *et al.* Cross-region reduction in 5-hydroxymethylcytosine in Alzheimer's

disease brain. *Neurobiol. Aging* **35**, 1850–1854 (2014).

197. Zhang, Y. *et al.* Selective loss of 5hmC promotes neurodegeneration in the mouse model of Alzheimer's disease. *FASEB J.* **34**, 16364–16382 (2020).

198. Shu, L. *et al.* Genome-wide alteration of 5-hydroxymenthylcytosine in a mouse model of Alzheimer's disease. *BMC Genomics* **17**, (2016).

199. James, S. J., Shpyleva, S., Melnyk, S., Pavliv, O. & Pogribny, I. P. Elevated 5-hydroxymethylcytosine in the Engrailed-2 (EN-2) promoter is associated with increased gene expression and decreased MeCP2 binding in autism cerebellum. *Transl. Psychiatry* **4**, e460 (2014).

200. Geiman, T. M. *et al.* DNMT3B interacts with hSNF2H chromatin remodeling enzyme, HDACs 1 and 2, and components of the histone methylation system. *Biochem. Biophys. Res. Commun.* **318**, 544–555 (2004).

201. Chen, C. C., Wang, K. Y. & Shen, C. K. J. The mammalian de novo DNA methyltransferases DNMT3A and DNMT3B are also DNA 5-hydroxymethylcytosine dehydroxymethylases. *J. Biol. Chem.* **287**, 33116–33121 (2012).

202. Zocher, S. *et al.* De novo DNA methylation controls neuronal maturation during adult hippocampal neurogenesis. *EMBO J.* **40**, (2021).

203. Kong, Q. *et al.* Conditional Dnmt3b deletion in hippocampal dCA1 impairs recognition memory. *Mol. Brain* **13**, (2020).

204. Nieto-Estevez, V. *et al.* HDAC1 Regulates Neuronal Differentiation. *Front. Mol. Neurosci.* **14**, (2022).

205. Pao, P. C. *et al.* HDAC1 modulates OGG1-initiated oxidative DNA damage repair in the aging brain and Alzheimer's disease. *Nat. Commun.* **11**, (2020).

206. Bahari-Javan, S. *et al.* HDAC1 regulates fear extinction in mice. *J. Neurosci.* **32**, 5062–5073 (2012).

207. Sharma, R. P., Grayson, D. R. & Gavin, D. P. Histone deactylase 1 expression is increased in the prefrontal cortex of schizophrenia subjects: analysis of the National Brain Databank microarray collection. *Schizophr. Res.* **98**, 111–117 (2008).

208. Zhao, P. *et al.* Essential roles of HDAC1 and 2 in lineage development and genome-wide DNA methylation during mouse preimplantation development. *Epigenetics* **15**, 369–385

(2020).

209. Gräff, J. *et al.* An epigenetic blockade of cognitive functions in the neurodegenerating brain. *Nature* **483**, 222–226 (2012).

210. Tan, Y. *et al.* Upregulation of histone deacetylase 2 in laser capture nigral microglia in Parkinson's disease. *Neurobiol. Aging* **68**, 134–141 (2018).

211. Singh, P. & Thakur, M. K. Reduced recognition memory is correlated with decrease in DNA methyltransferase1 and increase in histone deacetylase2 protein expression in old male mice. *Biogerontology* **15**, 339–346 (2014).

212. Singh, P. & Thakur, M. K. Histone Deacetylase 2 Inhibition Attenuates Downregulation of Hippocampal Plasticity Gene Expression during Aging. *Mol. Neurobiol.* **55**, 2432–2442 (2018).

213. Nakatsuka, D. *et al.* Histone Deacetylase 2 Knockdown Ameliorates Morphological Abnormalities of Dendritic Branches and Spines to Improve Synaptic Plasticity in an APP/PS1 Transgenic Mouse Model. *Front. Mol. Neurosci.* **14**, (2021).

214. Frankowski, H. *et al.* Knock-Down of HDAC2 in Human Induced Pluripotent Stem Cell Derived Neurons Improves Neuronal Mitochondrial Dynamics, Neuronal Maturation and Reduces Amyloid Beta Peptides. *Int. J. Mol. Sci.* **22**, 1–19 (2021).

215. Ito, S. *et al.* Tet proteins can convert 5-methylcytosine to 5-formylcytosine and 5-carboxylcytosine. *Science* **333**, 1300–1303 (2011).

216. Taylor, S. E. B., Smeriglio, P., Dhulipala, L., Rath, M. & Bhutani, N. A global increase in 5-hydroxymethylcytosine levels marks osteoarthritic chondrocytes. *Arthritis Rheumatol. (Hoboken, N.J.)* **66**, 90–100 (2014).

217. Park, J.-L. *et al.* Decrease of 5hmC in gastric cancers is associated with TET1 silencing due to with DNA methylation and bivalent histone marks at TET1 CpG island 3'-shore. *Oncotarget* **6**, 37647–37662 (2015).

218. Wang, K. C. *et al.* Ten-eleven translocation 1 dysfunction reduces 5-hydroxymethylcytosine expression levels in gastric cancer cells. *Oncol. Lett.* **15**, 278–284 (2018).

219. Moyon, S. *et al.* TET1-mediated DNA hydroxymethylation regulates adult remyelination in mice. *Nat. Commun.* **12**, (2021).

220. Greer, C. B. *et al.* Tet1 Isoforms Differentially Regulate Gene Expression, Synaptic Transmission, and Memory in the Mammalian Brain. *J. Neurosci.* **41**, 578–593 (2021).

221. Carroll, J. A., Striebel, J. F., Race, B., Phillips, K. & Chesebro, B. Prion infection of mouse brain reveals multiple new upregulated genes involved in neuroinflammation or signal transduction. *J. Virol.* **89**, 2388–2404 (2015).

222. Guijarro, I. M. *et al.* Neuroimmune Response Mediated by Cytokines in Natural Scrapie after Chronic Dexamethasone Treatment. *Biomolecules* **11**, 1–18 (2021).

223. López-Pérez, Ó. *et al.* BAMBI and CHGA in prion diseases: Neuropathological assessment and potential role as disease biomarkers. *Biomolecules* **10**, (2020).

224. Marcos-Carcavilla, A. *et al.* IL-1 family members as candidate genes modulating scrapie susceptibility in sheep: localization, partial characterization, and expression. *Mamm. Genome* **18**, 53–63 (2007).

225. Zhang, R. R. *et al.* Tet1 regulates adult hippocampal neurogenesis and cognition. *Cell Stem Cell* **13**, 237–245 (2013).

226. Chopp, M. & Li, Y. Treatment of neural injury with marrow stromal cells. *Lancet Neurology* vol. 1 92–100 (2002).

227. Bonab, M. M. *et al.* Aging of mesenchymal stem cell in vitro. *BMC Cell Biol.* **7**, (2006).

228. Calloni, R., Viegas, G. S., Türck, P., Bonatto, D. & Pegas Henriques, J. A. Mesenchymal stromal cells from unconventional model organisms. *Cytotherapy* vol. 16 3–16 (2014).

229. Ghaemmaghami, S. *et al.* Cell division modulates prion accumulation in cultured cells. *Proc. Natl. Acad. Sci. U. S. A.* **104**, 17971–17976 (2007).

230. Kanu, N. *et al.* Transfer of scrapie prion infectivity by cell contact in culture. *Curr. Biol.* **12**, 523–530 (2002).

231. Krejciova, Z. *et al.* Human stem cell-derived astrocytes replicate human prions in a PRNP genotype-dependent manner. *J. Exp. Med.* **214**, 3481–3495 (2017).

232. Jauković, A. *et al.* Specificity of 3D MSC Spheroids Microenvironment: Impact on MSC Behavior and Properties. *Stem cell Rev. reports* **16**, 853–875 (2020).

233. Sart, S., Tsai, A. C., Li, Y. & Ma, T. Three-Dimensional Aggregates of Mesenchymal Stem Cells: Cellular Mechanisms, Biological Properties, and Applications.

https://home.liebertpub.com/teb **20**, 365–380 (2013).

234. Liu, Y., Muñoz, N., Tsai, A. C., Logan, T. M. & Ma, T. Metabolic Reconfiguration Supports Reacquisition of Primitive Phenotype in Human Mesenchymal Stem Cell Aggregates. *Stem Cells* **35**, 398–410 (2017).

235. Zhang, Q. *et al.* Three-dimensional spheroid culture of human gingiva-derived mesenchymal stem cells enhances mitigation of chemotherapy-induced oral mucositis. *Stem Cells Dev.* **21**, 937–947 (2012).

236. Wang, Z. *et al.* Single-cell transcriptome atlas of human mesenchymal stem cells exploring cellular heterogeneity. *Clin. Transl. Med.* **11**, (2021).

237. Yin, J. Q., Zhu, J. & Ankrum, J. A. Manufacturing of primed mesenchymal stromal cells for therapy. *Nat. Biomed. Eng.* **3**, 90–104 (2019).

238. Jiang, B. *et al.* Spheroidal formation preserves human stem cells for prolonged time under ambient conditions for facile storage and transportation. *Biomaterials* **133**, 275–286 (2017).

239. Li, Y. *et al.* Three-dimensional spheroid culture of human umbilical cord mesenchymal stem cells promotes cell yield and stemness maintenance. *Cell Tissue Res.* **360**, 297–307 (2015).

240. Regmi, S. *et al.* Enhanced viability and function of mesenchymal stromal cell spheroids is mediated via autophagy induction. *Autophagy* **17**, 2991–3010 (2021).

241. Beraldo, F. H. *et al.* Role of α7 nicotinic acetylcholine receptor in calcium signaling induced by prion protein interaction with stress-inducible protein. *J. Biol. Chem.* **285**, 36542–36550 (2010).

242. Hall, G. N. M. *et al.* Cellular prion protein interaction with vitronectin supports axonal growth and is compensated by integrins. *J. Cell Sci.* **120**, 1915–1926 (2007).

243. Head, B. P., Patel, H. H. & Insel, P. A. Interaction of membrane/lipid rafts with the cytoskeleton: Impact on signaling and function: Membrane/lipid rafts, mediators of cytoskeletal arrangement and cell signaling. *Biochim. Biophys. Acta - Biomembr.* **1838**, 532–545 (2014).

244. Hirsch, T. Z., Martin-Lannerée, S. & Mouillet-Richard, S. Functions of the Prion Protein. *Prog. Mol. Biol. Transl. Sci.* **150**, 1–34 (2017).

245. Málaga-Trillo, E. *et al.* Regulation of Embryonic Cell Adhesion by the Prion Protein. *PLOS Biol.* **7**, e1000055 (2009).

246. Boilan, E. *et al.* Role of Prion protein in premature senescence of human fibroblasts. *Mech. Ageing Dev.* **170**, 106–113 (2018).

247. Wurm, S. & Wechselberger, C. Prion protein modifies TGF-beta induced signal transduction. *Biochem. Biophys. Res. Commun.* **349**, 525–532 (2006).

248. Besnier, L. S. *et al.* The cellular prion protein PrPc is a partner of the Wnt pathway in intestinal epithelial cells. *Mol. Biol. Cell* **26**, 3313–3328 (2015).

249. Sun, J. *et al.* Remarkable impairment of Wnt/β-catenin signaling in the brains of the mice infected with scrapie agents. *J. Neurochem.* **136**, 731–740 (2016).

250. Singh, A. *et al.* Prion protein regulates iron transport by functioning as a ferrireductase. *J. Alzheimers. Dis.* **35**, 541–552 (2013).

251. Singh, A. *et al.* Abnormal brain iron homeostasis in human and animal prion disorders. *PLoS Pathog.* **5**, (2009).

252. Singh, A., Qing, L., Kong, Q. & Singh, N. Change in the characteristics of ferritin induces iron imbalance in prion disease affected brains. *Neurobiol. Dis.* **45**, 930–938 (2012).

253. Basu, S. *et al.* Modulation of proteinase K-resistant prion protein in cells and infectious brain homogenate by redox iron: implications for prion replication and disease pathogenesis. *Mol. Biol. Cell* **18**, 3302–3312 (2007).

254. Voisset, C., Saupe, S. J. & Blondel, M. The various facets of the protein-folding activity of the ribosome. *Biotechnol. J.* **6**, 668–673 (2011).

255. Voisset, C. *et al.* The double life of the ribosome: When its protein folding activity supports prion propagation. *Prion* **11**, 89–97 (2017).

256. Bamia, A. *et al.* Anti-prion Drugs Targeting the Protein Folding Activity of the Ribosome Reduce PABPN1 Aggregation. *Neurotherapeutics* **18**, 1137–1150 (2021).

257. Gao, H. *et al.* Ferroptosis is a lysosomal cell death process. *Biochem. Biophys. Res. Commun.* **503**, 1550–1556 (2018).

258. Mou, Y. *et al.* Ferroptosis, a new form of cell death: opportunities and challenges in cancer. *J. Hematol. Oncol.* **12**, (2019).

259. Reichert, C. O. *et al.* Ferroptosis Mechanisms Involved in Neurodegenerative Diseases. *Int. J. Mol. Sci.* **21**, 1–27 (2020).

260. Khokha, R., Murthy, A. & Weiss, A. Metalloproteinases and their natural inhibitors in inflammation and immunity. *Nat. Rev. Immunol.* **13**, 649–665 (2013).

261. Minta, K. *et al.* Dynamics of cerebrospinal fluid levels of matrix metalloproteinases in human traumatic brain injury. *Sci. Rep.* **10**, (2020).

262. Cox, T. R. & Erler, J. T. Remodeling and homeostasis of the extracellular matrix: implications for fibrotic diseases and cancer. *Dis. Model. Mech.* **4**, 165–178 (2011).

263. Crocker, S. J., Pagenstecher, A. & Campbell, I. L. The TIMPs tango with MMPs and more in the central nervous system. *J. Neurosci. Res.* **75**, 1–11 (2004).

264. Liu, Y. *et al.* Matrix metalloproteinase-12 contributes to neuroinflammation in the aged brain. *Neurobiol. Aging* **34**, 1231–1239 (2013).

265. Song, K. *et al.* Synthetic prion Peptide 106-126 resulted in an increase matrix metalloproteinases and inflammatory cytokines from rat astrocytes and microglial cells. *Toxicol. Res.* **28**, 5–9 (2012).

266. Marbiah, M. M. *et al.* Identification of a gene regulatory network associated with prion replication. *EMBO J.* **33**, 1527–1547 (2014).

267. Moretto, E., Stuart, S., Surana, S., Vargas, J. N. S. & Schiavo, G. The Role of Extracellular Matrix Components in the Spreading of Pathological Protein Aggregates. *Front. Cell. Neurosci.* **16**, (2022).

268. Lee, J. A. *et al.* SerpinB2 (PAI-2) Modulates Proteostasis via Binding Misfolded Proteins and Promotion of Cytoprotective Inclusion Formation. *PLoS One* **10**, (2015).

269. Hirata, T. *et al.* Identification of a Golgi GPI-N-acetylgalactosamine transferase with tandem transmembrane regions in the catalytic domain. *Nat. Commun.* **9**, (2018).

270. Bate, C., Nolan, W. & Williams, A. Sialic Acid on the Glycosylphosphatidylinositol Anchor Regulates PrP-mediated Cell Signaling and Prion Formation. *J. Biol. Chem.* **291**, 160–170 (2016).

271. Hirata, T. *et al.* Loss of the N-acetylgalactosamine side chain of the GPI-anchor impairs bone formation and brain functions and accelerates the prion disease pathology. *J. Biol. Chem.* **298**, (2022).

272. Arnould, H. *et al.* Loss of prion protein control of glucose metabolism promotes neurodegeneration in model of prion diseases. *PLoS Pathog.* **17**, (2021).

273. Hu, H. *et al.* Proline-Rich Protein 11 Regulates Self-Renewal and Tumorigenicity of Gastric Cancer Stem Cells. *Cell. Physiol. Biochem.* **47**, 1721–1728 (2018).

274. Zhang, L. *et al.* Silencing of PRR11 suppresses cell proliferation and induces autophagy in NSCLC cells. *Genes Dis.* **5**, 158–166 (2017).

275. Zhou, L. *et al.* Overexpression of PRR11 promotes tumorigenic capability and is associated with progression in esophageal squamous cell carcinoma. *Onco. Targets. Ther.* **12**, 2677–2693 (2019).

276. Kaartinen, M. T. *et al.* F13A1 transglutaminase expression in human adipose tissue increases in acquired excess weight and associates with inflammatory status of adipocytes. *Int. J. Obes. (Lond).* **45**, 577–587 (2021).

277. Kaartinen, M. T. *et al.* Transglutaminases and Obesity in Humans: Association of F13A1 to Adipocyte Hypertrophy and Adipose Tissue Immune Response. *Int. J. Mol. Sci.* **21**, 1–20 (2020).